



Goundry, Amy Louise (2015) *Leishmania virulence factors: inhibitors of serine peptidases*. PhD thesis.

<http://theses.gla.ac.uk/6002/>

Copyright and moral rights for this work are retained by the author

A copy can be downloaded for personal non-commercial research or study, without prior permission or charge

This work cannot be reproduced or quoted extensively from without first obtaining permission in writing from the author

The content must not be changed in any way or sold commercially in any format or medium without the formal permission of the author

When referring to this work, full bibliographic details including the author, title, awarding institution and date of the thesis must be given

Enlighten:Theses
<http://theses.gla.ac.uk/>
theses@gla.ac.uk

***Leishmania* virulence factors: Inhibitors of serine peptidases**

Amy Louise Goundry
BSc (Hons)

Thesis submitted in fulfilment of the requirements for the
degree of Doctor of Philosophy

Institute of Infection, Immunity and Inflammation
College of Medical, Veterinary and Life Sciences
University of Glasgow

January 2015

Abstract

Leishmania spp. are protozoan parasites that cause a spectrum of pathologies in humans and other vertebrates, ranging symptomatically from cutaneous ulceration to visceral dissemination. In order to survive within the host, *Leishmania* are able to evade and modulate the host immune responses through the actions of their virulence factors; however, few putative virulence factors have been characterised during *in vivo* infection with *Leishmania*. The *Leishmania major* genome has revealed the presence of three peptide inhibitors of S1A family serine peptidases (ISPs), which are orthologues of a bacterial protease inhibitor, ecotin. Serine peptidases of the S1A family are absent in *Leishmania*; therefore, the ISPs have been proposed to inhibit the activity of host serine peptidases, such as those expressed by cells of the innate immune response. ISP2, which is expressed in the mammalian-infective metacyclic promastigote and amastigote stages, has previously been shown to inhibit neutrophil elastase (NE), a serine peptidase expressed by neutrophils, monocytes, and macrophages. This inhibition prevents the activation of a Toll-like receptor 4 (TLR4)-NE pathway during *Leishmania*-macrophage interaction promoting *Leishmania* survival and growth in macrophages *in vitro*.

The aims of this project were to assess whether the presence or absence of ISP2 in *L. major* affects parasite survival *in vivo*, and to investigate the effects of ISP2 on immune cell dynamics *in vivo*, specifically with regards to cell recruitment and activation, using the C57BL/6 mouse model. Parasite burdens were performed in mice infected with *L. major* wild-type (WT) parasites, a cell line deficient in *ISP2/3* ($\Delta isp2/3$), and a cell line re-expressing *ISP2/3* ($\Delta isp2/3:ISP2/3$). *L. major* $\Delta isp2/3$ parasites could not be detected at the site of inoculation by 5 wk post-infection compared with WT and $\Delta isp2/3:ISP2/3$ parasites, but parasites of all three cell lines were detected in the draining lymph nodes (dLNs) throughout the course of infection. These data were corroborated using *in vivo* bioluminescence imaging (BLI) of luciferase-expressing (LUC2) versions of these cell lines, in which only a low bioluminescent signal was observed at the site of inoculation with the LUC2-expressing $\Delta isp2/3$ cell line over the course of infection, compared with the LUC2-expressing *L. major* and $\Delta isp2/3:ISP2/3$ cell lines. These results suggest that ISP2 may be important in

the establishment and persistence of *Leishmania* infection by conferring parasite survival, particularly at the site of infection.

Serine peptidases of innate immune cells, such as NE, function in the proteolytic cleavage of cytokines, chemokines, and cell receptors, to regulate immune cell recruitment and activation. Flow cytometric analysis of innate cell populations at the site of inoculation, in response to *L. major* WT and $\Delta isp2/3$ parasites over 5 wk of infection, was conducted. This line of investigation revealed significantly higher numbers of monocytes, monocyte-derived macrophages, and monocyte-derived dendritic cells (moDCs) at 2 wk in $\Delta isp2/3$ infection. MoDCs have crucial functions in the induction of antigen-specific T helper 1 responses, which are considered to be important for parasite clearance. MoDCs at the site of $\Delta isp2/3$ infection showed an upregulation of the DC co-stimulatory molecule CD80 compared with those from WT infection suggesting an upregulation of DC maturation. MoDCs have also been shown to be the major producers of inducible nitric oxide synthase (iNOS) during *L. major* infection, which catalyses the production of nitric oxide that is responsible for the killing of *Leishmania*. Intracellular staining of iNOS through flow cytometric techniques showed that iNOS expression in moDCs was not affected by the presence or absence of ISP2; there was, however, an increase in iNOS expression in other innate cell types, the resident macrophages and DCs, monocytes, and monocyte-derived macrophages, at the site of $\Delta isp2/3$ infection compared with those from WT and $\Delta isp2/3:ISP2/3$ infections. At the 2 wk time-point, there was also a significant increase in the concentration of IFN- γ , a cytokine that induces iNOS expression, in response to $\Delta isp2/3$ infection compared with WT and $\Delta isp2/3:ISP2/3$ infections, as determined by ELISA. Quantitative *in vivo* BLI of myeloperoxidase (MPO) activity of activated phagocytes was determined over a period of 7 wk, which, also, indicated differences in phagocyte activation at the site of inoculation in *L. major* WT and $\Delta isp2/3$ infections. Taken together, these results indicate that the immune response is more primed towards *Leishmania* killing in $\Delta isp2/3$ infection compared with WT infection, which suggests that ISP2 modulates these immune responses to facilitate *Leishmania* survival.

Infections in transgenic mice deficient in NE, *Ela*^{-/-}, showed similar monocyte recruitment and moDC activation responses in $\Delta isp2/3$ infection compared with

WT and $\Delta isp2/3:ISP2/3$ infections, as those observed in the C57BL/6 mice. This indicates that NE may not be the major target for ISP2 *in vivo*, or that there may be compensations for the loss of NE by other serine peptidases in this model. Although the exact mechanism by which ISP2 modulates the recruitment and activation of the innate immune cells *in vivo* remains to be determined, this study has, for the first time, shown numerous differences in the innate immune responses induced following infection with either *L. major* WT or a mutant deficient in a putative virulence factor using *in vivo* techniques, such as *in vivo* imaging (IVIS) and flow cytometry, to compare the infections.

Table of Contents

1 Introduction	1
1.1 Leishmaniasis and the <i>Leishmania</i> parasite	1
1.1.1 Leishmaniases: Epidemiology, Pathology, and Treatment	1
1.1.2 <i>Leishmania</i> parasite: Structure and lifecycle	8
1.1.2.1 Development in the sandfly vector	8
1.1.2.2 Development in the mammalian host	11
1.2 Mammalian immune response to <i>Leishmania</i> spp.	12
1.2.1 Innate immune response	12
1.2.1.1 The complement system	12
1.2.1.2 Role of skin-resident cells.....	13
1.2.1.3 <i>Leishmania</i> -neutrophil interactions	13
1.2.1.4 <i>Leishmania</i> -macrophage interactions	15
1.2.1.5 <i>Leishmania</i> -dendritic cell interactions.....	17
1.2.2 Adaptive immune response	18
1.2.3 Second wave of innate cell infiltration	20
1.2.4 The role of cytokines during <i>Leishmania</i> infection.....	21
1.2.5 Experimental cutaneous leishmaniasis: The mouse models.....	22
1.3 <i>Leishmania</i> virulence factors and mechanisms of immune evasion and modulation	23
1.4 Inhibitors of serine peptidases (ISPs).....	25
1.4.1 Discovery of <i>Leishmania</i> ISPs	25
1.4.2 Role of ISP1 in flagellar pocket dynamics.....	27
1.4.3 Role of ISP2 as a potential virulence factor	28
1.5 Project aims	30
2 Materials and Methods	32
2.1 Promastigote parasite culture.....	32
2.1.1 <i>Leishmania</i> cell lines.....	32
2.1.2 Passage of cultures.....	33
2.1.2.1 Media and growth conditions	33
2.1.2.2 Antibiotic concentrations	33
2.1.3 Preparation and recovery of stabilates	33
2.1.4 Determination of culture density	33
2.1.5 Purification of <i>L. major</i> metacyclic promastigotes	34
2.1.6 Transfection and selection of <i>Leishmania</i> clones.....	34

2.1.7 Preparation of genomic DNA from <i>Leishmania</i> spp.	35
2.1.8 Preparation of protein extracts from <i>Leishmania</i> spp.	35
2.1.9 Luciferase reporter gene assay.....	35
2.2 Bacterial culture	36
2.2.1 <i>E. coli</i> strains	36
2.2.2 Transformation of <i>E. coli</i> with plasmid DNA.....	36
2.2.3 Culture of <i>E. coli</i>	36
2.2.3.1 Media and growth conditions	36
2.2.3.2 Antibiotic concentrations	37
2.2.4 Expression of recombinant proteins	37
2.3 Molecular biology techniques.....	38
2.3.1 Preparation of plasmid DNA from <i>E. coli</i>	38
2.3.2 Quantification of DNA concentration and purity.....	38
2.3.2 Agarose gel electrophoresis.....	38
2.3.3 Restriction endonuclease digestion.....	38
2.3.4 Gel extraction	39
2.3.5 Ethanol precipitation	39
2.3.6 Polymerase chain reaction (PCR)	39
2.3.6.1 High fidelity PCR	39
2.3.6.2 Colony PCR	39
2.3.6.3 PCR method of genotyping transgenic mice	40
2.3.7 Oligonucleotides used	40
2.3.8 Ligation	41
2.3.8.1 Cloning of PCR products into cloning vectors	41
2.3.8.2 Cloning of digested inserts into destination plasmids.....	41
2.3.9 DNA sequencing.....	41
2.3.10 Plasmids used.....	41
2.4 Protein techniques	42
2.4.1 SDS-PAGE	42
2.5 Antibody purification	43
2.5.1 Antibody storage	44
2.6 Immunostaining.....	44
2.6.1 Western blotting.....	44
2.6.2 Immunofluorescence microscopy	44
2.7 Flow cytometry	45
2.7.1 Staining cell surface antigens	45
2.7.2 Staining cytoplasmic intracellular antigens	46

2.7.3 Data acquisition and analysis	47
2.8 Enzyme-linked immunosorbent assay (ELISA)	47
2.9 Mice	47
2.9.1 Regulations	47
2.9.2 Strains	48
2.9.3 Mouse infections and inoculations	48
2.9.4 Measurement of lesions and tissues	49
2.9.4.1 Size measurements	49
2.9.4.2 Mass measurements	49
2.9.5 Tissue processing	49
2.9.5.1 Flow cytometry	49
2.9.5.2 ELISAs	50
2.9.5.3 Limiting dilution assays	50
2.9.6 Peritoneal macrophage isolation	50
2.9.7 Purification of amastigotes from tissues	51
2.10 Quantification of parasite burden from tissues	51
2.11 Bioluminescence imaging (BLI)	52
2.11.1 Preparation of luciferin	52
2.11.2 Preparation of luminol sodium salt	52
2.11.3 BLI image analysis	52
2.12 Statistical analysis	52
3 Localisation of the inhibitors of serine peptidases in <i>Leishmania major</i> ...	54
3.1 Introduction	54
3.1.1 ISP expression during the <i>Leishmania</i> lifecycle and inhibitory activity against host serine peptidases	54
3.1.2 Serine peptidases and the S1A serine peptidase family	55
3.1.3 S1A serine peptidase expression in the sandfly vector	55
3.1.4 S1A serine peptidase expression in the mammalian host	56
3.1.5 Aims	57
3.2 Results	57
3.2.1 Validation of affinity-purified anti-ISP1 and anti-ISP2 antibodies	57
3.2.2 Immunolocalisation of ISP1 and ISP2	61
3.3 Discussion	63
4 Comparison of parasite dissemination and burdens of <i>L. major</i> wild-type and <i>ISP2</i> gene mutants <i>in vivo</i>	70
4.1 Introduction	70

4.1.1 Considerations for an experimental mouse model to mimic natural <i>L. major</i> infection	70
4.1.2 The luciferase gene reporter system	75
4.1.3 The role of ISP2 on parasite survival <i>in vitro</i>	76
4.1.4 Aims	77
4.2 Results	77
4.2.1 Lesion measurements over the course of infection	77
4.2.2 Generation and characterisation of transgenic bioluminescent cell lines ...	79
4.2.3 Tracking parasite bioluminescence with the <i>in vivo</i> imaging system (IVIS)..	81
4.2.4 Measurements of tissues and quantification of parasite loads	88
4.3 Discussion	93
5 Comparison of the cellular immune response dynamics during infection with <i>L. major</i> wild-type and <i>ISP2</i> gene mutants <i>in vivo</i>	103
5.1 Introduction.....	103
5.1.1 Innate cell recruitment and activation during <i>L. major</i> infection in the mouse model.....	103
5.1.2 Role of serine peptidases in the mammalian immune response.....	104
5.1.3 Serine peptidase-deficient mice	107
5.1.4 <i>In vivo</i> methods to assess innate cell infiltration and activation.....	108
5.1.5 Aims	109
5.2 Results	110
5.2.1 Innate immune cell dynamics at the site of intradermal <i>L. major</i> inoculation	110
5.2.2 Imaging myeloperoxidase (MPO) activity of activated phagocytes during <i>L. major</i> infection	120
5.2.3 Quantification of the iNOS response, IFN- γ production, and DC maturation	128
5.2.4 The role of neutrophil elastase during <i>Leishmania</i> infection <i>in vivo</i>	134
5.2.4.1 Genotyping of transgenic <i>Ela</i> ^{-/-} mice	134
5.2.4.2 Lesion measurements over the course of <i>L. major</i> infection in <i>Ela</i> ^{-/-} mice	135
5.2.4.3 Imaging myeloperoxidase (MPO) activity of activated phagocytes in <i>Ela</i> ^{-/-} mice	136
5.2.4.4 Innate immune cell infiltration and activation at the site of inoculation at 2 wk post-infection in <i>Ela</i> ^{-/-} mice	141
5.2.4.5 Quantification of parasite loads in <i>Ela</i> ^{-/-} mice.....	143
5.3 Discussion	145
5.3.1 Innate cell recruitment and functions during <i>Leishmania</i> infection	146
5.3.1.1 The second wave of innate cell recruitment	148

5.3.1.2 Monocytes and monocyte-derived dendritic cells	151
5.3.1.3 Neutrophil-dendritic cell interactions.....	153
5.3.1.4 The iNOS response.....	154
5.3.2 <i>In vivo</i> imaging of the innate immune responses	155
5.3.3 Redundancy and synergistic effects of NSPs	158
5.3.3.1 MPO and NSPs	159
5.3.4 Future directions	160
5.3.5 Concluding remarks	161
6 General Discussion.....	163
References	172

List of Tables

1 Introduction

Table 1-1 Human-infective <i>Leishmania</i> species and their clinical forms.....	5
Table 1-2 Important cytokines and growth factors that mediate the immune response during <i>Leishmania</i> infection	22

2 Materials and Methods

Table 2-1 <i>Leishmania major</i> cell lines used in this study	32
Table 2-2 Competent <i>E. coli</i> strains used in the study	36
Table 2-3 Oligonucleotides used in this study.....	40
Table 2-4 Plasmids used or generated in this study.....	42
Table 2-5 Antibodies used for flow cytometry	46

5 Comparison of the cellular immune response dynamics during infection with *L. major* wild-type and *ISP2* gene mutants *in vivo*

Table 5-1 The effects of neutrophil serine proteases (NSPs), neutrophil elastase (NE), cathepsin G (CG), and proteinase 3 (PR3), on host biological targets.....	106
Table 5-2 Cell surface markers of CD11b ⁺ myeloid innate cell subsets.....	112

List of Figures

1 Introduction

Figure 1-1 Geographical distribution of cutaneous leishmaniasis and visceral leishmaniasis.	2
Figure 1-2 The <i>Leishmania</i> lifecycle within the sandfly vector.....	10
Figure 1-3 Neutrophil migration from the blood vessels to the site of infection	10
Figure 1-4 Mechanisms mediating healing versus non-healing in leishmaniasis	20
Figure 1-5 The early immune responses to infection with <i>Leishmania</i> spp.	21
Figure 1-6 Effect of <i>L. major</i> ISP2 on <i>Leishmania</i> -macrophage interactions	30

3 Localisation of the inhibitors of serine peptidases in *Leishmania major*

Figure 3-1 Validation of anti-ISP antibodies against extracts from <i>L. major</i> ISP gene mutants.....	60
Figure 3-2 ISP1 and ISP2 localisation in <i>L. major</i> promastigotes	62
Figure 3-3 ISP2 localisation in <i>L. major</i> amastigotes.....	63

4 Comparison of parasite dissemination and burdens of *L. major* wild-type and *ISP2* gene mutants *in vivo*

Figure 4-1 Lesion development in the footpads of C57BL/6 mice.....	78
Figure 4-2 Lesion development in the ears of C57BL/6 mice	79
Figure 4-3 <i>In vitro</i> luciferase reporter gene assays of LUC2-expressing cell lines	80
Figure 4-4 <i>In vitro</i> growth curves of promastigote cultures of <i>L. major</i> WT, $\Delta isp2/3$, $\Delta isp2/3:ISP2/3$ and the LUC2-expressing cell lines.....	81
Figure 4-5 <i>In vivo</i> bioluminescence imaging of LUC2-expressing cell lines at the site of inoculation	86
Figure 4-6 Quantification of bioluminescent signal from LUC2-expressing cell lines, and parasite burdens at the site of inoculation and in the draining lymph node	87
Figure 4-7 Parasite burdens during infection with <i>L. major</i> WT, $\Delta isp2/3$, and $\Delta isp2/3:ISP2/3$	92
Figure 4-8 Liver and spleen masses during infection with <i>L. major</i> WT, $\Delta isp2/3$, and $\Delta isp2/3:ISP2/3$	93

5 Comparison of the cellular immune response dynamics during infection with *L. major* wild-type and *ISP2* gene mutants *in vivo*

Figure 5-1 Myeloid cell composition at the site of inoculation during infection with <i>L. major</i> WT and $\Delta isp2/3$	111
Figure 5-2 Gating strategy to determine innate immune cell subsets in the ear dermis.	113
Figure 5-3 Dynamics of the innate immune cell populations at the site of inoculation during infection with <i>L. major</i> WT and $\Delta isp2/3$	119
Figure 5-4 Myeloid cell composition of the draining lymph node after intradermal inoculation with <i>L. major</i> WT or $\Delta isp2/3$	120
Figure 5-5 <i>In vivo</i> bioluminescence imaging of MPO activity of activated phagocytes at the site of inoculation during infection with <i>L. major</i> WT and <i>ISP2</i> gene mutants.....	126
Figure 5-6 MPO protein content of innate immune cells in the ear dermis of C57BL/6 mice at 2 wk post-infection with <i>L. major</i> WT and <i>ISP2</i> gene mutants	128
Figure 5-7 Inducible nitric oxide synthase (iNOS/NOS2) expression at the site of inoculation at 2 wk post-infection with <i>L. major</i> WT and <i>ISP2</i> gene mutants.....	130
Figure 5-8 IFN- γ concentration at 2 wk post-infection with <i>L. major</i> WT and <i>ISP2</i> gene mutants.....	131
Figure 5-9 Dendritic cell co-stimulatory molecule expression at 2 wk post-infection with <i>L. major</i> WT and $\Delta isp2/3$	133
Figure 5-10 Genotyping of transgenic neutrophil elastase deficient, <i>Ela</i> ^{-/-} , mice through PCR analysis.....	135
Figure 5-11 Lesion development in the ears of <i>Ela</i> ^{-/-} mice infected with <i>L. major</i> WT and <i>ISP2</i> gene mutants.....	136
Figure 5-12 <i>In vivo</i> bioluminescence imaging of MPO activity of activated phagocytes at the site of inoculation during infection with <i>L. major</i> WT and <i>ISP2</i> gene mutants in <i>Ela</i> ^{-/-} mice	140
Figure 5-13 Composition of the cellular infiltrate at the site of inoculation at 2 wk post-infection with <i>L. major</i> WT and <i>ISP2</i> gene mutants in <i>Ela</i> ^{-/-} mice	142
Figure 5-14 Dendritic cell co-stimulatory molecule expression at 2 wk post-infection with <i>L. major</i> WT and <i>ISP2</i> gene mutants in <i>Ela</i> ^{-/-} mice	143
Figure 5-15 Parasite burdens at 5 wk post-infection with <i>L. major</i> WT and <i>ISP2</i> gene mutants in <i>Ela</i> ^{-/-} mice.....	144
Figure 5-16 Lymph node diameters, and liver and spleen masses at 5 wk post-infection with <i>L. major</i> WT and <i>ISP2</i> gene mutants in <i>Ela</i> ^{-/-} mice	144

6 General Discussion

Figure 6-1 Immune responses at the site of <i>L. major</i> WT and Δ <i>isp2/3</i> infection at 2 wk	166
Figure 6-2 Potential effects of the prevention of TLR4 signalling cascades on immune responses <i>in vivo</i>	167
Figure 6-3 Potential effects of inhibiting serine peptidase activity by <i>L. major</i> ISP2 during <i>in vivo</i> infection.....	169

Acknowledgements

I would like to thank my supervisor Jeremy Mottram for his guidance over the past four years, and for giving me the opportunity to work on a great project in a great lab. I would also like to thank my co-supervisor Ana Paula Lima for her brilliant insights, and Elmarie Myburgh for her continuous support throughout this project. My assessors, Tansy Hammarton and Paul Garside, have also provided valuable feedback on my work from both the Parasitology and Immunology perspectives. Additional thanks to Paul for allowing me to use his group's antibodies for flow cytometry. I would also like to acknowledge the Medical Research Council, who funded my project.

Thanks to Ryan Ritchie and the staff at the JRF, particularly Colin, who provided a lot of help with the animal work. Thanks to Jillian Stephen for help with immunology protocols. And thanks to the omniscient Jim Scott, without whom the lab would fall into chaos.

Many thanks to the past and present members of level 6, who have made this experience a lot of fun; Alli, Andrea, Annelie, Antonio, Becky, Ben, Cat, Corinna, Craig, Cristina, Dan, Elaine, Elena, Elizabeth, Ellie, Esther, Fernanda, Fernando, Helena, Isabela, Jeziel, Juliana, Larissa, Luciana, Manuel, Mari, Marko, Marlene, Nath, Nick, Robyn, Sam, Saskia, Stephan, Susan, Tamsin, Tania, Tiago, Tom, Vivi, and Will.

And finally thanks to my parents, who have supported my quest to be an eternal student.

Author's Declaration

The research reported in this thesis is the result of my own original work, except where stated below, and has not been submitted for any other degree.

Amy Louise Goundry, September 2014

The *L. major* $\Delta isp1/2/3$, $\Delta isp1/2/3:ISP1$, $\Delta isp1/2/3:ISP2/3$, $\Delta isp2/3$, $\Delta isp2/3:ISP2/3$, and WT [*pXG-ISP2*] mutants were produced by Dr Sylvain Eschenlauer and Dr Lesley Morrison. The plasmid used for the generation of the *L. major*+LUC2 and $\Delta isp2/3$ +LUC2 cell lines, pGL2126, was generated by Dr Elmarie Myburgh. Protein purification of recombinant ISP1 and ISP2 was performed in-house by Alan Scott.

Some of the results presented in Chapter 3 have been published in Cellular Microbiology:

Morrison, L.S., Goundry, A., Faria, M.S., Tetley, L., Eschenlauer, S.C., Westrop, G.D., Dostalova, A., Volf, P., Coombs, G.H., Lima, A.P., and Mottram, J.C. (2012) Ecotin-like serine peptidase inhibitor ISP1 of *Leishmania major* plays a role in flagellar pocket dynamics and promastigote differentiation. *Cell Microbiol* 14 (8): 1271-86

List of Abbreviations

2P-IVM	intravital two-photon microscopy
4-ABAH	4-aminobenzoic acid hydrazide
α -ISP	anti-ISP antibody
AAT	α -1 antitrypsin
ACT	α -1-antichymotrypsin
ANOVA	analysis of variance
AP-1	activator protein 1
APC	antigen-presenting cell
ATP	adenosine triphosphate
BLAST	basic local alignment search tool
BLI	bioluminescence imaging
bp	base pair
BSA	bovine serum albumin
CCD	charge-coupled device
CD	cluster of differentiation
CG	cathepsin G
(L)CL	(localised) cutaneous leishmaniasis
CP	cysteine peptidase
CR	complement receptor
CRET	chemiluminescence resonance energy transfer
d	day
DALY	disability-adjusted life years
DAPI	4,6-diamidino-2-phenylindole
DC	dendritic cell
DCL	diffuse cutaneous leishmaniasis
DIC	differential interference contrast
dLN	draining lymph node
DMSO	dimethyl sulfoxide
DNA	deoxyribonucleic acid
dNTP	deoxynucleotide triphosphate
DPPI	dipeptidyl peptidase I
DTT	dithiothreitol
ECM	extracellular matrix
EDTA	ethylenediaminetetraacetic acid
ELISA	enzyme-linked immunosorbent assay
FACS	fluorescence-activated cell sorting
FCS	foetal calf serum
fPPG	filamentous proteophosphoglycan
g	gram
G	gauge
GIPL	glycoinositolophospholipid
gp63	glycoprotein 63
GPCR	G-protein coupled receptor
GPI	glycophosphatidylinositol
h	hour
HIV	human immunodeficiency virus
HOMEM	hemoflagellate-modified minimal essential medium
HRP	horseradish peroxidase
Hz	hertz
ICP	inhibitor of cysteine peptidase
IFN	interferon
IFT	intraflagellar transport
IL	interleukin
iNOS	inducible nitric oxide synthase

IPTG	isopropyl-β-D-thiogalactopyranoside
IRF3	interferon regulatory transcription factor 3
ISP	inhibitor of serine peptidase
IVIS	<i>in vivo</i> imaging system
kb	kilobase
kDa	kilodalton
L	litre
LACK	<i>Leishmania</i> homolog of receptors for activated C kinase
LB	lysogeny broth
LC	Langerhans cell
LDA	limiting dilution assay
LPG	lipophosphoglycan
LUC2	firefly luciferase
μ	micro
m	milli / metre
M	molar
MAC	membrane attack complex
Mb	megabase
MCL	mucocutaneous leishmaniasis
MHC	major histocompatibility complex
min	minute
MMR	macrophage mannose receptor
MNEI	monocyte neutrophil elastase inhibitor
MoDC	monocyte-derived dendritic cell
MPO	myeloperoxidase
MyD88	myeloid differentiation marker 88
n	nano
NADPH	nicotinamide adenine dinucleotide phosphate
NE	neutrophil elastase
NEI	neutrophil elastase inhibitor
NEO	neomycin resistance gene
NET	neutrophil extracellular trap
NF-κB	nuclear factor-κB
NK	natural killer
NO	nitric oxide
OD	optical density
OPB	oligopeptidase B
PAC	puromycin resistance gene
PAR	protease-activated receptor
PBS	phosphate buffered saline
(q)PCR	quantitative polymerase chain reaction
PDGF	platelet-derived growth factor
PG	phosphoglycan
PKDL	post-kala azar dermal leishmaniasis
PKR	protein kinase R
PPG	proteophosphoglycan
PR3	proteinase 3
PSA-2	promastigote surface antigen 2
PSG	promastigote secretory gel
PSGEMKA	buffer comprising 20 mM sodium phosphate, 104 mM sodium chloride, 5.5 mM D-glucose, 0.5 mM EDTA, 10 mM magnesium chloride, 10 mM potassium chloride and 0.02% (w/v) BSA
PV	parasitophorous vacuole
RFP	red fluorescent protein
rISP	recombinant ISP
ROI	region of interest
ROS	reactive oxygen species

rpm	revolutions per minute
SAT	streptothricin acetyltransferase (nourseothricin resistance gene)
SDS-PAGE	sodium dodecylsulphate polyacrylamide gel electrophoresis
sec	second
SEM	standard error of the mean
SGS	salivary gland sonicate
SKALP	skin-derived antileukoprotease
SLPI	secretory leukocyte protease inhibitor
SOC	super optimal broth with catabolite repression
(N)SP	(neutrophil) serine peptidase
SSG	sodium stibogluconate
STAT	signal transducers and activators of transcription
TBE	Tris-borate-EDTA
TBS(T)	Tris-buffered saline (with Tween-20)
TCR	T cell receptor
Tfh	T follicular helper
Th	T helper
Tip-DC	TNF-iNOS-producing dendritic cell
TLR	Toll-like receptor
TNF	tumour necrosis factor
Tr1	type 1 regulatory
(n)Treg	(natural) T regulatory
TRIF	TIR domain-containing adaptor inducing IFN- β
U	Unit
UV	ultraviolet
VL	visceral leishmaniasis
v/v	volume to volume
w/v	weight to volume
WHO	World Health Organization
wk	week
WT	wild-type

1 Introduction

1.1 Leishmaniasis and the *Leishmania* parasite

Leishmaniasis is a neglected tropical disease that manifests in a spectrum of pathologies in humans and other vertebrates, collectively known as the leishmaniasis; these range from ulcerative cutaneous lesions to systemic visceral infection. The leishmaniasis are caused by species of the protozoan parasite, *Leishmania*, of the family Trypanosomatidae, Order Kinetoplastida. *Leishmania* parasites are primarily transmitted to humans and other vertebrates through the bite of an infected phlebotomine sandfly.

1.1.1 Leishmaniasis: Epidemiology, Pathology, and Treatment

The leishmaniasis are endemic in over 98 countries and territories, principally in Africa, Asia, and Latin America, with more than 350 million people at risk of infection (Alvar et al., 2012). In the order of 12 million people are currently infected with *Leishmania*, which is commonly associated with poverty and poor socioeconomic conditions, as the malnourished and immunosuppressed are the most susceptible to infection. There are three major clinical forms of the disease; cutaneous, the most common form of the disease of which there are 0.7 to 1.2 million new cases annually; visceral, the most severe form of which there are 200 000 to 400 000 new cases annually; and mucocutaneous (Alvar et al., 2012). Cutaneous leishmaniasis is widely distributed, with 70 to 75% of cases occurring in ten countries: Afghanistan, Algeria, Brazil, Colombia, Costa Rica, Ethiopia, Iran, Peru, Sudan, and Syria; whereas more than 90% of visceral leishmaniasis cases occur in six countries: Bangladesh, Brazil, Ethiopia, India, South Sudan, and Sudan (Figure 1-1) (Alvar et al., 2012). Almost 90% of mucocutaneous leishmaniasis cases occur in Bolivia, Brazil, and Peru.

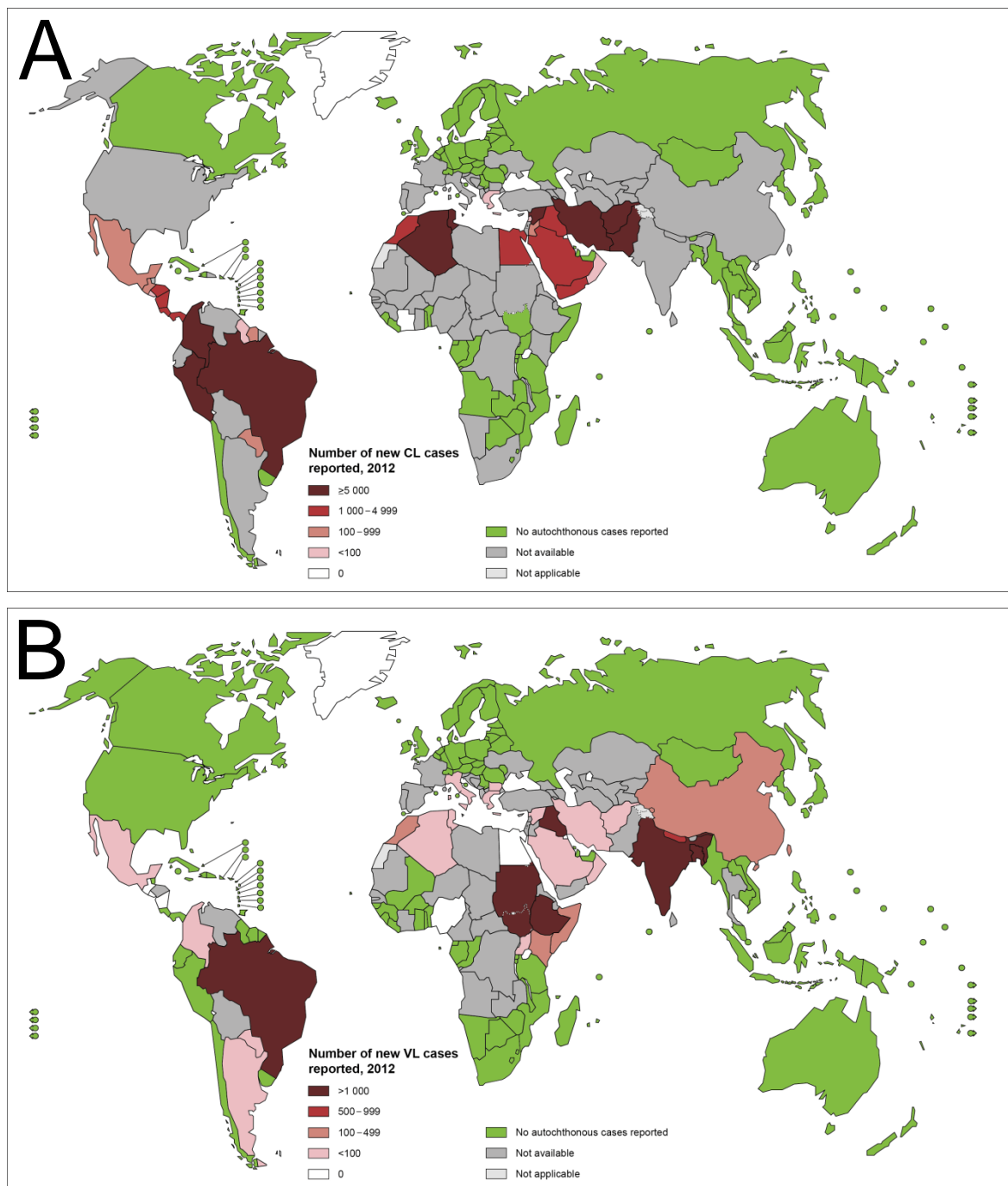


Figure 1-1 Geographical distribution of (A) cutaneous leishmaniasis and (B) visceral leishmaniasis. Source: World Health Organization (WHO) Global Health Observatory Map Gallery (<http://gamapserver.who.int/mapLibrary/app/searchResults.aspx>).

As the mortality caused by the leishmaniases, 20 000 to 40 000 deaths each year (Alvar et al., 2012), is low in comparison to deaths attributed to other infectious diseases in low-income countries, such as HIV, tuberculosis, and malaria, leishmaniasis has been neglected as a major public health problem. However, morbidity is more common than mortality in parasitic infections, producing long-lasting chronic infections as the parasites evade the host immune response to promote their development and survival within the host. Morbidity is, therefore, the principal burden of the leishmaniases, contributing to an estimated 2.4

million disability-adjusted life years (DALYs), which are the number of years lost due to ill-health, disability, or early death. There is also a life-long social and psychological stigma associated with leishmaniasis due to disfiguring scars caused during the disease.

There are over thirty species and subspecies of *Leishmania*, and around twenty of these are pathogenic to humans. The leishmaniases can be grouped into either zoonotic disease, in which the reservoir hosts are other mammals such as dogs and rodents, or anthroponotic disease, in which humans are the reservoir host.

There are two subgenera of *Leishmania*, *Leishmania* and *Viannia*, which were originally classified on the basis of the location of parasite colonisation and development in the gut of the sandfly vector (Lainson et al., 1977), and subsequently supported by phylogenetic analysis. Human-infective *Leishmania* species are separated into two categories based on their geographic distribution, which is dependent on the presence of the appropriate species of phlebotomine sandfly, of the family Psychodidae, for transmission. 'Old World' species of *Leishmania* are transmitted by sandflies of the genus *Phlebotomus*, present in the Eastern hemisphere, specifically Asia, Africa, and Southern Europe. 'New World' species of *Leishmania*, however, are transmitted by sandflies of the genus *Lutzomyia*, and are endemic in the Western hemisphere, which includes Mexico, Central America, and South America.

Humans infected with *Leishmania* exhibit a range of pathologies, the type and severity of which, generally depends on the species of *Leishmania*, as different species of *Leishmania* often display preferential tropisms, primarily dermatropism, mucotropism, and viscerotropism (Table 1-1). The species of *Leishmania* in conjunction with the immunological status of the host, particularly with regards to the innate inflammatory response and the balance between the cellular and humoral arms of the adaptive immune response, determine the outcome of the disease. The three main manifestations of the leishmaniases are cutaneous, mucosal, and visceral.

Localised cutaneous leishmaniasis (LCL) is the most common form of leishmaniasis, and is characterised by cutaneous ulceration at the site of the

sandfly bite on exposed skin, generally on the face, arms and legs. *L. major* and *L. tropica* are the species that cause the majority of LCL cases in the Old World. The development of multiple non-ulcerative papules, plaques, or nodules that resemble leprosy, is an indication of diffuse cutaneous leishmaniasis (DCL), which typically occurs in individuals with a defective cell-mediated immune response. DCL is usually caused by infection with *L. mexicana*, *L. amazonensis*, and *L. aethiopica*. There is a variable tendency for LCL lesions to spontaneously self-heal within 2 to 6 months for *L. major*, 3 to 9 months for *L. mexicana*, or 6 to 15 months for *L. tropica*, which normally results in life-long protection from the disease, although disfiguring scars are often left. Spontaneous self-resolving is not associated with DCL and relapses are frequent after treatment.

Mucocutaneous leishmaniasis (MCL) arises when parasites disseminate from the inoculation site, from less than 5% of LCL or DCL infections, to mucosal tissue. Damage associated with MCL includes the extensive destruction of mucosal membranes of the oro-nasal and pharyngeal cavities with disfiguring lesions and mutilation of the face, particularly the collapse of the nasal septum. MCL is primarily caused by members of the *Viannia* subspecies, such as *L. braziliensis*, *L. peruviana*, and *L. guyanensis*. Secondary bacterial infections, such as *Staphylococcus aureus*, are commonly associated with MCL, further complicating the treatment of this disease. Mucosal lesions of the oro-nasal cavities and the genital mucosa rarely occur in the Old World; these cases are mostly seen in India or Sudan, in patients with visceral leishmaniasis (VL) or post-kala azar dermal leishmaniasis (PKDL), and can be caused by *L. major*, *L. tropica*, *L. infantum*, and *L. donovani*.

VL is the most severe form of leishmaniasis. Parasites disseminate from the inoculation site and proliferate in liver, spleen, and bone marrow, causing undulating fever, weight loss, hepatomegaly, splenomegaly, and anaemia, resulting in host immunosuppression, and ultimately death in the absence of treatment. VL is usually caused by infection with *L. donovani* and *L. infantum*; these parasites have also been implicated as important pathogens in co-infections with HIV creating a lethal combination, which is especially important in the countries where the prevalence of these diseases overlap. The incidence of VL and HIV co-infections has been reported to be increasing in some areas of

Africa and India (Alvar et al., 2008). There is no spontaneous self-healing associated with MCL or VL, and both are difficult to treat. In addition, patients that have been treated for VL can develop PKDL within two years after apparent clinical cure of VL. PKDL patients exhibit a chronic cutaneous disease, which requires long and expensive treatment.

Table 1-1 Human-infective *Leishmania* species and their clinical forms. LCL, localised cutaneous leishmaniasis; DCL, diffuse cutaneous leishmaniasis; MCL, mucocutaneous leishmaniasis; VL, visceral leishmaniasis.

	Clinical forms			
	LCL	DCL	MCL	VL
Old World species	<i>L. (L.) major</i>		<i>L. (L.) major</i>	
	<i>L. (L.) tropica</i>		<i>L. (L.) tropica</i>	
	<i>L. (L.) aethiopica</i>	<i>L. (L.) aethiopica</i>		
	<i>L. (L.) infantum</i>		<i>L. (L.) infantum</i>	<i>L. (L.) infantum</i>
			<i>L. (L.) donovani</i>	<i>L. (L.) donovani</i>
New World species	<i>L. (L.) venezuelensis</i>			
	<i>L. (L.) mexicana</i>	<i>L. (L.) mexicana</i>		
	<i>L. (L.) amazonensis</i>	<i>L. (L.) amazonensis</i>		
	<i>L. (L.) infantum</i> (syn. <i>L. chagasi</i>)			<i>L. (L.) infantum</i> (syn. <i>L. chagasi</i>)
	<i>L. (V.) lainsoni</i>			
	<i>L. (V.) naiffi</i>			
	<i>L. (V.) peruviana</i>			
	<i>L. (V.) shawi</i>			
	<i>L. (V.) braziliensis</i>		<i>L. (V.) braziliensis</i>	
	<i>L. (V.) guyanensis</i>		<i>L. (V.) guyanensis</i>	
<i>L. (V.) panamensis</i>		<i>L. (V.) panamensis</i>		

Pentavalent antimonials, such as sodium stibogluconate (SSG) and meglumine antimoniate, have been the standard first-line treatments for VL for over 60 years. These chemotherapies are administered as daily intravenous or intramuscular injections for a period of at least 20 days and have efficacy around 90% in most parts of the world (reviewed in Singh and Sundar, 2014). However, pentavalent antimonials are highly toxic and have serious side effects associated with their use. Where drug resistance has emerged in endemic regions or where efficacy is low, notably the state of Bihar in India where unresponsiveness is as high as 65%, the second-line drugs, amphotericin B, paromomycin, or miltefosine, are used. Amphotericin B deoxycholate, a polyene antibiotic administered intravenously, complexes with sterols in the *Leishmania* plasma membrane increasing permeability through the formation of pores, which ultimately causes cell lysis (Saha et al., 1986). Amphotericin B is also effective against MCL. Several formulations of amphotericin B, including a liposomal amphotericin B, AmBisome, are now in use, which have similar efficacy to amphotericin B but are significantly less toxic (Sundar et al., 2010). Paromomycin, an aminoglycoside antibiotic administered intramuscularly, has a broad spectrum of activity against Gram-positive and Gram-negative bacteria, and *Leishmania*. Miltefosine, an alkyl phospholipid given orally for over 28 days, interferes with the synthesis of *Leishmania* phospholipids and sterols (Rakotomanga et al., 2007); it is now the first-line treatment for VL in India. However, miltefosine is potentially teratogenic and should not be used by pregnant women or women with child-bearing potential. Oral antifungals agents, such as ketoconazole, itraconazole, and fluconazole, have also shown variable efficacy in the treatment of leishmaniasis with minimal adverse effects. The incidence of VL and HIV co-infections has further complicated treatment, as the cure rate of SSG and miltefosine treatments significantly decreases in HIV patients and relapses are more frequent.

Sitamaquine, an 8-aminoquinoline drug used for the treatment of malaria, is currently in development by GlaxoSmithKline as an oral treatment for VL. Several combination treatments of available anti-leishmanial drugs have also been trialled (Sundar et al., 2011; Musa et al., 2012); these have the potential to increase efficacy, reduce the probability of selection of drug-resistant parasites, and reduce the duration and overall dose of treatment, thereby

reducing the occurrence of adverse effects, and the cost of treatment. As LCL caused by species of the Old World tends to resolve spontaneously, and is not a life-threatening condition, treatment is not typically recommended unless the lesions are disfiguring, painful, or have secondary infections. However, new approaches to treating LCL, DCL, and MCL are being explored; one such approach, as proposed by the Drugs for Neglected Diseases initiative (DNDi), is to combine chemotherapy with a therapeutic vaccine or an adjuvant to modulate the immune response in order to enhance recovery.

As yet, there are no prophylactic drugs or vaccines available for any form of leishmaniasis, as the diversity of the *Leishmania* species and the complexity of the immunological responses to the different species has hindered vaccine development. However, the feasibility for an effective vaccine remains viable, as long-lasting natural immunity to re-infection does occur following recovery from a primary infection. Some vaccine candidates utilise genetically-modified parasites that are avirulent through the deletion of all alleles of specific genes, such as those involved in polyamine or nucleotide metabolism, or proteases that have roles in the lifecycle or host-parasite interactions (reviewed in Chhajer & Ali, 2014). These live-attenuated parasites can deliver the full range of antigens to the antigen-presenting cells (APCs) allowing a robust immune response to be generated. Other second generation vaccine candidates exploit recombinant proteins, or use DNA cloned into mammalian expression vectors to encode leishmanial antigens, which may be species- or stage-specific, or conserved among species. These antigens will then be presented in the major histocompatibility complexes (MHCs) of APCs to prime an adaptive antigen-specific T cell response. Current recombinant protein vaccine candidates include the surface glycoprotein gp63, *Leishmania* activated C kinase (LACK), promastigote surface antigen 2 (PSA-2), and *Leishmania*-derived recombinant polyprotein (*Leish*-111f) (reviewed in Duthie et al., 2012; Kumar & Engwerda, 2014). It is necessary to fully understand the pathogenesis and generation of host-protective immunity during *Leishmania* infection to advance progress in vaccine research.

1.1.2 *Leishmania* parasite: Structure and lifecycle

Trypanosomatid kinetoplastids, such as *Leishmania* and *Trypanosoma*, are unicellular eukaryotic organisms containing membrane-bound organelles, including the nucleus, the Golgi body, and endoplasmic reticulum, as well as a cytoskeletal structure and a flagellum. Kinetoplastids also have a unique feature known as the kinetoplast, a disc-shaped granule containing many copies of circular specialised mitochondrial DNA, which is located within the single mitochondrion of *Leishmania*.

Leishmania parasites have a digenetic lifecycle with two key morphological forms; the flagellated, extracellular promastigote in the digestive tract of the sandfly vector, and the non-motile, obligate intracellular amastigote in the phagocytes of the mammalian host. Procyclic promastigotes, which are only present in the sandfly, are stumpy and only slightly motile, whereas the infective metacyclic promastigotes, which are inoculated into the host, are slender and highly active with an anterior flagellum at least twice the length of the cell body. Intermediate promastigote forms have also been identified in the sandfly, including nectomonads, leptomonads, and haptomonads (Rogers et al., 2002); the intermediate forms are often overlooked due to their subtle morphological differences and unknown functions. Promastigote development in the digestive tract of the sandfly differs between the two *Leishmania* subgenera, *Leishmania*, which develop exclusively in the midgut and foregut, and *Viannia*, which also have a phase of development in the hindgut (Lainson et al., 1977).

1.1.2.1 Development in the sandfly vector

Leishmaniasis is an example of anthroponosis, a vector-borne disease transmitted by the female phlebotomine sandfly from infected animals, with dogs and rodents as the main reservoirs, or from infected humans, to uninfected humans. Recently, a species of biting midge were implicated as the vector in the transmission of an *L. enriettii* complex to red kangaroos in Australia (Dougall et al., 2011). However, the development and transmission of *Leishmania* spp. with other potential vectors requires further evaluation (Seblova et al., 2012). Phlebotomine sandflies, of the family Psychodidae, have an average body length of 2 to 3 mm, which is much smaller in comparison to the adult tsetse fly (5 to

15 mm), the vector for trypanosome transmission, or the *Anopheles* mosquito (6 to 12 mm), the vector for the transmission of *Plasmodium* spp. that cause malaria. Only sandflies of the genus *Phlebotomus*, in the Old World, and *Lutzomyia*, in the New World, are involved in the transmission of *Leishmania*. There are more than 400 species in both these genera combined but less than 50 species actually transmit the parasites. Only the female is described as telmophage, an arthropod that severs the skin and superficial blood vessels of the host to feed on blood, which is required for egg development.

Naive sandflies become infected with *Leishmania* amastigotes during a blood meal from an infected mammalian host. The blood meal is encased in a film-like structure, composed of chitin and proteins, known as the peritrophic membrane, a matrix secreted by the midgut epithelium that separates the blood meal from the midgut tissue. Within 12 to 18 hours, the amastigotes undergo a morphological transformation into procyclic promastigotes, due to changes in environmental conditions, notably the decrease in temperature and increase in pH. The procyclic promastigotes attach to the microvillar surface of the midgut, through the binding of the abundant *Leishmania* surface molecule, lipophosphoglycan (LPG), and replicate as the blood meal continues to be digested (Pimenta et al., 1994). Between 48 to 72 hours, procyclic promastigotes also transform into the intermediate forms, the first of which is the non-dividing nectomonad (Gossage et al., 2003) (Figure 1-2). Procyclic promastigotes and nectomonads cluster in the anterior of the abdominal midgut. After three days, the peritrophic membrane, which protects the parasites from the hydrolytic enzymes of the gut (Pimenta et al., 1997), ruptures due to the activity of *Leishmania* chitinases (Rogers et al., 2008), allowing passage of the parasites to the thoracic midgut and stomodeal valve. At this time, the nectomonads transform into leptomonads (Gossage et al., 2003), which are responsible for the production of promastigote secretory gel (PSG) consisting of a mucin-like glycoprotein unique to *Leishmania* known as filamentous proteophosphoglycan (fPPG) (Rogers et al., 2002). Leptomonads replicate and subsequently differentiate into mammalian-infective metacyclic promastigotes in a process known as metacyclogenesis. PSG blocks the anterior of the thoracic midgut to provide a favourable environment for metacyclogenesis. PSG also plays a role in transmission, as the gel-like properties of fPPG cause a physical obstruction that

prevents the sandfly from taking an adequate blood meal (Stierhof et al., 1999), this forces the sandfly to regurgitate the PSG and the attached metacyclic promastigotes into the host (Rogers et al., 2004). The PSG obstruction also causes sandflies to increase biting persistence and to feed for longer, thereby enhancing parasite transmission (Rogers & Bates, 2007). Another intermediate form, the haptomonads, remain within the sandfly, through attachment of an anterior parasite structure, known as the hemidesmosome, to the cuticular intima of the stomodeal valve (Killick-Kendrick et al., 1974; Walters et al., 1989), whereas the metacyclic promastigotes migrate to the sandfly proboscis, where they are suspended in saliva ready to be transmitted to another potential host.

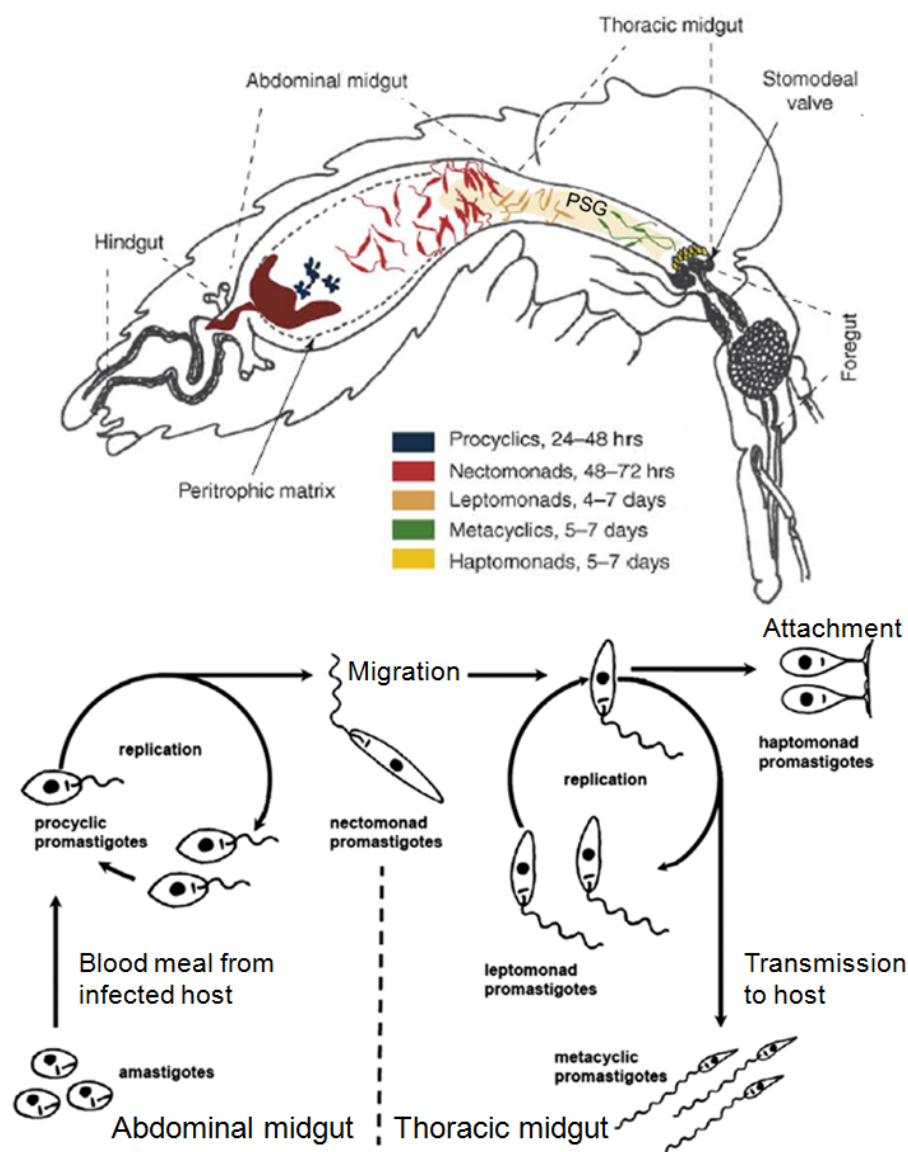


Figure 1-2 The *Leishmania* lifecycle within the sandfly vector. The *Leishmania* parasite undergoes several differentiation steps between the procyclic promastigote in the abdominal midgut and the metacyclic promastigote in the thoracic midgut and stomodeal valve. These intermediate forms include the nectomonad, leptomonad, and haptomonad promastigotes, but it is the metacyclic promastigote that is transmitted to the mammalian host when the sandfly takes a blood meal. Adapted from Kamhawi (2006) and Bates (2007) with permission.

1.1.2.2 Development in the mammalian host

As the *Leishmania*-infected sandfly uses its proboscis to break the skin of the host to gain access to the dermal capillaries during a blood meal, highly active and infective metacyclic promastigotes are regurgitated into the host dermis. The number of *Leishmania* parasites transmitted to the host by a sandfly can vary from 100 to 100 000 per bite (Kimblin et al., 2008), although both Kimblin et al. (2008) and Rogers et al. (2010) report an average inoculation dose of less than 600 parasites per bite, the majority of which are metacyclic promastigotes. *Leishmania* are internalised by host innate immune cells, mainly neutrophils, macrophages, monocytes, and dendritic cells (DCs). Macrophages are the major host cell type for *Leishmania*, providing an environment in which the parasites are able to grow and replicate whilst evading the host immune response. The metacyclic promastigotes then differentiate into the ovoid, non-motile amastigotes within a compartment in macrophages known as the parasitophorous vacuole (PV). After leaving the macrophages, the amastigotes can then infect local cells or disseminate to secondary sites in distant tissues resulting in tissue damage, and giving rise to the spectrum of clinical manifestations associated with the leishmaniasis.

Components of the sandfly saliva can contribute to the successful transmission and establishment of *Leishmania* infection. There are around 50 molecules present in sandfly saliva, which have vasodilatory, anti-coagulative, or immunomodulatory properties, in order to produce a favourable feeding environment. Individual molecules from sandfly saliva have been shown to coordinate the host immune response, such as maxadilan, a vasodilatory peptide (Morris et al., 2001; Rogers & Titus, 2003), and PpSp44 (Oliveira et al., 2008), which have been shown to enhance *L. major* virulence. Pre-exposure to salivary gland extract or uninfected sandflies can protect against *Leishmania* challenge in experimental models (Kamhawi et al., 2000; Carregaro et al., 2013), and immunisation with individual sandfly saliva proteins, such as LJM11 (Xu et al., 2011) and LJM19 (Gomes et al., 2008) from *Lu. longipalpis*, and PpSP15 from *P. papatasi* (Oliveira et al., 2008), can have the same prophylactic effect.

1.2 Mammalian immune response to *Leishmania* spp.

At the site of infection there is a complex interplay between the *Leishmania* parasites and the host immune response. Experimental models have been a powerful tool in dissecting these interactions in order to generate a description of the cellular dynamics at the site of infection, including the activation of effector cells, and to provide an explanation of how this leads to the formation of an adaptive immune and the range of pathologies caused by the different *Leishmania* species. In this section, a general overview of the innate and adaptive immune responses to *Leishmania* spp. through the use of experimental models will be presented, highlighting specific differences discovered between the well-studied *Leishmania* species that cause Old World cutaneous leishmaniasis, *L. major*, New World cutaneous leishmaniasis, *L. mexicana*, and Old World visceral leishmaniasis, *L. donovani*.

1.2.1 Innate immune response

Upon tissue damage to the microvasculature of the epidermis and dermis caused by the proboscis of the sandfly during *Leishmania* inoculation, a strong local inflammatory response is initiated, with the coordinated recruitment of innate immune cells. Despite differences in the local pathogenesis at the site of inoculation during infection with *Leishmania* spp. that cause LCL and VL, the early local inflammatory response during VL is not well characterised.

1.2.1.1 *The complement system*

Extracellular metacyclic promastigotes are first exposed to the non-specific humoral defence factors, including soluble serum proteins of the complement system, such as the opsonins. C3b, cleaved from C3, is one of the most potent opsonins; it binds extracellular microorganisms and the complement receptors, CR1 and CR3, on phagocytic cells, such as neutrophils and macrophages, to promote their phagocytic uptake and lytic clearance. However, *Leishmania* have evolved mechanisms of resisting lysis whilst exploiting opsonic complement factors for receptor-mediated entry into their target host cells. The major surface metalloprotease of *Leishmania*, glycoprotein gp63, enhances C3b cleavage to a proteolytically inactive fragment, iC3b, which is still able to

opsonise the parasites but cannot activate complement-mediated cytotoxic activity, such as the oxidative burst which releases reactive oxygen species (ROS) (Brittingham et al., 1995). LPG of metacyclic promastigotes also acts as a barrier preventing the insertion of the C5b-C9 membrane attack complex (MAC) into the *Leishmania* surface membrane to prevent pore formation (Späth et al., 2003). A major feature of *Leishmania* infection is that the parasites retreat into “safe target cells”, such as neutrophils, macrophages, monocytes, and DCs of the cellular innate response, by exploiting the phagocytic abilities of these cells, thereby providing passive protection against anti-leishmanial products in the extracellular environment.

1.2.1.2 Role of skin-resident cells

The skin acts as a barrier against infection, and cells in the skin are involved in surveillance and serve as an important source of immunomodulatory mediators once this barrier is penetrated. The epidermis is principally composed of keratinocytes, whilst the underlying dermis is formed of fibroblasts and is vascularised with blood and lymphatic vessels. Keratinocytes have been reported to contribute to the generation of protective T helper 1 (Th1) responses in *L. major* infection through the upregulation of cytokine expression (Ehrchen et al., 2010). Langerhans cells (LCs), a DC subset, are present in the skin and draining lymph nodes (dLNs); LCs have been reported to have an immunosuppressive function during *L. major* infection by driving the expansion of T regulatory (Treg) cells (Kautz-Neu et al., 2011). In addition to keratinocytes and LCs, mast cells, which are granulocytes that surround the blood vessels in the dermis, also have an indirect role in *Leishmania* infection through degranulation. Degranulation involves the release of granules consisting of heparin, histamine, serotonin, cytokines, and serine peptidases (SPs), which can influence innate cell recruitment (Maurer et al., 2006; Romão et al., 2009).

1.2.1.3 Leishmania-neutrophil interactions

Neutrophils, which are polymorphonuclear granulocytes, are one of the earliest innate immune cell types that are recruited to the site of infection, occurring a few hours after parasite inoculation (Peters et al., 2008). Neutrophils continuously circulate through dermal blood vessels and extravasate upon inflammation (Figure 1-3). Neutrophil chemotaxis is induced by the presence of

sandfly- and *Leishmania*-derived factors (Peters et al., 2008; van Zandbergen et al., 2002), complement C3 (Jacobs et al., 2005), and the production and secretion of chemokines by epithelial cells, keratinocytes, fibroblasts, and neutrophils, including CXCL1 (KC) and CXCL2 (MIP-2), which are homologues of human IL-8 (Müller et al., 2001). Neutrophils phagocytose metacyclic promastigotes to serve as temporary intermediate hosts for *Leishmania* (Laufs et al., 2002). Over the first day of infection, the majority of promastigotes, around 80 to 90%, are phagocytosed by neutrophils, whereas only 10 to 20% are directly phagocytosed by monocytes or macrophages as evidenced by flow cytometry and intravital two-photon microscopy (2P-IVM) (Peters et al., 2008; Thalhofer et al., 2011; Ribeiro-Gomes et al., 2012). *Leishmania* are able to reside and survive within the intracellular environment of the neutrophil (Mollinedo et al., 2010); in addition, *Leishmania* are able to evade the adaptive immune response, as other immune cells are unable to detect the parasites whilst inside the neutrophils. During this ‘silent’ phase of *Leishmania* growth, neutrophils are persistently recruited to, and maintained at, the infection site through the presence of chemokines.

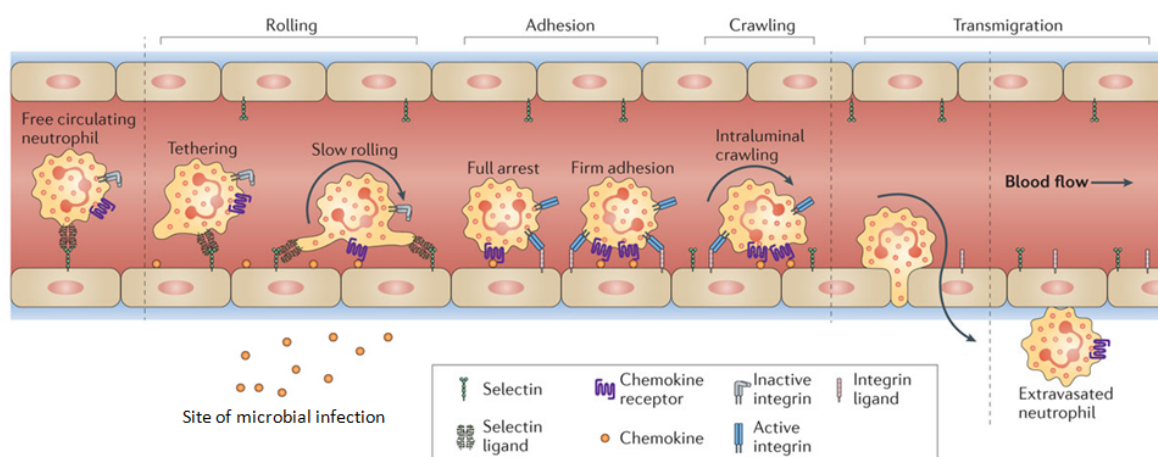


Figure 1-3 Neutrophil migration from the blood vessels to the site of infection. Neutrophils move along the endothelium, transiently adhering to selectins displayed on the endothelial surface, in a process called rolling. Upon microbial infection, chemokines are released from multiple sources at the site of infection. The chemokines become bound to proteoglycans on the endothelium, which causes an increase in the avidity of integrins of the chemoattracted neutrophils. The neutrophils then firmly adhere to the endothelium through the binding of integrin ligands, and are then able to transmigrate through the endothelium to the site of infection. Other immune cells, such as monocytes, can be recruited by this process, dependent upon the chemokines present on the endothelial surface. Adapted from Kolaczowska and Kubec (2013) with permission.

Neutrophils generate ROS, such as superoxide, O_2^- , hydrogen peroxide, H_2O_2 , and hypochlorous acid, HOCl, through the NADPH oxidase system upon activation; these microbicidal metabolites oxidise molecules, such as amino acids and

nucleotides. Neutrophils also contain azurophilic granules that contain myeloperoxidase (MPO), and proteolytic enzymes, such as collagenase, gelatinase, and SPs. Human neutrophil azurophilic granules also have defensins, which render target cell surface membranes more permeable. Neutrophils have recently been shown to release neutrophil extracellular traps (NETs), which are filamentous structures composed of chromatin with bound granular and cytoplasmic proteins, including histones, antimicrobial peptides, and proteolytic enzymes (Brinkmann et al., 2004). NETs are able to capture and kill microorganisms; however, although *L. major*, *L. amazonensis*, *L. donovani*, and *L. infantum* have been shown to induce NET formation, they evade the antimicrobial activities of the NETs due to their nuclease activity (Gabriel et al., 2010; Guimarães-Costa et al., 2009, 2014).

By three days, the numbers of neutrophils at the site of infection are highly reduced, as it is at this time, that inflammatory monocytes and macrophages become the predominant innate immune cells present (Thalhofer et al., 2011; Ribeiro-Gomes et al., 2012). Furthermore, through staining of the apoptotic cell marker, annexin V, it was observed that the apoptosis of neutrophils infected with live *L. major* is delayed from the average 6 to 12 hour life span to up to two days, through the reduction of caspase 3 activity, which coincides with the arrival of monocytes and macrophages to the site of infection (Aga et al., 2002).

1.2.1.4 Leishmania-macrophage interactions

Neutrophils may be the first host cell type, but macrophages are considered the main host cell type for the productive *Leishmania* infection. Upon infection with *Leishmania*, neutrophils secrete significantly higher levels of the chemokines CCL3 (MIP-1 α) and CCL4 (MIP-1 β) (van Zandbergen et al., 2004), which cause monocytes and macrophages to migrate to the site of infection, arriving at two or three days post-infection. Monocytes differentiate into either macrophages or DCs at the site of infection based on the presence of local growth factors and cytokines. There has been much debate as to how *Leishmania* infect macrophages; whether the parasites are released from the neutrophils and taken up directly by macrophages; or that macrophage clearance of apoptotic neutrophils harbouring parasites leads to the indirect uptake of *Leishmania* in a process termed the 'Trojan horse' (van Zandbergen et al., 2004); or that

parasites escape from the apoptotic neutrophils and are taken up directly by macrophages together with the apoptotic cells in a process termed the 'Trojan rabbit' (Peters et al., 2008; Ritter et al., 2009). van Zandbergen et al. (2004) used confocal microscopy with fluorescently-labelled parasites, neutrophils, and macrophages, to observe *in vitro* macrophages readily phagocytosing *Leishmania*-infected apoptotic neutrophils and the subsequent survival and replication of these parasites within the macrophages. Whereas, Peters et al. (2008) used 2P-IVM to observe, *in vivo*, viable parasites being released from apoptotic neutrophils surrounded by macrophages.

Leishmania reside within a PV inside the macrophage, which is formed by the fusion of the phagosome with late endosomes or lysosomes, containing acid hydrolases, in a process known as phagolysosomal biogenesis (Courret et al., 2002; Ndjamen et al., 2010). *Leishmania* facilitate the formation of a more suitable environment for their intracellular survival through the remodelling of the phagosomal compartments and the interruption of phagosome-lysosome fusion allowing sufficient time for the promastigotes to differentiate into the hydrolase-resistant amastigotes (reviewed in Moradin & Descoteaux, 2012).

The 'silent entry' of *Leishmania* parasites into macrophages is enhanced by the modulation of the macrophage intracellular signalling pathways by *Leishmania* to render them unresponsive to activating stimuli, or to downregulate or inhibit the antimicrobial effector functions. Macrophages produce toxic metabolites, such as ROS and nitric oxide (NO), which function as potent effectors against both extra- and intracellular *Leishmania*. IFN- γ , secreted by NK and Th1 cells predominantly, stimulates the expression of the inducible isoform of nitric oxide synthase (iNOS, also known as NOS2) of macrophages, which catalyses the conversion of L-arginine to L-citrulline and NO. *Leishmania* can induce the expression of immunomodulatory molecules to inhibit macrophage activation and suppress iNOS-mediated generation of NO (Cortez et al., 2011). The requirements for ROS and NO in the control of *Leishmania* spp. in experimental models may be species-dependent, as *L. major* and *L. donovani* can be sufficiently cleared by NO, whereas the clearance of *L. amazonensis* also requires ROS (Murray & Nathan, 1999; Mukbel et al., 2007).

Surviving the intracellular environment of macrophages, amastigotes replicate to further infect host cells in local or distant tissues, producing the spectrum of clinical manifestations of the leishmaniasis. Again, the mechanism by which this occurs is unclear; whether the infected macrophages burst, the PVs are released from the macrophages by exocytosis, or other uninfected macrophages engulf the infected macrophages (reviewed in Rittig & Bogdan, 2000).

1.2.1.5 *Leishmania-dendritic cell interactions*

The inflammatory monocytes recruited to the site of infection differentiate into either macrophages or DCs. Monocyte-derived DCs (moDCs) play an important role in the induction of protective antigen-specific Th1 responses during *Leishmania* infection (León et al., 2007; De Trez et al., 2009; Petritus et al., 2012). DCs migrate from the site of infection to the dLNs, and process antigen and present it to T cells of the adaptive immune response (Misslitz et al., 2004; Ritter et al., 2004; Ng et al., 2008). DCs are the major cell type harbouring *Leishmania* in the dLN and are also major producers of IL-12 during *L. major* infection (León et al., 2007). IL-12 stimulates T cells to form Th1 cells. However, the ability of *Leishmania* to induce IL-12 production from DCs may be species-dependent, as *L. mexicana* and *L. donovani* have been reported to suppress IL-12 production from DCs (Bennett et al., 2001; McDowell et al., 2002; Favila et al., 2014). In addition, moDCs have been shown to be major producers of iNOS during *L. major* infection, which can lead to parasite killing (De Trez et al., 2009; Petritus et al., 2012); whereas, it has been reported that in *L. mexicana* infection, moDCs produce less iNOS and migrate less efficiently to the dLN (Petritus et al., 2012).

L. major-activated DCs can also promote lymph node hypertrophy, which enables the recruitment of more naive T cells from the blood into the lymph node to be primed, enhancing the antigen-specific protective responses (Carvalho et al., 2012); *L. mexicana* infection, however, has been associated with minimal expansion of the dLN (Hsu & Scott, 2007).

1.2.2 Adaptive immune response

Antigen presentation via the MHC of DCs to the T cell receptor (TCR) of T cells, along with the cytokine response at the early stage of infection is fundamental in *Leishmania* disease progression; this essentially determines the type of adaptive immune response that will develop, with particular respect to the T helper cell subset that is induced. *Leishmania* antigens are presented through the MHC class I and II pathways leading, respectively, to the stimulation of *Leishmania*-specific CD8⁺ cytotoxic T cell responses, which have been reported to promote pathology (Novais et al., 2013), and CD4⁺ Th cell responses, which are important for resistance against *Leishmania*. MHC I molecules present peptide derived from cytosolic proteins, whereas MHC II molecules derives peptide from exogenous sources, such as endocytosed microorganisms that are degraded in phagolysosomes. *Leishmania* reside within phagolysosomal compartments; therefore, it is usually MHC II that is loaded with leishmanial peptide and thus, interaction and activation of naive CD4⁺ T cells occurs (Muraille et al., 2010).

There are two well-defined CD4⁺ T helper cell subsets, known as Th1 and Th2. In general, IL-12 from macrophages and DCs activates the STAT4 pathway of activated T cells to form Th1 cells, whereas other cellular sources, such as mast cells, basophils, and eosinophils, release IL-4, which activates the STAT6 pathway of activated T cells to form Th2 cells. IFN- γ secreted by Th1 cells increases the production of IL-12 from macrophages and DCs, creating a positive feedback loop driving the expansion of the Th1 cell subset, as evidenced during *L. major* infection (Park et al., 2000). IL-4 secreted by Th2 cells acts in an autocrine manner, causing cell activation and expansion of the Th2 subset, whilst inhibiting the differentiation of naive CD4⁺ T cells into Th1 cells, downregulating the expression of the IL-12 receptor on Th1 cells to render them unresponsive to IL-12 (Gollob et al., 1997), and limiting the recruitment of Th1 cells to the site of infection (Lazarski et al., 2013). Th2 cells also secrete IL-10, which inhibits the synthesis of IFN- γ and IL-2, which is responsible for the growth, proliferation, and differentiation of the effector T cells.

In *Leishmania* infection, Th1 cells generally promote cellular immunity by stimulating macrophage phagocytic and effector functions, such as the iNOS-

mediated generation of NO, to eliminate the parasites (Figure 1-4). Th2 cells, conversely, promote humoral immunity by helping B cells produce parasite-specific antibodies, which are usually insufficient to clear the parasites and control *Leishmania* infection (Figure 1-4). However, the adaptive immune responses are more complex than the proposed Th1/Th2 dichotomy, in that other CD4⁺ Th cell populations (Figure 1-4), and the plasticity of the T helper cell subset functions, have been reported (reviewed in O'Shea & Paul, 2010), as well as the pleiotropic activities of IL-4 and IL-13, such as in facilitating Th1 responses (reviewed in Alexander & Brombacher, 2012; Hurdal & Brombacher, 2014). In addition, *Leishmania* can subvert the development of the Th1 responses, through the selective inhibition of IL-12 and IL-1 production, a pro-inflammatory mediator, and encourage the induction and expansion of the counter-protective Th2 cells (reviewed in Bhardwaj et al., 2010; Shio et al., 2012), and the Treg cells (Figure 1-4) (reviewed in Belkaid et al., 2002), which regulate the effector T cell subsets. The outcome of disease can be influenced by the balance between the Th1 and Th2 responses, which is dependent upon the species of *Leishmania* and host genetic factors; however, *L. donovani* infections in experimental models are associated with the presence of both Th1 and Th2 cytokines (Miralles et al., 1994), and organ-specific immune responses may, in fact, provide more insight into the disease pathology in VL (Bunn et al., 2014).

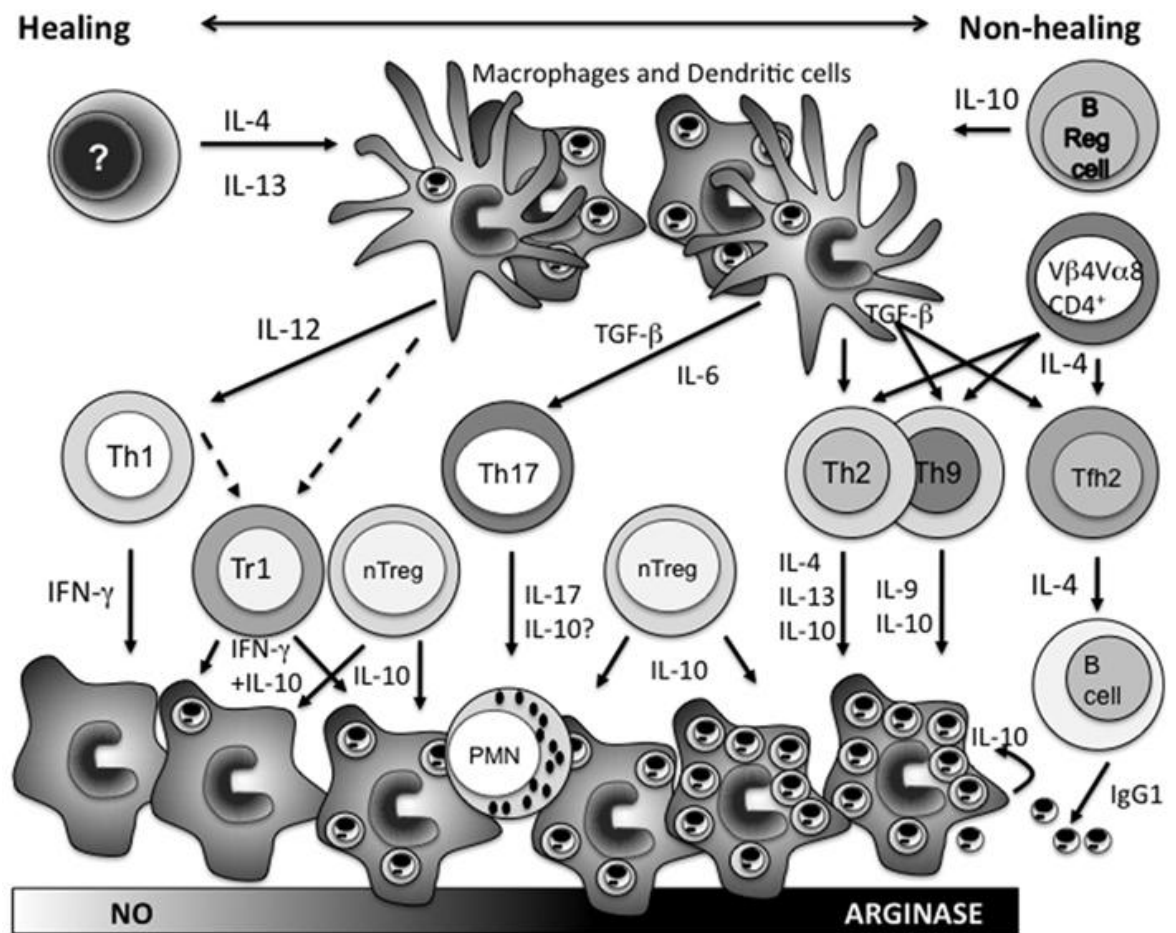


Figure 1-4 Mechanisms mediating healing versus non-healing in leishmaniasis. In general, parasite clearance is achieved through classical macrophage activation and nitric oxide (NO) production. Early IL-4 and IL-13 instruct macrophages and dendritic cells to produce IL-12, which drives the expansion of protective antigen-specific T helper 1 (Th1) cells that produce IFN- γ . IFN- γ stimulates the expression of inducible nitric oxide synthase (iNOS), which catalyses the production of NO. Persistent or non-healing infections, however, are associated with the presence of IL-10-producing T regulatory cells, such as type 1 regulatory (Tr1) cells and natural T regulatory (nTreg) cells, as well as the TGF- β /IL-4-driven Th2 and Th9 cells. IL-4, IL-9, IL-10, and IL-13 from Th2 and Th9 cells induce alternative macrophage activation and increase arginase expression enabling parasite survival and expansion. In addition, Th17 cells secrete IL-17, which stimulates neutrophil influx into lesions that is often associated with increased pathology. T follicular helper 2 (Tfh2) cells induce IgG1 production, the uptake of IgG1-opsonised parasites via macrophage Fc γ R stimulates IL-10 release from the host cell, which together with the influence of cytokines from the other non-Th1 CD4⁺ T cell populations promotes progressive disease. Reproduced from Alexander & Brombacher (2012) under the terms of the Creative Commons Attributions Non-Commercial License.

1.2.3 Second wave of innate cell infiltration

Through the use of flow cytometry, a second wave of innate cell infiltration, consisting of neutrophils, macrophages, monocytes, and DCs, beginning at 1 or 2 weeks post-infection has recently been described in experimental mouse models (Thalhofer et al., 2011; Ribeiro-Gomes et al., 2012). The role of these cells during this second wave of infiltration has not yet been characterised, in terms of their effects on the immune response at this later phase of infection, as by

this time, intracellular infections have fully transitioned into macrophages and DCs.

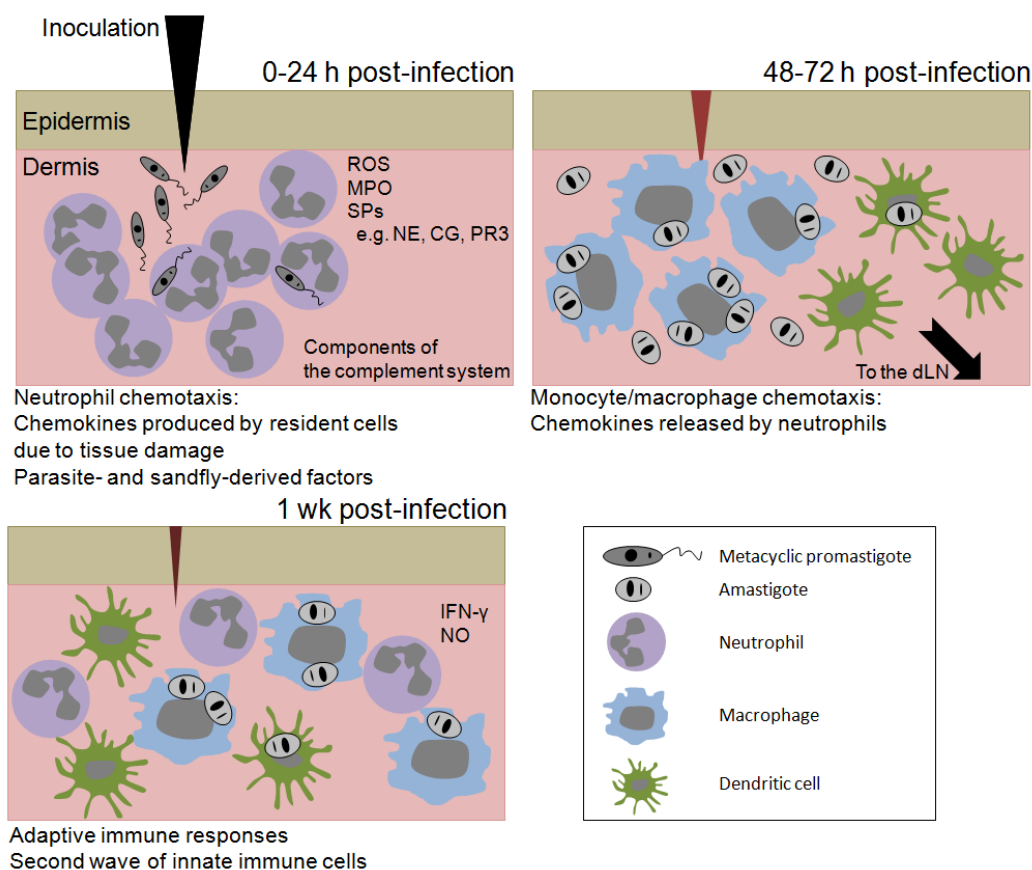


Figure 1-5 The early immune responses to infection with *Leishmania* spp. During the first 24 h post-infection, neutrophils are the principal innate immune cell at the site of inoculation and are the first host cell for *Leishmania*. In the defence against pathogens, neutrophils generate reactive oxygen species (ROS), and have granules consisting of myeloperoxidase (MPO) and serine peptidases (SPs), such as neutrophil elastase (NE), cathepsin G (CG), and proteinase 3 (PR3). By 3 d post-infection, macrophages have arrived at the site of inoculation to become the main host cell for intracellular *Leishmania*. Inflammatory monocytes also arrive which can differentiate into macrophages and dendritic cells. Dendritic cells process and present *Leishmania* antigen, and migrate to the draining lymph node (dLN) to induce a T cell response. By 1 wk post-infection, an antigen-specific T helper cell response has been mounted and innate cell effector functions, such as the inducible nitric oxide synthase (iNOS)-mediated generation of nitric oxide (NO), are activated through the action of IFN- γ secreted by Th1 cells. Also at this time-point, a second wave of innate cells to the site of infection occurs.

1.2.4 The role of cytokines during *Leishmania* infection

Cytokines, such as interferons, interleukins, and chemokines, have roles in cell signalling, such as in the activation of cell effector functions, and in the migration of cell populations. *Leishmania* are able to modulate the host cytokine responses to favour their survival. Table 1-2 summarises some of the common cytokines and growth factors that have important functions during *Leishmania* infections.

Table 1-2 Important cytokines and growth factors that mediate the immune response during *Leishmania* infection. The general functions of the cytokines and growth factors in immunity are given.

Name	Functions	Source
Interleukins		
IL-1	Pro-inflammatory Induces cytokine production	Monocytes/Macrophages Endothelial cells Epithelial cells
IL-2	T, B, and NK cell proliferation and activation	Th1 cells NK cells
IL-4	Induces Th2 cell differentiation	Th2 cells
IL-8	Neutrophil chemoattractant	Neutrophils Endothelial cells Fibroblasts
IL-10	Inhibits macrophages and DCs	Macrophages Th2 cells Treg cells
IL-12	Induces Th1 cell differentiation Stimulates IFN- γ production from cells	Macrophages DCs
IL-13	Inhibits macrophage activation Inhibits cytokine production	Th2 cells
IL-17	Neutrophil chemoattractant	Th17 cells
Interferons (IFNs)		
IFN- α and IFN- β (type I interferons)	Increases MHC I expression Activates NK cells Induces NO and IFN- γ expression	Macrophages
IFN- γ (type II interferon)	Activates macrophages Induces iNOS expression Increases MHC I and II expression	Th1 cells NK cells
Tumour necrosis factors (TNFs)		
TNF- α	Pro-inflammatory Induces cytokine production	Macrophages T cells NK cells
Transforming growth factors (TGFs)		
TGF- β	Inhibits macrophage activation Inhibits proliferation and activation of T cells	Monocytes/Macrophages Treg cells

1.2.5 Experimental cutaneous leishmaniasis: The mouse models

Various strains of mice differ in their susceptibility to cutaneous leishmaniasis; for example, C57BL/6 mice resolve lesions and recover after *L. major* challenge,

whereas BALB/c mice develop severe lesions. Cytokine profiles of these murine models during *L. major* infection reveal that the resistant C57BL/6 mice have high levels of IFN- γ and IL-2, but low levels of IL-4 and IL-10, which is characteristic of a Th1 cell-mediated response, whilst the converse is true for the susceptible BALB/c mice, indicating a polarisation towards a Th2 humoral response involving IL-4, IL-5, IL-10, and IL-13 (Locksley et al., 1991).

IL-12 is essential for parasite elimination as it drives the expansion of a Th1 response. Susceptible BALB/c mice produce less and respond poorly to IL-12 due to a downregulation of the IL-12 receptor β chain (Güler et al., 1996). Resistant C57BL/6 mice treated with monoclonal anti-IL-12 antibodies develop a Th2 response and are unable to contain the infection (Heinzel et al., 1995), whereas susceptible BALB/c mice treated with recombinant IL-12 or monoclonal anti-IL-4 antibodies develop a Th1 response and eliminate the infection (Heinzel et al., 1993; Chatelain et al., 1999).

Human cutaneous leishmaniasis caused by *L. major* has been extrapolated from the analysis of infections in these murine models; however, the human Th response is not fully understood and often widely variable Th cytokine profiles are reported due to few studies actually conducted, host genetic factors and immunological status, and the stage of disease (Louzir et al., 1998; Ajdary et al., 2000). Mouse models, therefore, provide a reproducible system to study the immune responses during *L. major* infection, particularly with regards to host-parasite interactions, which is not possible to investigate with clinical samples.

1.3 *Leishmania* virulence factors and mechanisms of immune evasion and modulation

Virulence factors are molecules expressed by the parasite to enable them to colonise and replicate within the host, and/or avoid or inhibit the host immune responses. Virulence factors contribute to the degree of pathogenicity caused by the parasite by facilitating the initiation, propagation, and persistence of *Leishmania* infection. *Leishmania* possess multiple infection-related molecules that are crucial for the parasites to establish successful intracellular infection; these invasive or evasive determinants are mostly cell surface-bound or

secreted/released molecules, such as gp63, LPG, proteophosphoglycans (PPGs), glycosylphospholipid (GIPL), and cysteine peptidases (CPs).

As mentioned earlier, *Leishmania* are able to avoid complement-mediated lysis, retreat into 'safe' target cells, such as the neutrophils, macrophages, and DCs, and resist the acidic environment of the PV, through the actions of LPG and gp63, in order to facilitate their survival in the host and initiate infection (reviewed in Franco et al., 2012). LPG has a lipid backbone coated with a polymer of repeating disaccharide-phosphate units with variable side-chain modifications attached to a glycan core that is inserted into the membrane via a glycosylphosphatidylinositol (GPI) anchor, and is capped by a neutral oligosaccharide. The most abundant surface protein, gp63, is a GPI-anchored zinc metalloprotease. To generate a persistent infection, *Leishmania* can alter host signalling pathways in macrophages and DCs to render the macrophages unresponsive to activating stimuli, through the Toll-like receptors (TLRs) for example, or to suppress the antimicrobial effector functions, such as the oxidative burst and iNOS-mediated generation of NO (reviewed in Shio et al., 2012). *Leishmania* modulate the expression of cytokines and chemokines to alter immune cell activation, IL-12 in particular (Piedrafita et al., 1999), and the migration of cell populations to the site of infection. LPG and other proteoglycans have been implicated in the inhibition of IL-2, IL-12, and IFN- γ production, whilst stimulating the production of IL-4 and IL-10 (Liu et al., 2009). Attenuation of T cell-mediated responses by interfering with the loading of *Leishmania* antigens onto MHC II, downregulating the macrophage and DC co-stimulatory cell surface molecules required to stimulate a T cell response, polarisation towards a Th2 phenotype, and induction of Treg cell activity, which suppress Th cell responses, are also common mechanisms of *Leishmania* immune evasion and exploitation (reviewed in Bhardwaj et al., 2010; Shio et al., 2012).

Leishmania cysteine peptidases, designated CPA, CPB, and CPC, have already been proven to be important *Leishmania* virulence factors (Mottram et al., 2004). When *L. mexicana*, which are particularly rich in CPs, are genetically-modified to be deficient in the multicopy *CPB* gene array, their ability to infect macrophages and lesion development in BALB/c mice is much reduced compared to infection with *L. mexicana* wild-type (WT) (Mottram et al., 1996), due to an

inability to induce IL-4 production (Pollock et al., 2003). CPB has been shown to inhibit IL-12 production in C3H and C57BL/6 mice, and induce IL-4 production in BALB/c mice, both of which prevent the host from mounting a protective Th1 response, and may enhance a counter-protective Th2 cell response (Alexander et al., 1998; Buxbaum et al., 2003; Pollock et al., 2003; Cameron et al., 2004).

Leishmania exosomes have been implicated in the priming of host target cells for *Leishmania* invasion and have been shown to have immunosuppressive effects on monocytes and moDCs (Silverman et al., 2010b; Hassani et al., 2011). However, the functions of the individual proteins of the exoproteome on immune modulation have yet to be elucidated. Despite much being known about the immune responses to *Leishmania* spp., few putative *Leishmania* virulence factors, other than LPG, gp63, and CPs, have been characterised in their interactions with host immune cells and the modulation of host immune responses, particularly using *in vivo* infection models.

1.4 Inhibitors of serine peptidases (ISPs)

1.4.1 Discovery of *Leishmania* ISPs

The haploid genome of *L. major* Friedlin has been completely sequenced showing 32.8 Mb distributed on 36 chromosomes with over 8000 predicted protein-coding genes, 36% of which have a putative function (Ivens et al., 2005). BLAST analysis of these protein-coding genes has led to the discovery of putative *Leishmania* virulence factors, such as the inhibitors of serine peptidases (ISPs) (Eschenlauer et al., 2009).

One of the major mechanisms used to control the activity of peptidases in mammals is through tight interaction with natural peptidase inhibitors, such as serpins and cystatins. Orthologues of mammalian peptidase inhibitors have not been identified in the *Leishmania* genome; orthologues of peptidase inhibitors from other pathogens, such as bacteria, however, have been detected, including ISPs and inhibitors of cysteine peptidases (ICPs) (Sanderson et al., 2003), which suggests that these inhibitors may be virulence factors that act upon host peptidases during *Leishmania* infection. Non-healing, progressive lesions were observed in BALB/c mice infected with *L. mexicana* WT parasites, ICP-deficient

mutants, and ICP re-expressing mutants, whilst BALB/c mice infected with mutants over-expressing ICP have severely reduced virulence and were able to significantly control lesion growth, due to reduced IL-4 and enhanced IFN- γ production (Besteiro et al., 2004; Bryson et al., 2009).

Peptidases of immune cells, particularly serine peptidases (SPs), have roles in fighting pathogenic infections, as they can have direct microbicidal activity against bacteria through the degradation of bacterial membranes (Belaouaj et al., 2000). SPs also have important functions in the modulation of host immune responses through the proteolytic modification of cytokines and chemokines, which can regulate immune cell activation and recruitment, and the activation or inactivation of specific cell receptors (discussed in Chapter 5). Very few studies have explored the roles of such peptidases during infection with *Leishmania*; Ribeiro-Gomes et al. (2004) have shown that the host SP, neutrophil elastase (NE), released from dying neutrophils, induces the microbicidal activity of macrophages infected with *L. major*.

Three ISPs have been identified in the *L. major* genome, designated ISP1, ISP2, and ISP3; these have also been identified in *L. mexicana*, *L. infantum*, and *L. braziliensis*. ISP1 and ISP2 are present in *T. brucei* but only ISP2 has been identified in *T. cruzi*. *Leishmania* ISPs are orthologues of the *Escherichia coli* protein, ecotin. Trypanosomatids are the only known eukaryotes to possess these ecotin-like natural peptide inhibitors, which suggests there may have been a horizontal gene transfer event between the bacteria and *Leishmania*, possibly during a co-infection in a mutual host (Opperdoes & Michels, 2007).

Ecotin is a homodimeric protein found in the periplasmic space between the inner and outer membranes of bacteria. Ecotin inhibits a wide range of SPs from the S1A trypsin-fold peptidase family of clan PA(S), which include trypsin, chymotrypsin, NE, cathepsin G (CG), and coagulation factors Xa and XIIIa (Chung et al., 1983; Eggers et al., 2004). The broad range of peptidases inhibited by ecotin can be explained by the fact that ecotin forms a head-to-tail dimer that interacts with two enzyme molecules via multiple binding sites (Yang et al., 1998). No *E. coli* peptidase has been identified that is sensitive to ecotin and there are no reports that ecotin inhibits SPs of other families or catalytic classes (Chung et al., 1983). Therefore, ecotin is hypothesised to protect the cell

against exogenous S1A peptidases, such as digestive or pancreatic peptidases, or SPs produced by the host immune cells during infection. It has been shown that *E. coli* expressing an inactive form of ecotin were more sensitive to NE than WT cells (Eggers et al., 2004). Ecotin has well-conserved orthologues in several pathogenic genera, including *Burkholderia*, *Pseudomonas*, *Salmonella*, *Serratia*, and *Yersinia* (Eggers et al., 2004; Clark et al., 2011; Ireland et al., 2014), although few studies have investigated the role of ecotin in virulence. Ecotin of *Burkholderia pseudomallei*, the causative agent of melioidosis, has been shown to be important for disease persistence in murine macrophages and the *in vivo* mouse model (Ireland et al., 2014). The genome of *L. major* reveals the presence of at least 153 identifiable peptidases, representing approximately 2% of the genome, which can be classified into the major catalytic types, aspartic, cysteine, metallo-, threonine, and serine peptidases (Ivens et al., 2005). *L. major* has 13 SPs belonging to six families but lacks genes encoding trypsin-fold SPs from the S1A family (Ivens et al., 2005); therefore, it is hypothesised that, like bacterial ecotin, *Leishmania* ISPs act against host-derived SPs (Eschenlauer et al., 2009).

L. major ISP1 (LmjF 15.0300), ISP2 (LmjF 15.0510), and ISP3 (LmjF 15.0520) are found in a cluster on chromosome 15. ISP3 (41.8 kDa) is not detected in any of the *Leishmania* lifecycle stages and has been suggested to be a pseudogene (Eschenlauer et al., 2009). ISP1 is a 16.5 kDa protein that can only be detected in procyclic and metacyclic promastigotes, whereas ISP2, a 17.5 kDa protein, is expressed in all three lifecycle stages with the levels of expression being greater in the infective metacyclic promastigotes and amastigotes (Eschenlauer et al., 2009). ISP1 and ISP2 share only 36% sequence identity with each other, and recombinant ISP2 (rISP2) has been shown to have high peptidase inhibitory activity against human NE, trypsin, and chymotrypsin, whereas rISP1 has peptidase inhibitory activity at least 10-fold lower than that of rISP2 (Eschenlauer et al., 2009; Morrison et al., 2012). This indicates that ISP2 may play a role in the inhibition of host SPs during mammalian infection.

1.4.2 Role of ISP1 in flagellar pocket dynamics

ISP1, which has low peptidase inhibitory activity, has been implicated in *Leishmania* flagellar homeostasis (Morrison et al., 2012). *L. major* ISP triple

knock-out mutant ($\Delta isp1/2/3$) populations have enlarged flagellar pockets with an accumulation of granular vesicles and membranous whorls, longer flagella, and are less motile than WT populations, but $\Delta isp1/2/3:ISP1$ populations have a phenotype similar to that of WT parasites (Morrison et al., 2012). Based on these results, it was proposed that ISP1 has an intracellular function involved in the regulation of intraflagellar transport (IFT), disruption of which affects flagellar pocket flux, including flagella biosynthesis and flagellar pocket distention, culminating in stress response-induced differentiation (Morrison et al., 2012).

1.4.3 Role of ISP2 as a potential virulence factor

The main way to investigate the role of putative virulence factors in disease progression and host-parasite interactions is to generate *Leishmania* mutants deficient in the putative virulence factor and compare the disease profiles with that of the WT parasites. Using *L. major* deficient in *ISP2* and *ISP3* ($\Delta isp2/3$), Eschenlauer et al. (2009) and Faria et al. (2011) showed that the *L. major* $\Delta isp2/3$ promastigotes were internalised more efficiently by macrophages of susceptible BALB/c and resistant C57BL/6 mice than *L. major* WT promastigotes respectively (Figure 1-6). A partial elimination of intracellular $\Delta isp2/3$ parasites, or reduced parasite burdens, at 24 h or 72 h post-infection was observed in macrophages from BALB/c and C57BL/6 mice respectively; this suggests that ISPs are important for the initiation and persistence of infection in the host and that early control of SPs can influence the outcome of infection (Faria et al., 2011). The presence of rISP2 or a peptidyl synthetic irreversible inhibitor to NE (NEI) with macrophages prior to *Leishmania* infection reduced the internalisation and elimination of $\Delta isp2/3$ parasites to WT levels, which elucidated NE as the primary target of ISP2 and revealed that NE activity present during early *Leishmania*-macrophage contact results in subsequent parasite death (Eschenlauer et al., 2009; Faria et al., 2011).

Internalisation of $\Delta isp2/3$ parasites returned to WT levels when macrophages were pre-treated with antibodies that block CD11b (Eschenlauer et al., 2009; Faria et al., 2011). CD11b of macrophages is implicated in various adhesive interactions and also mediates the uptake of complement-coated microorganisms, such as iC3b-coated *Leishmania* parasites. CD11b is a component of CR3, which is the receptor for the iC3b fragment; this suggests

that the increased uptake of *Δisp2/3* promastigotes is mediated by engagement of CR3 in macrophages of BALB/c and C57BL/6 mice. Internalisation and elimination of *Δisp2/3* parasites in macrophages returned to WT levels at 24 h post-infection, when macrophages were pre-treated with monoclonal antibodies that block TLR4 (Faria et al., 2011). This indicates that TLR4 is responsible for the enhanced uptake and elimination of *Δisp2/3* parasites in macrophages. In addition, neutralisation of both CD11b and TLR4 had similar effects to the neutralisation of either CD11b or TLR4 alone; it is plausible that they act in a common pathway. The decreased phagocytosis of *Δisp2/3* parasites when macrophages were pre-incubated with NEI, was no longer observed upon activation of TLR4, and *Δisp2/3* parasites were poorly infective to TLR4-defective macrophages from C3HeJ mice; these results indicate that NE activity promotes parasite internalisation through TLR4 (Faria et al., 2011).

ISP2 may also prevent the generation of ROS by preventing the activation of this TLR4-mediated response. When infected cultures were treated with EUK134, a superoxide scavenger, immediately after parasite internalisation, the numbers of *Δisp2/3* parasites at 24 h post-infection were similar to those at 3 h; this indicates that superoxide strongly contributes to the killing of intracellular *Δisp2/3* parasites (Faria et al., 2011).

Faria et al. (2014) have further elucidated the downstream responses of the TLR4-NE activation during *Δisp2/3* infection in macrophages, attributing parasite killing to a dependency of functional protein kinase R (PKR), which may be phosphorylated by the associated TLR4 adaptor proteins MyD88 or TRIF, leading to the induction of TNF- α and IFN- β production. This investigation also revealed that TLR2 and TLR4 may act conjointly in the enhanced internalisation of *Δisp2/3* promastigotes in macrophages (Faria et al., 2014). TLR4 signalling is commonly divided into the MyD88-dependent pathway, which ultimately leads to NF- κ B and AP-1 activation, and TRIF-dependent pathways, which can lead to the activation of interferon regulatory factor (IRF3), as well as NF- κ B and AP-1 (Ulrichs & Tavernier, 2008). The nuclear levels of the NF- κ B subunit p65 and IRF3 were reduced in *Δisp2/3* infection compared with that of WT infection (Faria et al., 2014).

In summary, Faria et al. (2011) proposed that *L. major* ISP2 inhibits the activity of NE preventing the activation of a TLR4-NE signalling cascade during early *Leishmania*-macrophage contact. Through the inhibition of NE activity, there is a downregulation of parasite phagocytosis, which is also mediated by engagement of CR3, and an inhibition of ROS production, exerting a beneficial effect for intracellular amastigote survival and growth in the macrophages. ISP2 is, therefore, proposed as an important virulence factor used by *L. major* to establish a productive infection in the mammalian host.

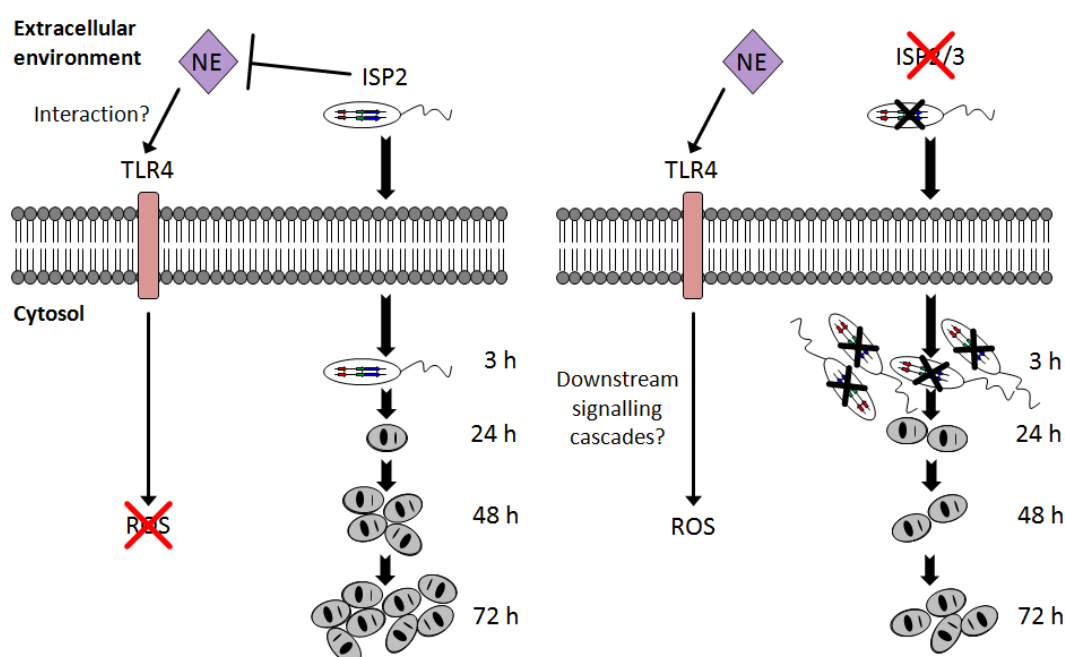


Figure 1-6 Effect of *L. major* ISP2 on *Leishmania*-macrophage interactions. ISP2 has been shown to inhibit the activity of the host serine peptidase, neutrophil elastase (NE). This prevents the activation of a Toll-like receptor 4 (TLR4)-NE signalling cascade during early *Leishmania*-macrophage contact *in vitro*, resulting in a downregulation of phagocytosis and an inhibition of reactive oxygen species (ROS) production. *L. major* deficient in *ISP2* and *ISP3*, $\Delta isp2/3$, are internalised more efficiently but have reduced parasite burdens by 24 h. Therefore, ISP2 may play a role in the establishment and persistence of infection in the mammalian host. There are still some mechanisms to be elucidated, such as the exact interaction of NE and TLR4, which leads to TLR4 activation, and the signalling cascades that are stimulated during the TLR4-NE interaction, and how the prevention of the TLR4 signalling cascade activation by *L. major* ISP2 inhibition of NE activity will affect the immune responses *in vivo*, for example, through the modulation of cytokine and chemokine production.

1.5 Project aims

Host serine peptidases, such as NE and CG, expressed by cells of the early innate immune response, including neutrophils, macrophages, monocytes, and mast cells, are heavily involved in the proteolytic modification of chemokines, and in cytokine and cell receptor activation, which can therefore impact upon cell recruitment and the activation of cell effector functions. It is hypothesised that

L. major ISP2 will inhibit the activity of these SPs during early infection to enable the initiation and persistence of *L. major* infection *in vivo*.

The aims of this project are to:

- Determine the subcellular localisation of ISP1 and ISP2 during the *Leishmania* lifecycle.
- Assess disease progression during *in vivo* infection with *L. major* WT and *ISP2* gene mutants, in terms of parasite burden, to determine whether *ISP2* confers parasite survival *in vivo*.
- Compare the innate immune cell dynamics at the site of inoculation after infection with *L. major* WT and *ISP2* gene mutants, with particular regards to the innate immune cell recruitment and activation, to determine whether *ISP2* affects functions associated to the activity of SPs during the immune response.
- Investigate the role of the serine peptidase, neutrophil elastase (NE), in mediating the immune responses to *L. major* WT and *ISP2* gene mutants *in vivo* through the use of NE-deficient (*Ela*^{-/-}) mice.

2 Materials and Methods

2.1 Promastigote parasite culture

2.1.1 *Leishmania* cell lines

The *Leishmania* cell lines used in this study are given in Table 2-1, together with a description of their genetic manipulation and the resistance genes used for their selection.

Table 2-1 *Leishmania major* cell lines used in this study.

<i>L. major</i> cell line	Description	Antibiotic resistance	Reference
<i>L. major</i> Friedlin wild-type (WT)	MHOM/JL/80/Friedlin		
$\Delta isp1/2/3$	Knock-out of ISP1, ISP2 and ISP3	Blasticidin Nourseothricin Hygromycin Phleomycin	(Morrison et al., 2012)
$\Delta isp1/2/3:ISP1$	Re-expression of ISP1 in $\Delta isp1/2/3$	Blasticidin Nourseothricin Hygromycin Phleomycin Puromycin	(Morrison et al., 2012)
$\Delta isp1/2/3:ISP2/3$	Re-expression of ISP2 and ISP3 in $\Delta isp1/2/3$	Blasticidin Nourseothricin Hygromycin Phleomycin Puromycin	(Morrison et al., 2012)
$\Delta isp2/3$	Knock-out of ISP2 and ISP3	Hygromycin Phleomycin	(Eschenlauer et al., 2009)
$\Delta isp2/3:ISP2/3$	Re-expression of ISP2 and ISP3 in $\Delta isp2/3$	Hygromycin Phleomycin Puromycin	(Eschenlauer et al., 2009)
WT [<i>pXG-ISP2</i>]	Overexpression of ISP2 in WT	Neomycin	(Morrison et al., 2012)
<i>L. major</i> +LUC2	<i>L. major</i> expressing firefly luciferase	Puromycin	

$\Delta isp2/3$ +LUC2	$\Delta isp2/3$ expressing firefly luciferase	Hygromycin Phleomycin Puromycin
$\Delta isp2/3:ISP2/3$ +LUC2	$\Delta isp2/3:ISP2/3$ expressing firefly luciferase	Hygromycin Phleomycin Puromycin Nourseothricin

2.1.2 Passage of cultures

2.1.2.1 Media and growth conditions

Leishmania major were grown in modified Eagle's medium, designated HOMEM medium (Gibco), supplemented with 10% (v/v) heat-inactivated foetal calf serum (FCS) (Gibco), and 100 U ml⁻¹ penicillin and 100 µg ml⁻¹ streptomycin solution (Sigma). Cultures were incubated at 25 °C.

2.1.2.2 Antibiotic concentrations

Cell lines in Table 2-1 were grown in the presence of the appropriate antibiotics. *ISP* gene re-expressing cell lines were selected with 50 µg ml⁻¹ puromycin (InvivoGen) and *ISP* gene overexpressing cell lines were selected with 50 µg ml⁻¹ G418 neomycin (InvivoGen). Bioluminescent cell lines were selected with 50 µg ml⁻¹ puromycin (InvivoGen) or 25 µg ml⁻¹ LEXSY NTC (nourseothricin) (Jena Bioscience).

2.1.3 Preparation and recovery of stabilates

Cultures were preserved in HOMEM medium supplemented with 20% FCS and 5% dimethyl sulfoxide (DMSO). Cryovials were stored at -80 °C overnight then transferred to liquid nitrogen storage for cryopreservation. Stabilates were recovered in HOMEM/20% FCS and incubated at 25 °C.

2.1.4 Determination of culture density

A 1:1 ratio of parasites from culture and 2% formaldehyde solution was prepared, 10 µl of fixed cells were placed on a Neubauer chamber (Weber Scientific), and parasites were counted on an inverted light microscope. Within the centre square of the grid on the haemocytometer, three lines of squares

were counted, the count was divided by 3 to give an average, and the culture density was calculated as follows:

$$\text{Parasites / ml} = \text{count} \times 5 \text{ (total cells in centre square)} \times 2 \text{ (dilution factor)} \times 10^4 \text{ (volume of chamber)}$$

2.1.5 Purification of *L. major* metacyclic promastigotes

Parasites were harvested from culture, which had been in stationary-phase for 3 days, at 1000 x g for 10 min and resuspended in HOMEM. Metacyclic promastigotes were isolated using peanut lectin agglutination (Sacks et al., 1985). Peanut lectin (Sigma) was added at 50 µg ml⁻¹ and incubated at room temperature for 20 min to agglutinate procyclic promastigotes. Metacyclic promastigotes were recovered from the supernatant after centrifugation at 100 x g for 5 min. Metacyclic promastigotes were washed twice in 1x phosphate buffered saline (PBS) [137 mM NaCl, 2.7 mM KCl, 10 mM Na₂HPO₄, 1.8 mM KH₂PO₄] at 1000 x g for 5 min then resuspended in the appropriate volume of PBS.

2.1.6 Transfection and selection of *Leishmania* clones

For each transfection, 5x10⁷ log-phase promastigotes were centrifuged at 1000 x g for 5 min, and resuspended in 100 µl Human T Cell Nucleofactor Solution, provided as part of the Human T Cell Nucleofactor Kit (Lonza). Approximately 10 µg DNA, prepared in up to 10 µl molecular grade water, was added and the solution was transferred to a cuvette. Parasites were electroporated using program U-033 on the Amaxa Nucleofactor™ II. A negative control, in which 10 µl molecular grade water was used instead of DNA, was performed for each transfection. After transfection, the solution was transferred to 10 ml HOMEM/20% FCS, the culture was then split into two flasks of 5 ml to yield two populations, and flasks were incubated at 25 °C overnight.

After the parasites had recovered, the appropriate concentration of selection antibiotic was added to the flasks, including the negative controls. Serial dilution into round-bottom 96-well plates was performed to generate clones of the transfected parasites. Dilutions were as follows: dilution 1 consisted of 4 ml

culture and 20 ml HOMEM/10% FCS supplemented with the appropriate antibiotic; dilution 2 consisted of 2 ml of dilution 1 and 22 ml HOMEM; and dilution 3 consisted of 4 ml of dilution 2 and 22 ml HOMEM. One plate was used for each dilution at 200 μ l per well. Plates were incubated at 25 °C for 3 to 4 weeks.

2.1.7 Preparation of genomic DNA from *Leishmania* spp.

Total genomic DNA from *Leishmania* was purified from a cell pellet harvested from 10 ml of *Leishmania* culture using the DNeasy Blood & Tissue kit (Qiagen), following the manufacturer's protocol for "Purification of Total DNA from Animal Blood or Cell (Spin-Column)". Samples were stored at -20 °C.

2.1.8 Preparation of protein extracts from *Leishmania* spp.

Promastigotes were harvested at the desired lifecycle stage at 1000 x g for 10 min and washed in PBS. Cells were lysed in 1x SDS-PAGE sample buffer [45 mM Tris pH 6.8, 10% (v/v) glycerol, 1% (w/v) SDS, 0.01% bromophenol blue, 50 mM DTT] at 10^7 cells in 10 μ l, briefly vortexed and boiled for 5 min on a heat block. Samples were stored at -20 °C.

2.1.9 Luciferase reporter gene assay

To quantify luciferase activity of bioluminescent cell lines, the Luciferase Reporter Gene Assay (Roche) was used. The assay was performed in duplicate for each cell line; promastigotes were centrifuged at 1000 x g for 10 min, washed in phenol red-free RPMI 1640 (PAA), then resuspended in phenol red-free RPMI 1640 at the required number of cells per 100 μ l. The cell suspensions, and a medium only control, were added to a 96-well white, clear-bottom plate (Greiner Bio-One) at 100 μ l per well, to which 100 μ l luciferase substrate was added. Luminescence was read every 2 min over 30 min using an EnVision Multilabel Reader with a <700 nm luminescence emission filter or a PHERAstar FS (BMG Labtech).

2.2 Bacterial culture

2.2.1 *E. coli* strains

The *E. coli* strains used in this study are given in Table 2-2, together with a description of their main features and uses.

Table 2-2 Competent *E. coli* strains used in the study.

<i>E. coli</i> strains	Features	Uses
DH5 α (Invitrogen)	<i>recA1</i> for insert stability <i>endA1</i> to improve yield and quality of plasmid DNA	Transformations of plasmid DNA or ligation reactions for DNA amplification and purification
<i>dam</i> ⁻ / <i>dcm</i> ⁻ (New England Biolabs)	Methyltransferase-deficient cells	Used to generate unmethylated plasmid DNA
One Shot BL21(DE3)pLysS (Invitrogen)	Produces T7 lysozyme to reduce basal level expression of the gene of interest	Transformation of plasmid DNA for recombinant protein expression and purification

2.2.2 Transformation of *E. coli* with plasmid DNA

Aliquots of 50 μ l of competent cells were thawed on ice, to which 1 μ l DNA was added. Cells were incubated on ice for 30 min. Cell transformation was performed using the heat shock method, in which cells were incubated in a 42 °C waterbath for 45 sec then immediately incubated on ice for 2 min. The cells were recovered through the addition of 450 μ l SOC (Invitrogen) or lysogeny broth (LB) medium and subsequent incubation in a 37 °C incubator shaking at 225 rpm for 1 h. Transformed cells, up to 100 μ l, were spread onto LB agar plates supplemented with the appropriate antibiotic for selection. Plates were inverted and incubated at 37 °C overnight.

2.2.3 Culture of *E. coli*

2.2.3.1 Media and growth conditions

For cells required for the purification of plasmid DNA, individual colonies were selected from the LB agar plates with a sterile pipette tip, placed in 5 ml LB

medium supplemented with the appropriate antibiotic and grown overnight in a 37 °C incubator shaking at 225 rpm overnight.

For cells required for the expression of recombinant proteins, 5 ml LB cultures were prepared as described above. Four 1 L conical flasks containing 400 ml LB medium supplemented with the appropriate antibiotic were prepared. A volume of 1 ml from the 5 ml overnight culture was transferred to each of the 1 L conical flasks, which were grown to an appropriate cell density in a 37 °C incubator shaking at 225 rpm.

2.2.3.2 Antibiotic concentrations

Plasmids used in this study had either ampicillin or chloramphenicol resistance genes. To select for *E. coli* harbouring the plasmid, ampicillin solution, prepared from ampicillin sodium salt (Sigma) in water, or chloramphenicol (Sigma), prepared in ethanol, were added to the culture medium at a final concentration of 100 µg ml⁻¹.

2.2.4 Expression of recombinant proteins

The cell density of the 400 ml cultures was determined using the optical density at 600 nm (OD₆₀₀) measured on a BioPhotometer (Eppendorf), using medium only as a blank reference. When the OD₆₀₀ was between 0.6 and 0.8, protein expression was induced with 0.1 mM isopropyl-β-D-thiogalactopyranoside (IPTG). For recombinant ISP1 expression, the cultures were incubated at 18 °C overnight, and for recombinant ISP2 expression, the cultures were further incubated at 37 °C for 4 h. After induction, cells were harvested at 5000 x g for 15 min, washed with ice-cold PBS then centrifuged at 5000 x g for 15 min. The cell pellet was stored at -20 °C until required for protein purification, which was performed in-house.

2.3 Molecular biology techniques

2.3.1 Preparation of plasmid DNA from *E. coli*

Plasmid DNA from *E. coli* was purified from a cell pellet harvested from 5 ml of LB culture using the QIAprep Spin Miniprep kit (Qiagen), following the manufacturer's protocol for "QIAprep Spin Miniprep Kit Using a Microcentrifuge".

2.3.2 Quantification of DNA concentration and purity

DNA concentration, given in ng ml^{-1} , and purity were quantified on a NanoDrop 1000 Spectrophotometer (NanoDrop), through absorption at 260 nm (A_{260}), and the ratio of A_{260} to A_{280} (nucleic acids to proteins) respectively.

2.3.2 Agarose gel electrophoresis

Agarose gels were made by dissolving 1% (w/v) agarose, or 0.7% (w/v) agarose for gel extraction protocols, into 0.5x Tris-borate-EDTA (TBE) buffer [20 mM Tris, 20 mM boric acid, 0.5 mM EDTA, pH 7.2] by briefly heating in a microwave. After cooling, SYBR Safe DNA gel stain (Invitrogen) was added at 1:20 000 and the gel was left to set. 6x loading dye [0.25% (w/v) bromophenol blue, 0.25% (w/v) xylene cyanol FF, 30% glycerol] was added to the DNA samples for loading. A 1 kb Plus DNA ladder (Invitrogen) was loaded at 0.1 μg per mm lane width alongside the samples as a reference. Electrophoresis was performed between 60 and 120 V until the loading dye had run down at least 80% of the gel. Agarose gels were viewed under UV light on a Molecular Imager Gel Doc XR system (Bio-Rad) using Quantity One software (Bio-Rad).

2.3.3 Restriction endonuclease digestion

DNA was digested using restriction endonucleases (New England Biolabs) according to the manufacturer's guidelines regarding reaction buffer and reaction incubation temperature. For double digests, the optimum reaction buffer was chosen using the 'Double Digest Finder' tool on the New England Biolabs website. Digestion of large concentrations of DNA were performed in 100 to 200 μl volumes and incubated overnight.

2.3.4 Gel extraction

DNA was extracted and purified from 0.7% agarose gels using the QIAquick Gel Extraction kit (Qiagen), following the manufacturer's protocol for "QIAquick Gel Extraction Kit using a Microcentrifuge".

2.3.5 Ethanol precipitation

To purify and concentrate DNA for transfection into *Leishmania* spp., a 10% volume of 3 M sodium acetate pH 5.2 and one volume of 100% isopropanol were added to the sample. The sample was centrifuged at 13 000 x g for 30 min at 4 °C. The DNA pellet was washed in 700 µl 70% ethanol and centrifuged at 13 000 x g for 30 min at 4 °C. The supernatant was removed and the DNA pellet was air-dried in a fume hood. The DNA pellet was resuspended in 30 µl molecular grade water for *Leishmania* transfection.

2.3.6 Polymerase chain reaction (PCR)

2.3.6.1 High-fidelity PCR

Polymerase chain reactions (PCRs), in a volume of 50 µl with 100 ng template DNA, generally consisted of the final concentrations of: 0.2 µM each of the oligonucleotide primers, 200 µM dNTPs (Sigma), 2.5 U *PfuTurbo* DNA polymerase (Agilent Technologies), 1x *pfu* reaction buffer (Agilent Technologies), and molecular grade water. PCR reactions were performed in either a Hybaid Px2 Thermo Cycler (Thermo Scientific) or a Robocycler Gradient 96 (Stratagene), and were typically as follows: an initial denaturation step of 95 °C for 2 min, followed by 30 cycles of denaturation at 95 °C for 50 sec, annealing at 65 °C for 40 sec, optimised for each reaction, and extension at 72 °C for 50 sec, determined by the extension rate of the polymerase and the length of the amplified product, then a final extension step for 10 min at 72 °C. To A-tail the PCR product for cloning into a generic cloning vector, 1 µl *Taq* polymerase (New England Biolabs) was added for 20 min at 72 °C after the final extension step.

2.3.6.2 Colony PCR

Colonies were picked from LB agar plates with a sterile pipette tip and mixed in a PCR mix, in a volume of 20 µl, consisting of the final concentrations of: 0.2 µM

each of the oligonucleotide primers, 200 μ M dNTPs (Sigma), 0.5 U *Taq* polymerase (New England Biolabs), 1x ThermoPol Reaction Buffer (New England Biolabs), and molecular grade water. PCR reactions were performed in a Hybaid Px2 Thermo Cycler (Thermo Scientific) and were typically as follows: an initial denaturation step of 95 °C for 1 min, followed by 25 cycles of denaturation at 95 °C for 30 sec, annealing at 55 °C for 30 sec, and extension at 72 °C for 1 min, then a final extension step for 10 min at 72 °C.

2.3.6.3 PCR method of genotyping transgenic mice

PCRs to genotype NE-deficient mice (*Ela*^{-/-}), in a final volume of 25 μ l with 200 ng DNA, consisted of the final concentrations of: 0.2 μ M each of the oligonucleotide primers, 200 μ M dNTPs (Sigma), 0.5 U *Taq* polymerase (New England Biolabs), 1x ThermoPol Reaction Buffer (New England Biolabs), and molecular grade water. PCR reactions were performed as follows: an initial denaturation step of 94 °C for 5 min, followed by 30 cycles of denaturation at 94 °C for 1 min, annealing at 56 °C for 1 min, and extension at 72 °C for 2 min, then a final extension step for 5 min at 72 °C.

2.3.7 Oligonucleotides used

Oligonucleotides primers, OL3978 and OL3979 in Table 2-3, were designed using Vector NTI software (Invitrogen) and synthesised by Eurofins MWG Operon.

Table 2-3 Oligonucleotides used in this study. Descriptions and sequences are given. Restriction endonuclease sites are underlined, and start or stop codons are in bold.

Oligo number	Description	Oligonucleotide sequence
OL3336 (forward)	Wild-type neutrophil elastase gene	AGACTATCCAGCCGGACTCT
OL3337 (reverse)		ACCAACAATCTCTGAGGGCA
OL3338 (forward)	NEO gene (Disrupts wild-type neutrophil elastase gene in <i>Ela</i> ^{-/-} mice)	ATGATTGAACAAGATGGATTGCAC
OL3339 (reverse)		TTCGTCCAGATCATCCTGATCGAC

OL3978 (forward)	Amplification of the SAT gene and addition of a <i>Bam</i> HI restriction site	GCAGGATCCATGAAGATTTCCGGTGATCCCTGAGC
OL3979 (reverse)	Amplification of the SAT gene and addition of a <i>Sex</i> AI restriction site	TGCACCAGGTTTAGGCGTCATCCTGTGCTCCCCGA

2.3.8 Ligation

2.3.8.1 Cloning of PCR products into cloning vectors

PCR products, with A-overhangs, were ligated into pGEM-T Easy Vector (Promega) then transformed into competent *E. coli* cells following the manufacturer's instructions. Transformants were selected based on blue/white colony screening and confirmed by colony PCR with T7 and SP6 primers.

2.3.8.2 Cloning of digested inserts into destination plasmids

Digested inserts were ligated into similarly digested plasmids at a 3:1 insert:vector ratio, in a 20 µl reaction volume comprising T4 DNA ligase (New England Biolabs), T4 DNA ligase buffer (New England Biolabs), and molecular grade water. Ligation reactions were incubated at 16 °C overnight, after which 2 µl of the ligation reaction was transformed into competent *E. coli* cells, which were plated onto LB agar plates supplemented with the appropriate antibiotic for selection. Colonies were selected and verified by colony PCR using vector-specific primers or through restriction digest analysis of the purified plasmid.

2.3.9 DNA sequencing

DNA sequencing was performed by DNA Sequencing and Services at the University of Dundee and analysed using CLC Genomics Workbench 4 (CLC Bio).

2.3.10 Plasmids used

Plasmids used and generated in this study are listed in Table 2-4, together with a description of their use in this study.

Table 2-4 Plasmids used or generated in this study.

Plasmid number	Backbone	Description
pGL573	pGEM-T	Contains SAT gene Used to change the resistance cassette of pGL2127 to generate pGL2276
pGL998	PET15b	Protein expression of recombinant <i>L. major</i> ISP1
pGL999	PET15b	Protein expression of recombinant <i>L. major</i> ISP2
pGL2126		Contains LUC2 and PAC genes
pGL2127	pRIB (pGL631) (Misslitz et al., 2000) Integrates into the	Contains mCherry and PAC genes
pGL2276	<i>Leishmania</i> rRNA locus	Contains mCherry and SAT genes Used to generate pGL2357
pGL2357		Contains LUC2 and SAT genes

2.4 Protein techniques

2.4.1 SDS-PAGE

Leishmania protein extracts were separated on sodium dodecyl sulphate (SDS) polyacrylamide gels. Each 12% separating polyacrylamide gel was prepared in a volume of 12.5 ml [3.55 ml distilled water, 3.15 ml 1.5 M Tris pH 8.8, 5 ml 30% acrylamide solution, 125 µl 10% SDS, 125 µl 10% ammonium persulfate, 5 µl TEMED] and cast in a 1.0 mm mini gel cassette (Invitrogen). A 5% stacking gel was prepared in a volume of 4 ml [2.25 ml distilled water, 500 µl Tris pH 6.8, 650 µl 30% acrylamide solution, 40 µl 10% SDS, 40 µl 10% ammonium persulfate, 4 µl TEMED], cast over the 12% separating gel and a cassette comb (Invitrogen) was set in place. A Spectra Multicolor Broad Range Protein Ladder (Thermo Scientific) was used as a protein marker. Electrophoresis was performed in an XCell SureLock Mini-Cell Electrophoresis System (Invitrogen) with 1x SDS-PAGE running buffer [25 mM Tris, 192 mM glycine, 0.1% (w/v) SDS].

2.5 Antibody purification

Anti-ISP1 and anti-ISP2 antibodies were purified from sheep antisera (Eschenlauer et al., 2009) using AminoLink Plus Coupling Resin (Thermo Scientific). To prepare the AminoLink Plus Coupling Resin (Thermo Scientific), 4 ml of slurry was centrifuged at 1000 rpm for 5 min, to remove the storage solution, leaving 2 ml resin. The resin was washed twice in 10 ml PBS at 1000 rpm for 5 min.

Recombinant ISP protein was concentrated to approximately 10 mg in 1 ml using a Vivaspin 2 Centrifugal Concentrator with a molecular weight cut-off value (MWCO) of 10 000 (Sartorius Stedim Biotech) centrifuged at 3000 rpm for 10 min. The concentrated protein was collected and diluted in 3 ml coupling buffer [0.1 M sodium phosphate, 0.15 M sodium chloride, pH 7.2]. The protein solution was added to the resin with 40 μ l cyanoborohydride solution [5 M sodium cyanoborohydride in 1 M sodium hydroxide] and incubated on a rotating mixer at 4 °C overnight to immobilise the protein.

All centrifugations, including wash steps, were performed at 1000 rpm for 5 min at 4 °C. The resin with the immobilised protein was centrifuged, washed in 4 ml coupling buffer then washed in 10 ml quenching buffer [1 M Tris pH 7.4]. Thereafter, 2 ml quenching buffer and 40 μ l cyanoborohydride solution were added and incubated on a rotating mixer at room temperature for 30 min. The resin was washed three times in 6 ml wash buffer [1 M sodium chloride, 0.05% sodium azide] then washed in 10 ml ImmunoPure (Protein A) IgG Binding Buffer (Thermo Scientific). After which, 2.5 ml binding buffer and 5 ml anti-sera were incubated on a rotating mixer at 4 °C overnight.

The 10 ml solution was gently pipetted into a 2 ml column (Thermo Scientific) and allowed to run until the resin had settled. The resin was washed with 20 ml binding buffer then eluted with 8 ml IgG Elution Buffer (Thermo Scientific). Elutions were collected in 0.5 ml fractions and protein concentration was determined using the absorbance at 260 nm, measured on a BioPhotometer (Eppendorf) using water as a blank reference. For re-use, the column was washed with 20 ml wash buffer and stored upright at 4 °C.

2.5.1 Antibody storage

Antibody solutions of 0.5 ml were neutralised with 25 μ l 1 M Tris pH 9. Sodium azide was added, at a final concentration of 0.01% (w/v), to inhibit microbial growth, and glycerol was used, at a final concentration of 20%, as a cryoprotectant. Antibodies were stored at -20 °C.

2.6 Immunostaining

2.6.1 Western blotting

Proteins from SDS-PAGE gels were transferred onto Hybond C-Super nitrocellulose membranes (Amersham) using the XCell SureLock XCell II Blot Module (Invitrogen) in the presence of transfer buffer [25 mM Tris, 192 mM glycine, 20% methanol] at 30 V for 1 h. Membranes were blocked in Tris-buffered saline (TBS) [10 mM Tris pH 8, 150 mM NaCl, pH 7.4] supplemented with 0.05% Tween-20 (TBST) and 5% (w/v) Marvel at 4 °C overnight. Freshly affinity-purified primary antibodies to either rISP1 or rISP2 were used at 1:50 (v/v) in TBST with 5% (w/v) Marvel, and purified anti-oligopeptidase B (OPB) antibodies (Munday et al., 2011) were used at 1:20 000 (v/v) for 2 h at room temperature. The donkey anti-sheep IgG-HRP (Santa Cruz Biotechnology) secondary antibody was used at a 1:10 000 dilution for 1 h. The reactive bands were detected using ECL Western Blotting Detection Reagent (Amersham).

2.6.2 Immunofluorescence microscopy

Parasites were harvested at 1000 x g for 5 min and washed twice in PBS at 1000 x g for 3 min. Cells were resuspended in 100 μ l PBS and fixed in 1% methanol-free formaldehyde (Thermo Scientific) for 30 min at room temperature. Cells were permeabilised with 0.1% Triton X-100 detergent for 10 min then reactive products were neutralised with 0.1 M glycine for 10 min at room temperature. Cells were centrifuged at 2000 rpm for 10 min then resuspended in an appropriate volume of PBS. A volume of 200 μ l of cells was added to each well of an 8-well chamber slide (Lab-Tek) and parasites were left to adhere to the slide for 10 min at room temperature. Excess PBS was removed from the well and

cells were blocked in blocking buffer [0.1% (v/v) Triton X-100, 0.1% (w/v) BSA, in PBS] for 1 h at room temperature.

Freshly affinity-purified primary antibodies were used at a 1:50 (v/v) dilution in blocking buffer and slides were incubated for 2 h at room temperature. A secondary antibody only control was performed, in which blocking buffer was used instead of primary antibody, to determine background fluorescence. The wells were washed three times with PBS and incubated with donkey anti-sheep Alexa Fluor 488-conjugated antibody (Invitrogen) at 1:2000 (v/v) in blocking buffer for 1 h in a dark box at room temperature. The wells were washed three times in PBS, the chamber was removed, and VectaShield Mounting Medium with DAPI (Vector Laboratories) was applied to the slide.

Cells were observed and imaged at 100x magnification on a DeltaVision RT or DeltaVision Core epifluorescent microscope (Applied Precision) equipped with DAPI (381-399 nm) and FITC (461-489 nm) filters, and images were captured with a CoolSNAP HQ or HQ² camera (Photometrics) respectively.

2.7 Flow cytometry

2.7.1 Staining cell surface antigens

All steps were performed at 4 °C and all centrifugation steps were performed at 380 x g for 5 min. Single-cell suspensions from mouse ear or lymph nodes were incubated with an anti-Fc- γ III/II (CD16/32) receptor antibody (2.4G2, BD Biosciences) for 30 min, washed twice with PBS, then stained in the dark with the fluorochrome-conjugated antibodies, given in Table 2-5, for 30 min. The appropriate rat IgG2a, rat IgG2b, rat IgG2c, or Armenian hamster IgG isotype controls were used. After staining of surface markers, the cells were washed twice with PBS, and stained with Fixable Viability Dye eFluor 506 or eFluor 660 (eBioscience) for 30 min, following the manufacturer's protocol. The cells were washed twice in FACS buffer [1% dialysed FCS, 0.05% sodium azide, 2 mM EDTA, in PBS] then fixed with methanol-free formaldehyde (Thermo Scientific) for 5 min. Cells were washed twice in FACS buffer, then resuspended in FACS buffer and passed through a Nitex mesh with a pore size of 50 μ m (Cadisch).

2.7.2 Staining cytoplasmic intracellular antigens

Single-cell suspensions were blocked with an anti-Fc- γ III/II (CD16/32) receptor antibody (2.4G2, BD Biosciences), cell surface antigens were stained, and Fixable Viability Dye eFluor 660 (eBioscience) was added as above. All subsequent steps were performed at room temperature and all centrifugation steps were performed at 380 x g for 5 min. The cells were then washed twice with PBS, pulse-vortexed and fixed in 100 μ l IC Fixation Buffer (eBioscience) for 20 min in the dark. Cells were washed twice in 1x Permeabilization Buffer (eBioscience) then cytoplasmic intracellular antigens, given in Table 2-5, were stained for 20 min in the dark. Cells were washed twice with FACS buffer, then resuspended in FACS buffer and passed through a Nitex mesh with a pore size of 50 μ m (Cadisch).

Table 2-5 Antibodies used for flow cytometry.

Marker	Fluorophore	Clone	Manufacturer
Cell surface antigens			
CD11b	APC	M1/70	eBioscience
CD11b	PE-Cy7	M1/70	eBioscience
CD11c	PE	N418	eBioscience
CD11c	PerCP-Cy5.5	N418	eBioscience
CD45	APC-Cy7	30-F11	BD Biosciences
CD80 (B7-1)	FITC	16-10A1	eBioscience
CD86 (B7-2)	PE-Cy7	GL1	eBioscience
F4/80	APC	BM8	eBioscience
Ly-6C	eFluor 450	HK1.4	eBioscience
Ly-6C	PerCP-Cy5.5	HK1.4	eBioscience
Ly-6G	PE	1A8	BD Biosciences
Ly-6G	APC-Cy7	1A8	BD Biosciences
Ly-6G (Gr-1)	PE	RB6-8C5	eBioscience

MHCII (I-A/I-E)	APC-eFluor780	M5/114.15.2	eBioscience
MHCII (I-A/I-E)	eFluor 450	M5/114.15.2	eBioscience
MHCII (I-A/I-E)	FITC	M5/114.15.2	eBioscience
MHCII (I-A/I-E)	FITC	2G9	BD Biosciences
Cytoplasmic intracellular antigens			
Myeloperoxidase (MPO)	FITC	8F4	Hycult Biotech
NOS2	PE	CXNFT	eBioscience

2.7.3 Data acquisition and analysis

The data were collected using either a MACSQuant Analyzer (Miltenyi Biotec) or a BD LSR II Flow Cytometer (BD Biosciences), and analysed using FlowJo. Compensation settings were optimised using lymph node cells single-stained with anti-mouse CD4 antibodies conjugated to the corresponding fluorophores used in Table 2-5, (RM4-5, eBioscience and GK1.5, BD Biosciences). Live (based on Fixable Viability Dye staining) innate immune cells from the ear and draining lymph node were identified based on size (forward scatter) and granularity (side scatter), as well as by surface phenotype as indicated in the text and figure legends.

2.8 Enzyme-linked immunosorbent assay (ELISA)

The mouse IFN- γ ELISA Ready-Set-Go! kit (eBioscience) was used following the manufacturer's protocol, using supernatant isolated from mouse ears and draining lymph nodes as samples. Plates were read on a Dynex MRX TC II microplate reader (Dynex Technologies) at 450 nm.

2.9 Mice

2.9.1 Regulations

All procedures were conducted under Home Office Licence, after institutional ethical review. Prior to the removal of tissues or organs, mice were culled using

approved Schedule 1 methods, either by exposure to rising concentrations of carbon dioxide gas, generally for mice infected in the ear, or the dislocation of the neck for mice infected in the footpad.

2.9.2 Strains

Female BALB/cJ and C57BL/6J mice were purchased from Charles River Laboratories International, and female neutrophil elastase (NE)-deficient mice (129-S2-Ela2), *Ela*^{-/-}, were obtained from the in-house breeding facility, but were originally from MRC Harwell. Mice were typically inoculated between 8 to 14 weeks of age.

Ela^{-/-} were originally generated in the 129X1/SvJ background through the disruption of the endogenous NE gene with a targeting vector containing neomycin phosphotransferase cDNA driven by the phosphoglycerate kinase promoter (PGK-neo) (Belaouaj et al., 1998). Mice were then backcrossed to C57BL/6 mice for at least 10 generations.

2.9.3 Mouse infections and inoculations

For intradermal inoculations, the ear dermis was inoculated with 10^4 metacyclic promastigotes in 10 μ l PBS, and for the controls, injected with 10 μ l PBS or with the needle only, whilst the mice were kept under general anaesthesia with 2% isoflurane/1.5 L O₂.min⁻¹. Injections were performed using a 0.3 ml 29G insulin syringe (VWR).

For subcutaneous inoculations, the footpad was inoculated with up to 2×10^6 parasites in 40 μ l. Injections were performed using a 0.3 ml 29G insulin syringe (VWR). Parasites were routinely passaged in BALB/c mice, in this manner, to maintain infectivity. Once the lesion size of the infected footpad was above 3 mm, the mice were culled, and the footpads and draining popliteal lymph nodes were removed and placed into flasks containing HOMEM/10% FCS supplemented with 0.5% gentamicin solution (Sigma) then incubated at 25 °C to obtain promastigotes.

To elicit peritoneal macrophages, up to 0.5 ml of 3% thioglycollate was injected into the peritoneal cavity using a syringe with 25G needle attached, and mice were culled between 4 and 24 h later. Elicited peritoneal macrophages were used as positive controls for some flow cytometry experiments. Other intraperitoneal injections, of luciferin and luminol, were performed using a 1 ml syringe with 25G needle attached.

2.9.4 Measurement of lesions and tissues

2.9.4.1 Size measurements

For lesion progression, the infected ear or footpad thickness was measured weekly with a dial caliper, with the uninfected ear or footpad as a control. Draining lymph nodes were removed and three diameter measurements were taken with a Vernier caliper.

2.9.4.2 Mass measurements

To obtain the mass measurements of the liver and spleen, glass universals containing a volume of HOME/10% FCS supplemented with 0.5% gentamicin solution were weighed before and after the addition of the excised organs. The difference corresponded to the mass of the organ.

2.9.5 Tissue processing

2.9.5.1 Flow cytometry

Ears were deposited in PBS and cut repeatedly with surgical scissors, 4 mg ml⁻¹ collagenase D (Roche) and 100 U ml⁻¹ DNase I were added, then the tissue was incubated in a Thermomixer Comfort Eppendorf shaking incubator (Eppendorf) at 37 °C shaking at 1000 rpm for 45 min. Digested tissue was transferred to a gentleMACS C tube (Miltenyi Biotec) containing RPMI 1640 and processed in the gentleMACS dissociator (Miltenyi Biotec). Tissue homogenates were filtered through a 40 µm cell strainer (BD Biosciences).

Draining retromaxillary lymph nodes were collected and mechanically dissociated with the back of a syringe through a 70 µm cell strainer (BD Biosciences).

Homogenised tissue samples were centrifuged at 380 x g for 10 min at 4 °C, washed in PBS, and resuspended in 1 ml PBS. Cell number was then determined by taking 10 µl of cells with a 1:1 ratio of cells to trypan blue (Sigma), and counting on a Neubauer chamber, as described earlier.

2.9.5.2 ELISAs

Ears and draining retromaxillary lymph nodes were removed and placed in ice-cold PBS, samples were then transferred to 2 ml conical microcentrifuge tubes (Thermo Scientific) containing 500 µl T-PER Tissue Protein Extraction Reagent (Thermo Scientific) with 1% protease inhibitor cocktail (Roche). Lysis was performed by adding two 5 mm stainless steel beads (Roche) to each tube and running the samples on a TissueLyser LT (Qiagen) at 50 Hz for 2 min. Samples were then centrifuged at 13 000 rpm for 10 min at 4 °C. The supernatant was transferred to a new Eppendorf and stored at -80 °C.

2.9.5.3 Limiting dilution assays (LDAs)

Ears were sprayed with 70% ethanol and deposited in 500 µl HOME supplemented with 1% (v/v) penicillin/streptomycin, and 1% (v/v) gentamicin solution, cut repeatedly with surgical scissors, then digested with 4 mg ml⁻¹ collagenase D and incubated at 37 °C for 2 h. Digested tissue was transferred to a gentleMACS C tube and processed in the gentleMACS dissociator. Tissue homogenates were filtered through a 70 µm cell strainer (BD Biosciences).

Draining retromaxillary lymph nodes were collected and mechanically dissociated with the back of a syringe through a 70 µm cell strainer (BD Biosciences).

2.9.6 Peritoneal macrophage isolation

Peritoneal macrophages were isolated from mice, either injected with thioglycollate or not, which were used as controls in flow cytometry. Mice were culled by CO₂ asphyxiation. Mice were sprayed with 70% ethanol and the skin incised at the abdomen and pulled away to reveal the peritoneum, which was sprayed again with 70% ethanol. The cavity was filled with up to 10 ml RPMI 1640 supplemented with 1% (v/v) penicillin/streptomycin and 0.5% gentamicin, using

a charged syringe with 26G needle attached. The mouse was shaken for 30 sec to dislodge cells in the peritoneal cavity. The peritoneal fluid was removed using an empty syringe with a 21G needle attached. Cells were harvested by centrifugation at 1500 rpm for 10 min at 4 °C. Macrophages were then washed in PBS.

2.9.7 Purification of amastigotes from tissues

Mouse organs were removed, cut into small pieces and transferred to a Dounce glass tissue grinder with 400 ml PSGEMKA buffer (Hart et al., 1981) until no large pieces remained. Then 50 mg saponin was resuspended in 1 ml PSGEMKA buffer and added to the 400 ml crude suspension. The crude suspension was centrifuged at 3400 rpm for 10 min, the supernatant was discarded, and the pellet was washed three times in PSGEMKA buffer. The pellet was resuspended in a final volume of 100 ml PSGEMKA buffer. A column was prepared with glass wool and a 100 ml sephadex solution (2.5 g sephadex CM25 swelled in 100 ml PSGEMKA at 4 °C overnight). The 100 ml amastigote suspension was pipetted into the column. The first 100 ml of flow-through was discarded and the subsequent volume collected as the amastigote preparation. The amastigote preparation was centrifuged at 3400 rpm for 10 min and the pellet was washed three times in PSGEMKA buffer.

2.10 Quantification of parasite burden from tissues

Quantification of parasite burdens were performed using the LDA method (Titus et al., 1985). Ear and lymph node homogenates were resuspended in 3.2 ml and 1.6 ml HOMEM/20% FCS supplemented with 1% (v/v) penicillin/streptomycin respectively; liver and spleen homogenates were resuspended in 6.4 and 3.2 ml respectively. The cell homogenates were submitted to 2-fold serial dilutions in 96-well flat-bottom plates. Samples were performed in duplicate. Plates were sealed and incubated in humidified box at 25 °C for 7 to 10 d, after which the wells were visually analysed for the presence of parasites. The highest dilution well was used to estimate the number of parasites multiplied by the dilution factors. Parasite numbers are given as total per tissue or organ.

2.11 Bioluminescence imaging (BLI)

2.11.1 Preparation of luciferin

A stock solution of D-luciferin potassium salt (Promega) was prepared at 15 mg ml⁻¹ in PBS. The solution was filtered through a 0.2 µm syringe filter. Luciferin was administered at 150 mg per kg body weight, 10 µl per g body weight, intraperitoneally.

2.11.2 Preparation of luminol sodium salt

A stock solution of luminol sodium salt (Sigma) was prepared at 50 mg ml⁻¹ in PBS. The solution was filtered through a 0.2 µm syringe filter. Luminol was administered at 200 mg per kg body weight, 4 µl per g body weight, intraperitoneally.

2.11.3 BLI image analysis

Mice were anaesthetised at 4% isoflurane/1.5 L O₂ min⁻¹ then bioluminescent light emission was imaged at 10 to 15 min after luciferin or luminol injection, using the IVIS Spectrum bioluminescence imaging system (Caliper Life Sciences). Mice were maintained under anaesthesia at 1.5% isoflurane/1.5 L O₂ min⁻¹ whilst in the IVIS. Imaging was performed with an open emission filter, for 1 min exposures, large binning, and 1 f/stop, and captured with a charge-coupled device (CCD) camera. Analysis was performed using Living Image software (Caliper Life Sciences). The absolute unit of photon emission was given as radiance (photons/second/cm²/steradian). Regions of interest (ROIs) were manually selected over the entire ear to quantify the amount of photon emission as total photon flux in photons per second (photons sec⁻¹).

2.12 Statistical analysis

Statistical analysis was performed using GraphPad Prism 5. The analysis of significance of the data was performed by an unpaired t-test when comparing data from WT and $\Delta isp2/3$ infections, or one-way ANOVA with Tukey post-test when comparing data from WT, $\Delta isp2/3$, and/or $\Delta isp2/3:ISP2/3$ or WT [pXG-

ISP2] infections with controls, as indicated in the figures. Scores showing statistical significance are indicated in the figures with asterisks.

3 Localisation of the inhibitors of serine peptidases in *Leishmania major*

3.1 Introduction

3.1.1 ISP expression during the *Leishmania* lifecycle and inhibitory activity against host serine peptidases

Three ecotin-like peptide inhibitors of serine peptidases, ISPs, have been identified in the *L. major* genome, designated ISP1, ISP2, and ISP3. Of the three ISPs, only ISP1 and ISP2 are detected at the protein level during the *Leishmania* lifecycle (Eschenlauer et al., 2009). ISP3 is not detected in any of the *Leishmania* lifecycle stages and has been suggested to be a pseudogene. There does, however, appear to be stage-regulated expression of ISP1 and ISP2; ISP1 is expressed during the vector-borne promastigote stages, whereas ISP2 is expressed in all three lifecycle stages, with particularly high levels in the infective metacyclic promastigote and amastigote stages (Eschenlauer et al., 2009).

The inhibitory activities of ISP1 and ISP2 have been tested against serine peptidases that *L. major* may come into contact with during its lifecycle, either in the mammalian host or the sandfly vector. The SPs chosen included those of the S1A trypsin-fold peptidase family of clan PA(S), of which bacterial ecotin has already been shown to inhibit (Chung et al., 1983; Eggers et al., 2004). Unexpectedly, however, recombinant ISP1 has been shown to have no inhibitory activity towards bovine trypsin, and low inhibitory activity against human NE, with only 50% inhibition at 670 nM (Morrison et al., 2012). Recombinant ISP1 also has low inhibitory activity against sandfly midgut extract with only 40% inhibition at 6.7 μ M, compared to 60% inhibition at 2 nM for recombinant ISP2 (Morrison et al., 2012). ISP1 was, in fact, shown to have an endogenous role in flagellar homeostasis of *Leishmania* promastigotes (Morrison et al., 2012), the target of which is, as yet, unidentified, as *Leishmania* lack endogenous S1A serine peptidases (Ivens et al., 2005).

Recombinant ISP2, however, has been shown to inhibit the human serine peptidases, NE, trypsin, and chymotrypsin with K_i s of 7.7 (\pm 1.4) nM, 83 (\pm 2.3)

nM, and 19 (± 4.2) nM respectively (Eschenlauer et al., 2009). These data indicate a potential role for ISP2 in the inhibition of host SP activity.

3.1.2 Serine peptidases and the S1A serine peptidase family

SPs are ubiquitously found in prokaryotes and eukaryotes, and are responsible for various functions in humans and other mammals, including immunity, digestion, development, reproduction, blood coagulation, and fibrinolysis. As of 2014, the SPs have been grouped into 16 clans, based on catalytic mechanism, and 53 families, based on common ancestry. The majority of SPs belong to the S1 family of clan PA, of which there are subfamilies that are distinguished based on their substrate specificity; these are trypsin-like, chymotrypsin-like, and elastase-like serine peptidases. *Leishmania* spp., including *L. major*, *L. mexicana*, *L. infantum*, and *L. braziliensis* lack S1 serine peptidase homologues. There are six subfamilies within the S1 family, but subfamilies S1A and S1B are the most well-defined, in that S1B serine peptidases are involved in intracellular protein turnover, whereas S1A peptidases mediate extracellular processes. Like ecotin, ISP2 has been shown to have inhibitory activity against S1A serine peptidases, suggesting it may be involved in protecting the parasite against the digestive S1A serine peptidases in the sandfly gut and/or modulating the immune response in the mammalian host through the inhibition of the activity of host SPs with roles in immunity. However, the inhibitory activity of neither ecotin nor the ISPs has been tested against SPs of the other S1 subfamilies.

3.1.3 S1A serine peptidase expression in the sandfly vector

Trypsin and chymotrypsin are two of the most studied S1A serine peptidases. These SPs are common endoprotease digestive enzymes, found in the digestive systems of many species of animals including blood-feeding arthropods. Trypsin and chymotrypsin are the main digestive enzymes in the midgut of Diptera flies, which includes the subfamily Phlebotominae (Ramalho-Ortigão et al., 2003; Telleria et al., 2010). These SPs are produced and secreted by midgut epithelial cells upon the ingestion of blood and are active within the midgut lumen. They have been shown to be a potential barrier to *Leishmania* growth and development; however, the peritrophic membrane, a matrix secreted by the

midgut epithelium that separates the blood meal from the midgut tissue, typically protects *Leishmania* from these enzymes.

3.1.4 S1A serine peptidase expression in the mammalian host

Upon inoculation of *Leishmania* into the skin of the mammalian host, a local inflammatory immune response is initiated, and *Leishmania* encounter innate immune cells and their antimicrobial components, including SPs. The most abundant leukocyte in mammals, the neutrophils, are a major source of SPs, and are the first immune cells to be recruited to the site of *Leishmania* infection. Three S1A serine peptidases, often referred to as neutrophil serine peptidases (NSPs), NE, CG, and proteinase 3 (PR3), are stored in high concentrations in the cytoplasmic azurophilic (or primary) granules of neutrophils. Azurophilic granules also contain other antimicrobial factors, such as MPO and defensins, as well as a monocyte chemotactic antibiotic protein, azurocidin. However, NE is also localised in the nuclear envelope (Clark et al., 1980; Benson et al., 2003). Granules fuse with the phagolysosome, a cytoplasmic body formed upon sequestration of microorganisms by the fusion of the phagosome with a lysosome. In conjugation with antimicrobial factors, these NSPs digest phagocytosed microorganisms within the phagolysosomes.

Catalytically active NSPs can also be released extracellularly from both activated and apoptotic neutrophils, as they also play a vital role in the modulation of the immune response through the processing of cytokines, chemokines, and growth factors, as well as the cleavage and activation of specific cell surface receptors (reviewed in Pham, 2008). Extracellular secretion occurs by highly controlled exocytosis upon neutrophil activation at sites of inflammation. Extracellular NSPs can bind to the neutrophil cell surface through interactions with chondroitin sulfate and heparin sulfate proteoglycans; there is up to a 20-fold increase in neutrophil surface-bound NSPs upon neutrophil activation (Campbell & Owen, 2007). Surface-bound NSPs function in the regulation of leukocyte function by peptidase signalling through cell surface binding sites or other surface proteins.

In addition, activated neutrophils release NETs, which are web-like structures of decondensed chromatin that ensnare extracellular microorganisms, in an active

process termed NETosis (Brinkmann et al., 2004). NSPs are found bound to NETs in high concentrations, along with histones, active MPO, and other antimicrobial peptides (Papayannopoulos et al., 2010; Metzler et al., 2011).

Inflammatory monocytes are another source of all three of the mentioned NSPs, whilst other sources of NE and PR3 include mast cells and the other granulocytes, the eosinophils and basophils. CG and NE have both been shown to localise to peroxidase-positive cytoplasmic granules in monocytes (Kargi et al., 1990); whilst in mast cells, eosinophils, and basophils, NE has been found in secretory granules. NE has also been found in association with CR3 on neutrophils, macrophages, and NK cells (Cai & Wright, 1996). Immunofluorescence performed by Faria et al. (2011) revealed that NE was localised to the surface of elicited macrophages from C57BL/6 mice.

3.1.5 Aims

The protein expression of the ISPs throughout the *Leishmania* lifecycle has previously been reported (Eschenlauer et al., 2009); however, the localisation of the ISPs within these lifecycle stages has not been investigated. *In vitro* studies have shown that *L. major* ISP2 inhibits the activity of NE, which in turn prevents the activation of a TLR4-NE signalling cascade in macrophages (Faria et al., 2011). The aim of this chapter is to determine the localisation of ISP1 and ISP2 within *L. major* promastigotes and amastigotes to provide an indication of potential interactions of the ISPs with the host SPs.

3.2 Results

3.2.1 Validation of affinity-purified anti-ISP1 and anti-ISP2 antibodies

To determine the localisation of ISP1 and ISP2 in *L. major* WT, polyclonal antibodies were first affinity-purified from sheep serum using the AminoLink Plus Coupling Resin (Thermo Scientific). The cross-reactivity of the anti-ISP1 and anti-ISP2 antibodies was then tested against recombinant ISP1 (rISP1) and ISP2 (rISP2) proteins (Figure 3-1, A and B), which had been expressed and purified from *E. coli*. The molecular weights of the recombinant ISPs were as expected

(Figure 3-1, A and B), as the predicted sizes of ISP1 and ISP2 are 16.5 kDa and 17.5 kDa respectively (Eschenlauer et al., 2009). The ISP2 antibody did not cross-react with ISP1 (Figure 3-1B), but the ISP1 antibody recognised both ISP1 and ISP2 (Figure 3-1A). The specificity of the ISP1 antibody was then tested against cell extracts from *L. major* WT promastigotes, an *ISP2/3* double knock-out ($\Delta isp2/3$) generated by Eschenlauer et al. (2009), and an *ISP1/2/3* triple knock-out ($\Delta isp1/2/3$) generated by Morrison et al., 2012) (Figure 3-1C). It appears as though two bands were detected in WT parasite extracts, which could be due to the cross-reactivity of the ISP1 antibody resulting in detection of both the ISP1 and ISP2, while only one band was detected in cell lines deficient in *ISP2*, $\Delta isp2/3$, representing ISP1 (Figure 3-1C). In accordance with this, no bands were detected in the extracts from $\Delta isp1/2/3$ parasites (Figure 3-1C). Antibodies against oligopeptidase B (OPB), an 83 kDa enzyme present in various *Leishmania* species including *L. major*, were used as to show equal loading of the protein samples (Munday et al., 2011).

Previously, Eschenlauer et al. (2009) had shown that ISP1 and ISP2 are expressed in log-phase promastigotes, which they referred to as procyclic promastigotes, and in purified metacyclic promastigotes. Cell extracts were prepared from stationary-phase cultures for Figure 3-1, the populations of which consist of procyclic and metacyclic promastigotes, as well as the other intermediate forms, the nectomonad, leptomonad, and haptomonad promastigotes. Therefore, the levels of ISP expression in the cell lines are likely to vary between samples collected at different times, dependent upon the composition of the culture population, as ISP2 was shown to be more highly expressed in metacyclic promastigotes compared to the procyclic promastigotes (Eschenlauer et al., 2009). This could explain the differences observed between ISP levels in the different Western blots, given in Figure 3-1, with extracts from the same cell line collected at different times.

The antibodies were also tested against an *ISP1* re-expressor ($\Delta isp1/2/3:ISP1$) (Figure 3-1D) and an *ISP2/3* re-expressor ($\Delta isp1/2/3:ISP2/3$) (Figure 3-1E) in the triple knock-out background, generated by Morrison et al. (2012). ISP1 and ISP2 were detected in the promastigote forms of WT, and the re-expressing cell lines, $\Delta isp1/2/3:ISP1$ and $\Delta isp1/2/3:ISP2/3$ (Figure 3-1, D and E respectively), but not

in $\Delta isp1/2/3$. Again, two bands were detected in $\Delta isp1/2/3:ISP1$ with the ISP1 antibody (Figure 3-1D), this could indicate post-translational modification of ISP1, as in this cell line ISP2 should not be present and in the background cell line, $\Delta isp1/2/3$, no bands were detected. The expression of ISP1 and ISP2 in the re-expressing cell lines was higher than that detected in WT parasites (Figure 3-1, D and E respectively), which has been shown to occur from genes integrated into the ribosomal locus under a polymerase I promoter (Lodes et al., 1995; Miszlitz et al., 2000).

Additionally, the ISP2 antibody was used to confirm the presence or absence of ISP2 in the cell lines, which would be used for *in vivo* experiments, discussed in Chapters 4 and 5. These cell lines included an ISP2 over-expressor (WT [*pXG-ISP2*]) generated by Morrison et al. (2012) (Figure 3-1F), and an *ISP2/3* re-expressor in the double knock-out background ($\Delta isp2/3:ISP2/3$) generated by Eschenlauer et al. (2009) (Figure 3-1G). A single band, around 17 kDa, the predicted size for ISP2, was detected in the extracts from WT, WT [*pXG-ISP2*], and $\Delta isp2/3:ISP2/3$ parasites, but not $\Delta isp2/3$ parasites. The expression of ISP2 in the overexpressing cell line, which express ISP2 from episomal plasmids, and the re-expressing cell line was, again, higher than that detected in WT parasites (Figure 3-1, F and G respectively).

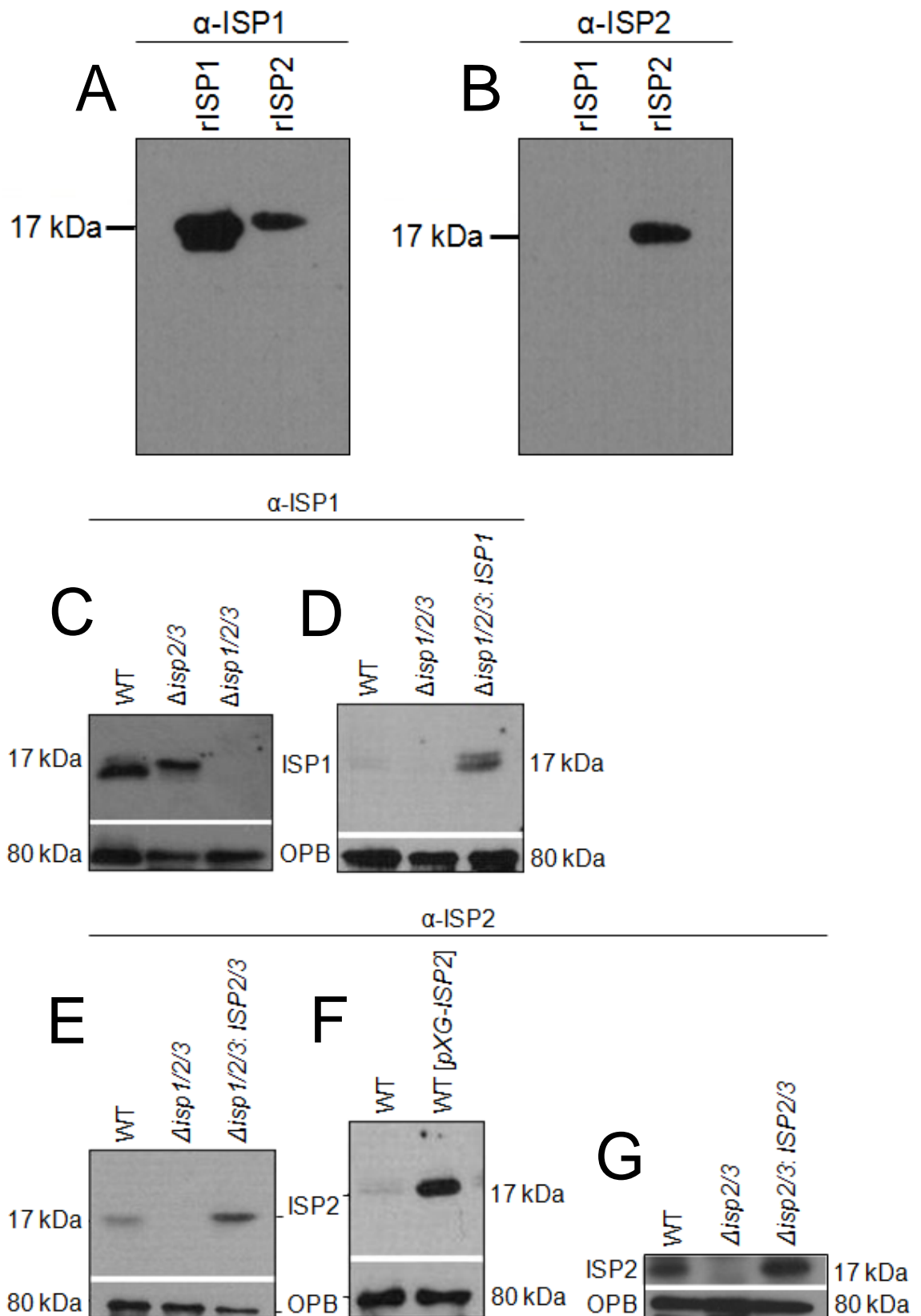


Figure 3-1 Validation of anti-ISP antibodies against extracts from *L. major* ISP gene mutants. Western blots of recombinant ISP1 and ISP2 using purified A) anti-ISP1 (α -ISP1) or B) anti-ISP2 (α -ISP2) primary antibody. Western blots of cell extracts from 10^7 promastigotes of *L. major* WT, Δ isp1/2/3, Δ isp1/2/3:ISP1, Δ isp1/2/3:ISP2/3, WT [pXG-ISP2], Δ isp2/3, or Δ isp2/3:ISP2/3 using purified C and D) α -ISP1, or E to G) α -ISP2. Antibodies against oligopeptidase B (OPB) were used as a loading control.

3.2.2 Immunolocalisation of ISP1 and ISP2

To determine the localisation of ISP1 and ISP2 in *L. major* promastigotes, immunofluorescence was performed using the ISP antibodies against promastigotes from culture. The $\Delta isp1/2/3$ cell line was chosen as a negative control; as neither α -ISP1 nor α -ISP2 had cross-reacted with extracts from this cell line in the Western blots (Figure 3-1, C to E). ISP1 and ISP2 were not detected in immunofluorescence performed with the $\Delta isp1/2/3$ promastigotes (Figure 3-2, A and B respectively), including in the intermediate promastigote form, the haptomonad (Figure 3-2, C and D respectively), which is easily distinguished from the other promastigote forms by the hemidesmosome structure, an expansion of the flagellar tip (Wakid & Bates, 2004).

In *L. major* WT promastigotes, ISP1 and ISP2 were generally localised in the cytosol, with punctate distribution, and along the flagellum, with a noticeable accumulation at the tip of the flagellum (Figure 3-2, G to I). There was also prominent labelling of ISP1 and ISP2 in the haptomonad promastigotes, with an accumulation in the hemidesmosome structure (Figure 3-2, E and F). The hemidesmosome is an expansion of the flagellar tip that enables attachment of haptomonads to the cuticular intima of the stomodeal valve in the sandfly (Killick-Kendrick et al., 1974; Walters et al., 1989). ISP2 was also present on the cell surface of the haptomonad promastigotes (Figure 3-2F), which was not observed for ISP1 (Figure 3-2E).

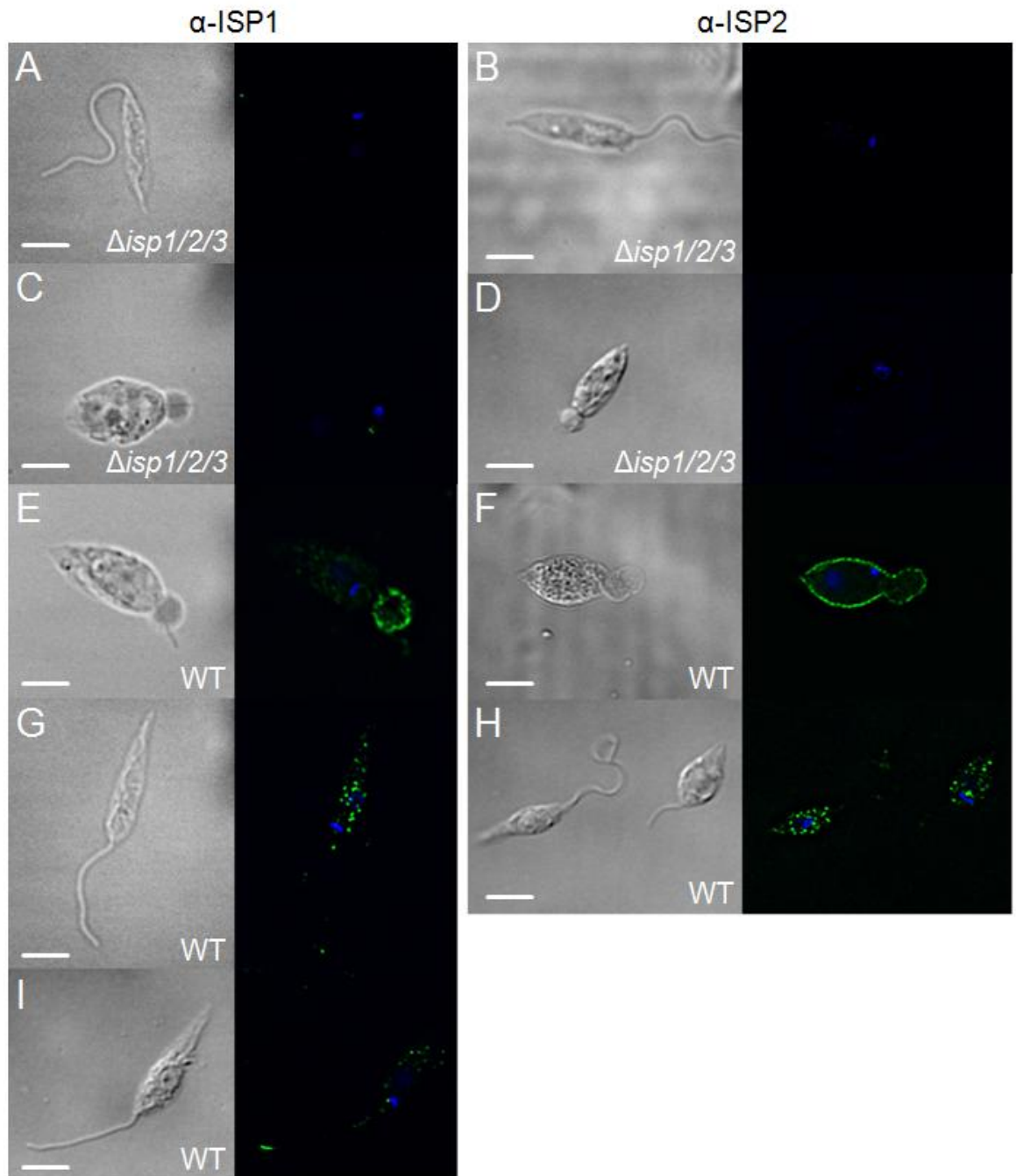


Figure 3-2 ISP1 and ISP2 localisation in *L. major* promastigotes. Fixed *L. major* promastigotes were labelled with α -ISP1 (A, C, E, G, and I) or α -ISP2 (B, D, and F) and donkey anti-sheep Alexa 488-secondary antibody. Nuclear and kinetoplast DNA were stained with DAPI. Left panel, DIC image. Right panel, merged image of ISP (green) and DAPI (blue). Scale bar = 5 μ m.

Eschenlauer et al. (2009) previously showed that only ISP2 was expressed in the amastigote lifecycle stage. To determine where ISP2 is localised, amastigotes were harvested from the footpads of *L. major* WT- and Δ *isp2/3*-infected mice and labelled with the ISP2 antibodies. The Δ *isp2/3* cell line was used as a negative control in these experiments, as ISP2 had not been detected in the extracts from this cell line in the Western blots (Figure 3-1G), and this cell line would be used for the following *in vivo* infections in Chapters 4 and 5. ISP2 was

not detected in immunofluorescence performed with the $\Delta isp2/3$ amastigotes, and as was observed in the promastigotes, ISP2 in WT amastigotes had punctate localisation within the cytosol (Figure 3-3).

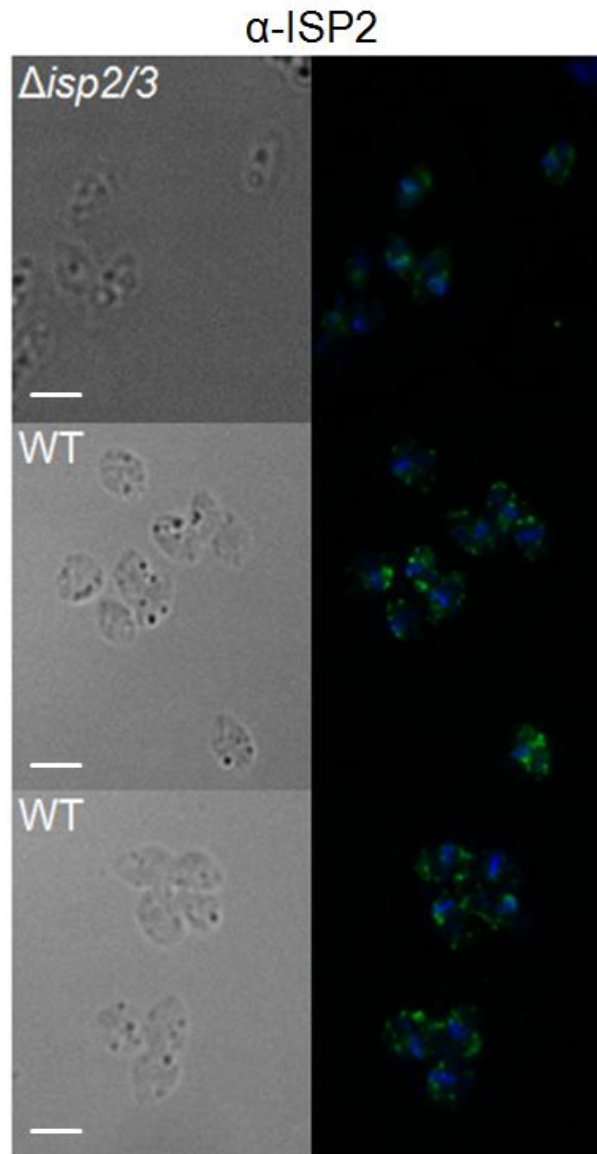


Figure 3-3 ISP2 localisation in *L. major* amastigotes. Fixed *L. major* amastigotes were labelled with α -ISP2 and donkey anti-sheep Alexa 488-secondary antibody. Nuclear and kinetoplast DNA were stained with DAPI. Left panel, DIC image. Right panel, merged image of ISP2 (green) and DAPI (blue). Scale bar = 5 μ m.

3.3 Discussion

Ecotin of Gram-negative bacteria is a periplasmic protein, which has been shown to be required for *Burkholderia pseudomallei* infection of macrophages (Chung et al., 1983; Ireland et al., 2014). *L. major* ISP1 and ISP2 were generally localised in the cytosol and along the flagellum in the promastigote stage of the

Leishmania lifecycle (Figure 3-2, G to I), with a similar cytosolic localisation of ISP2 in the amastigote stage (Figure 3-3).

Interestingly, ISP1 and ISP2 showed prominent labelling in the hemidesmosome structure of haptomonad promastigotes (Figure 3-2, E and F), which are one of the intermediate promastigote forms found during development in the sandfly vector. The hemidesmosome is involved in the attachment of haptomonad promastigotes to the chitin lining of the stomodeal valve in the sandfly (Killick-Kendrick et al., 1974). However, the proteomic composition and further potential roles of the hemidesmosome are still unknown. The localisation within the other promastigote forms, the procyclic, nectomonad, leptomonad, and metacyclic promastigotes, was not assessed on an individual basis as there are only subtle morphological differences, such as the length of the cell body and flagellum, by which to distinguish these forms (Rogers et al., 2002); however, all the promastigotes observed and imaged had the same cytosolic and flagellar localisation. High resolution immuno-electron microscopic analysis could be performed to further determine the subcellular localisation of ISP1 and ISP2 in *L. major* WT promastigotes. The hemidesmosome localisation, in addition to the flagellar localisation, would mean that the ISPs are in close contact with the sandfly SPs, such as trypsin and chymotrypsin, which ISP2, in particular, has been shown to inhibit (Eschenlauer et al., 2009). ISP2 could, therefore, aid in the protection against the proteolytic activity of these enzymes in the sandfly gut (Borovsky & Schlein, 1987). In addition, metacyclic promastigotes are internalised by neutrophils, which are considered the first host cell type for *Leishmania*; azurophilic granules containing NSPs fuse with the *Leishmania*-containing phagosomes (Mollinedo et al., 2010). Microorganisms are degraded in these vacuoles due to acidification and exposure to antimicrobial peptides and proteolytic enzymes, which occurs through the fusion of tertiary granules. However, *Leishmania* are able to survive in the intracellular environment of the neutrophil, as they can selectively prevent the fusion of tertiary granules impeding phagosome acidification and ROS production (al Tuwaijri et al., 1990; Mollinedo et al., 2010). There are no reports that host proteases directly affect *Leishmania* viability, which may be due to the inhibition of NSPs by ISP2. Furthermore, targets of the NSPs, such as the cytokines and cell receptors, are

not present in this environment; therefore, it is unlikely that the inhibition of intracellular NSPs by ISP2 affects cellular responses in neutrophils.

ISP1, which is only expressed, in the promastigote lifecycle stages (Eschenlauer et al., 2009), has low inhibitory activity against trypsin and NE, and has been shown to have an endogenous role in flagellar pocket dynamics and promastigote differentiation (Morrison et al., 2012). ISP1 may target an exogenous SP that has yet to be identified.

ISP1 and ISP2 have not been detected in the *Leishmania* secretome (or exoproteome) (Silverman et al., 2008; Peysseon et al., 2013), in which over 300 proteins are secreted in a non-classical, vesicle-based mechanism (Silverman et al., 2010a). The vast majority of characterised *Leishmania* secreted proteins do not have an identifiable secretion signal sequence, typically only GPI-anchored surface proteins, such as gp63, LPG, and PPGs, have a signal sequence (Silverman et al., 2008). Protein secretion from *Leishmania* can be induced by a temperature shift, as would be experienced by the parasite during transition from the sandfly vector, around 25°C, to the mammalian host at 37°C (Silverman et al., 2010a; Hassani et al., 2011). *Leishmania* exosomes (or microvesicles) have been implicated in the priming of host target cells for *Leishmania* invasion and the modulation of host immune responses (Silverman et al., 2010b; Hassani et al., 2011). *L. donovani* exosomes had immunosuppressive effects on human monocytes and moDCs, but this was dependent upon the composition of the exosome cargo (Silverman et al., 2010b). Further studies are required into the potential exosome localisation of the ISPs. *In vitro* assays by Faria et al. (unpublished) showed that *L. major* WT and $\Delta isp2/3:ISP2/3$ promastigotes, but not $\Delta isp2/3$ promastigotes, inhibit cytokine secretion from macrophages, but this does not occur in Transwell plates. In the Transwell assays, parasites were separated from the macrophages suggesting that the parasites do require contact to exert the effects associated with ISP2.

L. major amastigotes also showed cytosolic localisation of ISP2. *Leishmania* metacyclic promastigotes differentiate into amastigotes inside the PV of macrophages and DCs (Courret et al., 2002; Körner et al., 2006). Macrophages are recruited to the site of *Leishmania* inoculation at 2 to 3 d post-infection to become the main host cell type for the productive *Leishmania* infection

(Thalhofer et al., 2011; Ribeiro-Gomes et al., 2012). SPs have not been detected in the PVs of macrophages and DCs, but NE has been found localised to the cell surface of macrophages, possibly in association with CR3 (Cai & Wright, 1996; Faria et al., 2011). It is still not known whether macrophage clearance of apoptotic neutrophils harbouring parasites leads to the indirect uptake of *Leishmania* (van Zandbergen et al., 2004), or parasites escape or are released from apoptotic neutrophils and are taken up directly by macrophages together with the apoptotic cells (Peters et al., 2008; Ritter et al., 2009). Once the parasites have been internalised by the macrophages and DCs, however, it is unlikely that ISP2 will have any effect, as the NSPs are primarily found bound to the surface of these cells, or in the extracellular environment. NE released from neutrophils has been shown to induce parasite killing in *L. major*-infected C57BL/6 macrophages *in vitro* (Ribeiro-Gomes et al., 2004, 2007). However, *in vivo* the number of neutrophils present at the site of *Leishmania* infection is very low by the time macrophages become the predominant infected host cell. In addition, there will be extracellular parasites present; therefore, the neutrophil-macrophage co-cultures used by Ribeiro-Gomes et al. (2004, 2007) may not reflect the situation at the site of infection *in vivo*.

It has also been reported that C57BL/6 mice infected with *L. mexicana* have higher numbers of degranulated mast cells than BALB/c mice at 3 d post-infection (Villaseñor-Cardoso et al., 2008). Mast cells are another source of NE and PR3. ISP2 may have effects throughout *Leishmania* infection due to the continuous cellular recruitment of SP sources. It is not clear how amastigotes are released from macrophages and DCs; the cells may burst or the PVs may be released by exocytosis. ISP2 from extracellular amastigotes could possibly inhibit the activity of NSPs released by cellular degranulation events, as has been shown with neutrophils and mast cells that occur later in *Leishmania* infection. It was hypothesised by Eschenlauer et al. (2009) and Faria et al. (2011) that ISP2 would have an effect during the early phase of mammalian infection, specifically on the innate immune response involving neutrophils. ISP2 of metacyclic promastigotes and amastigotes could, however, mean the inhibition of NSPs over the course of *L. major* infection. This means ISP2 could have a multitude of effects on *Leishmania* disease progression, due to differential concentrations of NSPs, based on the cell populations present and timings of degranulation events,

as well as the numerous functions of NSPs *in vivo*, such as the regulation of cell recruitment and activation.

Faria et al. (2011) showed that ISP2 inhibits the activity of NE; the other NSPs, CG and PR3, are also potential targets of ISP2 during *Leishmania* infection in the mammalian host. Once released from the innate immune cells into the extracellular environment, the NSPs are able to remain active through several mechanisms, despite the presence of naturally occurring protease inhibitors. The main inhibitor of NE, CG, and PR3 is α -1 antitrypsin (AAT, or α -1 proteinase inhibitor) from the serpin family, which is produced predominantly by hepatocytes, in addition to other sources including epithelial cells, neutrophils, and macrophages (Korkmaz et al., 2010). AAT is the most abundant serpin present in human blood at between 1.2 and 2 mg ml⁻¹ in a healthy human. Monocyte neutrophil elastase inhibitor (MNEI) synthesised and secreted by neutrophils and macrophages also inhibits all three NSPs. Another inhibitor of CG is the serpin, α -1-antichymotrypsin (ACT). Serpins function by presenting their reactive site as a substrate for the protease, which traps the enzyme and distorts its catalytic site (Huntington, 2011). Elafin (or skin-derived antileukoprotease, SKALP) from the chelonianin family inhibits NE and PR3, and secretory leukocyte protease inhibitor (SLPI), also from the chelonianin family and secreted by epithelial cells, neutrophils, and macrophages, inhibits NE and CG. These inhibitors regulate excessive extracellular activity of the NSPs. However, the NSPs can evade the action of the host protease inhibitors. High local concentrations of NSPs at sites of inflammation can overwhelm the action of the protease inhibitors, and through the binding of NSPs to the surface of neutrophils and other innate immune cells, the protease inhibitors are unable to gain access to the NSPs. The addition of *L. major* ISP2 at the site of infection could overcome this protease-protease inhibitor equilibrium, and inhibit the activity of NSPs, leading to a modulation of the host immune responses.

Faria et al. (2011) have previously shown that the NE produced by RAW 264.7 monocytes/macrophages *in vitro*, which have not been exposed to other SP sources, was sufficient for the upregulation of *L. major* Δ isp2/3 promastigote internalisation compared with that of WT promastigotes. In addition, ISP2 produced by *L. major* WT was sufficient to inhibit the activity of NE found on

macrophages isolated from the peritoneal cavity of C57BL/6 mice preventing the upregulation of internalisation and the production of ROS. Macrophages are considered the main host cell for *Leishmania* spp. so these data are important in showing that ISP2 can suppress the microbicidal activities of these host cells to allow intracellular parasite survival and growth. However, *in vivo* there is an influx of other inflammatory cells to the site of infection, including neutrophils and monocytes, which are important sources of the putative target S1A serine peptidases. It is not known yet whether the internalisation and parasite killing processes of these phagocytic cell types are affected in the same way as the macrophages by *L. major* ISP2. There could be an important role for ISP2 in the establishment of the initial *L. major* infection, as neutrophils are considered the primary host cell type for *Leishmania*. Faria et al. (2011) also showed that ISP2 produced by *L. major* WT is sufficient to inhibit the activity of NE on macrophages *in vitro*, however the case *in vivo* will likely be very different. The site of *Leishmania* infection will be flooded with SPs from multiple sources, including the neutrophils, monocytes, macrophages, and mast cells. Addition of exogenous NE to C57BL/6 macrophages during interaction with *L. major* WT and $\Delta isp2/3$ promastigotes *in vitro* caused an increase in internalisation of WT parasites in a dose-dependent manner, and reduced intracellular parasites at 72 h post-infection, but there was no effect on the uptake of $\Delta isp2/3$ parasites (Faria et al., 2011). The addition of parasites to co-cultures of macrophages and neutrophils could give a better indication of whether the additional presence of NSPs from other innate cells affects the inhibitory activity of ISP2, consequently affecting the internalisation and parasite killing processes of the macrophages. This also poses the question as to whether the ISP2 produced by *L. major* is sufficient to inhibit the activity of NE to enable parasite survival in phagocytic cells *in vivo*. *L. major* $\Delta isp2/3$ parasites were internalised more efficiently by macrophages *in vivo* at 3 h after an intraperitoneal infection of C57BL/6 mice, in the presence of the resident and recruited cells (Faria et al., 2011). The parasite burdens within these macrophages were determined after 24 h of culture *in vitro* to evaluate parasite survival, which showed the same as the *in vitro* macrophage infection assays, with higher parasite burdens of *L. major* WT compared to $\Delta isp2/3$ parasites.

Although the expression of ISP2 is abundant in *L. major* WT, if there is no secretion of ISP2, will cell surface localisation allow for the inhibition of the extracellular SP activity and the activity of those that are bound to the surface of the innate immune cells? Furthermore, would this contribute to differences in disease progression depending on the initial parasite dose? Addition of exogenous NE promoted higher internalisation and reduced parasite burdens of *L. major* WT *in vivo* (Faria et al., 2011), which suggests the ISP2 produced by *L. major* WT is sufficient to inhibit the activity of the NE at the site of inoculation. In this case, however, an intraperitoneal infection was used, which is not the best model for *L. major* infection, as will be discussed in Chapter 4, as the parasites are able to disperse further, and therefore, the concentration of SPs may be lower, in contrast to the low dose intradermal inoculations of *Leishmania*, where the parasites and SPs are limited to the site of inoculation. In addition, it has been reported that the innate cell recruitment differs based on the site of inoculation, in that neutrophils are not necessarily the principal responders in peritoneal infections, which could alter the contribution of SPs in the different sites of inoculation (Ribeiro-Gomes et al. 2014). To address whether ISP2 is able to promote *L. major* survival *in vivo*, it would be useful to assess the parasite burden in infected macrophages from dermal sites.

The activation of specific cell receptors by NSPs has also had an effect on the production and secretion of cytokines and chemokines: an increase in CXCL1 (KC), CXCL2 (MIP-2), TNF- α , and IL-6 release has been observed from C57BL/6 macrophages infected with *L. major* $\Delta isp2/3$ promastigotes compared with those infected with WT promastigotes (Faria et al., unpublished). This suggests that preventing the activation of the TLR4-NE signalling cascade by ISP2 could have additional effects that have not, as yet, been fully studied. One of the major functions of NSPs is the proteolytic modification of cytokines and chemokines (Pham, 2008). It is possible that these functions are also affected by the presence of *L. major* ISP2 *in vivo*, in that, inhibition of NSP activity could modulate the recruitment and activation of specific innate immune cell types *in vivo*, which will be discussed in Chapter 5. In Chapters 4 and 5, the role of *L. major* ISP2 in parasite survival and the modulation of innate immune responses *in vivo* will be assessed.

4 Comparison of parasite dissemination and burdens of *L. major* wild-type and *ISP2* gene mutants *in vivo*

4.1 Introduction

4.1.1 Considerations for an experimental mouse model to mimic natural *L. major* infection

At the site of *Leishmania* infection, there is a complex interplay between the parasites and the cells, and other components, of the host immune response. *In vivo* experimental animal models have been a powerful tool in dissecting these host-parasite interactions and elucidating the roles of immune cells, cytokines, chemokines, and signal transduction cascades, during infection with the different *Leishmania* species. However, heterogeneity in the parameters that can affect the immune response in animal models exists between studies. This creates a challenge in relating and assembling the findings made in such studies together in order to generate a potential description of the host immune responses that may be relevant to the human disease. To more reliably translate and extrapolate the discoveries made in animal models to that of the corresponding human disease, there is a requirement for a reproducible model of “natural” infection, with focus on *L. major* infection, as proposed by Belkaid et al. (2000). In terms of the animal model, these factors include the host species or strain, the sex and age of the host, and the site of inoculation. Whilst in terms of the parasite, these include the *L. major* strain, the inoculation dose, and the lifecycle stage. Other considerations are the method of parasite delivery, whether parasites are delivered by needle inoculation or sandfly bite, the needle gauge, the volume of parasite suspension injected, and the use of sandfly salivary components, as well as the time-points after infection which are assessed.

The inbred mouse strains, C57BL/6 and BALB/c, have long been used to investigate the mechanisms involved in the differentiation of polarised Th1 or Th2 responses during *L. major* infection that control resistance or susceptibility to infection respectively. The resistance and susceptibility disease phenotypes of

mouse strains to *L. major* infections have been determined based on their ability to resolve cutaneous lesions, the parasite burdens at the site of inoculation and in the dLNs, and the T helper response profile induced during infection. The homogeneity of the genetic backgrounds of the defined inbred mouse strains has provided reproducible systems for studying the immune responses in experimental diseases that resemble the spectrum of clinical manifestations of leishmaniasis observed in humans. Obviously, this is not the case in human disease, where the host genetics of the individual can affect the outcome of disease, but this is impossible to replicate in experimental models of infection. *L. major* infection in BALB/c mice leads to the development of non-healing lesions due to uncontrolled parasite replication, which is attributed to the development of Th2 cells (Locksley et al., 1991). The C57BL/6 mouse model, however, is thought to be more relevant to the human cutaneous disease, due to the spontaneous healing of localised lesions following *L. major* infection, which is typically seen in immunocompetent patients with cutaneous leishmaniasis. The resistance phenotype of C57BL/6 mice involves the production of IFN- γ by Th1 cells, which stimulates the synthesis of iNOS generating the production of NO, a potent cytotoxin responsible for the killing of *Leishmania* parasites (Locksley et al., 1991; Park et al., 2000). There are other murine models available, which exhibit resistance to *L. major*, including C3H/He, CBA/H, and 129/Sv (Lipoldová & Demant, 2006), although these models are less frequently used because less is known about the immune response mechanisms mediating the resistance to *L. major* in these models. Recently, humanised mice, in which human hematopoietic stem cells are transplanted into immunodeficient NOD-*scid* *IL2 γ* ^{null} mice, have been used to characterise *L. major* infection in the context of the cellular components of the human immune system, such as T, B, and NK cells (Wege et al., 2012). This novel model of a human immune system in a murine environment could be useful to characterise interactions between specific human immune cell subsets and the *Leishmania* parasites; however, a systemic disease, with no self-healing, developed upon *L. major* infection, which is not indicative of an *L. major* infection in immunocompetent humans. It is important to take into account the genetic background of transgenic mice used in studies for the selection of appropriate controls, and to be able to explain discoveries in the context of human disease. Often overlooked is the fact that differences have been reported in the immune response of the mouse models to

Leishmania attributed to the sex and age of the host (Giannini, 1974; Alexander, 1988; Snider et al., 2009). To reduce biological variation in studies, mice are of the same strain and sex, and are often age-matched.

Generally lesion size over the course of *L. major* infection is taken as a measure of disease progression. Weekly dial or vernier caliper measurement of footpad thickness after subcutaneous inoculation of *L. major* is the simplest technique to track lesion formation and resolution. However, sandfly bites are typically intradermal, rather than subcutaneous or intraperitoneal, as the proboscis is less than 0.5 mm in length, and so can only penetrate the superficial layers of the skin. Intradermal inoculations can be performed at the base of the tail or in the ear pinna. The skin is comprised of specialised cells, such as keratinocytes, LCs, as well as dermal macrophages and DCs, which rapidly respond to tissue damage and pathogen invasion by producing inflammatory mediators. The cellular composition of the skin can vary so even the site of intradermal inoculation, the tail or ear, can affect the generation of the T helper cytokine profile, in terms of IFN- γ and IL-4, and the severity of disease (Baldwin et al., 2003). Differences in the cellular compositions of the tissue at the site of inoculation can affect the production of inflammatory mediators and the recruitment of innate immune cells, as has been shown in the phagocyte response to intradermal, subcutaneous, and intraperitoneal inoculation of *L. major* (Goncalves et al., 2011; Ribeiro-Gomes et al., 2014).

L. major Friedlin, a laboratory substrain first isolated from a patient in Israel, is often used to study *L. major* infections, as this substrain has been completely sequenced and is easily available (Ivens et al., 2005; Peacock et al., 2007). When investigating the role of *Leishmania* virulence factors in host-parasite interactions and disease progression it is necessary to use a laboratory strain, of which the gene sequence is known, in order to genetically manipulate the parasites to generate cell lines deficient in, or harbouring mutant versions of, the putative virulence factor. Other *L. major* substrains are occasionally used including LV39, isolated from a gerbil in Russia, and IR75 and IR173, which were isolated from humans in Iran. Different substrains have been shown to induce distinct immune responses, as has been shown in the role of B cells in the development of Th2 responses for the susceptibility of BALB/c mice to LV39

infection, but not IR75 or IR173 (Ronet et al., 2008). In addition, to achieve the same level of parasite killing in infected macrophages, LV39 has been shown to require 25 to 500-fold greater concentrations of IFN- γ than that required for the killing of IR173 (Noben-Trauth et al., 2003). All these substrains have been continually passaged *in vitro*; long-term *in vitro* culture has been demonstrated to reduce *Leishmania* infectivity and virulence in animal models compared to those which have been passed through animals (Giannini, 1974). Substrains may also differ from wild *L. major* strains isolated from patients (Kébaïer et al., 2001).

The average number of parasites transmitted by individual sandflies has been determined to be less than 1000 per bite, although the range is from 100 to 100 000 parasites per bite, of which the majority are metacyclic promastigotes (Warburg & Schlein, 1986; Kimblin et al., 2008; Rogers et al., 2010). Parasites collected in the stationary-phase of *in vitro* growth are heterogeneous populations composed of procyclic, nectomonad, leptomonad, haptomonad, and metacyclic promastigotes, of which metacyclic promastigotes comprise less than 20% of the population (da Silva & Sacks, 1987; Morrison et al., 2012). *L. major* metacyclic promastigotes can be purified through negative selection with peanut agglutination (Sacks et al., 1985), which enables control over the composition of the promastigote inoculation into the experimental model. The infective amastigote lifecycle stage can also be used in infections; these can be harvested from the lesions of infected animals and immediately re-inoculated into the experimental model, or grown in axenic culture (Wenzel et al., 2012). The use of amastigotes for *in vivo* infection does not reflect a natural sandfly-derived infection, however, if a putative virulence factor is differentially expressed or stage-specific it may be necessary to use amastigotes (Leifso et al., 2007). High dose inoculation of parasites or the inoculation of amastigotes has been used in studies to induce a faster or greater immune response to the parasites. It has been shown that the use of low dose inocula, 100 metacyclic *L. major* promastigotes, produces a “silent” phase of parasite growth, in which parasites are present but there is no detectable lesion over the first few weeks of infection (Lira et al., 2000; Kimblin et al., 2008), which may prevent the detection of differences between the infection profiles caused by different cell lines. However, excessive parasites present in high dose inocula may be

internalised by other immune cell types, forcing an immune response that may not be representative of a “natural” infection.

The proboscis of the sandfly is less than 0.5 mm long with a diameter of around 30 μm (Peters et al., 2008); there are no syringe needles available that can replicate these dimensions, so it is important to consider the needle gauge and the depth at which the inoculation is performed. It is important to distinguish the parasite-specific immune responses from the inflammatory responses to tissue damage, as has been demonstrated by Peters et al. (2008), who showed that neutrophil recruitment to needle injection in the absence of parasites was not as prolonged as when parasites were inoculated. In addition, the volume of saline, in which the parasites are often suspended, may contribute to tissue damage.

During a sandfly bite, salivary components are transmitted along with the *Leishmania* parasites. Selective components of the sandfly saliva, such as anti-hemostatic or immunomodulatory molecules, or homogenised salivary gland lysate or salivary gland sonicate (SGS), can be co-inoculated with *Leishmania* into experimental models, which has been shown to exacerbate the disease, producing destructive lesions with greater parasite burdens (Titus & Ribeiro, 1988; Belkaid et al., 1998). Pre-exposing mice to the bites of uninfected sandflies, SGS, or specific salivary proteins, however, abrogates these effects (Kamhawi et al., 2000; Teixeira et al., 2014). In *Leishmania* endemic regions, it is likely that individuals will have prior exposure to sandfly saliva from the bites of uninfected sandflies. The composition of the sandfly saliva is likely to vary between sources, in terms of the sandfly species and on an individual sandfly basis. If the purpose of a study is to investigate the role of a putative *Leishmania* virulence factor *in vivo*, the addition of sandfly saliva components prior to or upon *Leishmania* infection may mask the effects caused by the virulence factor.

In this study, disease progression and immune cell dynamics at the site of infection and in the dLN was assessed in response to *L. major* Friedlin WT and *ISP2* gene mutant infection, using a low-dose intradermal model of infection. Resistant C57BL/6 mice, female and usually 8 to 10 weeks old upon inoculation, were used. Mice were infected using a 29G insulin needle, which has a 0.3 mm needle diameter, into the ear dermis with a parasite inoculation dose of 10 000

purified metacyclic *L. major* promastigotes in only 10 µl PBS. A dose of 10 000 metacyclic promastigotes was chosen, as it was within the range determined for the number of parasites transmitted by a sandfly bite, and thought to enable differences between the immune responses to *L. major* WT and the *ISP2* gene mutants to be more easily observed. Salivary gland components were not used, as the intention of this study is to determine the differences caused by *L. major* *ISP2*. The expression of *ISP2* has been shown to be more highly expressed in metacyclic promastigotes and amastigotes compared to procyclic promastigotes (Eschenlauer et al., 2009); therefore, it is expected that if *ISP2* is to have an effect on the modulation of the host immune responses, it will be upon the early responses.

4.1.2 The luciferase gene reporter system

To quantify parasite burden *in vivo* at a specific time-point during infection, often large groups of animals must be euthanised and the tissue of interest taken for microscopic examination, limiting dilution analysis (LDA), or quantitative PCR (qPCR) amplification of parasite DNA. These estimations are often based on a limited sample size, which may not be representative of the parasite burden in the entire organ, particularly if not all the infected tissue is excised or analysed. Non-invasive bioluminescence imaging (BLI) of luciferase-expressing pathogens in live animals has been available for almost 20 years (Contag et al., 1995). Real-time imaging of luciferase-expressing parasites *in vivo* has negated the use of numerous animals for the purpose of determining parasite burdens and tracking disease progression, in accordance with the National Centre for the Replacement, Refinement and Reductions of Animals in Research (NC3Rs). Animals are inoculated with the luciferase-expressing parasites then injected with D-luciferin substrate at each imaging time-point, which enables real-time longitudinal imaging of live, metabolically active parasites in the same individual animals over the entire course of the experiment. D-luciferin is rapidly oxidised with adenosine triphosphate (ATP) by the luciferase-emitting photons, and this bioluminescent signal can be detected with a charge-coupled device (CCD) camera in an *in vivo* imaging system (IVIS) to non-invasively visualise and monitor the infections inside the live animal. The use of the same animals also minimises the biological variation often seen within

and between animal groups, and between time-points investigated in the parasite burden quantification methods.

In vivo BLI has become a powerful tool in following the dissemination of pathogens at the tissue/organ level in many infectious disease models, including trypanosomes (Myburgh et al., 2013), and some *Leishmania* species, such as *L. amazonensis* (Lang et al., 2005; Reimão et al., 2013), *L. donovani* (de La Llave et al., 2011), *L. infantum* (Michel et al., 2011), *L. tropica* (Talmi-Frank et al., 2012), and *L. major* (de La Llave et al., 2011; Giraud et al., 2014), and evaluating the effect of drugs on parasites *in vivo* (Lang et al., 2005; Michel et al., 2011; Reimão et al., 2013). The BLI system, as yet, has not been used to investigate parasite survival and growth of luciferase-expressing cell lines deficient in putative virulence factors directly compared with the luciferase-expressing reference strain.

4.1.3 The role of ISP2 on parasite survival *in vitro*

In vitro studies conducted by Faria et al. (2011) showed that *L. major* deficient in *ISP2* and *ISP3* ($\Delta isp2/3$) were internalised more efficiently by thioglycollate-elicited macrophages of C57BL/6 mice than *L. major* WT parasites or a cell line re-expressing *ISP2* and *ISP3* ($\Delta isp2/3:ISP2/3$). The numbers of intracellular $\Delta isp2/3$ parasites then dropped by 50% by 24 h post-infection, attributed to the production of ROS, compared with *L. major* WT parasites, indicating a role in the establishment of a productive infection (Faria et al., 2011).

To investigate whether this effect also occurred *in vivo*, Faria et al. (2011) inoculated 2×10^7 stationary-phase promastigotes directly into the peritoneal cavity of C57BL/6 mice, and again $\Delta isp2/3$ parasites were found at higher numbers than WT parasites at 3 h post-infection. After cultivation of the parasites for 24 h *in vitro*, intracellular $\Delta isp2/3$ parasites were approximately half the initial number compared to WT parasites. To follow on from this work, the role of *L. major* *ISP2* will be investigated *in vivo*. A low dose intradermal infection model will be employed to determine whether the *ISP2* present in a low parasite dose, 10^4 metacyclic promastigotes, inoculated intradermally is sufficient to confer *L. major* survival in the C57BL/6 mouse model at later stages of infection.

4.1.4 Aims

In vitro studies indicate that ISP2 is required for *L. major* intracellular survival and growth in macrophages upon early parasite-macrophage contact (Faria et al., 2011). In this chapter, the role of ISP2 on parasite survival in a low dose intradermal C57BL/6 infection model will be evaluated up to 10 wk post-infection through the comparison of infection profiles with *L. major* WT parasites, the cell line deficient in *ISP2/3*, Δ *isp2/3*, and the cell line re-expressing *ISP2/3*, Δ *isp2/3:ISP2/3*. As ISP3 is not detected in any *Leishmania* lifecycle stage, and is thought to be a pseudogene (Eschenlauer et al., 2009), it is assumed that differences observed between these cell lines is due to the role of ISP2.

The aims of this chapter are to:

- Monitor lesion progression over the course of infection
- Generate reporter cell lines expressing firefly luciferase (LUC2)
- Track disease progression through BLI
- Evaluate parasite burdens in various organs

4.2 Results

4.2.1 Lesion measurements over the course of infection

Typically lesion size is taken as a measure of disease progression over the course of *L. major* infection, although lesion size does not always directly correlate with parasite burden (Belkaid et al., 2000; Lira et al., 2000; Kimblin et al., 2008; Giraud et al., 2014). Lesion size was first evaluated following low dose subcutaneous inoculation of 10^4 *L. major* WT or Δ *isp2/3* metacyclic promastigotes into the footpads of C57BL/6 mice (Figure 4-1). Metacyclic promastigotes were harvested from *in vitro* culture using peanut lectin agglutination (Sacks et al., 1985), resuspended in PBS, and inoculated into mice. Over the first 5 wk post-infection, the lesions of Δ *isp2/3*-infected mice were significantly higher than those of WT-infected mice. After 5 wk, the lesions of

WT-infected mice began to increase in size, becoming significantly larger than those of $\Delta isp2/3$ -infected mice, which were decreasing at this point.

The lesion size was then evaluated in the low dose intradermal infection model following inoculation of 10^4 *L. major* WT or $\Delta isp2/3$ metacyclic promastigotes into the ears of C57BL/6 mice, as this will be the model of infection used in this study. The mean ear thickness of the uninfected ears of these mice over the course of this experiment was 0.3 mm. Due to the thinness of the ear, accurate measurements were more technically difficult than the footpad thickness measurements. There were no significant differences between the lesions of WT- or $\Delta isp2/3$ -infected mice (Figure 4-2).

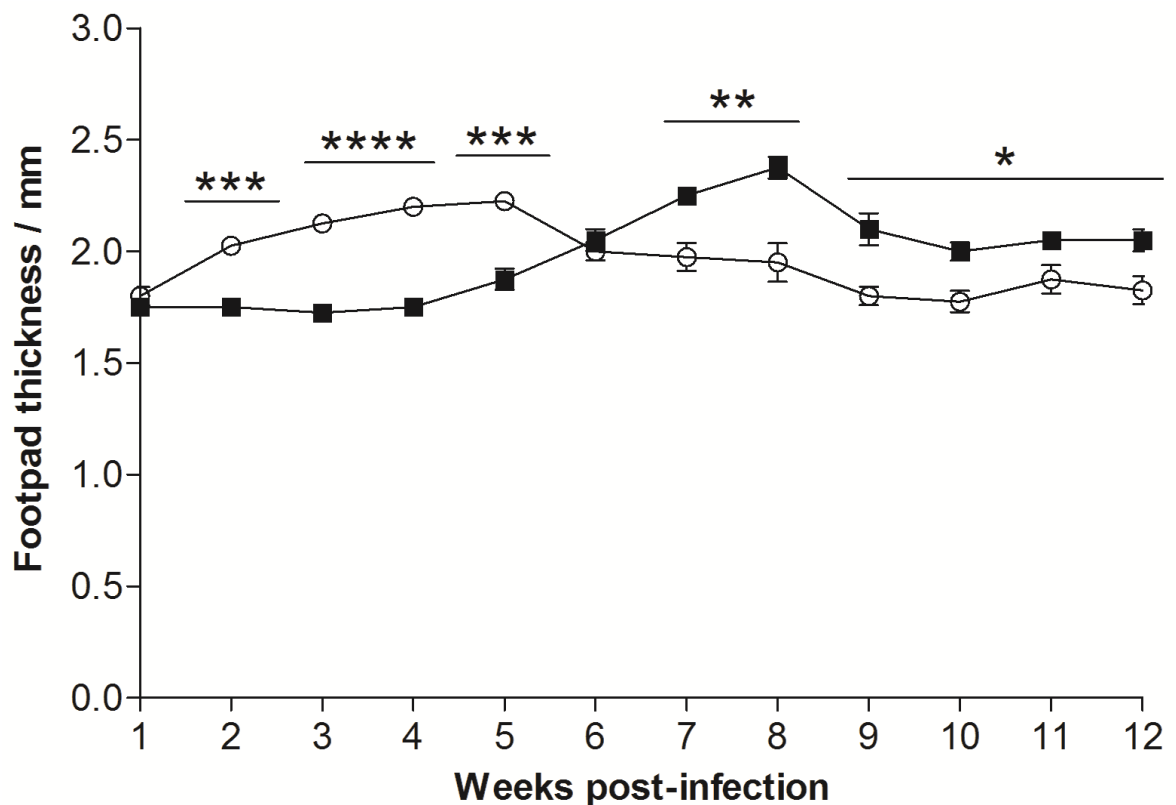


Figure 4-1 Lesion development in the footpads of C57BL/6 mice. Purified metacyclic promastigotes (10^4 in 40 μ l PBS) were subcutaneously inoculated into the footpads of C57BL/6 mice ($n=4$). Footpad thickness was measured weekly with a dial caliper. ■, WT; ○, $\Delta isp2/3$. Error bars represent S.E.M. Asterisks indicate statistical significance between the groups at $p < 0.05$ (*), $p < 0.01$ (**), $p < 0.001$ (***), and $p < 0.0001$ (****), as determined by an unpaired t-test.

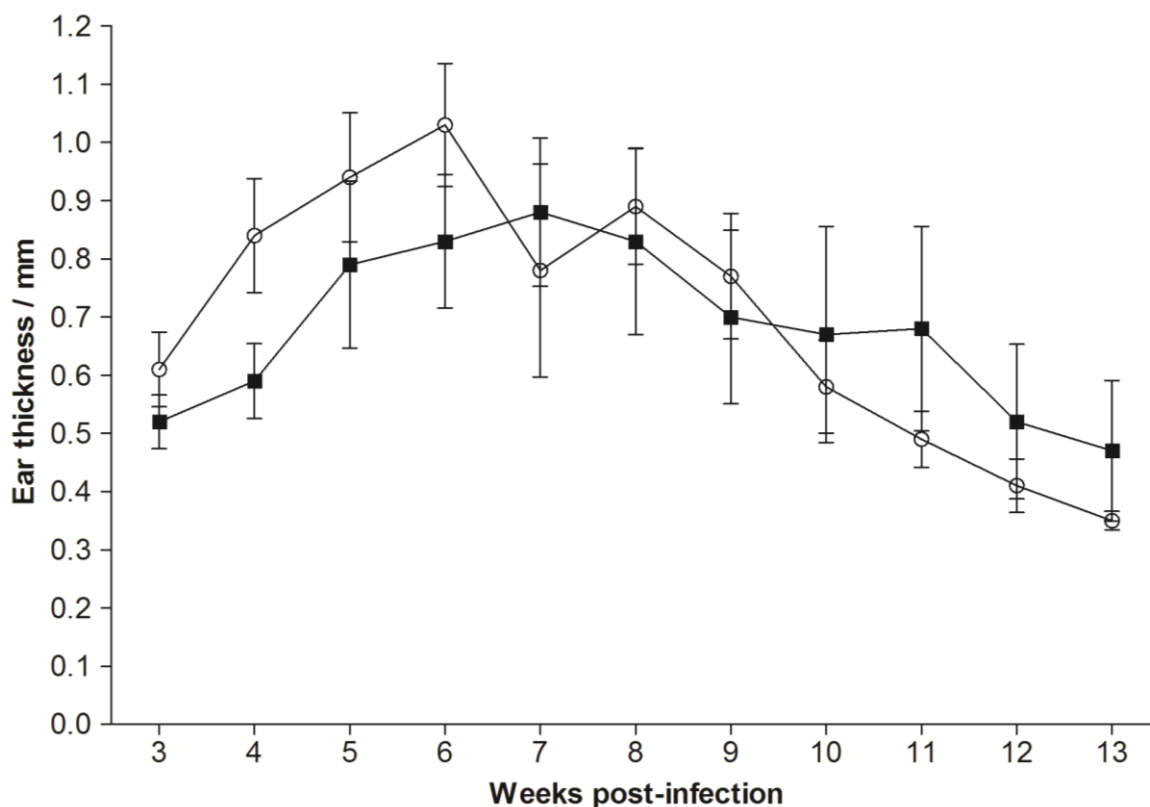


Figure 4-2 Lesion development in the ears of C57BL/6 mice. Purified metacyclic promastigotes (10^4 in $10 \mu\text{l}$ PBS) were intradermally inoculated into the ears of C57BL/6 mice ($n=5$). Ear thickness was measured weekly with a dial caliper. ■, WT; ○, $\Delta isp2/3$. Error bars represent S.E.M.

4.2.2 Generation and characterisation of transgenic bioluminescent cell lines

To enable longitudinal monitoring of transgenic bioluminescent cell lines *in vivo*, *L. major* cell lines expressing the firefly luciferase (LUC2) reporter gene were generated. Transgenic parasites were generated through the integration of the *luc2* gene into the *Leishmania* 18S ribosomal RNA locus of the genome through homologous recombination. This enabled stable constitutive gene expression under the control of the ribosomal promoter, as opposed to episomal expression, which has been reported to cause varying levels of expression due to the copy number variation of the transfected plasmids in each parasite (Roy et al., 2000). Plasmids containing the *luc2* gene, pGL2126 and pGL2357, which have puromycin (PAC) and streptothricin (SAT) resistance cassettes respectively, had a pRIB backbone (pGL631) and were linearised with *PacI* and *PmeI*. The DNA was transfected into the *L. major* WT, $\Delta isp2/3$, and $\Delta isp2/3:ISP2/3$ cell lines. Several clones of the transfected cell lines giving high levels of *in vitro* LUC2 expression were then selected, as assessed through bioluminescent signal using the Luciferase Reporter Gene Assay (Roche) with the parental cell lines as controls.

The levels of *in vitro* bioluminescence were compared between the clones of each cell line at different stages of *in vitro* parasite growth. One clone of each of the bioluminescent cell lines, *L. major*+LUC2, Δ *isp2/3*+LUC2, and Δ *isp2/3:ISP2/3*+LUC2, was chosen, which had the closest levels of LUC2 expression within a particular range. Figure 4-3 shows the *in vitro* bioluminescence, with metacyclic promastigotes of the clones chosen for *in vivo* infections, as this is the lifecycle stage that will be used for the *in vivo* infections. The graph shows that the *in vitro* bioluminescence of the *L. major*+LUC2 cell line was significantly higher than that of the Δ *isp2/3*+LUC2 and Δ *isp2/3:ISP2/3*+LUC2 cell lines, despite attempts to select clones with similar levels of LUC2 expression.

The *in vitro* growth rates of the LUC2-expressing cell lines, *L. major*+LUC2, Δ *isp2/3*+LUC2, and Δ *isp2/3:ISP2/3*+LUC2, were compared against the parental cell lines, parasites lacking the *luc2* gene, *L. major* WT, Δ *isp2/3*, and Δ *isp2/3:ISP2/3*, showing there was no difference in the *in vitro* growth phenotype (Figure 4-4).

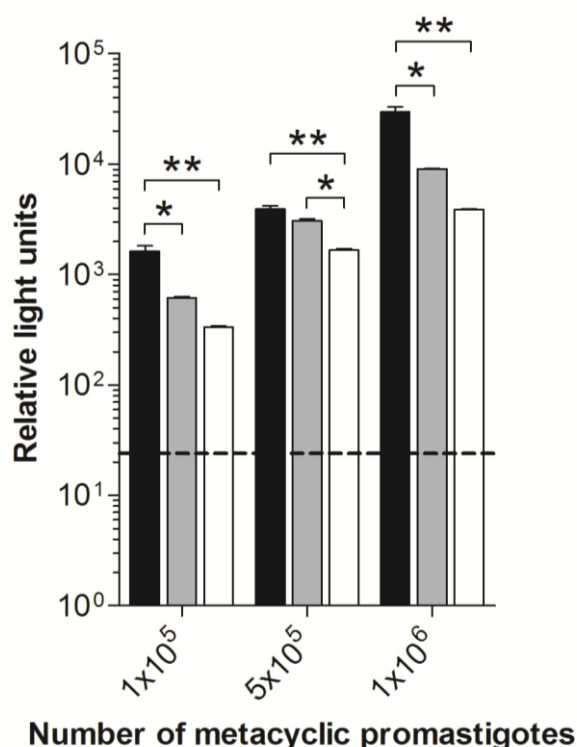


Figure 4-3 *In vitro* luciferase reporter gene assays of LUC2-expressing cell lines. Assays were performed using purified metacyclic promastigotes in the Luciferase Reporter Gene Assay (Roche). Black bar, *L. major*+LUC2; grey bar, Δ *isp2/3*+LUC2; white bar, Δ *isp2/3:ISP2/3*+LUC2. Data are shown on a logarithmic scale. Error bars represent S.E.M of replicate wells. Dashed line indicates background bioluminescence, the mean bioluminescence from wells containing 10^6 purified metacyclic promastigotes of *L. major* WT, Δ *isp2/3*, or Δ *isp2/3:ISP2/3*. Asterisks indicate statistical significance between the groups at $p < 0.05$ (*) and $p < 0.01$ (**), as determined by one-way ANOVA with Tukey post test.

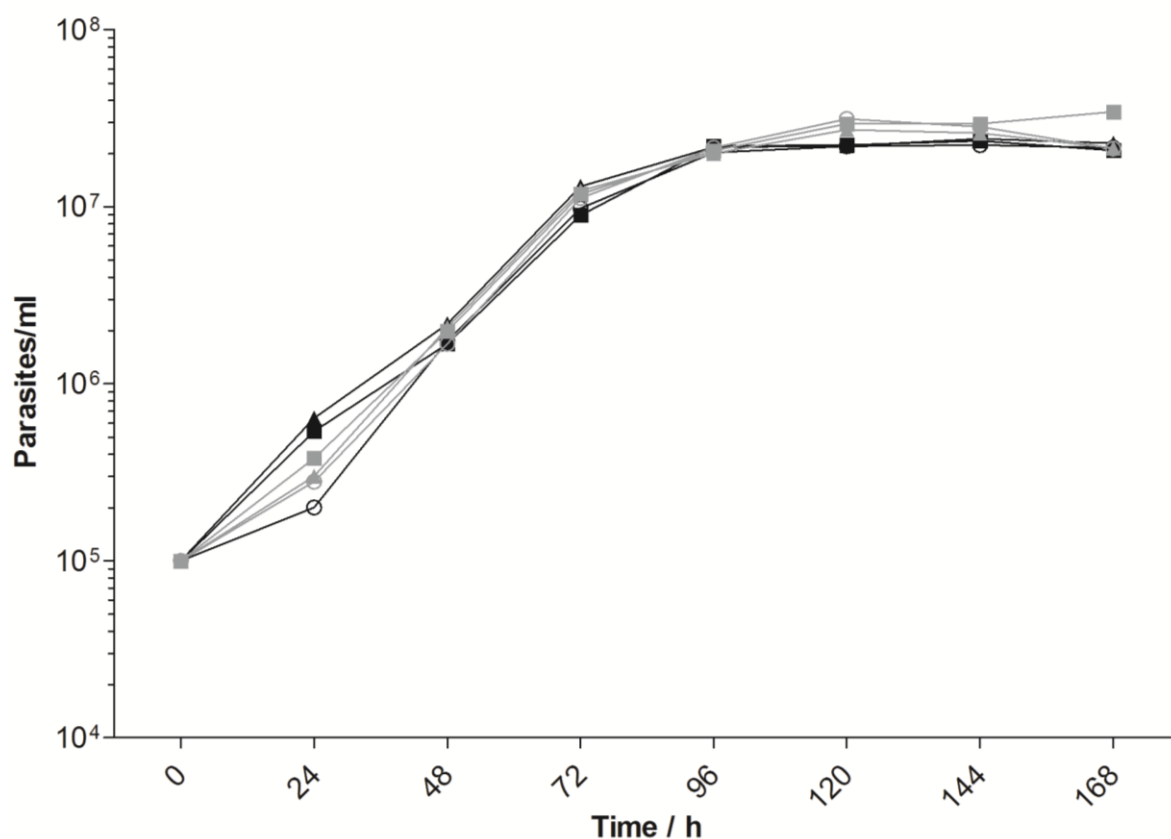


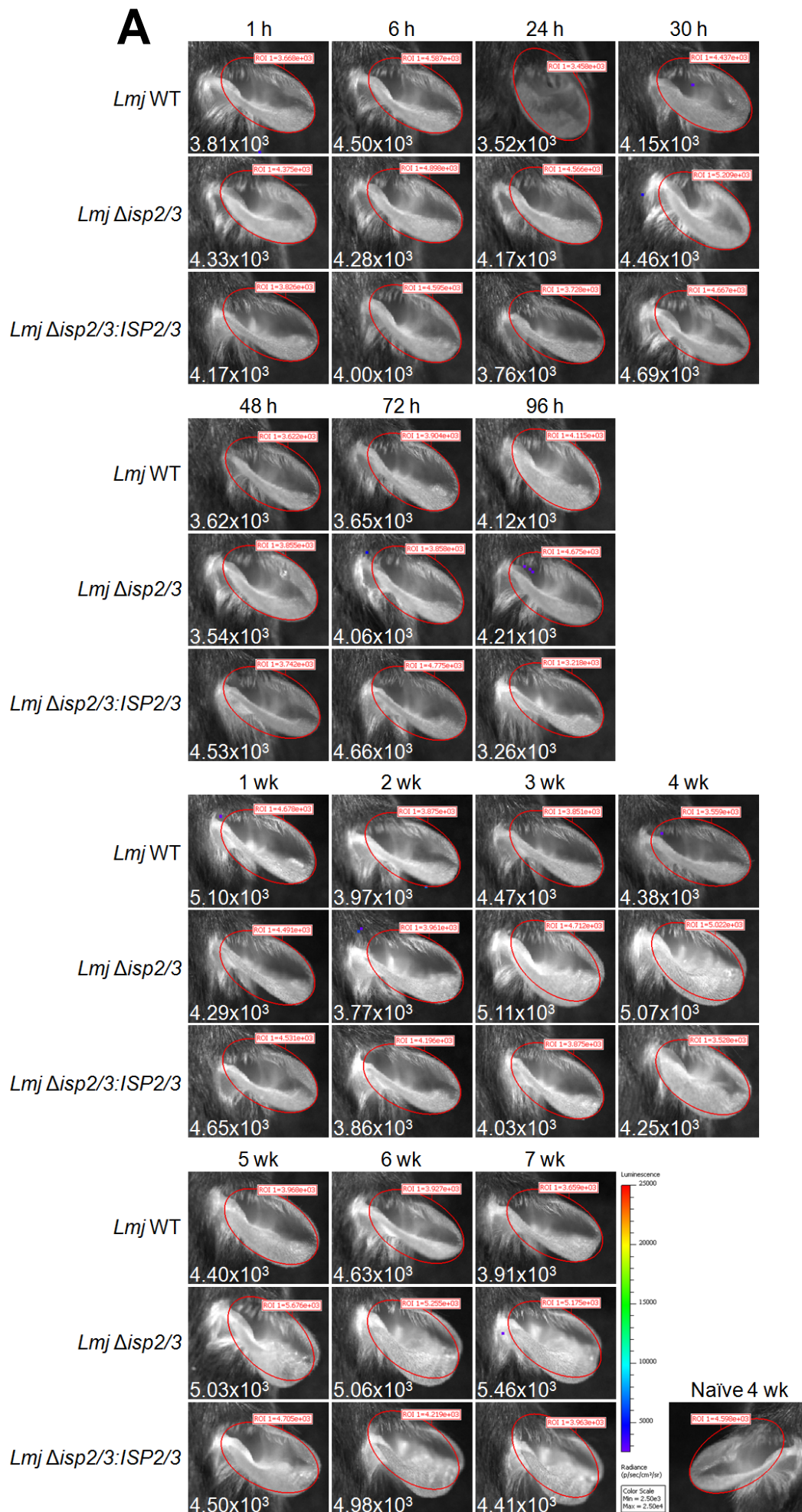
Figure 4-4 *In vitro* growth curves of promastigote cultures of *L. major* WT, Δ isp2/3, Δ isp2/3:ISP2/3 and the LUC2-expressing cell lines. Promastigote cultures were started at 10^5 cells ml⁻¹ and cell densities were determined daily for 7 d. Data shown on a logarithmic scale. ■, WT; ○, Δ isp2/3; ▲, Δ isp2/3:ISP2/3; ■, *L. major*+LUC2; ○, Δ isp2/3+LUC2; ▲, Δ isp2/3:ISP2/3+LUC2.

4.2.3 Tracking parasite bioluminescence with the *in vivo* imaging system (IVIS)

BLI of the three LUC2-expressing cell lines, *L. major*+LUC2, Δ isp2/3+LUC2, and Δ isp2/3:ISP2/3+LUC2 (from Figure 4-3), in the mouse model, enabled the parasite presence in localised cutaneous infections to be imaged in real-time over a period of 7 wk. This made it possible to observe and compare the dynamics of infection, in terms of parasite loads, at both early and late time-points. Metacyclic promastigotes, 10^4 , were inoculated into the ear dermis of C57BL/6 mice. For each time-point after parasite inoculation, mice were injected with the luciferase substrate, D-luciferin, into the peritoneal cavity to induce the bioluminescence from the LUC2-expressing parasites. Mice were anaesthetised then imaged in the IVIS using a CCD camera to detect and capture the photons emitted from the bioluminescent parasites between 10 and 15 min after luciferin injection. Based on preliminary kinetic studies, 10 to 15 min was the optimal time to capture the peak of the luciferase-specific signal from the ear.

Figure 4-5 shows representative images of one mouse per group over the course of infection. A region of interest (ROI) was created that covered the entire surface of the ear, in order to measure the total flux, the photons per second (photons sec^{-1}) over the ROI. The same ROI was used to evaluate the bioluminescent signal in all mice at all time-points, and values given in white are the mean bioluminescent signal for each group, as plotted in Figure 4-6A. A pseudo-coloured image representing the bioluminescence was overlaid onto a photograph as an anatomical reference. Images from the control mice, which were mice inoculated with the parental cell lines, parasites lacking the *luc2* gene, *L. major* WT, $\Delta\text{isp2/3}$, and $\Delta\text{isp2/3:ISP2/3}$, show the background bioluminescence from the ear to be approximately 4.3×10^3 photons sec^{-1} , which is the same as that exhibited in the naive ear of infected mice (Figure 4-5A). A representative image from a naive ear of an infected mouse at 4 wk is shown, as at this time-point ears infected with the LUC2-expressing parasites had a peak bioluminescent signal. One hour after parasite inoculation, there was a bioluminescent signal from the ears of mice inoculated with the LUC2-expressing parasites (Figure 4-5B), 1.5-fold higher for *L. major*+LUC2 and $\Delta\text{isp2/3:ISP2/3}$ +LUC2 infections, and 1.2-fold higher for $\Delta\text{isp2/3}$ +LUC2 infection, as compared to the signal from the control mice (Figure 4-6A). This initial signal decreased to levels seen in the control mice by 24 h and remained low until 1 wk post-infection for the *L. major*+LUC2 and $\Delta\text{isp2/3:ISP2/3}$ +LUC2 infections, and 2 wk post-infection for the $\Delta\text{isp2/3:ISP2/3}$ +LUC2 infection, at which point the signal began to increase above that of the initial signal for all LUC2-expressing groups. This signal continued to increase up to 5 wk post-infection, at 1.04×10^5 photons sec^{-1} for the *L. major*+LUC2 infection, but only up to 3 wk, at 4.12×10^5 photons sec^{-1} for the $\Delta\text{isp2/3:ISP2/3}$ +LUC2 infection showing, on average, a 17-fold and 63-fold increase from the initial signals for these groups respectively. The signal from the ears of $\Delta\text{isp2/3}$ +LUC2-infected mice stayed low over the course of infection, as compared with mice infected with the *L. major*+LUC2 and $\Delta\text{isp2/3:ISP2/3}$ +LUC2 cell lines; the highest signal being at 3 wk post-infection, at 1.03×10^4 photons sec^{-1} , only 2-fold higher than the initial signal for this group. After the respective peaks, the signals in all the groups began to decrease, with the signal from only the $\Delta\text{isp2/3}$ +LUC2-infected mice returning to a level equivalent to the background signal by 7 wk post-infection.

At 7 wk post-infection, mice were culled, and the ears and superficial cervical dLNs were removed to determine the parasite burdens in these tissues (Figure 4-6, B and C). In the ear samples, parasites could only be detected in the $\Delta isp2/3:ISP2/3+LUC2$ group, of which only 3 out of 5 ears had detectable parasites, with a mean of 10^3 parasites per ear (Figure 4-6B). Parasites could be detected in the dLNs of all groups, although there was no significant difference in the parasite numbers between the groups, which had means between 1×10^5 and 2×10^5 parasites per dLN (Figure 4-6C).



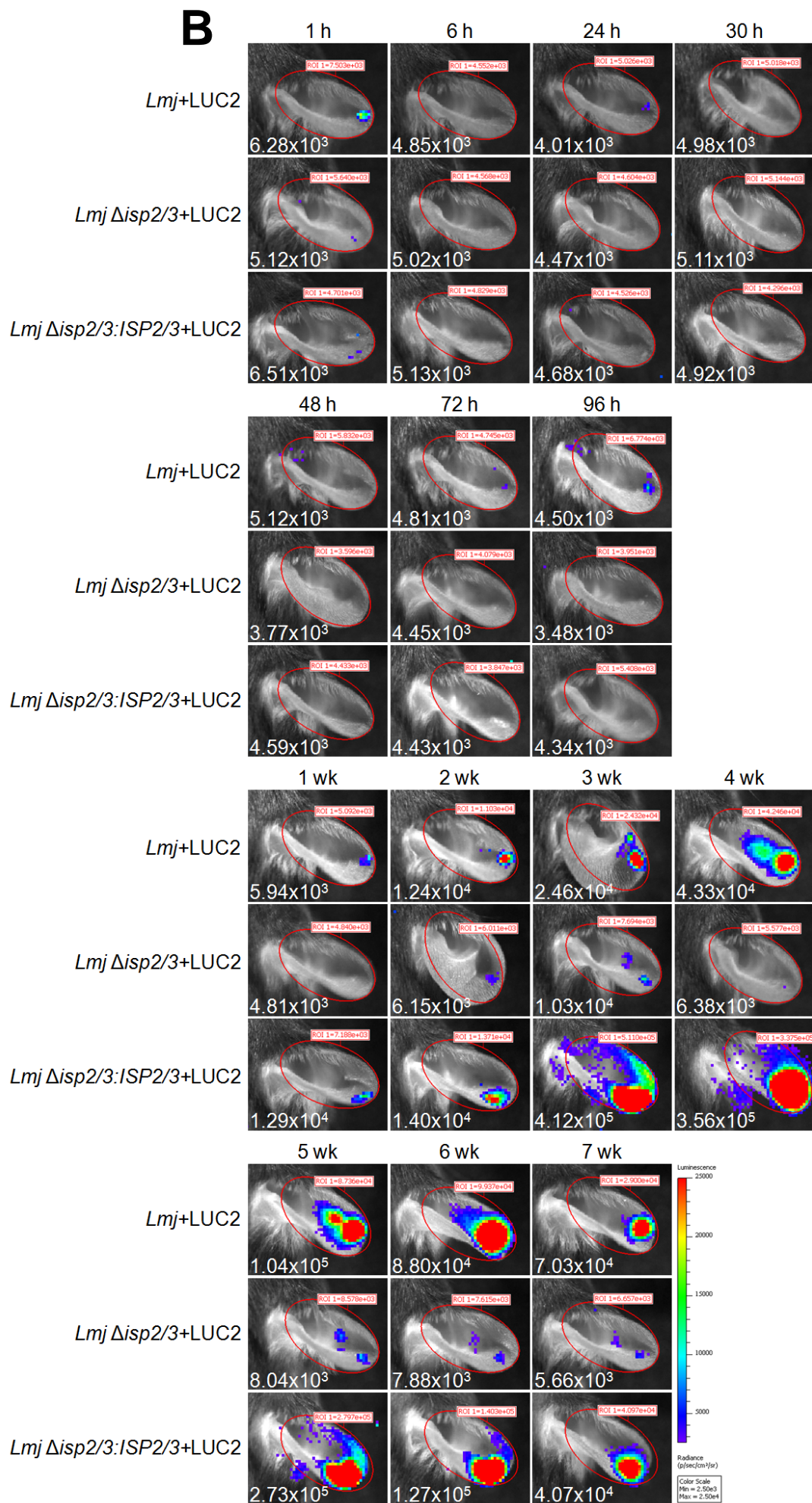


Figure 4-5 *In vivo* bioluminescence imaging of LUC2-expressing cell lines at the site of inoculation. Purified metacyclic promastigotes (10^4 in $10\ \mu\text{l}$ PBS) were intradermally inoculated into the ears of C57BL/6 mice ($n=2$ for *L. major* WT, $\Delta\text{isp}2/3$, and $\Delta\text{isp}2/3:\text{ISP}2/3$, and $n=5$ for LUC2-expressing *L. major*, $\Delta\text{isp}2/3$, and $\Delta\text{isp}2/3:\text{ISP}2/3$). Mice were imaged in the IVIS 10 to 15 min after intraperitoneal D-luciferin injection. Representative images of one mouse per group over the course of infection for **A)** the control mice infected with *L. major* WT, $\Delta\text{isp}2/3$, and $\Delta\text{isp}2/3:\text{ISP}2/3$ parasites, including an image from a naive ear at 4 wk post-infection, and **B)** the mice infected with *L. major*+LUC2, $\Delta\text{isp}2/3$ +LUC2, and $\Delta\text{isp}2/3:\text{ISP}2/3$ +LUC2 cell lines. The colour scale indicates bioluminescent radiance in photons/second/ cm^2 /steradian. The red oval indicates the region of interest (ROI) and the value in the red box indicates the total flux, given in photons per second (photons sec^{-1}), over the ROI in the individual image shown. The same colour scale and ROI was applied to all images analysed. The value in white gives the mean total flux for the group at each time-point.

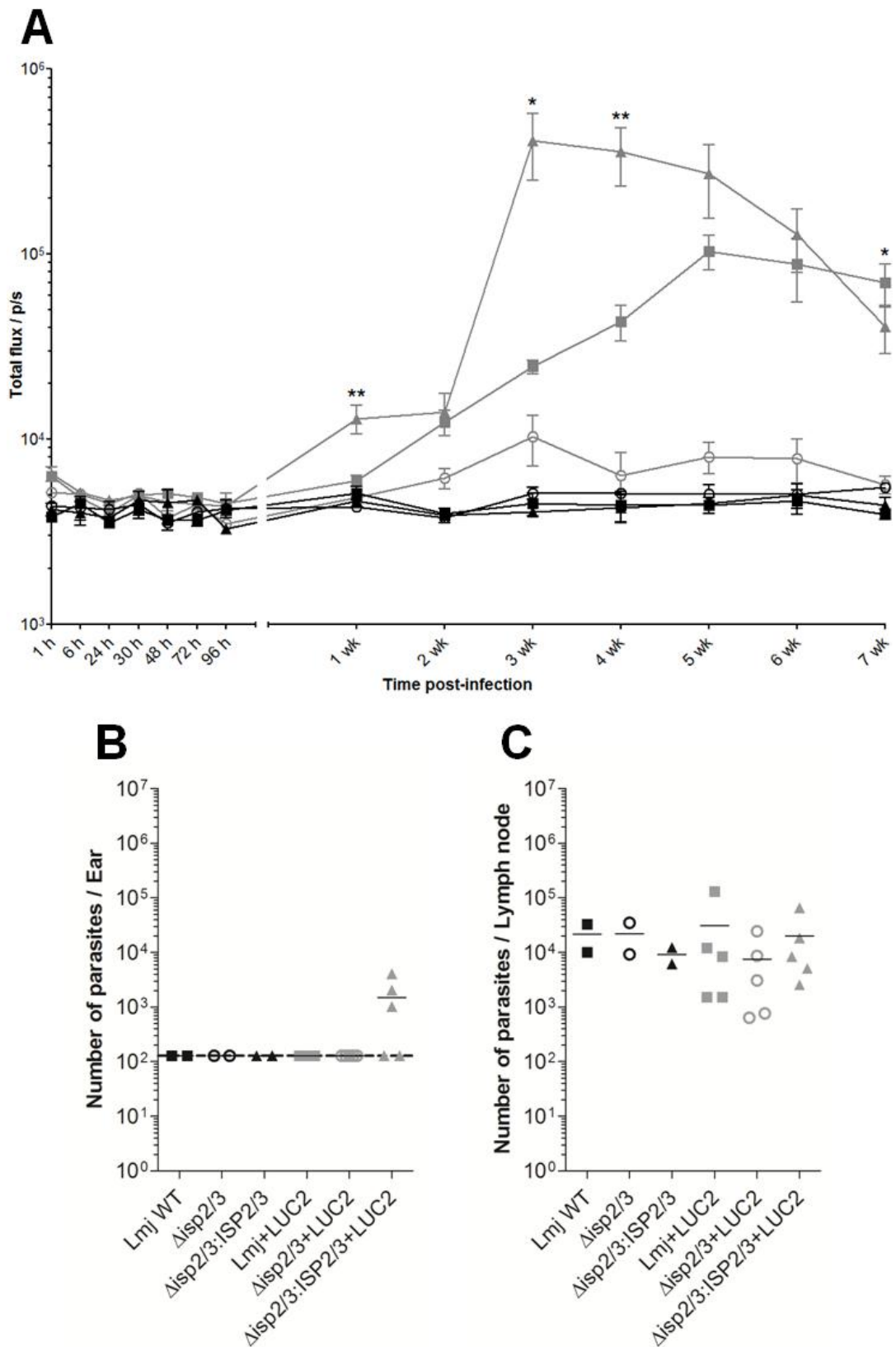


Figure 4-6 Quantification of bioluminescent signal from LUC2-expressing cell lines, and parasite burdens at the site of inoculation and in the draining lymph node. **A)** The mean total flux over the ROI of the ear, given in photons per second (photons sec^{-1}), for each group of infected mice at each time-point over the course of 7 wk infection. ■, *L. major* WT; ○, Δ isp2/3; ▲, Δ isp2/3:ISP2/3; ■, *L. major*+LUC2; ○, Δ isp2/3+LUC2; ▲, Δ isp2/3:ISP2/3+LUC2. Error bars represent S.E.M. Asterisks indicate statistical significance between the LUC2-expressing groups at $p < 0.05$ (*) and $p < 0.01$ (**), as measured by one-way ANOVA with a Tukey post test. Parasite loads in **B)** the ear and **C)** the dLN at 7 wk post-infection, as determined by LDA. Parasite loads from the individual samples are shown with the lines indicating the mean for the group. Dashed line indicates the lower limit of detection. Data are shown on a logarithmic scale.

4.2.4 Measurements of tissues and quantification of parasite loads

To further evaluate any pathological features of infection and parasite burdens, the ears and dLNs, as well as the livers and spleens, were removed from C57BL/6 mice intradermally inoculated with 10^4 metacyclic promastigotes of *L. major* WT, $\Delta isp2/3$, or $\Delta isp2/3:ISP2/3$. The mean diameters of the dLNs were calculated by taking the average of three diameter measurements around the dLN with a vernier caliper. The masses of the livers and spleens were also evaluated. The ears, dLNs, livers, and spleens were then homogenised and limiting dilutions were performed.

Lymph node diameter was measured at 2, 5, and 10 wk post-infection (Figure 4-7A). At 2 wk post-infection, there was no significant difference in the dLN diameter of WT-, $\Delta isp2/3$ -, and $\Delta isp2/3:ISP2/3$ -infected mice, which ranged between 1.3 and 2.4 mm in diameter. By 5 wk post-infection, the dLN diameter of WT- and $\Delta isp2/3$ -infected mice was 2-fold and 2.3-fold higher than measurements taken at 2 wk post-infection, respectively. Whereas the mean dLN diameter of $\Delta isp2/3:ISP2/3$ -infected mice at 5 wk post-infection was only 1.4 mm greater than that observed at 2 wk post-infection. The mean dLN diameter of $\Delta isp2/3$ -infected mice, 3.7 mm, was significantly larger than $\Delta isp2/3:ISP2/3$ -infected mice, 2.6 mm, at 5 wk post-infection. At 10 wk post-infection, the mean dLN diameters for the groups were similar to those observed at 5 wk post-infection, although there was no significant difference between the parasite groups.

LDAs were performed using ears infected for 2, 5, and 10 wk; however, at 2 wk post-infection, parasites could not be detected in the ears of mice infected with any of the parasite groups, WT, $\Delta isp2/3$, or $\Delta isp2/3:ISP2/3$. At 5 wk post-infection, in the first experiment, parasites could not be detected in any of the ears infected with $\Delta isp2/3$ parasites (Figure 4-7B, first column), and in a second experiment, $\Delta isp2/3$ parasites could not be detected in 4 out of the 5 ears (Figure 4-7B, second column). In both these experiments, WT parasites could be detected in all, but one, of the ear samples (Figure 4-7B, first and second columns), with mean parasite loads of 2.1×10^4 and 6.4×10^3 parasites per ear in the two independent experiments respectively. At 10 wk post-infection, $\Delta isp2/3$ parasites could, again, not be detected in the ears, and at this time-point, WT

parasites could only be detected in 3 out of the 5 ears, with a mean parasite load of less than 1000 (Figure 4-7B, third column). At both 5 and 10 wk post-infection, the mean parasite loads in $\Delta isp2/3:ISP2/3$ -infected ears were significantly higher than those of $\Delta isp2/3$ - and WT-infected ears, at 1.9×10^6 and 2.8×10^5 parasites per ear in the two independent experiments respectively (Figure 4-7B, second and third columns).

Parasites were detected in the dLNs of mice infected with all of the parasite groups, WT, $\Delta isp2/3$, or $\Delta isp2/3:ISP2/3$, at 5 and 10 wk post-infection, and there was no significant difference in the parasite loads between these groups (Figure 4-7C, second and third columns). At 5 wk post-infection, the mean parasite loads of WT infections in the dLNs were 2.3×10^4 and 8.6×10^4 parasites per dLN in the first and second experiments respectively (Figure 4-7C, first and second columns). In the first experiment, the mean parasite loads of WT infections in the ear and dLN were similar at 2.1×10^4 and 2.3×10^4 parasites respectively (Figure 4-7, B and C, first column), whereas in the second experiment, the mean parasite load in the dLN was approximately 13-fold higher than those at the site of infection, the ear, at this time-point (Figure 4-7, B and C, second column). In the first experiment at 5 wk post-infection, there was a significantly higher WT parasite load in the ear compared with $\Delta isp2/3$ infection, and this was also observed in the dLN (Figure 4-7, B and C, first column). However, in the second experiment at 5 wk post-infection, although there were significantly more $\Delta isp2/3:ISP2/3$ parasites in the ear compared with WT and $\Delta isp2/3$ parasites, there was no significant difference in the parasite loads between the parasite groups in the dLNs (Figure 4-7, B and C, second column). These differences may be due to biological variations between the animal groups used for each experiment. At 10 wk post-infection, there was, again, no significant difference in the parasite loads between the parasite groups in the dLNs; however, the mean parasite loads of $\Delta isp2/3:ISP2/3$ infections at 10 wk was 2.5×10^5 parasites per dLN, which was higher than that observed for WT and $\Delta isp2/3$ infections, which were 1.1×10^3 and 2.7×10^2 parasites per dLN respectively (Figure 4-7C, third column). Of note, the parasite loads for WT and $\Delta isp2/3$ infections at 10 wk were lower than those observed at 5 wk, which is depicted in Figure 4-7D, in addition to two other LDAs performed at 12 and 14 wk post-infection comparing WT and $\Delta isp2/3$ infections in the dLN following an ear dermis inoculation of

these parasite cell lines. These data show that both *L. major* WT and $\Delta isp2/3$ parasites persist in the dLN beyond 10 wk post-infection.

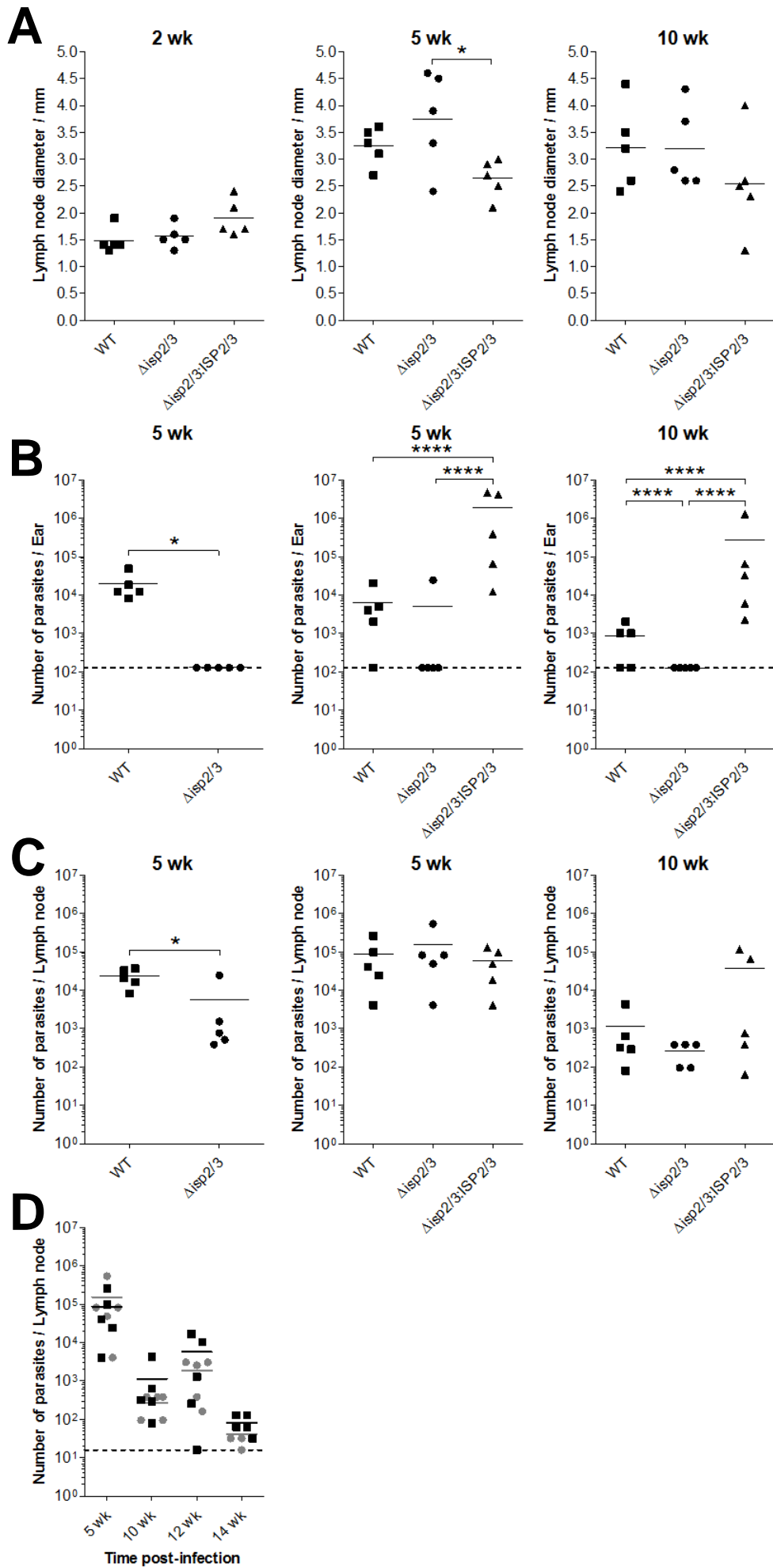


Figure 4-7 Parasite burdens during infection with *L. major* WT, $\Delta isp2/3$, and $\Delta isp2/3:ISP2/3$. Purified metacyclic promastigotes (10^4 in $10\ \mu\text{l}$ PBS) were intradermally inoculated into the ears of C57BL/6 mice ($n=5$ for each time-point). The parasite loads of the ear and dLN in the first column at 5 wk were collected from the same mice, and the data represented in the second column, 5 wk, and third column, 10 wk, were collected from the same mice respectively. **A)** The dLNs were removed at 2, 5, and 10 wk post-infection, and the diameter was measured by vernier caliper. Parasite loads in the **B)** ear and the **C)** dLN at 5 and 10 wk post-infection were determined by LDA. **D)** Graph showing the parasite loads in the dLNs of mice infected with WT (■) or $\Delta isp2/3$ (●) parasites at 5 (C, second column), 10 (C, third column), 12, and 14 wk post-infection from independent experiments. Dashed lines indicate the lower limit of detection. Asterisks indicate statistical significance between the groups at $p < 0.05$ (*) and $p < 0.0001$ (****), as measured by an unpaired t-test or a one-way ANOVA with a Tukey post test.

Mass measurements and limiting dilutions of the livers and spleens were also performed at 2, 5, and 10 wk post-infection, to determine whether parasites from any of the three cell lines had disseminated beyond the dLN. There were no significant differences in the masses of the livers and spleens of mice infected in the ear with *L. major* WT, $\Delta isp2/3$, or $\Delta isp2/3:ISP2/3$ parasites (Figure 4-8), except at 2 wk post-infection in which the liver mass from WT-infected mice was higher than that of $\Delta isp2/3$ -infected mice (Figure 4-8A, first column). No parasites were detected for any of the groups at any of the time-points investigated.

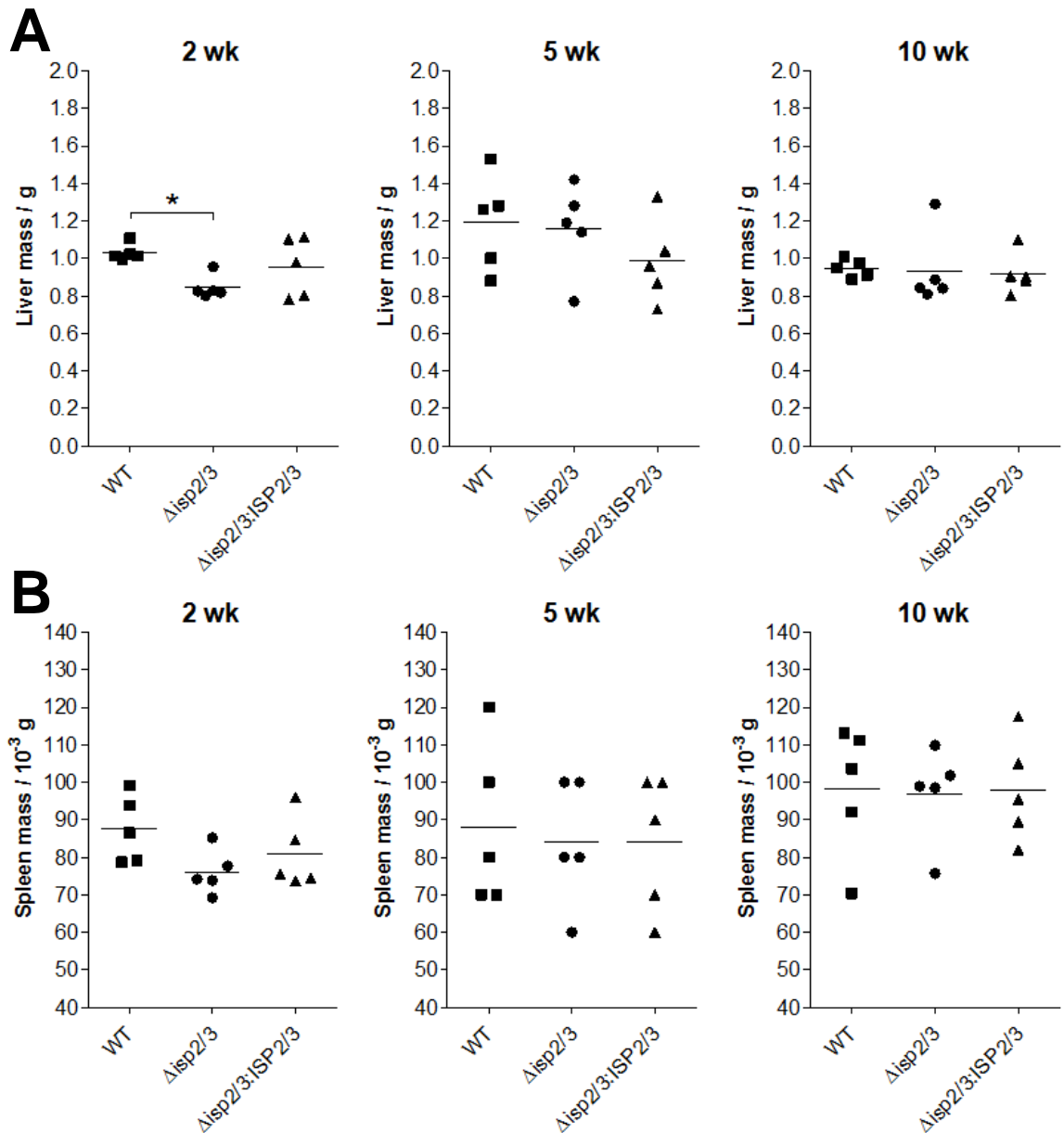


Figure 4-8 Liver and spleen masses during infection with *L. major* WT, Δ isp2/3, and Δ isp2/3:ISP2/3. Purified metacyclic promastigotes (10^4 in 10 μ l PBS) were intradermally inoculated into the ears of C57BL/6 mice ($n=5$ for each time-point). The A) livers and B) spleens were removed at 2, 5, and 10 wk post-infection, and the masses were measured. Asterisks indicate statistical significance between the groups at $p < 0.05$ (*), as measured by one-way ANOVA with a Tukey post test.

4.3 Discussion

The results of this chapter suggest that *L. major* ISP2 confers parasite survival at the site of inoculation *in vivo*. Eschenlauer et al. (2009) and Faria et al. (2011) previously demonstrated that *L. major* mutants deficient in *ISP2/3*, Δ isp2/3, had reduced parasite burdens after an initial upregulation of internalisation, as compared with *L. major* WT infections, in macrophages from BALB/c and C57BL/6 mice respectively. To follow on from these previous *in vitro* experiments, it has been shown here, through BLI (Figure 4-5 and 4-6) and LDA

(Figure 5-7B) techniques, that this phenotype can also be observed *in vivo*, further indicating an important role for ISP2 in the establishment and persistence of *Leishmania* infection. ISP2 has been shown to inhibit host serine peptidases of the S1A family, including NE and CG (Eschenlauer et al., 2009; Faria et al., 2011; Morrison et al., 2012), which are expressed by mammalian innate immune cells, including neutrophils, monocytes, and macrophages. S1A serine peptidases play many roles in the modulation of the immune response, including proteolytic modification of chemokines to regulate immune cell recruitment, and in the activation of immune cells through the cleavage of cytokines and cell surface receptors. Therefore, ISP2 may inhibit the activity of host SPs *in vivo* to modulate the innate immune responses facilitating *L. major* survival, which will be discussed in Chapter 5.

The use of a reproducible *L. major* infection model is important in the study of putative *L. major* virulence factors, as the disease profile observed in response to *L. major* mutants deficient in, or overexpressing, the putative virulence factor may reveal its function in the modulation of host immune responses and hence indicate their potential as vaccine candidates. In this study, in which low dose parasite inocula were used, differences were observed in the lesion progression profiles (Figure 4-1 and 4-2) and parasite loads, reflected in the BLI (Figure 4-6) and LDAs (Figure 4-7), between *L. major* WT and $\Delta isp2/3$ infections; this indicates that the use of a low dose intradermal infection model for *L. major* is robust enough to detect differences caused by single *L. major* virulence gene mutations. Infection with *L. major* $\Delta isp2/3:ISP2/3$ parasites, which has been shown to slightly overexpress ISP2 (as shown in Chapter 3), resulted in significantly higher parasite loads at the site of infection, assessed by LDA at 5 wk post-infection (Figure 4-7B) and BLI of a LUC2-expressing $\Delta isp2/3:ISP2/3$ cell line over the course of infection (Figure 4-6A), compared with *L. major* WT and $\Delta isp2/3$ infections, further confirming the importance of ISP2 for parasite survival. Interestingly, parasites of all three cell lines persisted in the dLNs (Figure 4-7C), which may reflect differences in the environment between the site of infection and the dLN, such as the differences in the presence of SPs, the activity of which ISP2 has been shown to inhibit. It is likely that the SP composition at the site of infection and the dLN will be different due to differences in the cellular compositions between these two locations, in that

there are more neutrophils, macrophages, and monocytes at the site of infection but not all of these migrate to the dLN (León et al., 2007).

Lesion size is often taken as a measure of disease progression over the course of *L. major* infection (Späth et al., 2000; Jacobs et al., 2005). Faria et al. (2011) had previously performed footpad inoculations of C57BL/6 mice with *L. major* WT and $\Delta isp2/3$ parasites, reporting no significant differences between the lesion sizes of the two groups over 10 wk. This does not match the infection profiles reported in this study for both footpad and ear inoculation of *L. major* WT and $\Delta isp2/3$ parasites, in which the lesions of $\Delta isp2/3$ -infected mice developed and resolved more rapidly than WT-infected mice (Figure 4-1 and 4-2). The differences observed are most likely due to the parasite inocula, as Faria et al. (2011) used 2×10^6 stationary-phase promastigotes, whereas 10^4 metacyclic promastigotes were used in this study. Stationary-phase cultures are composed of procyclic and metacyclic promastigotes, as well as the other intermediate promastigote forms. Although there are no significant differences in the *in vitro* growth curves between *L. major* WT and $\Delta isp2/3$ promastigotes (Figure 4-4), the quantification of the composition of promastigote forms in the stationary-phase culture has not been conducted for these cell lines. In addition, it has already been shown that ISP2 is more highly expressed in infective metacyclic promastigotes and amastigotes compared to procyclic promastigotes (Eschenlauer et al., 2009); therefore, using the same number of metacyclic promastigotes allows for a better comparison of the *in vivo* infections between the parasite groups.

A “silent” phase of parasite growth has been described in *L. major* infection models upon inoculation with a low parasite dose. Lira et al. (2000) inoculated 100 *L. major* Friedlin metacyclic promastigotes into the footpads of C57BL/6 mice and only observed lesion development at 6 to 8 wk post-infection, compared to a high dose of 10^6 metacyclic promastigotes, which caused footpad swelling at 1 wk post-infection, with a peak at 3 wk post-infection. The footpad lesion development caused by low dose inocula shown by Lira et al. (2000) more closely resembles the lesion development in this study in which 10^4 *L. major* Friedlin WT metacyclic promastigotes were inoculated into the footpad (Figure 4-1), as lesion development was not evident until 5 wk post-infection. The

kinetics of the lesion development in the ear of C57BL/6 mice infected with *L. major* Friedlin WT parasites performed in this study (Figure 4-2) also closely resembles trends shown by Baldwin et al. (2003), who likewise used 10^4 *L. major* Friedlin metacyclic promastigotes in the ear model showing lesion formation around 3 wk and a peak lesion size at 5 to 6 wk, and Cangussú et al. (2009) who used 10^3 *L. major* Friedlin metacyclic promastigotes also showing lesion formation around 3 wk and a delayed peak lesion size at 7 wk. The lesion profiles reported in these papers suggest that the experimental model used in this investigation is reproducible for *L. major* Friedlin infection. Recently, Schuster et al. (2014) proposed a method to standardise the measurement of lesions in the ear, as the techniques varied in the scientific literature including thickness measured by dial or vernier caliper, diameter of the induration measured by vernier caliper, a scoring system based on diameter, and lesional volume. This report found that all these techniques failed to represent what is visually observed, particular in the early stages of erythema swelling and when lesions show signs of necrosis (Schuster et al., 2014). Lesion development should, therefore, be considered in qualitative terms, rather than as a quantitative measure of disease progression. The use of BLI can help improve the monitoring of lesion development, as not only does BLI reflect the parasite loads at the site of inoculation, the imaging system takes a photograph as an anatomical reference, which could act as a direct two-dimensional record of lesion development over time.

Lesion size does not always correlate with parasite burden particularly when a low parasite dose is used (Lira et al., 2000), in fact, it is more coincident with the onset of immunity in terms of cellular infiltration (Belkaid et al., 2000). The absence of lesion formation during the first few weeks after a low dose inoculation of *L. major* suggests that host immune responses mediating cellular infiltration and parasite killing are avoided, as parasite loads peak after this period. Morphometric analysis of the number and type of cells composing the ear dermis over the course of a 10^3 *L. major* Friedlin metacyclic promastigote infection in C57BL/6 mice show an accumulation of leukocytes from 4.5 wk post-infection coinciding with the start of lesion development (Cangussú et al., 2009). In this study, lesion development after infection with *Disp2/3* parasites is evident even after 2 or 3 wk of infection and appears to be higher than that of

WT infection (Figure 4-2), even though $\Delta isp2/3$ parasites could not be detected in LDAs at 5 wk post-infection (Figure 4-7B); these results suggest that contrary to what is observed for *L. major* WT infection, mechanisms regulating cellular infiltration and parasite killing may be upregulated, or no longer inhibited by ISP2, during $\Delta isp2/3$ infection. Furthermore, the dLNs of $\Delta isp2/3$ -infected mice at 5 wk post-infection were significantly larger than those of $\Delta isp2/3:ISP2/3$ -infected mice (Figure 4-7A), which may indicate lymph node hypertrophy, which is the expansion of the lymph nodes to promote the increase of naive T cells into the lymph node in order to generate a protective antigen-specific immune response (Hsu & Scott, 2007; Carvalho et al., 2012).

The parasite loads detected in the ear for *L. major* WT infections (Figure 4-7B) are consistent with those of Belkaid et al. (2000), who inoculated 100 *L. major* Friedlin metacyclic promastigotes into the ear dermis. They showed low parasite loads of less than 1000 parasites at 2 wk post-infection, with the peak parasite load at 4 wk, over 10^5 parasites, but lesions only becoming apparent at 5 wk (Belkaid et al., 2000). Parasite burdens in this study were determined by the LDA method; however, other techniques are available, such as qPCR of *Leishmania* transcripts, such as *ssrRNA* (de La Llave et al., 2011). The detection limit of the LDAs for the ear samples was over 10^2 parasites. The detection limit was calculated based on sample preparation, as the first few wells of the LDA plates consisted of dense material from the ear that prevented the detection of any extracellular parasites. This dense material, which probably consisted of high concentrations of toxic products, may have also prevented parasite growth, as even after a couple of weeks of incubation there were no parasites in these wells. LDAs only detect amastigotes that are able to differentiate and survive as promastigotes in culture in the presence of antibiotics. The LDA method is also subject to error due to loss of parasites in the tissue harvesting and homogenising steps. In addition, technical and biological variation can occur in these quantification methods, which makes the results difficult to reproduce, as demonstrated by the two 5 wk post-infection LDA experiments performed on the ears of *L. major* WT- and $\Delta isp2/3$ -infected mice (Figure 4-7B, first and second columns). Contamination arose in some LDAs previously performed with ear samples, which prevented the parasite burdens from being calculated; this was eventually overcome by increasing the concentration of the antibiotic,

gentamicin, in the growth medium, although the gentamicin may also have had an effect on the parasite growth (Daneshvar et al., 2003). Parasites were not detected in any ear sample for any parasite-infected group, WT, *Δisp2/3*, or *Δisp2/3:ISP2/3*, at 2 wk post-infection. It is thought that only 10% of the metacyclic promastigotes inoculated into mice survive and transition into amastigotes, based on parasite loads determined by the abundance of *L. major* transcripts (Giraud et al., 2014). In studies that have monitored *L. major* parasite burdens in the site of infection over time after a low dose inoculation in resistant C57BL/6 mice, parasites have not been detected less than 3 or 4 wk post-infection at the site of inoculation assessed by LDA (Belkaid et al., 2000; Lira et al., 2000). However, the use of qPCR methods has detected a low abundance of the parasite transcripts over this early phase of infection (Giraud et al., 2014). Additionally, Baldwin et al. (2003) investigated the parasite burdens in the dLNs at 5, 10, and 15 wk post-infection, showing a decline over the course of infection, as was shown in this study for both *L. major* WT and *Δisp2/3*-infected mice.

BLI of the three LUC2-expressing cell lines, *L. major*, *Δisp2/3*, and *Δisp2/3:ISP2/3*, in the mouse model enabled the infections to be followed over the long-term, in order to compare the dynamics of infection in the initial stages, as was previously evaluated by Faria et al. (2011), and at late time-points. This is the first study to use the BLI system to compare the infection profiles of different parasite gene mutants. de La Llave et al. (2011) and Giraud et al. (2014) used firefly luciferase-expressing *L. major* IR173 to monitor disease progression in the ear dermis of C57BL/6 mice after inoculation with 10^4 metacyclic promastigotes. Four phases were described; phase 1, from 0 to 4 days, during which bioluminescence was similar to the background values; phase 2, from 4 to 29 days, where the signal increased, peaking around 19 days; phase 3, from 29 to 47 days, where the signal decreased to background levels but lesion development was still ongoing; and phase 4, from 47 to 118 days, in which there was no signal but the lesion was slowly resolving. A similar bioluminescent profile was observed for *L. major* Friedlin in this study. There were no significant differences in the bioluminescent signal from the LUC2-expressing parasites over the first week of infection (Figure 4-6A). *In vitro* luciferase reporter gene assays with 10^5 to 10^6 metacyclic promastigotes showed that LUC2

expression, as determined by bioluminescence, of the *L. major*+LUC2 cell line was significantly higher than that of the Δ *isp2/3*+LUC2 or Δ *isp2/3:ISP2/3*+LUC2 cell lines (Figure 4-3). However, *in vivo* imaging of these cell lines 1 h after intradermal inoculation with 10^4 metacyclic promastigotes showed that the *L. major*+LUC2 and Δ *isp2/3:ISP2/3*+LUC2 cell lines had mean signals of 6.28×10^3 photons sec^{-1} and 6.51×10^3 photons sec^{-1} respectively, whereas the mean signal from the ears infected with the Δ *isp2/3*+LUC2 cell line was 5.12×10^3 photons sec^{-1} , almost halfway between the background signal of ears infected with the parental cell lines, parasites not expressing luciferase, 4.3×10^3 photons sec^{-1} , and the *L. major*+LUC2 and Δ *isp2/3:ISP2/3*+LUC2 infected groups (Figure 4-6A). The difference between the bioluminescent signal of these cell lines *in vitro* and *in vivo* could be attributed to differences in the luciferase kinetics *in vitro* and *in vivo*, or it may indicate the parasite condition. Perhaps the cell lines are experiencing different metabolic stresses due to differences in internalisation, as Δ *isp2/3* parasites are internalised more efficiently by macrophages *in vitro* and Faria et al. (2011) also recovered macrophages with high parasite loads of intracellular Δ *isp2/3* parasites after a 3 h infection in the peritoneal cavity of C57BL/6 mice. Similarly Eschenlauer et al. (2009) showed high Δ *isp2/3* parasite burdens in the footpad of BALB/c mice after 24 h of infection. However, the parasite loads have not been assessed earlier than 3 h post-infection, particularly in this low dose intradermal infection model. By 1 wk post-infection the bioluminescent signal of the LUC2-expressing Δ *isp2/3:ISP2/3* cell line was already significantly higher than that of the *L. major*+LUC2 and Δ *isp2/3*+LUC2 infections. Changes in the kinetics of *in vitro* parasite growth are classically associated with changes in parasite virulence; however, the growth curves of the cell lines used in this study were similar to that of *L. major* WT parasites (Figure 4-4). The signal from the ears infected with *L. major*+LUC2 also began to increase at 1 wk, but the signal from Δ *isp2/3:ISP2/3*+LUC2 infections was higher than that of *L. major*+LUC2 infections over 5 wk, which is when the signal began to decline. The signal from the ears infected with the Δ *isp2/3*+LUC2 cell line, however, remained low over the course of infection, which could indicate that the parasites had been reduced to numbers no longer detectable, or that the parasites were in a bad condition. These data in conjunction, with the parasite burdens at the site of inoculation, again indicate a role of ISP2 in *in vivo* survival.

BLI can be used to reflect parasite burden, as often the numbers of parasites at the site of infection can be detected by BLI imaging before a detectable lesion develops (de La Llave et al., 2011). As with lesion size and parasite burdens, however, the lesion size does not directly correlate with the bioluminescent signal, as de La Llave et al. (2011) showed a peak lesion size followed 10 d after the peak bioluminescent signal. The bioluminescent signal itself though can be directly correlated with parasite burden, although it is necessary to determine the relationship between each luciferase-expressing cell line and the bioluminescence before making assumptions as to the parasite loads in each tissue. In this study, clones of *L. major*+LUC2, Δ *isp2/3*+LUC2, and Δ *isp2/3:ISP2/3* were chosen, which were as closely matched for luciferase expression *in vitro* as possible, as it is not possible to obtain clones of different cell lines with exactly the same levels of expression. Even with the levels of luciferase expression being similar for the same lifecycle stages *in vitro*, differences in parasite growth and condition, particularly *in vivo*, mean that it is important to determine the relationship of the parasite burdens and bioluminescence for each luciferase-expressing cell line. Reimão et al. (2013) and Myburgh et al. (2013) also directly imaged plates of serially diluted luciferase-expressing *L. amazonensis* and *Trypanosoma brucei* on the IVIS respectively, to determine the correlation between parasite number and photons detected. The BLI signal strength can vary depending of the *Leishmania* lifecycle stage and parasite condition, as well as the tissue location, due to light absorption and scattering, the kinetics of luciferin distribution, and the availability of co-factors, such as ATP (Thalhofer et al., 2010). The detection sensitivity has been shown to differ depending on *in vivo* or *ex vivo* measurements of tissues infected with luciferase-expressing parasites (Michel et al., 2011). Bioluminescence from different organs cannot be compared within the same animal, but for a given organ, the bioluminescence can reflect differences in the parasite loads between animals infected with the same cell line. *In vivo* imaging of luciferase-expressing cell lines also does not give any information on whether the parasites are intracellular or extracellular. Differences between the bioluminescent signals immediately after inoculation can, therefore, reflect the infection efficiency in each animal. Prior to infection, the levels of bioluminescence from purified metacyclic promastigotes of each of the three LUC2-expressing cell lines showed significant differences in *in vitro* luciferase reporter gene assays (Figure 4-4), although no data was

collected on the bioluminescence of amastigotes. Michel et al. (2011) demonstrated that the signal from luciferase-expressing *L. infantum* amastigotes is lower than that of exponentially growing promastigotes, which could be attributed to the fact that amastigotes generally display lower metabolic activity. Combined *in vivo* imaging and reverse transcription qPCR assays of *L. major* transcripts have been proposed to determine parasite burdens *in vivo* in relation to the bioluminescent signal (de La Llave et al., 2011; Giraud et al., 2014).

The ear dermis was chosen as the site of inoculation to resemble a “natural” infection and this was also a good choice for imaging LUC2-expressing parasites, as due to the thinness of the ear pinna, there is a lack of quenching of the light emission. However, signals from the dLN were not detected due to the deeper location and hence quenching from overlying tissues, blood, as well as the dark skin and hair pigment of the C57BL/6 mice. Firefly luciferase has a maximum emission of 562 nm. Parasites expressing red-shifted luciferase (PpyRE9H), which has a maximum emission of 617 nm, can be imaged in deeper tissues (McLatchie et al., 2013); this system is more sensitive, detecting fewer than 100 *T. brucei*. The enhanced sensitivity of red-shifted luciferase may be useful in the early stages of infection, when the signal is low for LUC2-expressing parasites, and also to capture dissemination to the dLN in C57BL/6 mice.

Recently, Giraud et al. (2014) used the BLI model of infection with simultaneous analysis of inflammatory processes and immune responses in the site of infection and the dLN by determining the abundance of mouse transcripts for the T cell subsets, CD4, CD8, and Foxp3, as well as related cytokines, including IL-4, IL-10, IFN- γ , and IL-12p40, over the course of infection. High IL-4 transcript abundance was detected at the peak of BLI signal and parasite burden, whereas CD4, IFN- γ , and IL-12p40 transcript abundance corresponded with a decrease in BLI signal and parasite burden (Giraud et al., 2014). The resistance of a mouse model is based on the resolution of lesion size, the clearance of parasites from the site of infection and the dLN, and the development of a Th1 response. Giraud et al. (2014) have provided the first study linking these factors in a “natural” infection model using BLI imaging to provide a better understanding of the dynamics of lesion progression, parasite burden, and cellular infiltration. In the next chapter,

the innate immune responses, in terms of immune cell recruitment and activation, in response to *L. major* WT, $\Delta isp2/3$, and $\Delta isp2/3:ISP2/3$ infections will be discussed, to explain the differences in disease profiles observed in this chapter.

It has been shown that mice displaying progressive lesions following primary inoculation display an absence of cutaneous lesions upon re-inoculation (Courret et al., 2003). Persistence of *L. major* within the host after lesion resolution has been attributed to the role of IL-10 produced by CD4⁺CD25⁺ regulatory T cells (Belkaid et al., 2002). Due to the differences observed in the disease profiles of *L. major* WT, $\Delta isp2/3$, and $\Delta isp2/3:ISP2/3$ infections, it may be of interest to investigate whether there is any effect on concomitant immunity.

Taken together, the low dose intradermal C57BL/6 infection model for *L. major* Friedlin is characteristic of other *L. major* low dose infection models shown in other reports, indicating that this model is highly reproducible, in terms of lesion progression and parasite burdens. This model is also much more representative of a human infection, as opposed to the subcutaneous high dose model. This model has allowed the comparison of disease profiles upon infection with *L. major* WT and *ISP2* gene mutants enabling the investigation into the role of the *L. major* virulence factor, *ISP2*, in parasite survival and growth. The results presented indicate the importance of *ISP2* in the establishment and persistence of *Leishmania* infection *in vivo*. BLI has also become a powerful tool in assessing the efficacy of drugs, and in tracking the dissemination of various luciferase-expressing cell lines. This study has shown that the BLI method can be applied to sensitively evaluate the role of putative virulence factors *in vivo*.

5 Comparison of the cellular immune response dynamics during infection with *L. major* wild-type and *ISP2* gene mutants *in vivo*

5.1 Introduction

5.1.1 Innate cell recruitment and activation during *L. major* infection in the mouse model

Upon *L. major* inoculation into the skin, a strong local inflammatory immune response is initiated due to tissue damage caused by the inoculation method. Neutrophils are one of the earliest innate immune cell types that infiltrate the site of infection, occurring less than an hour after parasite inoculation, to form a “plug” of neutrophils in the broken epidermis (Peters et al., 2008). Neutrophils are recruited by sandfly- and *Leishmania*-derived factors (van Zandbergen et al., 2002; Peters et al., 2008), as well as chemokines, such as CXCL1 (KC) and CXCL2 (MIP-2), produced by epithelial cells, keratinocytes, fibroblasts, and neutrophils (Müller et al., 2001). Neutrophils phagocytose metacyclic promastigotes to serve as intermediate hosts for *Leishmania* (Laufs et al., 2002; Peters et al., 2008). By three days post-infection, inflammatory monocytes and macrophages become the predominant innate immune cells present at the site of infection (Ribeiro-Gomes et al., 2012). Monocytes and macrophages are recruited by CCL3 (MIP-1 α) and CCL4 (MIP-1 β) secreted by neutrophils (van Zandbergen et al., 2004). Macrophages become the major host cell type harbouring intracellular *Leishmania* at the site of infection. Inflammatory monocytes differentiate into either monocyte-derived macrophages or monocyte-derived dendritic cells at the site of infection based on the presence of local growth factors and cytokines. DCs are proposed to be important in the generation of an adaptive immune response; DCs migrate from the site of infection to the dLNs to present antigen to naive T cells inducing an antigen-specific T cell response (León et al., 2007).

Neutrophils can contribute to inflammation through the process of degranulation or the formation of NETs, both of which release granule components into the extracellular environment. Neutrophils generate ROS, which oxidise molecules,

such as amino acids and nucleotides, and have cytoplasmic azurophilic granules consisting of antimicrobial factors, such as MPO, and proteolytic enzymes, including SPs. Macrophages and DCs are also able to phagocytose *L. major*. In addition, they produce toxic metabolites, such as NO, which is catalysed by iNOS (De Trez et al., 2009).

5.1.2 Role of serine peptidases in the mammalian immune response

Serine peptidases of neutrophils, often referred to as neutrophil serine proteases (NSPs), are stored in high concentrations of their active form in azurophilic granules. The NSPs can digest phagocytosed microorganisms through the fusion of azurophilic granules with phagolysosomes harbouring the microorganisms (Belaouaj et al., 2000). Upon neutrophil activation, following exposure to inflammatory stimuli, the NSPs are secreted into the extracellular environment where they have key roles in the regulation of host immune responses. The NSPs are also released from apoptotic neutrophils, and are found bound to NETs. Neutrophil elastase (NE), cathepsin G (CG), and proteinase 3 (PR3) are the main NSPs; these are also found in monocytes. Mast cells, eosinophils, and basophils are also sources of NE and PR3, whilst NE has been found in association with CR3 on the surface of macrophages (Cai & Wright, 1996).

The primary function of these SPs, of the S1A trypsin-fold family of clan PA, is to specifically process cytokines and chemokines to either enhance or abolish their function or stability, such as their affinity for their receptor. Proteolytic modification by these SPs is typically achieved through limited N-terminal cleavage of the respective cytokine or chemokine (reviewed in Pham, 2008). There are around 50 chemokines, which are highly specific immunomodulators broadly categorised as homeostatic or inflammatory. Migration of immune cells to the site of inflammation is mediated by a concentration gradient of active chemokines, which is sensed through the use of cognate G protein-coupled receptors (GPCRs). The cleavage of cytokines and chemokines by NSPs can, therefore, either enhance or terminate the immune response. In addition, NSPs can promote or prevent the activation of specific cell receptors leading to the modulation of intracellular signalling cascades, which can impact upon the production and release of chemokines, and the activation of cell effector

processes (Ribeiro-Gomes et al., 2007; Benabid et al., 2012). Table 5-1 highlights targets of the NSPs, including cytokines, chemokines, growth factors, receptors, and adhesion molecules, which have already been identified and characterised.

NSPs have also been implicated in the initiation of the adaptive immune response through the activation of lymphocytes, as well as the cleavage of extracellular matrix (ECM) components to facilitate leukocyte egress from blood vessels (reviewed in Pham, 2006).

Table 5-1 The effects of neutrophil serine proteases (NSPs), neutrophil elastase (NE), cathepsin G (CG), and proteinase 3 (PR3), on host biological targets. Adapted from Wiedow & Meyer-Hoffert (2005) and Pham (2008) with permission.

Target	Regulated by	Potential effect during an inflammatory response
Cytokines		
IL-1 β	Pro-form activated by PR3	Induces cell proliferation and differentiation
IL-2	Inactivated by NE	Inhibits differentiation of antigen-specific T cells
IL-6	Inactivated by NE, CG, and PR3	Wide variety of biological functions
IL-8 (or CXCL8)	Activated by PR3	Increases neutrophil chemotaxis
IL-18	Pro-form activated by PR3 Inactivated by NE	Induces release of IFN- γ from NK cells and Th1 cells
IL-32	Activated by PR3	Induces production and secretion of TNF- α , IL-6, IL-8, and CXCL2
TNF- α	Pro-form activated by NE, CG, and PR3 Mature form degraded by NE and CG	Regulates immune cells, including the production of cytokines, cell proliferation and differentiation, and apoptosis
Chemokines		
Chemerin	Pro-form activated by NE and CG	Increases APC chemotaxis, such as macrophages and DCs
CCL3 (or MIP-1 α)	Inactivated by NE, CG, and PR3	Abrogates monocyte/macrophage chemotaxis
CCL5 (or RANTES)	Inactivated by CG	Abrogates T cell, basophil, and eosinophil chemotaxis
CCL15 (or MIP-1 δ)	Activated by CG	Increases neutrophil and monocyte chemotaxis
CXCL2 (or MIP2)	Activated by CG	Increases neutrophil chemotaxis
CXCL5 (or ENA-78)	Activated by CG	Increases neutrophil chemotaxis
CXCL8 (or IL-8)	Activated by PR3 Inactivated by NE and CG	Affects neutrophil chemotaxis

CXCL12 (or SDF-1 α)	Inactivated by NE and CG	Abrogates lymphocyte chemotaxis
Growth factors		
TGF- β	Soluble form released by NE	Blocks activation of monocyte-derived cells and lymphocytes Regulates differentiation of Treg and Th17 cells
Receptors		
IL-2 receptor α	Cleaved by NE and PR3	Inhibits cellular response to IL-2
IL-6 receptor	Cleaved by CG	Inhibits cellular response to IL-6
CXCR4	Cleaved by NE and CG	Abrogates lymphocyte chemotaxis through CXCL12 binding
CD2, CD4, and CD8	Cleaved by NE and CG	Impairs T cell activation
CD14	Cleaved by NE and CG	Impairs LPS-induced cell activation
CD23	NE and CG release soluble fragments	Stimulates ROS and pro-inflammatory cytokine production in monocytes
CD43 (or sialophorin)	Cleaved by NE	Regulates monocyte and lymphocyte adhesion
CD87 (or urokinase receptor)	Cleaved by NE and CG	Regulates cell migration
CR1 (or CD35)	Cleaved by NE	Inhibits complement activation
TLR4	Activated by NE	Activates cell signalling through MyD88/IRAK/TRAF-6 pathway Upregulation of IL-6, IL-8, and TNF- α production
TNF receptor	Cleaved by NE	Inhibits cellular response to TNF- α
Protease-activated receptor 2 (PAR-2)	Cleaved by NE, CG, and PR3	Affects release of pro-inflammatory mediators, such as CCL3 and CXCL8, from epithelial cells
GCSF receptor	Cleaved by NE	Inhibits cellular response to GCSF causing inhibition, proliferation, and differentiation of granulocytes and macrophages
Formyl peptide receptor (FPR)	Cleaved by CG	Abrogates neutrophil and monocyte chemotaxis
Progranulin	Inactivated by NE	Suppresses oxidative burst and release of proteases by neutrophils
Adhesion molecules		
Intercellular adhesion molecule 1 (ICAM-1)	Cleaved by NE and CG	Affects leukocyte transmigration Increases neutrophil infiltration
Vascular cell adhesion protein 1 (VCAM-1)	Cleaved by NE and CG	Affects monocyte and lymphocyte adhesion to vascular endothelium

Antimicrobial peptides		
LL-37	Pro-form activated by PR3	Active against bacterial infection

Excessive extracellular activity of NSPs can contribute to tissue damage; therefore, the activity of the NSPs is tightly controlled by natural inhibitors. The liver produces inhibitors, such as the serpins, AAT and ACT, which are distributed throughout the body in plasma. Serpins are irreversible inhibitors, which function by presenting their reactive site as a substrate for the protease, trapping the enzyme and distorting its catalytic site through a conformational change of the serpin (Huntington, 2011). There are also tissue-specific inhibitors, such as the chelonianins, elafin and SLPI.

Other human SPs involved in immunity, which are in the same clan as the NSPs, are the granzymes, produced by NK cells and cytotoxic T cells, and chymase and tryptase of mast cells. These trypsin-like SPs have different substrate specificities to the elastase-like, NE and PR3. Granzymes mediate apoptosis of virus-infected and tumour cells, whereas chymase and tryptase are involved in the clearance of extracellular pathogens, degradation of ECM components, and blood coagulation. Based on the localisation and functions of the SPs *in vivo*, and previous *in vitro* studies on the roles of ISP2 (Faria et al., 2011), it is more likely that ISP2 inhibits the activity of the SPs produced by neutrophils and monocytes, which play prominent roles during *L. major* infection. In addition, Eschenlauer et al. (2009) and Faria et al. (2011) have previously shown that ISP2 is a strong inhibitor of NE activity.

5.1.3 Serine peptidase-deficient mice

The generation of mice deficient in the individual NSPs, NE encoded by the *Elane* gene, also known as the *Ela2* gene, CG encoded by the *Ctsg* gene, and PR3 encoded by the *Prtn3* gene, or combinations of these NSPs, have enabled investigation into the contribution of these NSPs as antimicrobial molecules and their roles in the regulation of inflammation. In general, homozygous transgenic mice were generated through targeted gene disruption of the specific genes in embryonic stem cells, and germline transmission of the mutant gene loci was enabled through the generation and breeding of chimeric mice; NE^{-/-} (Belaouaj et al., 1998), CG^{-/-} (MacIvor et al., 1999), NE^{-/-}PR3^{-/-} (Kessenbrock et al., 2008),

and NE^{-/-}CG^{-/-} mice (Tkalcevic et al., 2000) have so far been generated. In these transgenic mice, the NSPs are no longer expressed from bone marrow-derived cells.

NSPs have direct microbicidal properties against bacteria through the disruption of bacterial membranes (Belaouaj et al., 2000). NE-deficient mice are more susceptible to Gram-negative bacterial infections, such as *Escherichia coli* and *Klebsiella pneumonia* (Belaouaj et al., 1998), whereas CG-deficient mice are more susceptible to infections with the Gram-positive, *Staphylococcus aureus* (Reeves et al., 2002).

Mice deficient in both NE and CG, or NE alone, have been shown to have a defect in neutrophil recruitment in response to zymosan, with decreases in the production of CXCL1, CXCL2, TNF- α , and IL-1 β (Adkison et al., 2002; Young et al., 2004). In mice deficient in both NE and PR3, there is an accumulation of progranulin, due to an inability to degrade this anti-inflammatory factor, which functions in the suppression of the oxidative burst; this potentially inhibits neutrophil activation and can lead to a decrease in recruitment of immune cells (Kessenbrock et al., 2008).

The role of host NSPs in the modulation of immune responses during parasitic infections has not been fully assessed, particularly with the use of these NSP-deficient mice.

5.1.4 *In vivo* methods to assess innate cell infiltration and activation

Gross et al. (2009) established a method of imaging MPO activity *in vivo* using the redox-sensitive compound, luminol. Luminol-induced bioluminescence enables quantitative longitudinal monitoring of MPO activity of activated phagocytes. MPO constitutes about 5% of the protein in azurophilic granules of neutrophils and approximately 1% of the protein in monocytes. MPO is also found in macrophages and other polymorphonuclear leukocytes, such as eosinophils, basophils, and mast cells. Upon phagocyte activation, large quantities of active MPO are secreted into the phagosomes to catalyse a reaction between hydrogen peroxide, H₂O₂, generated during the phagosomal oxidative burst, with chloride

ions, Cl^- , to produce antimicrobial hypochlorous acid, HOCl. HOCl oxidises various molecules including DNA, proteins, and lipids. Luminol is a small uncharged molecule that can penetrate the plasma membrane and phagosomal membrane to enable quantification of MPO activity in these innate cell types *in vivo*. Bioluminescence is specific to MPO activity, as the signal is abolished in *Mpo*^{-/-} mice and upon treatment with 4-ABAH, a potent inhibitor of MPO activity (Gross et al., 2009; Zhang et al., 2013). The exact interaction with luminol is currently unknown; whether HOCl directly or indirectly oxidises luminol, or whether products from other reactions catalysed by MPO, such as the oxidation of NO, oxidise luminol to produce light. This luminol-based *in vivo* imaging technique has been used in animal models for acute inflammation, such as acute dermatitis, arthritis, and tumours (Gross et al., 2009; Zhang et al., 2013), but, as yet, has not been utilised to monitor the dynamics of phagocyte activation in models of infectious disease, including *Leishmania*.

5.1.5 Aims

In the previous chapter, the disease progression of *L. major* WT and the *ISP2* gene mutants was examined *in vivo*, revealing reduced parasite loads of an *L. major* *ISP2/3*-deficient mutant, $\Delta isp2/3$, at the site of inoculation compared with WT infection. In this chapter, the role of *ISP2* on the modulation of host immune responses at the site of inoculation, and in the dLN, in the low dose intradermal C57BL/6 infection model, discussed in Chapter 4, with *L. major* Friedlin WT and the *ISP2* gene mutants will be assessed *in vivo*. Flow cytometric analysis and novel *in vivo* BLI techniques will be used to evaluate innate cell infiltration and activation over the course of infection; this type of analysis has not previously been performed in the study of putative virulence factors *in vivo*. The sequence of local inflammatory events during infection with *L. major* WT, $\Delta isp2/3$, a cell line re-expressing *ISP2/3*, $\Delta isp2/3:ISP2/3$, or a cell line overexpressing *ISP2*, WT [*pXG-ISP2*], may indicate a role for *ISP2* in the modulation of immune responses during infection with *Leishmania*. In addition, transgenic mice deficient in NE, *Ela*^{-/-}, will be used to assess the role of this host NSP in the generation of immune responses to *L. major* WT and the *ISP2* gene mutants *in vivo*.

The aims of this chapter are to:

- Analyse the recruitment of the innate cell populations at the site of inoculation over the course of infection by flow cytometry
- Monitor phagocyte activation at the site of inoculation over the course of infection through BLI
- Assess the activation state of effector cells, in terms of the iNOS response and DC maturation through the expression of co-stimulatory markers
- Determine the cytokine microenvironment at the site of inoculation and in the dLN with regards to the levels of IFN- γ
- Evaluate the role of NE in these immune responses through the use of *Ela*^{-/-} mice

5.2 Results

5.2.1 Innate immune cell dynamics at the site of intradermal *L. major* inoculation

The cellular innate immune response at the site of infection was examined following intradermal inoculation with 10^4 *L. major* WT or Δ *isp2/3* metacyclic promastigotes into the ears of C57BL/6 mice. Innate cell subsets within the ear were analysed by flow cytometry from 1 d to 5 wk post-infection. The gating strategy excluded dead cells through staining with a fixable viability dye, in which dead cells were irreversibly labelled. Cells of the myeloid lineage were then identified and gated based on CD11b expression, which is expressed on the surface of many leukocytes, such as monocytes, macrophages, NK cells, specific subsets of DCs, neutrophils, and other granulocytes (Larson & Springer, 1990; Ribeiro-Gomes et al., 2012). The percentage of these cells within the live cell population in the ear increased from 1 to 5 wk post-infection for those infected with WT parasites, and 1 to 4 wk post-infection for Δ *isp2/3* parasites (Figure 5-1A). The total cell numbers within the ear were assessed by manual cell counts on a haemocytometer showing that the cell number was higher in ears infected with WT or Δ *isp2/3* parasites than the naive ears at almost every time-point studied (Figure 5-1B), suggesting cellular infiltration to the infected site. There were increases in the total cell number from 2 wk post-infection for both WT

and $\Delta isp2/3$ infections, which became higher than in the initial phase of infection, less than 1 wk post-infection; however, the only significant difference was at 2 d post-infection, in which the total cell number was higher in $\Delta isp2/3$ infection than WT infection (Figure 5-1B).

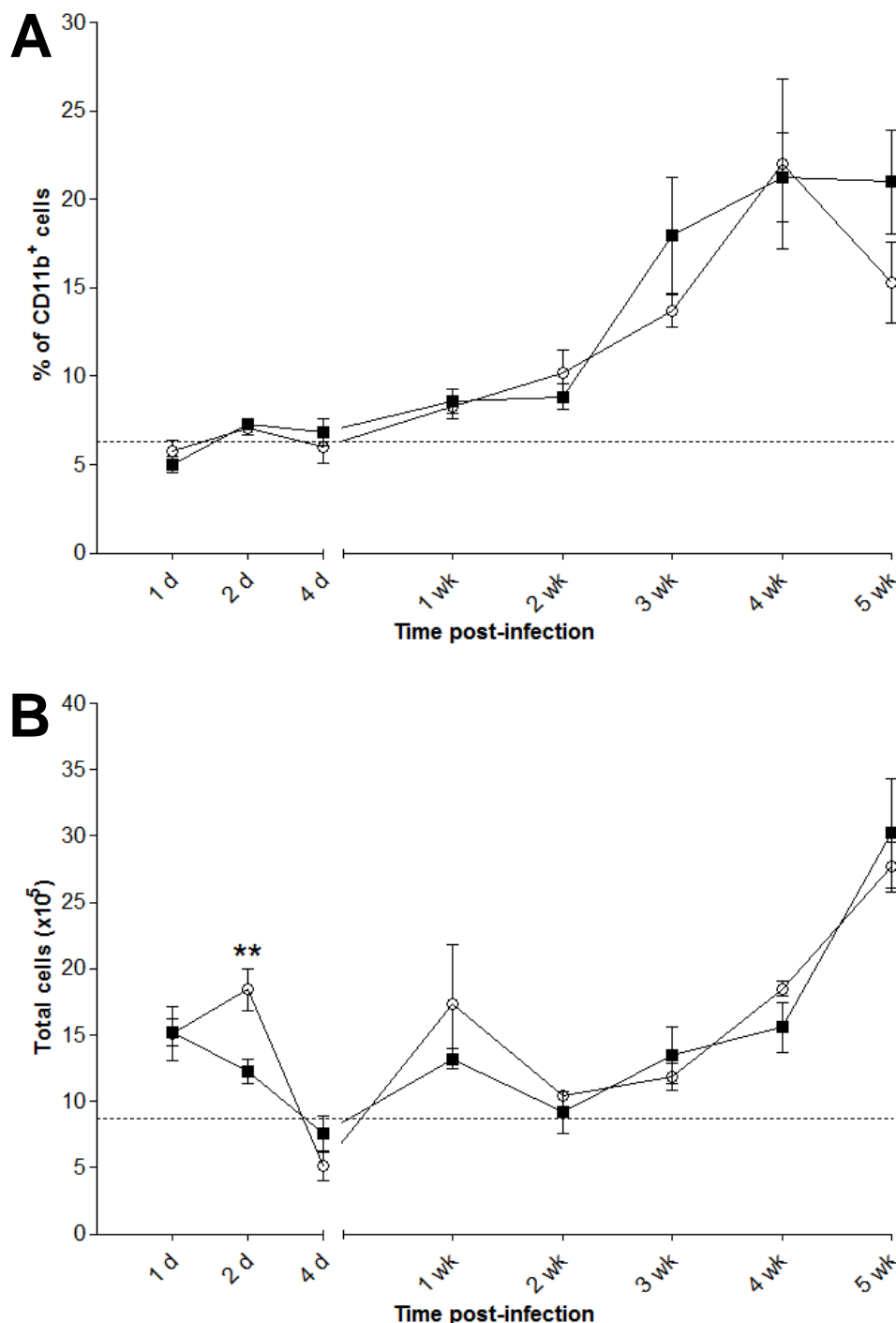


Figure 5-1 Myeloid cell composition at the site of inoculation during infection with *L. major* WT and $\Delta isp2/3$. Purified metacyclic promastigotes (10^4 in $10 \mu\text{l}$ PBS) were intradermally inoculated into the ears of C57BL/6 mice ($n=5$ for each group at each time-point). **A)** Changes in the percentages of CD11b⁺ cells within the live cell population assessed by flow cytometry. **B)** Total cells in the ear dermis assessed by cell counts on a haemocytometer. ■, WT; ○, $\Delta isp2/3$. Results are expressed as means per group at each time-point after infection, a representative of two independent experiments. Error bars represent S.E.M. Dashed lines represent A) the mean percentage of CD11b⁺ cells within the live cell population of a naive ear and B) the mean total cells in a naive ear. Asterisks indicate statistical significance between WT and $\Delta isp2/3$ at $p < 0.01$ (**), as measured by an unpaired *t*-test.

The CD11b⁺ innate cell subsets were further classified based on their surface antigen profiles, to investigate neutrophils, macrophages, DCs, monocytes, and the monocyte-derived macrophages and DCs (moDCs) (Table 5-2). The gating strategy used in this investigation was based on that proposed by Ribeiro-Gomes et al. (2012), as it encompassed all the innate immune cells that are thought to be important during *Leishmania* infection, and the recruitment of which may be affected by the inhibition of SP activity (Table 5-1). This gating strategy also allowed the reproducibility of the intradermal *L. major* infection models used in this study and that of Ribeiro-Gomes et al. (2012) to be shown, in terms of innate immune cell recruitment at the site of inoculation, and enabled comparisons of the innate immune cell dynamics to site of inoculation with *L. major* WT parasites to that of the *ISP2* gene mutants. An example of the gating strategy for the innate immune cell subsets of the ear dermis is given in Figure 5-2.

Table 5-2 Cell surface markers of CD11b⁺ myeloid innate cell subsets.

Cell type	Region in Figure 5-2	Ly6C	Ly6G	CD11c	MHCII
Neutrophils	2	Intermediate	Positive		
Resident dermal macrophages	5	Negative	Negative	Negative	Positive
Resident dermal dendritic cells	6	Negative	Negative	Positive	Positive
Inflammatory monocytes	7	High	Negative	Negative	Negative
Monocyte-derived macrophages	8	High	Negative	Negative	Positive
Monocyte-derived dendritic cells	9	High	Negative	Positive	Positive

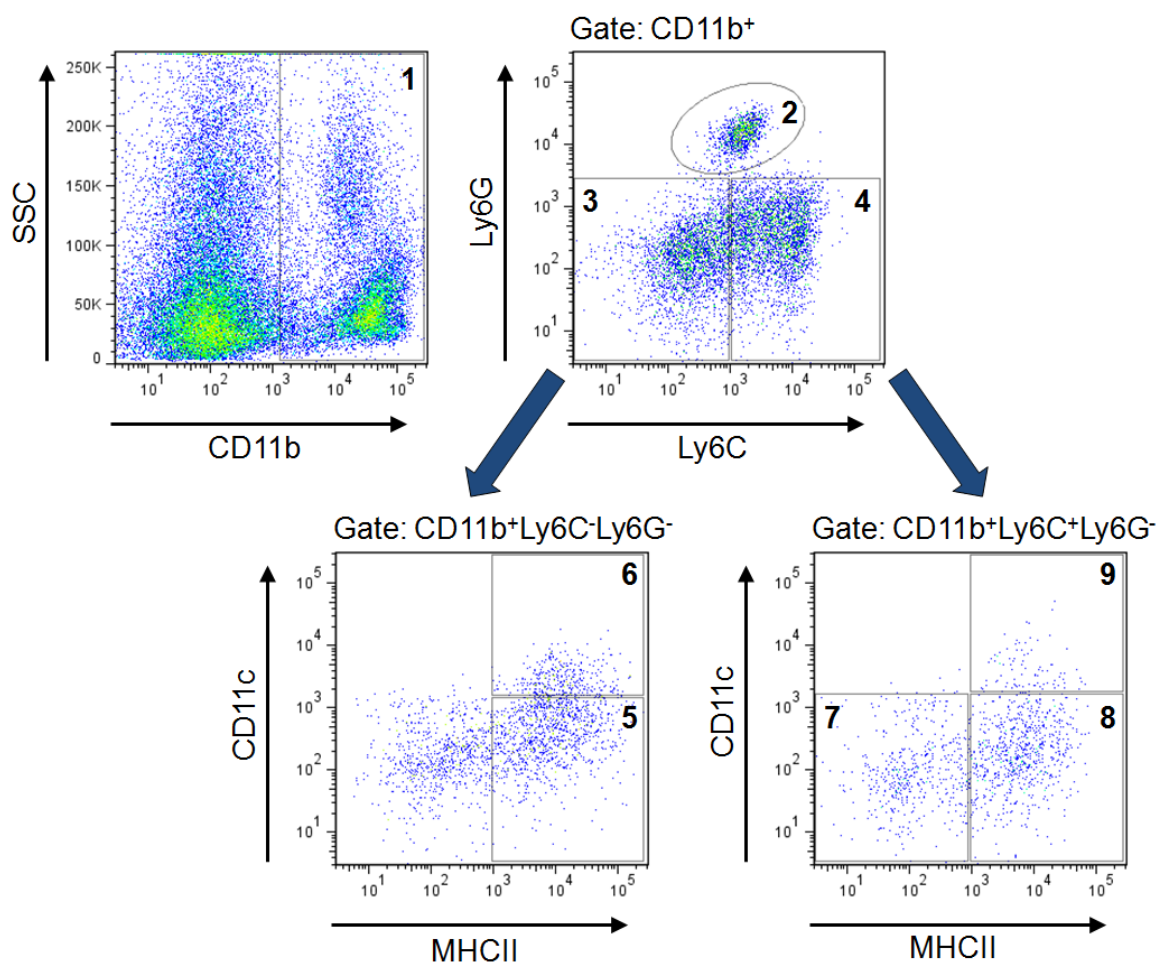


Figure 5-2 Gating strategy to determine innate immune cell subsets in the ear dermis. Subpopulations of $CD11b^+$ myeloid cells (region 1) were gated on Ly6C and Ly6G expression; regions 3 and 4 were further gated on CD11c and MHCII expression. The subpopulation of $CD11b^+$ myeloid cells were defined as follows: $Ly6C^{int}Ly6G^+$ neutrophils (region 2); $Ly6C^-Ly6G^-CD11c^-MHCII^+$ resident macrophages (region 5); $Ly6C^-Ly6G^-CD11c^+MHCII^+$ resident dendritic cells (region 6); $Ly6C^{hi}Ly6G^-$ inflammatory monocytes (region 7); $Ly6C^{hi}Ly6G^-CD11c^-MHCII^+$ monocyte-derived macrophages (region 8); and $Ly6C^{hi}Ly6G^-CD11c^+MHCII^+$ monocyte-derived dendritic cells (region 9).

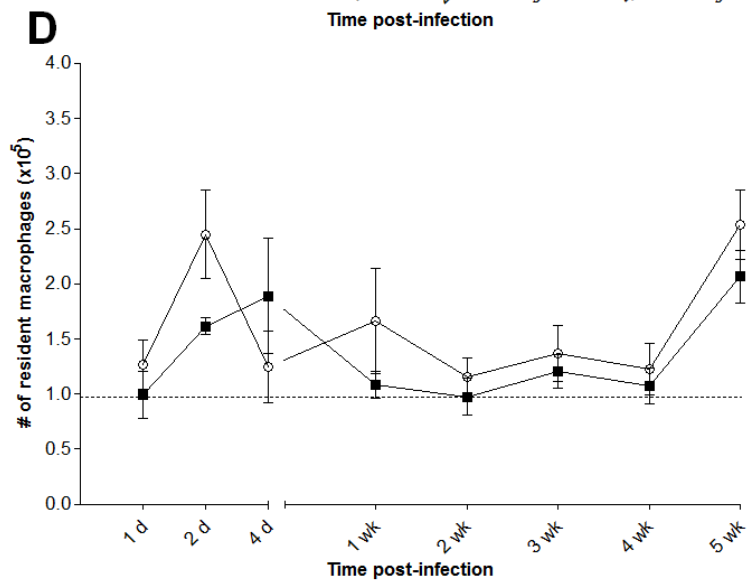
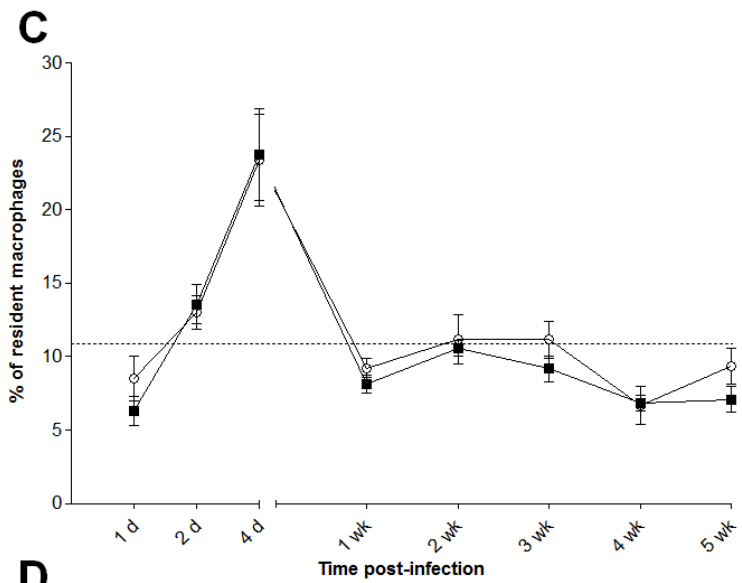
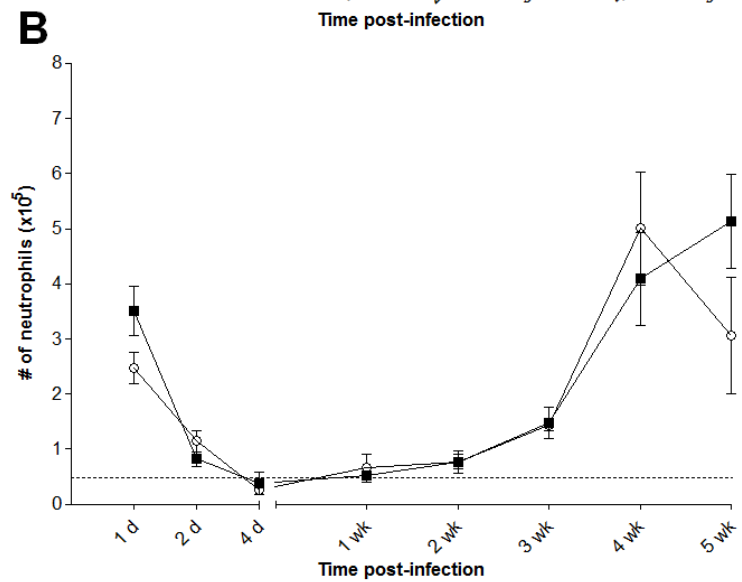
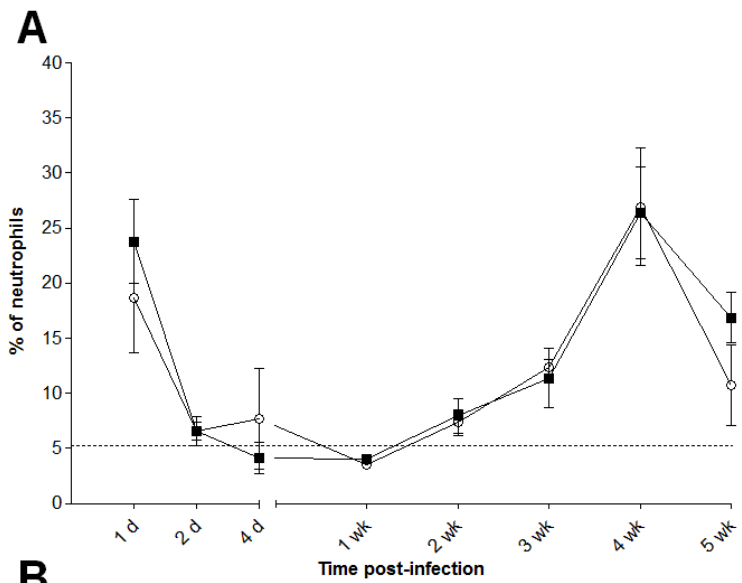
The graphs shown in Figure 5-3 indicate the percentage of each cell type within the $CD11b^+$ population (Figure 5-3, top panels) and the total number of each cell type, as calculated through manual cell counts (Figure 5-3, bottom panels), plotted as means per group at each time-point. To demonstrate how the innate cell populations in *L. major* WT- and $\Delta isp2/3$ -infected ears differed from the naive ear, presented on the graphs are the mean percentages and numbers of each cell type in the naive ear, which were used as a control at each time-point. The $CD11b^+$ cells of naive ears were comprised of large percentages and numbers of resident dermal macrophages and DCs (Figure 5-3, C to F), but low percentages and numbers of monocytes and monocyte-derived cells (Figure 5-3, G to L). Mice were also injected in the ear with PBS, in order to distinguish parasite-specific immune responses from tissue damage-induced inflammation;

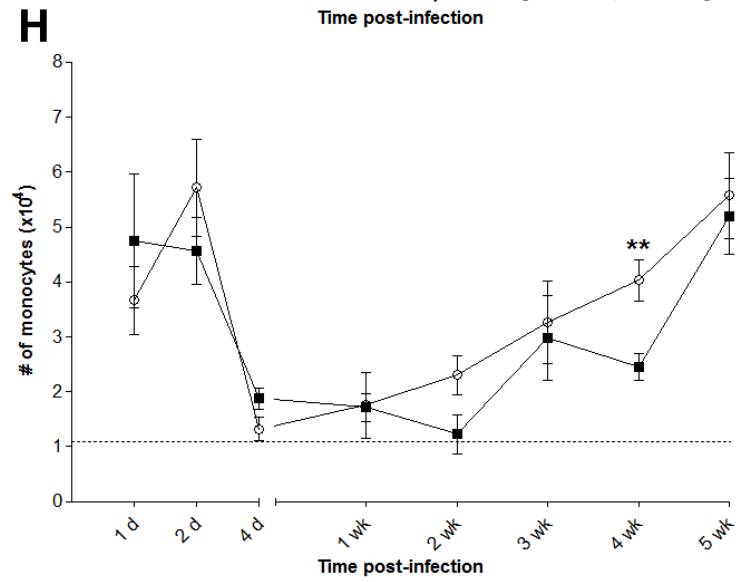
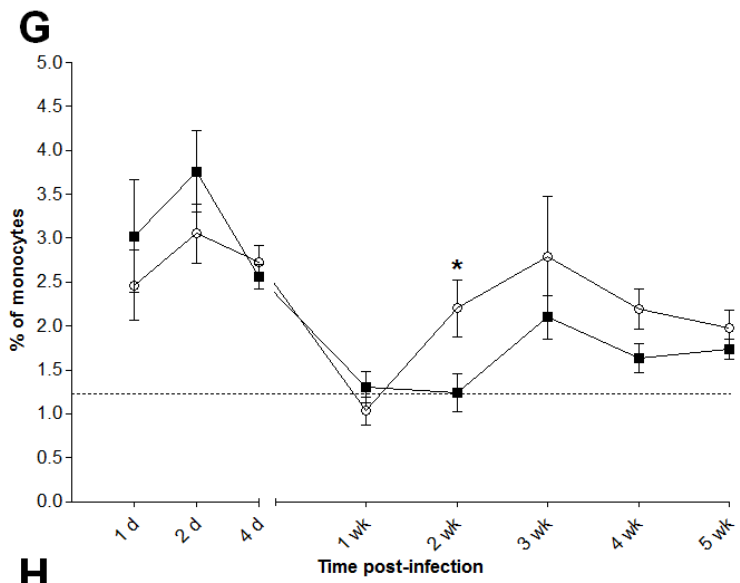
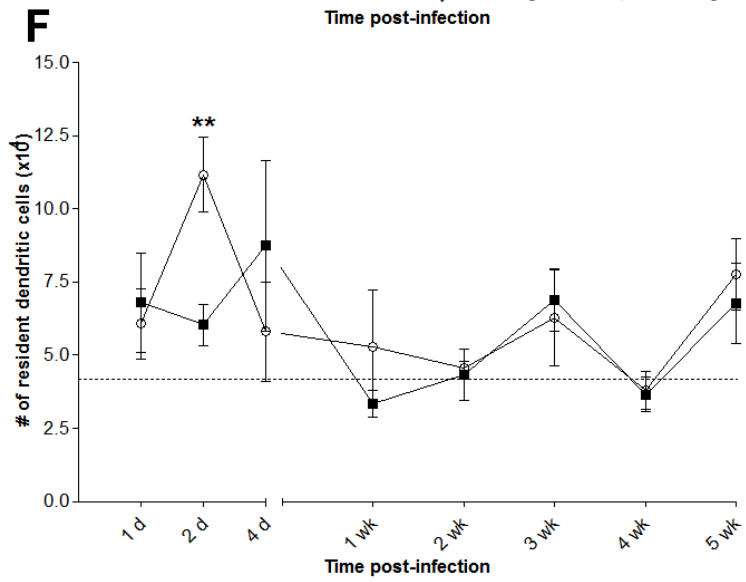
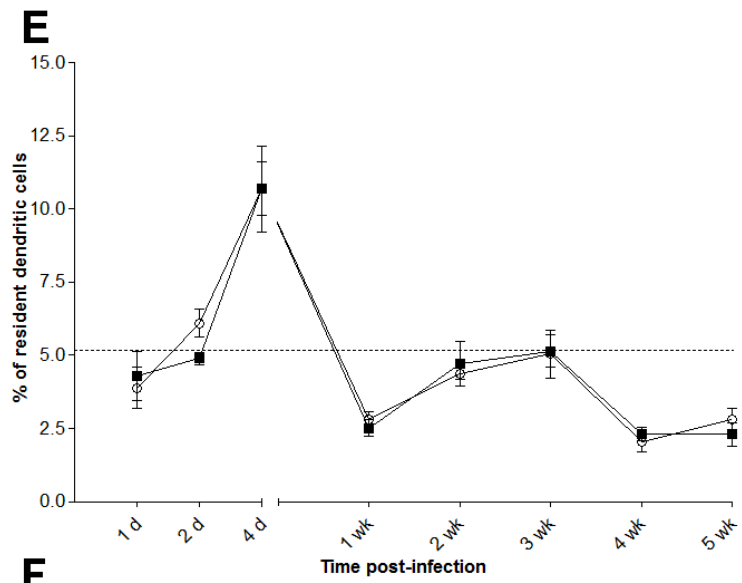
however, at the time-points studied, there was no difference in the innate cell populations between PBS-injected and naive ears. This has been shown by other groups, who only report a difference in neutrophil recruitment between sham injected and naive ears at 1 h post-infection (Ribeiro-Gomes et al., 2012).

Neutrophils constituted the largest percentage of the CD11b⁺ population at 1 d in both WT and $\Delta isp2/3$ infections (Figure 5-3A), which was also reflected in higher numbers of neutrophils (Figure 5-3B). The neutrophils then decreased to levels equivalent to those of a naive ear until 2 wk post-infection, at which a second wave of neutrophils was observed, which peaked at 4 wk in both WT and $\Delta isp2/3$ infections (Figure 5-3, A and B). The percentages of dermal macrophages and DCs within the CD11b⁺ population showed a peak at 4 d (Figure 5-3, C and E), at which the neutrophils were at a baseline level. After this point, the percentages of dermal macrophages and DCs were lower than that of a naive ear, which likely reflects a substantial infiltration of other CD11b⁺ cell subsets. The numbers of dermal macrophages and DCs did not differ significantly to that of a naive ear from 1 wk, except at 5 wk, where the numbers of macrophages were significantly higher than the naive ear for WT and $\Delta isp2/3$ infections (Figure 5-3D).

There was a peak in the percentage of inflammatory monocytes in both WT and $\Delta isp2/3$ infections at 2 d (Figure 5-3G), followed by peaks in the percentages of monocyte-derived macrophages and moDCs at 4 d (Figure 5-3, I and K). A second wave of these monocyte cell types was observed after a decrease to levels seen in naive ears at 1 wk; these second waves peaked at 2 wk for $\Delta isp2/3$ infections, but 3 wk for WT infections, as proportion of the CD11b⁺ population (Figure 5-3, G, I, and K). The decrease in the percentages of these monocyte cell types after their peaks may be due to the considerable increase in the percentage of neutrophils within the CD11b⁺ population, as the total numbers of the monocytes, monocyte-derived macrophages, and moDCs continued to increase up to 5 wk for both WT and $\Delta isp2/3$ infections (Figure 5-3, H, J, and L). There was a significantly higher percentage and total number of monocyte-derived macrophages and moDCs, and higher percentage of inflammatory monocytes at 2 wk post-infection for $\Delta isp2/3$ infection compared with WT infection (Figure 5-3, G to L).

The percentage of CD11b⁺ cells within the live cell populations of the dLNs were also assessed from 1 to 5 wk after intradermal inoculation with *L. major* WT or Δ *isp2/3* metacyclic promastigotes. Figure 5-4 shows a significantly higher percentage of CD11b⁺ cells in the dLNs of Δ *isp2/3*-infected mice at 2 wk post-infection than WT-infected mice.





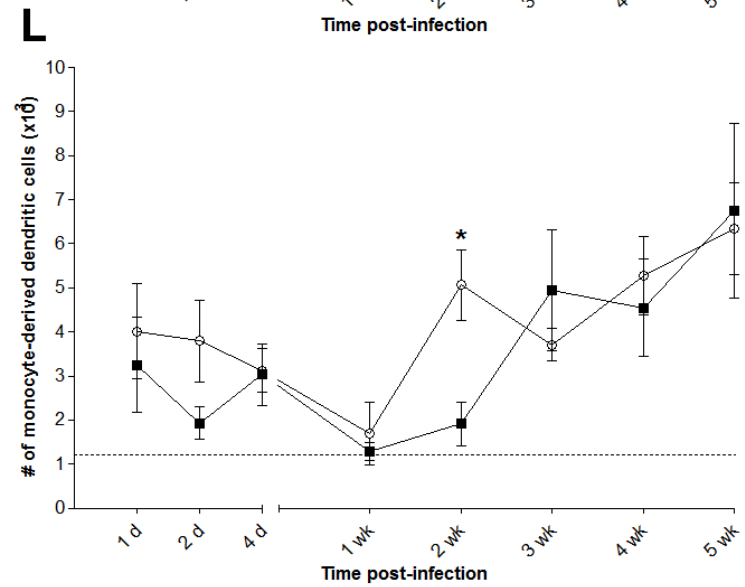
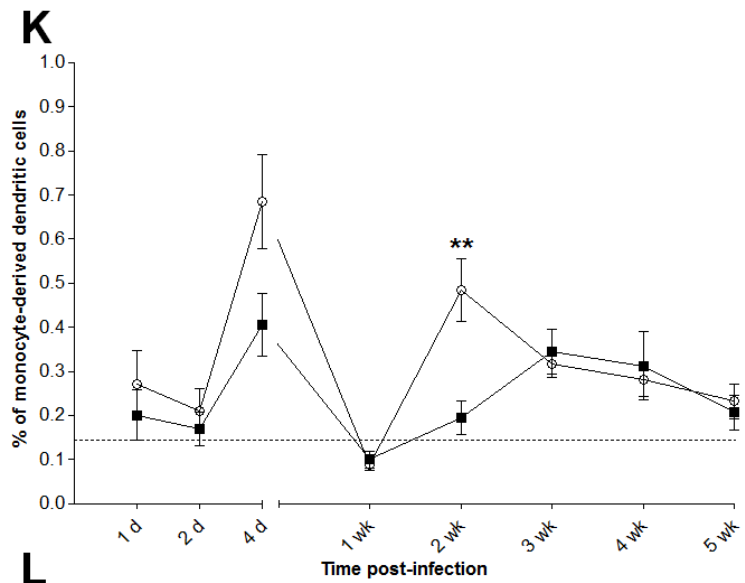
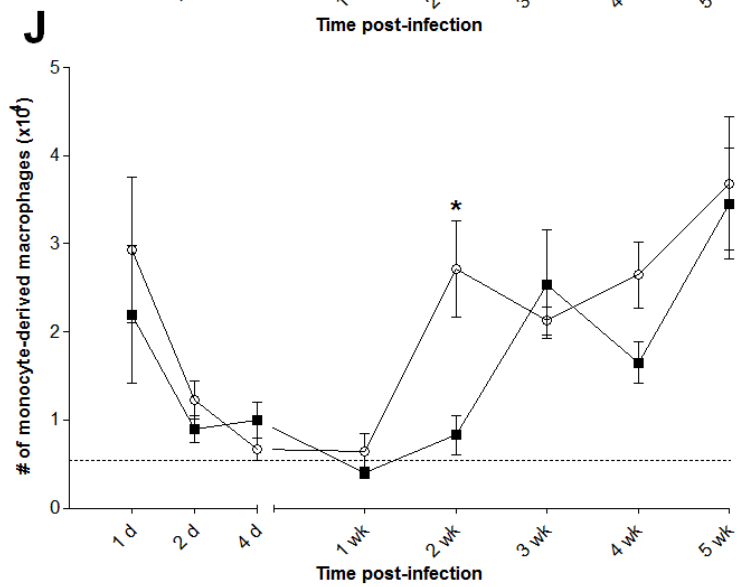
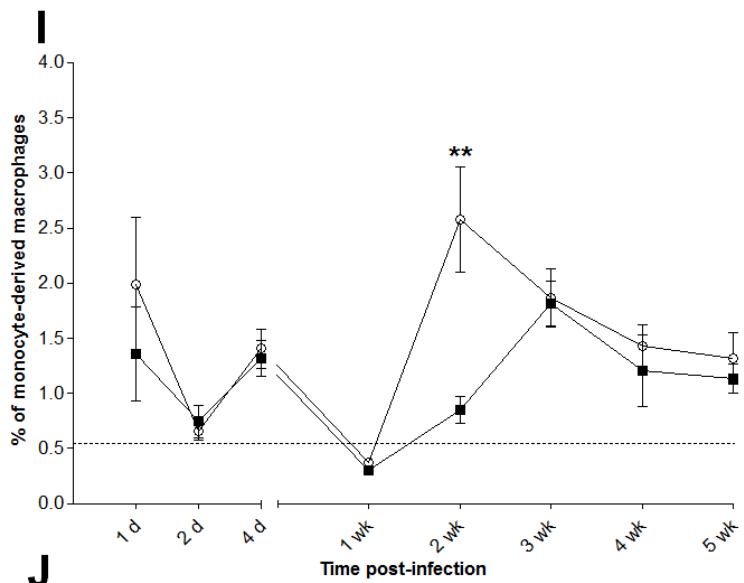


Figure 5-3 Dynamics of the innate immune cell populations at the site of inoculation during infection with *L. major* WT and Δ isp2/3. Purified metacyclic promastigotes (10^4 in 10 μ l PBS) were intradermally inoculated into the ears of C57BL/6 mice (n=5 for each time-point). Changes in the percentages of each cell type within the CD11b⁺ population (top panels) and changes in the total number of each cell type (bottom panels) per ear during infection with *L. major* WT (■) or Δ isp2/3 (○). Innate immune cell types are defined as given in Table 5-2 and Figure 5-2; neutrophils (A and B), dermal macrophages (C and D), dermal dendritic cells (E and F), inflammatory monocytes (G and H), monocyte-derived macrophages (I and J), and monocyte-derived dendritic cells (K and L). Results are expressed as means per group (n=5) at each time-point after infection, a representative of two independent experiments. Error bars represent S.E.M. Dashed lines represents the mean percentage of each cell type within the CD11b⁺ population (top panels) and the mean numbers of each cell type (bottom panels) in a naive ear. Asterisks indicate statistical significance between WT and Δ isp2/3 at $p < 0.05$ (*) and $p < 0.01$ (**), as measured by an unpaired *t*-test.

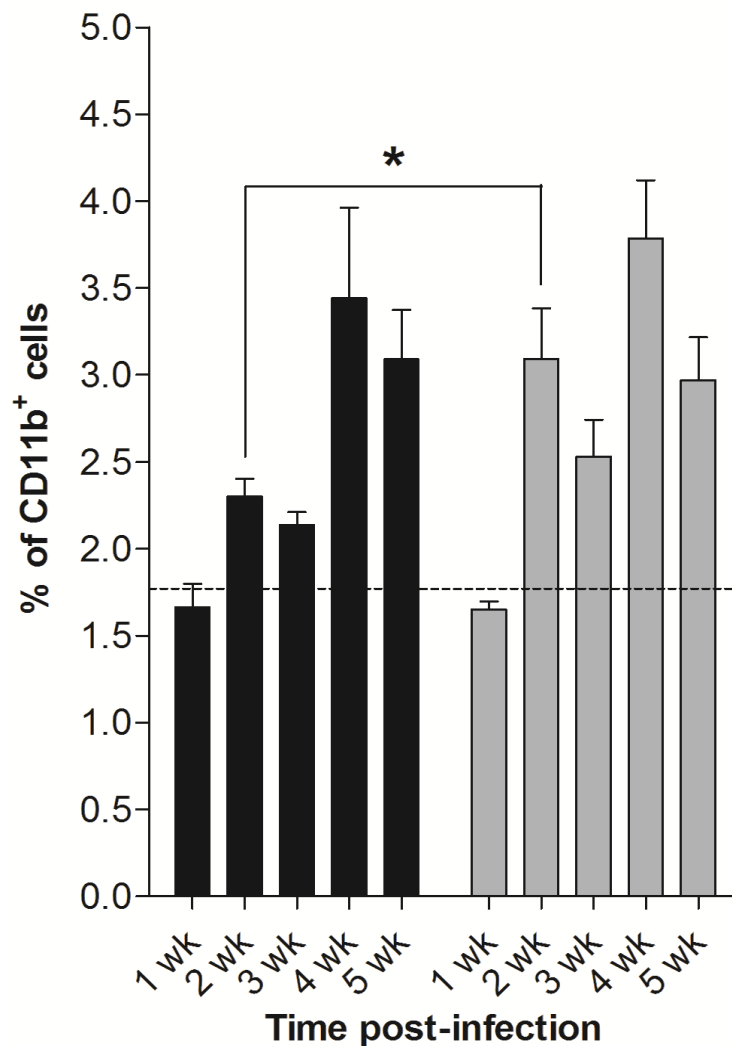


Figure 5-4 Myeloid cell composition of the draining lymph node after intradermal inoculation with *L. major* WT or Δ isp2/3. Purified metacyclic promastigotes (10^4 in 10 μ l PBS) were intradermally inoculated into the ears of C57BL/6 mice ($n=5$ for each time-point). The percentage of CD11b⁺ within the live cell population of the dLN was assessed during infection with *L. major* WT (black bars) or Δ isp2/3 (grey bars). Single cell suspensions from the dLNs were stained with the pan-myeloid cell marker, CD11b. Bars represent the means per group at each time-point after infection. Error bars represent S.E.M. Dashed lines represents the mean percentage of CD11b⁺ cells within the live cell population in naive dLNs. Asterisks indicate statistical significance between WT and Δ isp2/3 at $p < 0.05$ (*), as measured by an unpaired *t*-test.

5.2.2 Imaging myeloperoxidase (MPO) activity of activated phagocytes during *L. major* infection

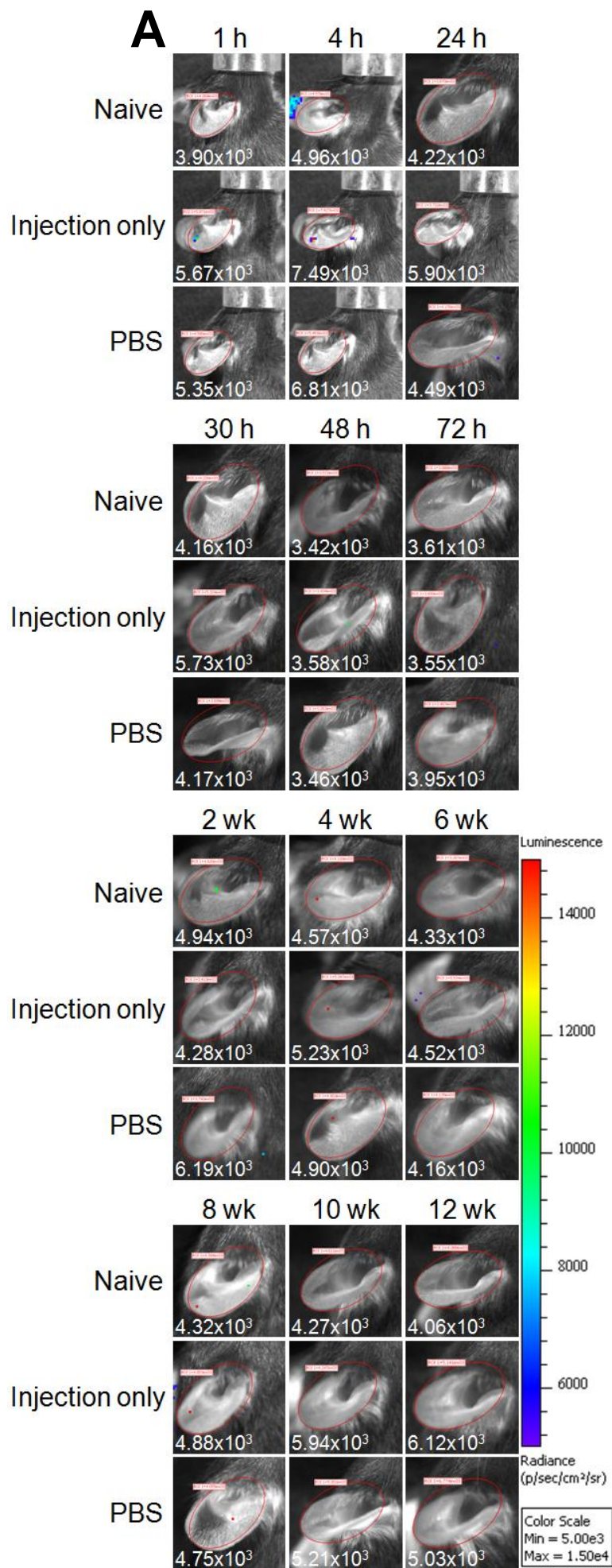
Luminol was used to non-invasively monitor MPO activity during the course of infection with *L. major* WT and *ISP2* gene mutants *in vivo*. *L. major* WT, Δ isp2/3, and an *ISP2* overexpressor, WT [*pXG-ISP2*], were inoculated into the ear dermis of C57BL/6 mice at a dose of 10^4 metacyclic promastigotes. For controls, ears were injected with an equivalent volume of PBS, or the needle only; naive ears were also imaged to provide the background signal for the BLI. For each time-point after parasite inoculation, mice were intraperitoneally injected with

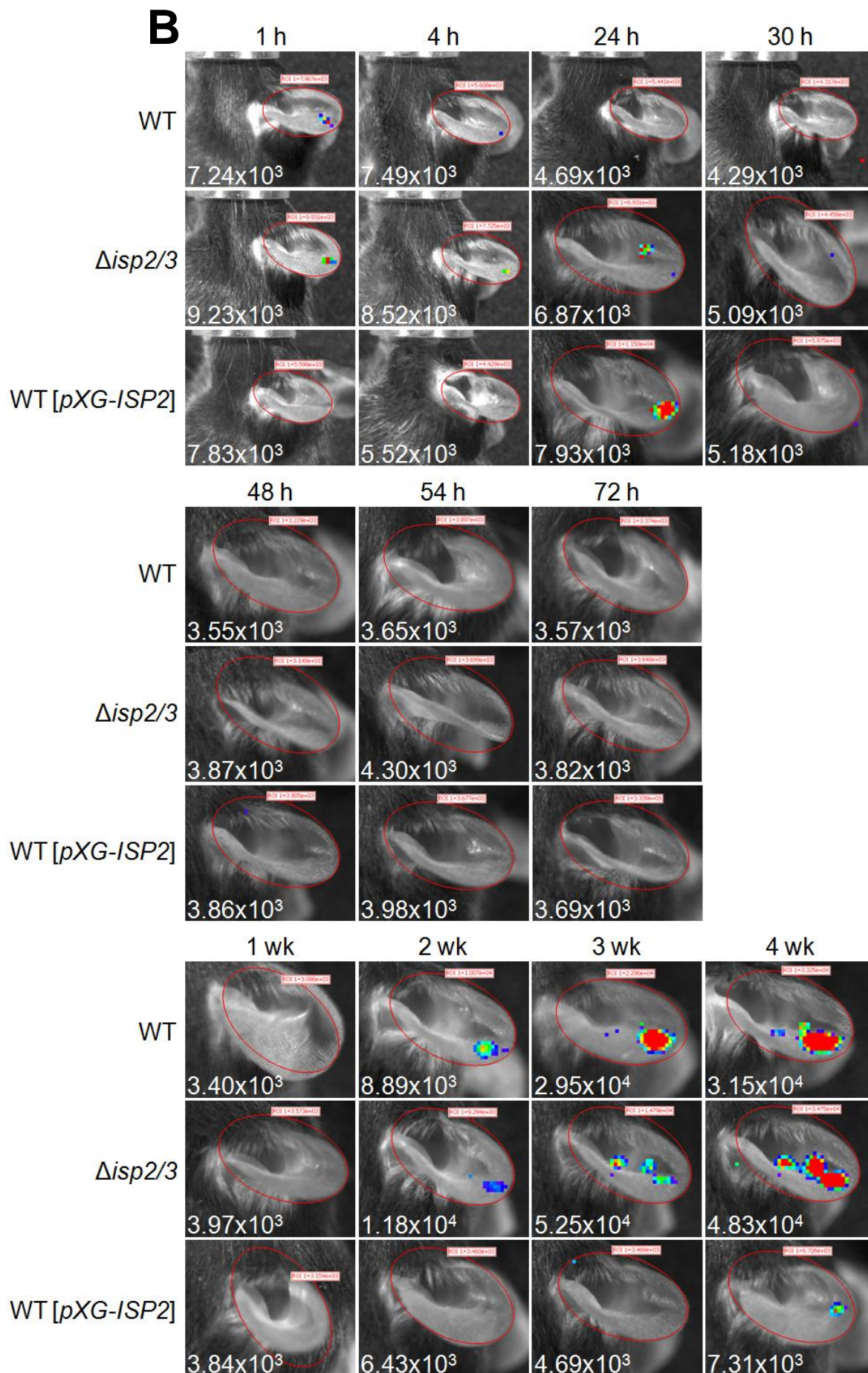
luminol to generate an MPO-specific bioluminescent signal. Mice were anaesthetised then imaged in the IVIS using a CCD camera to detect and capture the photons emitted between 10 and 15 min after luminol injection. Figure 5-5A shows representative images of one mouse for each of the control groups, and Figure 5-5B shows representative images of one mouse per group infected with either *L. major* WT, $\Delta isp2/3$, or WT [pXG-ISP2] parasites over the course of infection.

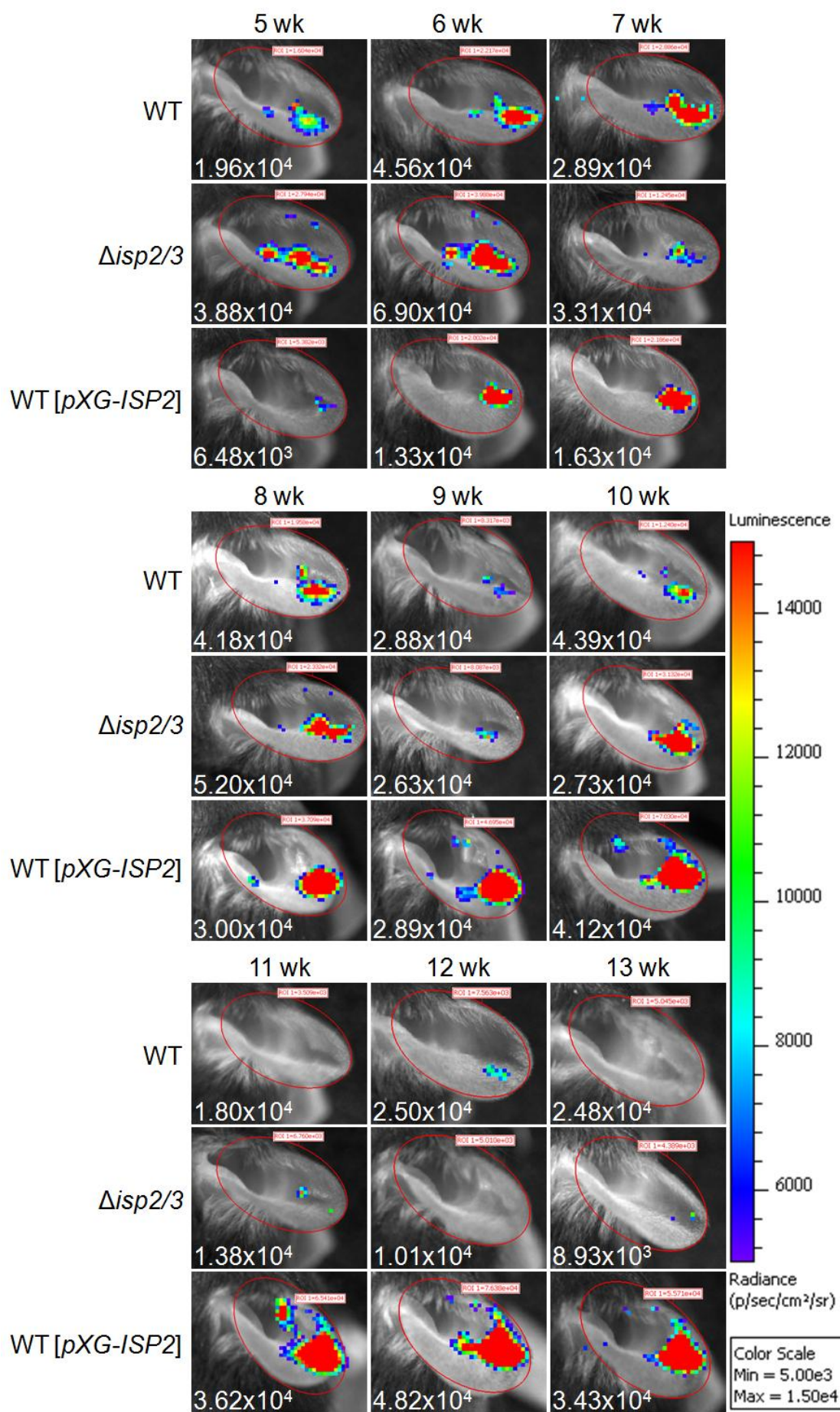
Figure 5-5C shows the average MPO-specific bioluminescent signal from the ears of each mouse group at each time-point studied. There was a low MPO-specific bioluminescent signal from the ears infected with all three *L. major* cell lines at 1 h post-infection, which was significantly different from the background signal from the naive ear, but not from the PBS and needle only controls. The bioluminescent signal from the PBS and needle only controls at 1 h was between that from the parasite groups and the naive ears, from which they were not significantly different. There was a slight increase in the signal from the PBS and needle only controls at 4 h, but the signal from these groups decreased to that of a naive ear by 24 h, which was on average 4.1×10^3 photons sec^{-1} over the course of infection. The signal from the PBS and needle only control groups remained around 4.7×10^3 photons sec^{-1} over the next 13 wk, which was not significantly different from that of the naive ear. The signal from the parasite-infected ears also decreased to the level of the background signal by 48 h.

At 2 wk post-infection, there was an increase in the bioluminescent signal from ears infected with WT and $\Delta isp2/3$ parasites, which continued to increase at 3 wk, and was maintained around the same level until 11 wk for WT infection and 9 wk for $\Delta isp2/3$ infection. Over 3 to 6 wk, the average bioluminescent signal from $\Delta isp2/3$ -infected ears appeared to be higher than that from WT-infected ears. This may indicate differences in the activation status of the phagocytes; as the only differences in innate immune cell recruitment were higher numbers of monocyte-derived cells at 2 wk in $\Delta isp2/3$ infection compared with WT infection, as evidenced by flow cytometry (Figure 5-3). At 9 wk, the signal from $\Delta isp2/3$ -infected ears began to decrease and by 13 wk the signal was almost equivalent to the background signal, whereas the decrease in signal from WT-infected mice from 11 wk was not as pronounced. This stage may show the

resolution of the disease with fewer phagocytes present, as these time-points were not assessed by flow cytometry. The signal from WT [*pXG-ISP2*]-infected ears was much more delayed, not beginning to increase until 4 wk, and reaching the peak around 12 wk. The overexpression of ISP2 may, therefore, lead to inhibition of innate cell recruitment to the site of infection. The respective peaks in bioluminescent signal for each of the parasite groups during this second wave was approximately 6 to 7-fold higher than their initial signal at 1 h.







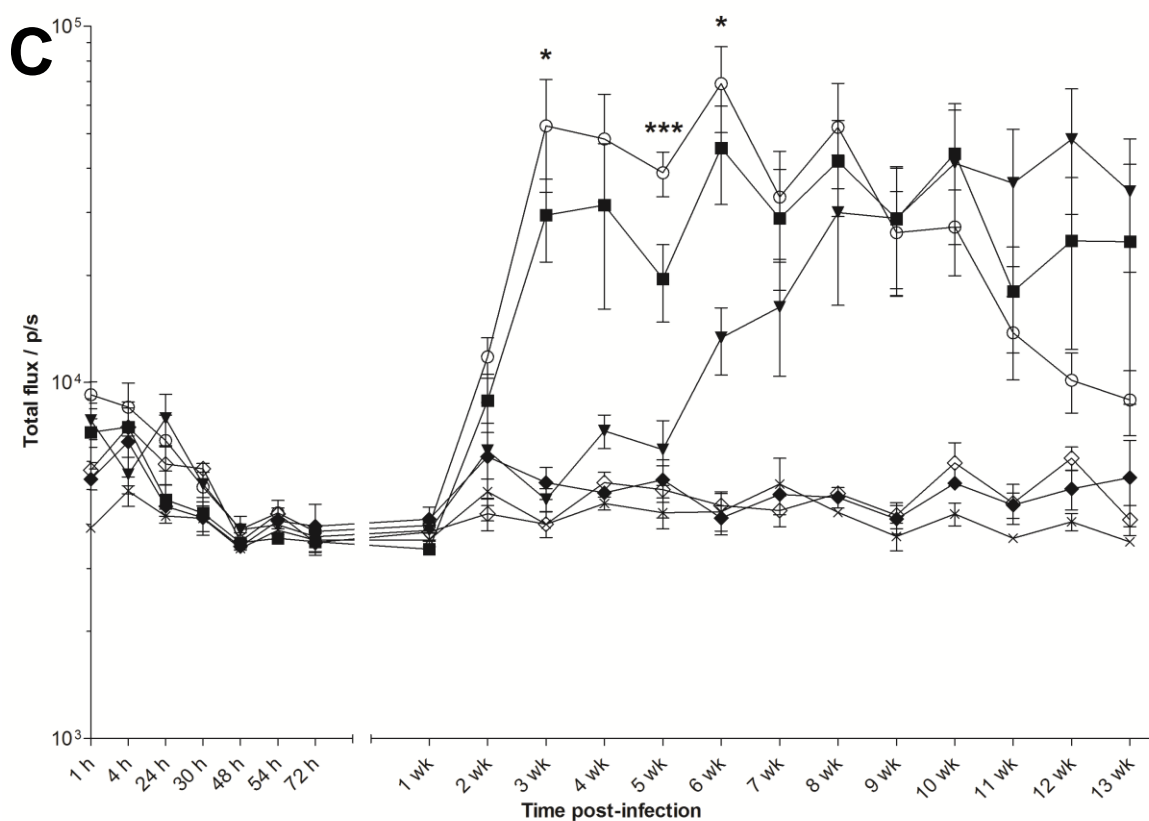


Figure 5-5 *In vivo* bioluminescence imaging of MPO activity of activated phagocytes at the site of inoculation during infection with *L. major* WT and *ISP2* gene mutants. C57BL/6 mice were inoculated in the ear with 10^4 *L. major* WT, Δ isp2/3, WT [pXG-ISP2] metacyclic promastigotes (n=5 for each group). Mice were imaged in the IVIS 10 to 15 min after intraperitoneal luminol injection. Representative images of one mouse per group over the course of infection for **A**) the controls, which were the naive ears, ears injected with the needle only, or ears injected with 10 μ l PBS (n=4 for each group), and **B**) ears infected with *L. major* WT, Δ isp2/3, and WT [pXG-ISP2]. The colour scale indicates bioluminescent radiance in photons/second/cm²/steradian. The red oval indicates the region of interest (ROI) and the value in the red box indicates the total flux, given in photons per second (photons sec⁻¹), over the ROI in the individual image shown. The same colour scale and ROI was applied to all images analysed. The value in white gives the mean total flux for the group at each time-point over the course of 13 wk infection. **C**) The mean total flux for the group at each time-point over the course of 13 wk infection. ■, WT; ○, Δ isp2/3; ▼, WT [pXG-ISP2]; ◆, PBS; ◇, injection only; ×, naive. Data are shown on a logarithmic scale. Error bars represent S.E.M. Asterisks indicate statistical significance between the parasite groups at $p < 0.05$ (*) and $p < 0.001$ (***), as measured by one-way ANOVA with a Tukey post test.

MPO is known to be contained within the granules of neutrophils and monocytes (Tay et al., 1998), but whether MPO is present in macrophages of mice is still unclear, as certain tissue macrophages in humans have been shown to be MPO-positive (Daugherty et al., 1994; Nagra et al., 1997). Therefore, flow cytometry was performed, using intracellular staining with an anti-MPO antibody, to analyse the MPO protein content in the cell types analysed in this investigation (Table 5-2). This information of MPO protein content could provide a better indication of which innate cell types contributed to the differences observed in the bioluminescent signal of MPO activity detected using luminol between *L. major* WT and the *ISP2* gene mutants *in vivo* (Figure 5-5).

Mice were intradermally inoculated with metacyclic promastigotes of *L. major* WT, $\Delta isp2/3$, or $\Delta isp2/3:ISP2/3$, which stably expresses *ISP2*, rather than WT [*pXG-ISP2*]; the ears were processed and analysed 2 wk post-infection, the time-point at which differences were observed in the innate immune cell populations in the ear after infection with WT or $\Delta isp2/3$ parasites (Figure 5-3). The graphs showing the percentage of CD11b⁺ cells within the total live cell population (Figure 5-6A) and the percentage of each innate cell type within the CD11b⁺ population (Figure 5-6, B to E) were analysed as in Figure 5-1 to 5-3. However, Figure 5-6C represents all Ly6C^{hi} cells, which incorporates the inflammatory monocytes, monocyte-derived macrophages, and moDCs, as too few cells were analysed to make reliable distinctions between these cell types. The percentages of each of these innate cell types in response to WT and $\Delta isp2/3$ infection at 2 wk was similar to that seen earlier (Figure 5-1 and 5-3). The use of the $\Delta isp2/3:ISP2/3$ cell line corroborated the differences observed previously in the Ly6C^{hi} monocyte and monocyte-derived cell populations in the WT and $\Delta isp2/3$ infections at this time-point (Figure 5-3, G, I, and K, and Figure 5-6C); the cell populations in response to WT and $\Delta isp2/3:ISP2/3$ infections were not significantly different, but between infections with $\Delta isp2/3$ and $\Delta isp2/3:ISP2/3$, which slightly overexpresses *ISP2* (Figure 3-1), were significantly different. However, there was also a significantly higher percentage of neutrophils in the $\Delta isp2/3$ infection compared with $\Delta isp2/3:ISP2/3$ infection (Figure 5-6B), whereas no significant difference was observed between $\Delta isp2/3$ and WT infections (Figure 5-3A and Figure 5-6B).

Figure 5-6F shows that there was significantly more MPO⁺ staining within the CD11b⁺ population of ears infected with $\Delta isp2/3$ parasites, than $\Delta isp2/3:ISP2/3$ and WT parasites, although this difference was not significantly different. Intracellular staining of MPO showed that almost all neutrophils were MPO⁺, 97%, and approximately 48% of Ly6C^{hi} cells were MPO⁺, regardless of the ear samples analysed, i.e. parasite-infected, PBS-injected, or naive. Resident macrophages and DCs had negligible MPO staining at 0.25% and 4.7% respectively. This indicates that MPO can be used as an additional stain to distinguish between these innate cell types in mice. Due to the levels of MPO staining within each of these cell types and the percentage of each of these cell types within the CD11b⁺ population, MPO⁺ neutrophils (Figure 5-6G) and MPO⁺ Ly6C^{hi} cells (Figure

5-6H) were significantly higher in $\Delta isp2/3$ infection compared with WT and $\Delta isp2/3:ISP2/3$ infections. This suggests that either of these cell types could contribute to the MPO-specific bioluminescent signal *in vivo* when these phagocytes are activated.

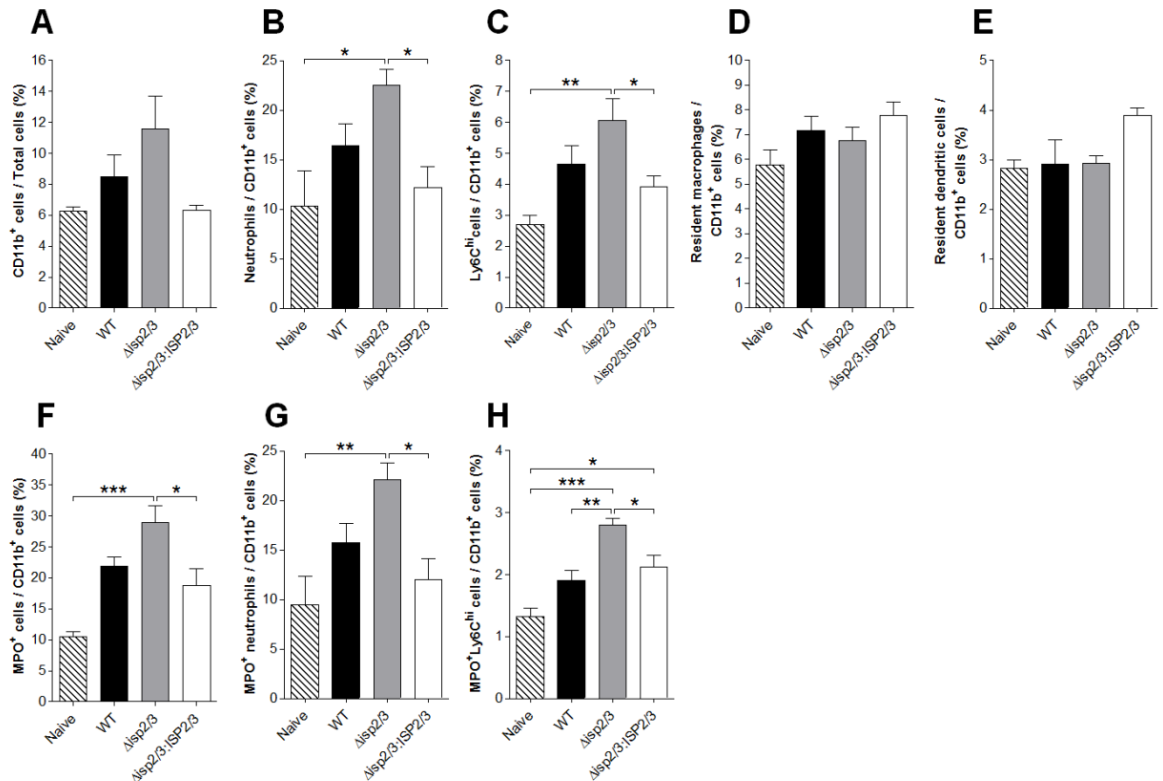


Figure 5-6 MPO protein content of innate immune cells in the ear dermis of C57BL/6 mice at 2 wk post-infection with *L. major* WT and *ISP2* gene mutants. Purified metacyclic promastigotes (10^4 in $10 \mu\text{l}$ PBS) of *L. major* WT, $\Delta isp2/3$, and $\Delta isp2/3:ISP2/3$ were intradermally inoculated into the ears of C57BL/6 mice ($n=5$). Innate immune cell populations of the ear were analysed by flow cytometry as shown in Figure 5-2. The intracellular MPO staining was then assessed for each cell population in each of the groups; data are presented as the percentage of each MPO⁺ cell type within the CD11b⁺ population for each group. Percentages of A) CD11b⁺ cells within the live cell population, and B) neutrophils, C) Ly6C^{hi} cells, D) dermal macrophages, and E) dermal dendritic cells, F) total MPO⁺ cells, G) MPO⁺ neutrophils, and H) MPO⁺ Ly6C^{hi} cells within the CD11b⁺ population. Asterisks indicate statistical significance between groups at $p < 0.05$ (*), $p < 0.01$ (**) and $p < 0.001$ (***), as measured by one-way ANOVA with a Tukey post test.

5.2.3 Quantification of the iNOS response, IFN- γ production, and DC maturation

As there were differences between the innate cell recruitment and activation during infection with *L. major* WT and the *ISP2* gene mutants, the expression of iNOS within these innate cell types was investigated. iNOS, also known as NOS2, produces the toxic metabolite, NO, which is known to control *L. major* infection (Stenger et al., 1994; Vouldoukis et al., 1995; De Trez et al., 2009; Petritus et al., 2012). The differences observed in the innate immune cell recruitment and

activation at the site of infection occurred during the second wave of innate cell infiltration, starting at 2 wk post-infection; therefore, the focus of the subsequent investigations were during this stage of infection.

Mice were intradermally inoculated with *L. major* WT, $\Delta isp2/3$, or $\Delta isp2/3:ISP2/3$ metacyclic promastigotes, the ears were processed and analysed at 2 and 5 wk post-infection. There was prominent iNOS expression in the parasite-infected ears at both 2 (Figure 5-7, A and B) and 5 wk post-infection (Figure 5-7C). There was a significantly higher percentage of iNOS⁺ cells in $\Delta isp2/3$ -infected ears compared with those infected with WT and $\Delta isp2/3:ISP2/3$ parasites at 2 wk, but by 5 wk, there was no significant difference between the groups. The higher iNOS expression in $\Delta isp2/3$ -infected ears at 2 wk was due to an increase in iNOS expression in the resident macrophages, resident DCs, inflammatory monocytes, and monocyte-derived macrophages (Figure 5-7, E to H). The level of iNOS expression within the moDCs was high in response to all the parasite groups (Figure 5-7I), suggestive of the iNOS-producing moDCs that have been described in *L. major* infection (De Trez et al., 2009). Conversely, the level of iNOS expression within the neutrophils was low (Figure 5-6D).

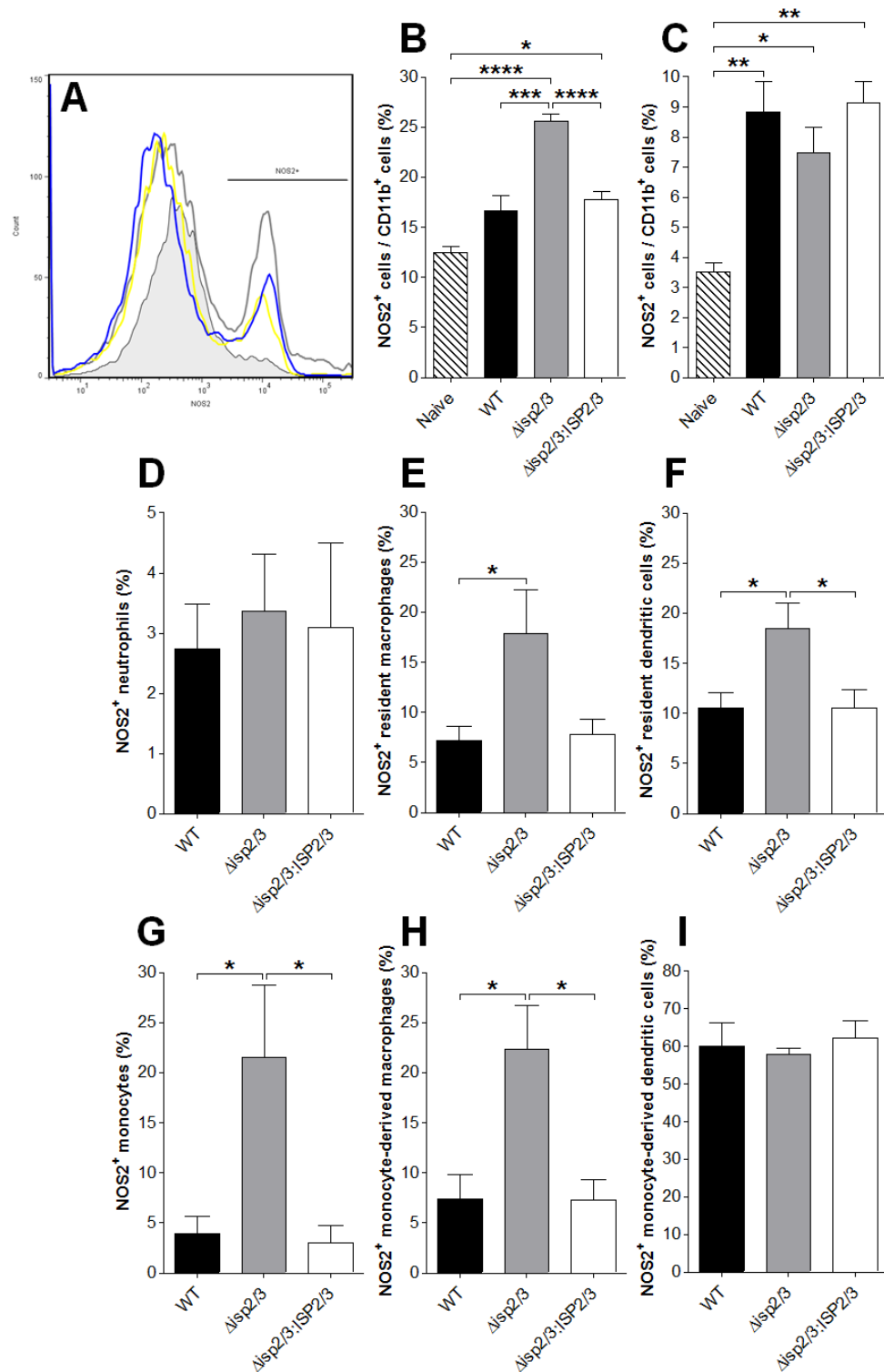


Figure 5-7 Inducible nitric oxide synthase (iNOS/NOS2) expression at the site of inoculation at 2 wk post-infection with *L. major* WT and *ISP2* gene mutants. Purified metacyclic promastigotes (10^4 in $10\ \mu\text{l}$ PBS) of *L. major* WT, Δ isp2/3, and Δ isp2/3:ISP2/3 were intradermally inoculated into the ears of C57BL/6 mice ($n=5$). Innate immune cell populations of the ear were analysed by flow cytometry as shown in Figure 5-2; data are presented as the percentage of iNOS/NOS2⁺ cells within each cell type for each group. **A)** Histogram to show the iNOS⁺ cells within the CD11b⁺ population at 2 wk post-infection. Shaded area represents the cells from a naive ear. Blue line, WT; grey line, Δ isp2/3; yellow line, Δ isp2/3:ISP2/3. Percentage of iNOS⁺ cells within the CD11b⁺ population at **B)** 2 wk and **C)** 5 wk post-infection. Percentage of iNOS⁺ **D)** neutrophils, **E)** resident macrophages, **F)** resident dendritic cells, **G)** inflammatory monocytes, **H)** monocyte-derived macrophages, and **I)** monocyte-derived dendritic cells, as assessed by flow cytometry. Asterisks indicate statistical significance between groups at $p < 0.05$ (*), $p < 0.01$ (**), and $p < 0.0001$ (****), as measured by one-way ANOVA with a Tukey post test.

IFN- γ secreted by Th1 cells stimulates the expression of iNOS, which produces NO. High levels of IFN- γ can be an indication of the polarisation of the adaptive immune response towards a Th1 response, which is associated with the control of *Leishmania* infection (Locksley et al., 1991; Park et al., 2000; De Trez et al., 2009). The concentration of IFN- γ at the site of inoculation and in dLN of mice infected with *L. major* WT, Δ *isp2/3*, and Δ *isp2/3:ISP2/3* parasites, at 2 wk post-infection was assessed by ELISA (Figure 5-8, A and B respectively). At the site of inoculation, the concentration of IFN- γ in Δ *isp2/3*-infected ears was significantly higher than that of WT- and Δ *isp2/3:ISP2/3*-infected ears (Figure 5-8A). Although the mean concentration of IFN- γ in the dLNs of Δ *isp2/3*-infected mice appeared higher than that of WT and Δ *isp2/3:ISP2/3* infections, there was no significant difference between the WT, Δ *isp2/3*, and Δ *isp2/3:ISP2/3* infections (Figure 5-8B).

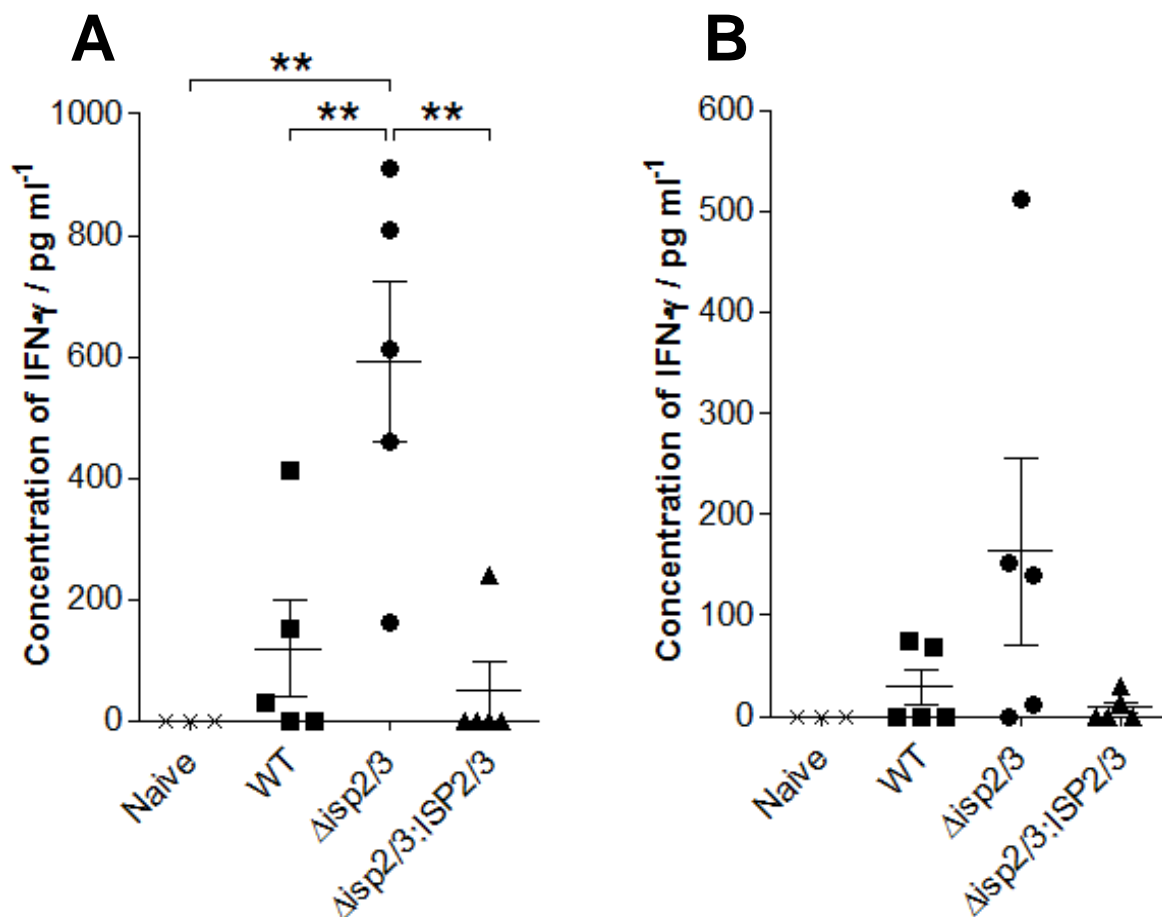


Figure 5-8 IFN- γ concentration at 2 wk post-infection with *L. major* WT and *ISP2* gene mutants. Purified metacyclic promastigotes (10^4 in 10 μ l PBS) of *L. major* WT, Δ *isp2/3*, and Δ *isp2/3:ISP2/3* were intradermally inoculated into the ears of C57BL/6 mice ($n=5$). ELISAs were performed using supernatants isolated from the **A**) ears and **B**) dLNs. Mean with error bars representing S.E.M. Asterisks indicate statistical significance between groups at $p < 0.01$ (**), as measured by one-way ANOVA with a Tukey post test.

DCs are proposed to be important in the generation of an adaptive immune response during *Leishmania* infection; DCs migrate from the site of infection to the dLNs to present antigen to naive T cells in order to induce an antigen-specific T cell response (León et al., 2007). To assess the activation of the DC populations, the resident DCs and the moDCs, flow cytometry was performed to determine the surface expression of CD86 and CD80. CD86 and CD80 are co-stimulatory molecules that work in tandem to prime a T cell response through T cell activation (Moser, 2001). CD86 is a marker of early DC maturation, whereas CD80 is a marker of mature DCs (Zheng et al., 2004). CD80 and CD86 have also been reported to activate the Th1 and Th2 developmental pathways respectively (Kuchroo et al., 1995), which has been shown to play a role during *L. major* infection (Brown et al., 1996). Mice were intradermally inoculated with *L. major* WT or $\Delta isp2/3$ parasites, the ears were processed and analysed at 2 wk post-infection. There was a significantly higher percentage of moDCs in response to $\Delta isp2/3$ infection compared with WT infection (Figure 5-9A), as seen previously (Figure 5-3K). However, there was also a significantly higher percentage of resident DCs in WT infection compared with $\Delta isp2/3$ infection, although there was no significant difference from the naive ear (Figure 5-9B).

There was no difference in the surface staining of CD86 on moDCs (Figure 5-9C) and resident DCs (Figure 5-9D) from parasite-infected or naive ears. There was, however, a significant increase in CD80 expression on moDCs from $\Delta isp2/3$ -infected ears compared with those from WT-infected and naive ears (Figure 5-9E). In addition, there appeared to be an increase in CD80 expression on resident DCs from $\Delta isp2/3$ -infected ears, although this was not significantly different from WT-infected or naive ears (Figure 5-9F).

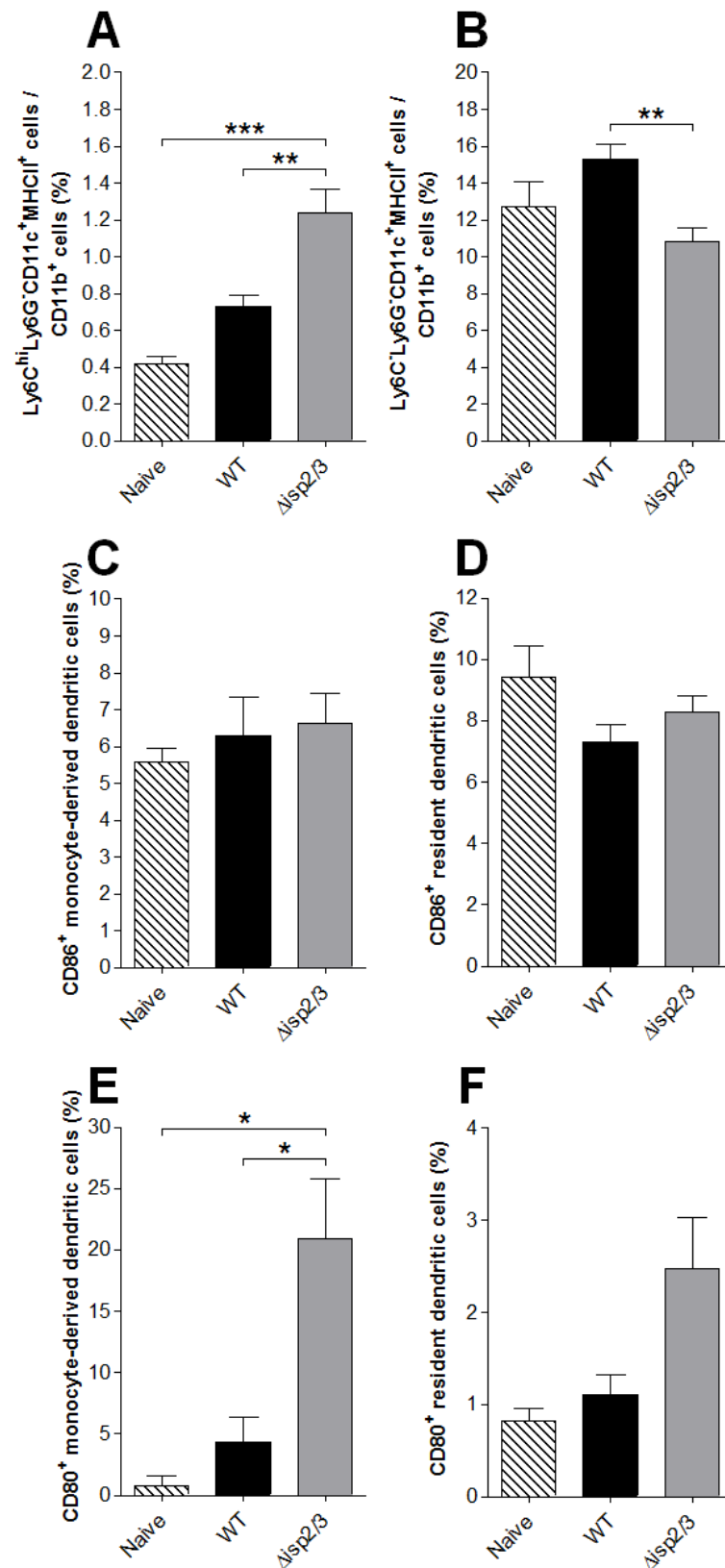


Figure 5-9 Dendritic cell co-stimulatory molecule expression at 2 wk post-infection with *L. major* WT and Δ isp2/3. Purified metacyclic promastigotes (10^4 in 10 μ l PBS) of *L. major* WT and Δ isp2/3 were intradermally inoculated into the ears of C57BL/6 mice (n=5). Innate immune cell populations of the ear were analysed by flow cytometry as shown in Figure 5-2. Percentage of **A**) monocyte-derived dendritic cells and **B**) resident dendritic cells within the CD11b⁺ population at 2 wk post-infection. Percentage of CD86⁺ **C**) monocyte-derived dendritic cells and **D**) resident dendritic cells. Percentage of CD80⁺ **E**) monocyte-derived dendritic cells and **F**) resident dendritic cells. Asterisks indicate statistical significance between groups at $p < 0.05$ (*), $p < 0.01$ (**), and $p < 0.001$ (***), as measured by one-way ANOVA with a Tukey post test.

5.2.4 The role of neutrophil elastase (NE) during *Leishmania* infection *in vivo*

Mice deficient in NE, *Ela*^{-/-}, were used to investigate the role of this host NSP in the generation of immune responses to *L. major* WT and the *ISP2* gene mutants *in vivo*.

5.2.4.1 Genotyping of transgenic *Ela*^{-/-} mice

Ela^{-/-} mice used in this study were previously generated through the disruption of the endogenous NE gene with a targeting vector containing neomycin phosphotransferase cDNA driven by the phosphoglycerate kinase promoter (PGK-neo) (Belaouaj et al., 1998). *Ela*^{-/-} mice are currently maintained in a C57BL/6 genetic background.

PCR was performed on DNA purified from the ear tissue of C57BL/6 and *Ela*^{-/-} mice to check the presence of the NE gene in C57BL/6 mice (Figure 5-10A, lanes 1 and 2), and the neomycin marker in *Ela*^{-/-} mice (Figure 5-10A, lanes 7 and 8). Samples from lanes 1, 2, 7, and 8, were re-run in Figure 5-10B, because no band, representing the wild-type NE gene in C57BL/6 mice, was observed in lane 2 of Figure 5-10A. Figure 5-10B shows that this band (lane 2) is much fainter and may not have been detected or loaded correctly in Figure 5-10A. DNA from C57BL/6 mice was negative for the neomycin marker (Figure 5-10A, lanes 3 and 4). Multiple bands were observed in PCR with the NE primers against DNA from *Ela*^{-/-} mice, although there were no bands present the same size as the wild-type NE gene (Figure 5-10A, 5 and 6); the presence of multiple bands is due to the disruption of the NE gene.

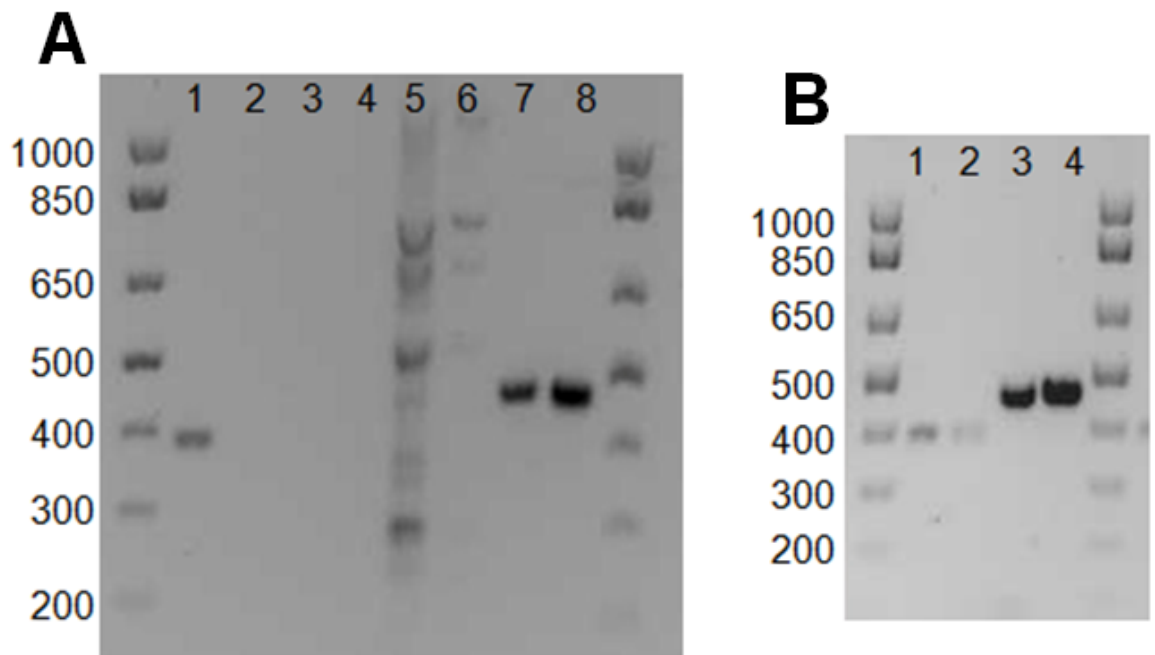


Figure 5-10 Genotyping of transgenic neutrophil elastase deficient, *Ela*^{-/-}, mice through PCR analysis. **A)** Two independent DNA samples from C57BL/6 mice with primers for the wild-type neutrophil elastase gene (lanes 1 and 2) and the neomycin marker (lanes 3 and 4). Two independent DNA samples from *Ela*^{-/-} mice with primers for the wild-type neutrophil elastase gene (lanes 5 and 6) and the neomycin marker (lanes 7 and 8). **B)** Samples from lanes 1, 2, 7, and 8 of Figure 5-10A, were run on a separate gel, lanes 1, 2, 3, and 4 respectively, to check the loading of lane 2 of A.

5.2.4.2 Lesion measurements over the course of *L. major* infection in *Ela*^{-/-} mice

Lesion size was evaluated in the ears of *Ela*^{-/-} mice following intradermal inoculation of 10⁴ *L. major* WT, Δ *isp2/3*, or WT [*pXG-ISP2*] metacyclic promastigotes (Figure 5-11). Ear thickness did not change in ears injected with PBS or the needle only, or in the naive ears, which were, on average, 0.25 mm over the course of infection. WT- and Δ *isp2/3*-infected ears showed a similar lesion profile, in which ear thickness began to increase at 2 wk post-infection, peaking and gradually decreasing from 4 wk onwards. WT [*pXG-ISP2*]-infected ears showed a much more delayed lesion progression, which did not begin to increase until 5 wk post-infection and continued to increase up to 11 wk post-infection.

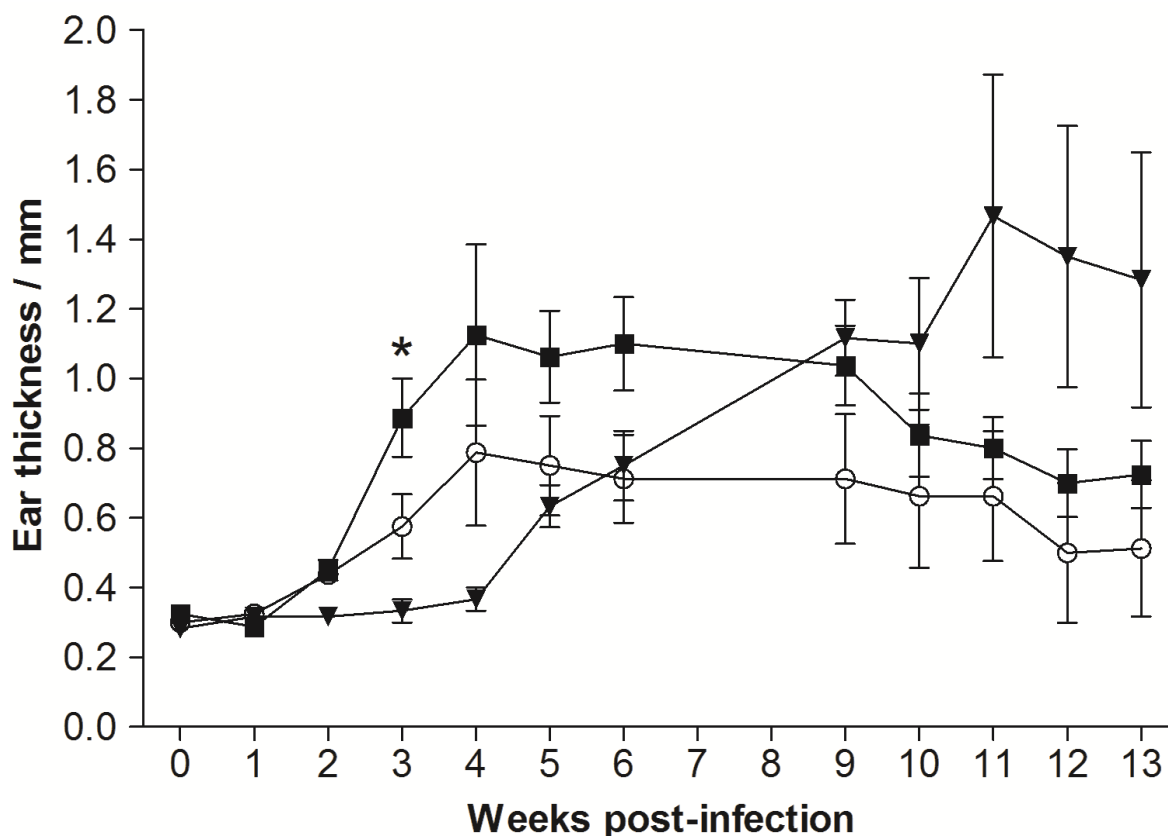


Figure 5-11 Lesion development in the ears of *Ela*^{-/-} mice infected with *L. major* WT and *ISP2* gene mutants. The ears of *Ela*^{-/-} mice were infected with 10⁴ *L. major* WT (n=4), Δ isp2/3 (n=4), or WT [pXG-ISP2] (n=3) metacyclic promastigotes. Ear thickness was measured weekly using a dial caliper. Average ear thickness over 13 wk of infection. ■, WT; ○, Δ isp2/3; ▼, WT [pXG-ISP2]. Error bars represent S.E.M. Asterisks indicate statistical significance between groups at $p < 0.05$ (*), as measured by one-way ANOVA with Tukey post-test.

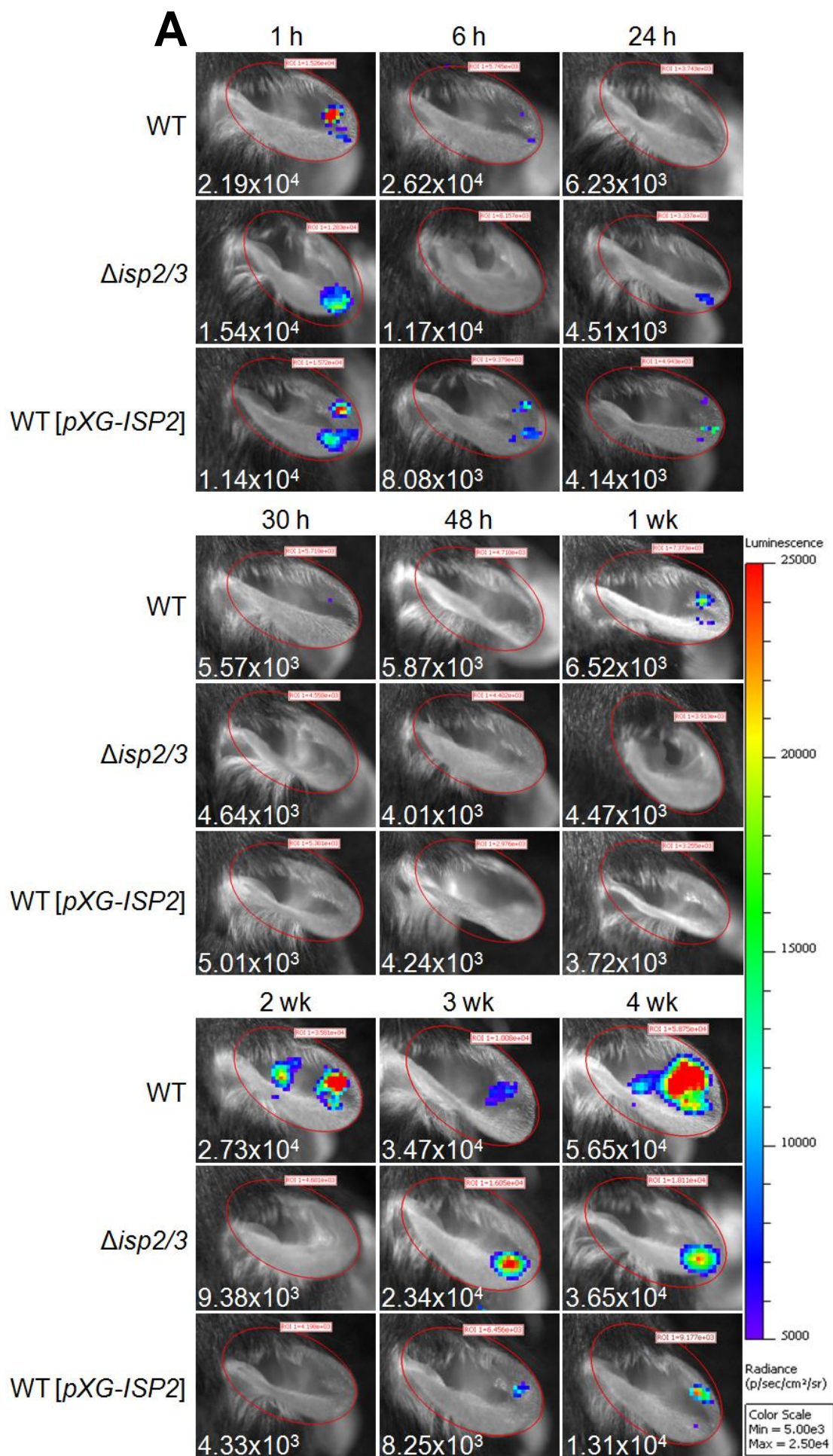
5.2.4.3 Imaging myeloperoxidase (MPO) activity of activated phagocytes in *Ela*^{-/-} mice

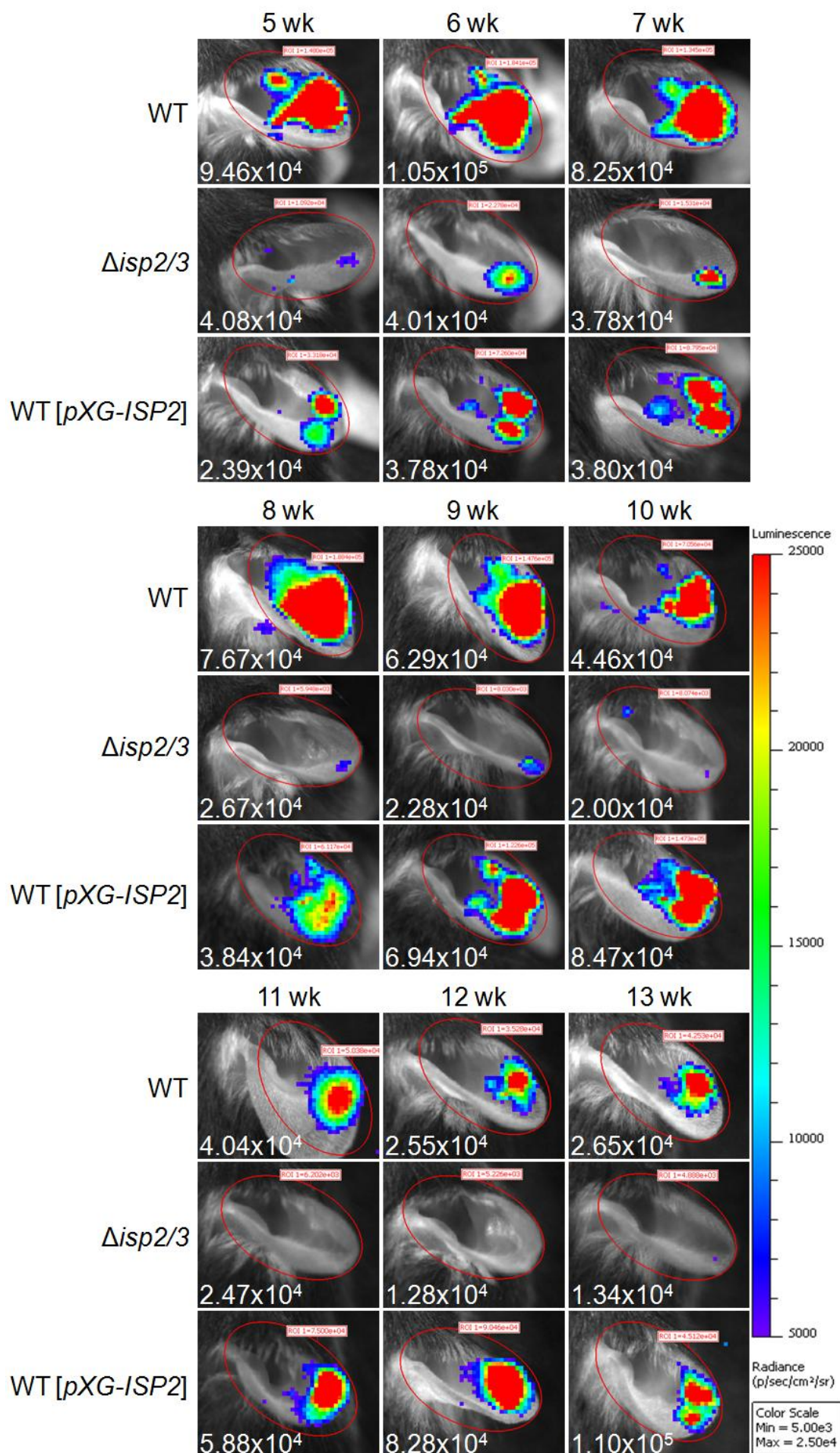
To determine whether NE plays a role in regulating phagocyte activation during infection with *L. major* WT and the *ISP2* gene mutants, luminol was used to non-invasively monitor MPO activity at the site of inoculation over the course of infection, as described earlier. *L. major* WT, Δ isp2/3, and WT [pXG-ISP2] parasites were inoculated into the ear dermis of *Ela*^{-/-} mice at a dose of 10⁴ metacyclic promastigotes. Controls were performed as in the C57BL/6 mice, ears were injected with an equivalent volume of PBS or the needle only. The bioluminescent signal from the control ears was low over the course of the experiment (Figure 5-12B). Naive ears were also imaged to provide the background signal for the BLI. Figure 5-12A shows representative images of one mouse per group infected with either *L. major* WT, Δ isp2/3, or WT [pXG-ISP2] parasites over the course of infection.

As in the C57BL/6 mice, there was a low MPO-specific bioluminescent signal from the ears infected with all three *L. major* cell lines at 1 h post-infection, although this was not significantly different from the background signal of the naive ear, or from the PBS and needle only controls (Figure 5-12B). The signal from the controls and the parasite-infected ears decreased to that of a naive ear by 24 h, which was on average 4.7×10^3 photons sec^{-1} over the course of infection. There was no significant difference in the MPO-specific bioluminescent signal between the parasite groups over the first 48 h.

At 2 wk post-infection, there was an increase in the bioluminescent signal from ears infected with WT and $\Delta\text{isp}2/3$ parasites, which continued to increase until 6 wk for WT infection and 5 wk for $\Delta\text{isp}2/3$ infection. From 1 wk post-infection, the average bioluminescent signal from WT-infected ears appeared to be higher than that from $\Delta\text{isp}2/3$ -infected ears. The peaks in bioluminescent signal for WT- and $\Delta\text{isp}2/3$ -infected ears during this second wave was approximately 4.7 and 2.7-fold higher than their initial signal at 1 h, respectively. The signal from WT [*pXG-ISP2*]-infected ears did not reach a peak during the course of this experiment; the signal began to increase at 3 wk post-infection and continued to increase over the next 10 wk. The increase in lesion formation (Figure 5-11) and the continuous increase in MPO-specific bioluminescence in the WT [*pXG-ISP2*]-infected ears suggest that the infection is more persistent than the WT and $\Delta\text{isp}2/3$ infections.

LDAs were performed on the dLNs of the mice infected with *L. major* WT, $\Delta\text{isp}2/3$, and WT [*pXG-ISP2*] parasites at 13 wk post-infection (Figure 5-12C). Parasite burdens in the dLNs of WT [*pXG-ISP2*]-infected mice were significantly higher than those of $\Delta\text{isp}2/3$ infection, and WT parasite burdens also seemed higher than those of $\Delta\text{isp}2/3$ infection, although this was not significantly different.





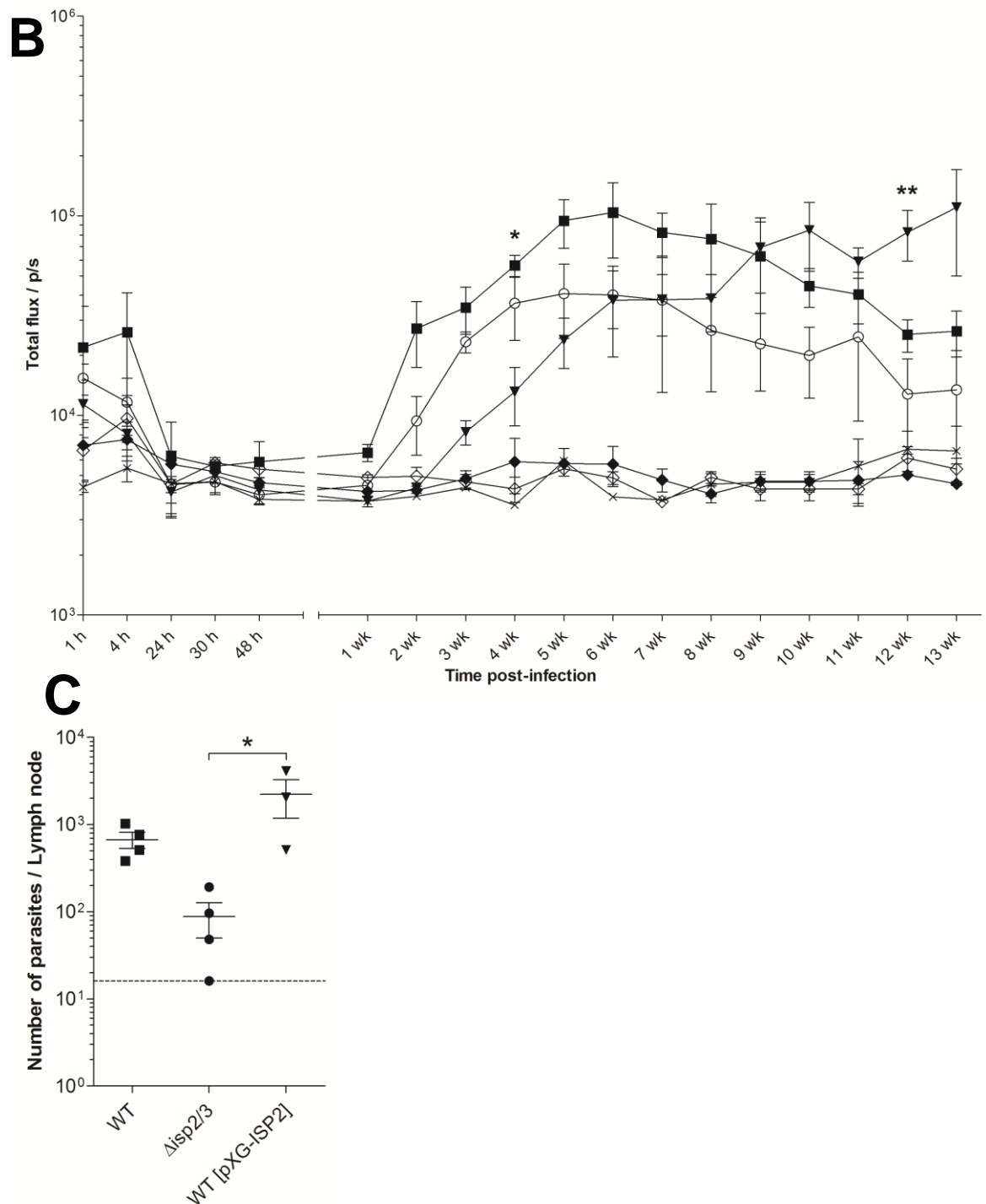


Figure 5-12 *In vivo* bioluminescence imaging of MPO activity of activated phagocytes at the site of inoculation during infection with *L. major* WT and *ISP2* gene mutants in *Ela*^{-/-} mice. *Ela*^{-/-} mice were inoculated in the ear with 10⁴ *L. major* WT (n=4), $\Delta isp2/3$ (n=4), WT [pXG-ISP2] (n=3) metacyclic promastigotes. Mice were imaged in the IVIS 10 to 15 min after intraperitoneal luminol injection. **A**) Representative images of one mouse per group over the course of infection for ears infected with *L. major* WT, $\Delta isp2/3$, and WT [pXG-ISP2]. The colour scale indicates bioluminescent radiance in photons/second/cm²/steradian. The red oval indicates the region of interest (ROI) and the value in the red box indicates the total flux, given in photons per second (photons sec⁻¹), over the ROI in the individual image shown. The same colour scale and ROI was applied to all images analysed, including the controls. The value in white gives the mean total flux for the group at each time-point. **B**) The mean total flux for the group at each time-point over the course of 13 wk infection. ■, WT; ○, $\Delta isp2/3$; ▼, WT [pXG-ISP2]; ◆, PBS; ◇, injection only; ×, naive. **C**) Parasite burdens in the dLNs of *Ela*^{-/-} mice determined by LDA at 13 wk post-infection. Data are shown on a logarithmic scale. Error bars represent S.E.M. Asterisks indicate statistical significance between the parasite groups at $p < 0.05$ (*) and $p < 0.01$ (**), as measured by one-way ANOVA with a Tukey post test.

5.2.4.4 Innate immune cell infiltration and activation at the site of inoculation at 2 wk post-infection in *Ela*^{-/-} mice

In C57BL/6 mice, the major differences observed in the innate cell recruitment and activation between *L. major* WT and Δ *isp2/3* intradermal infections occurred at 2 wk. Therefore, to assess the role of NE in these responses, the cellular immune response at the site of inoculation was examined in *Ela*^{-/-} mice at 2 wk post-infection following intradermal inoculation with 10⁴ *L. major* WT, Δ *isp2/3*, or Δ *isp2/3:ISP2/3* metacyclic promastigotes. Innate cell populations, given in Table 5-2, were analysed by flow cytometry as shown in Figure 5-2.

The percentage of CD11b⁺ cells within the live cell population in Δ *isp2/3*-infected ears was significantly higher than that of WT- and Δ *isp2/3:ISP2/3*-infected ears (Figure 5-13A). As in the C57BL/6 mice, there were significantly higher percentages of inflammatory monocytes, monocyte-derived macrophages, and moDCs in Δ *isp2/3*-infected ears compared with WT- and Δ *isp2/3:ISP2/3*-infected ears (Figure 5-13, C to E), and this was reflected in higher numbers of these cells (Figure 5-13, G to I), although there was only a significant difference in the moDCs. There was also a significantly higher percentage of neutrophils (Figure 5-13B), which was not observed in the C57BL/6 mice (Figure 5-3A), but there were no significant differences in the numbers of neutrophils between the groups (Figure 5-13F).

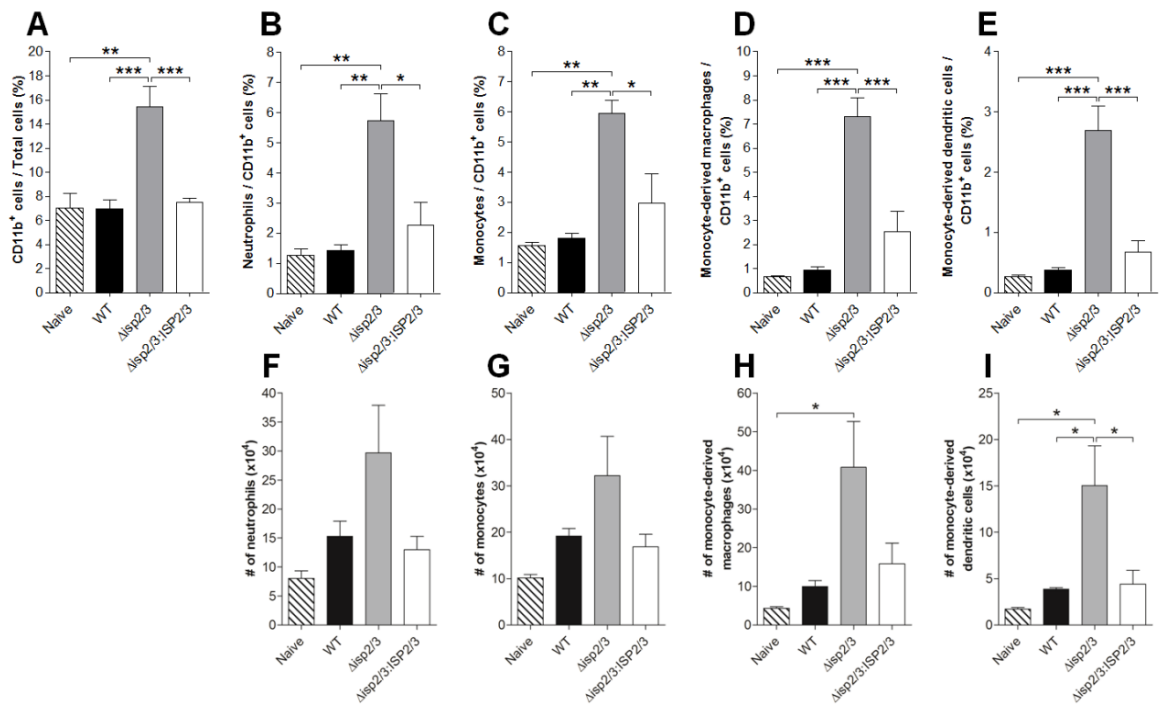


Figure 5-13 Composition of the cellular infiltrate at the site of inoculation at 2 wk post-infection with *L. major* WT and *ISP2* gene mutants in *Ela*^{-/-} mice. Purified metacyclic promastigotes (10^4 in 10 μ l PBS) of *L. major* WT, $\Delta isp2/3$, and $\Delta isp2/3:ISP2/3$ were intradermally inoculated into the ears of *Ela*^{-/-} mice. **A**) Percentage of CD11b⁺ cells within the live cell population, assessed by flow cytometry. Percentages of each cell type within the CD11b⁺ population (top panel) and changes in the total number of each cell type (bottom panel) per ear. Innate immune cell types are defined as given in Table 5-2 and Figure 5-2; Ly6C^{int}Ly6G⁺ neutrophils (**B** and **F**), Ly6C^{hi}Ly6G⁻ inflammatory monocytes (**C** and **G**), Ly6C^{hi}Ly6G⁺CD11c⁺MHCII⁻ monocyte-derived macrophages (**D** and **H**), and Ly6C^{hi}Ly6G⁺CD11c⁺MHCII⁺ monocyte-derived dendritic cells (**E** and **I**). Results are expressed as means per group ($n=5$). Error bars represent S.E.M. Asterisks indicate statistical significance between groups at $p < 0.05$ (*), $p < 0.01$ (**), and $p < 0.001$ (***), as measured by one way ANOVA with Tukey post test.

Ear dermal cells were additionally stained to evaluate the expression of the co-stimulatory molecules, CD80 and CD86, on the DC populations in the *Ela*^{-/-} mice infected with *L. major* WT, $\Delta isp2/3$, and $\Delta isp2/3:ISP2/3$ parasites for 2 wk. As in the C57BL/6 mice, there was no difference in the surface staining of CD86 on moDCs (Figure 5-14A) and resident DCs (Figure 5-14B) from the parasite-infected or naive ears. There was, however, a significant increase in CD80 expression on moDCs (Figure 5-14C) and resident DCs (Figure 5-14D) from $\Delta isp2/3$ -infected ears compared with those from naive ears and those infected with WT and $\Delta isp2/3:ISP2/3$ parasites.

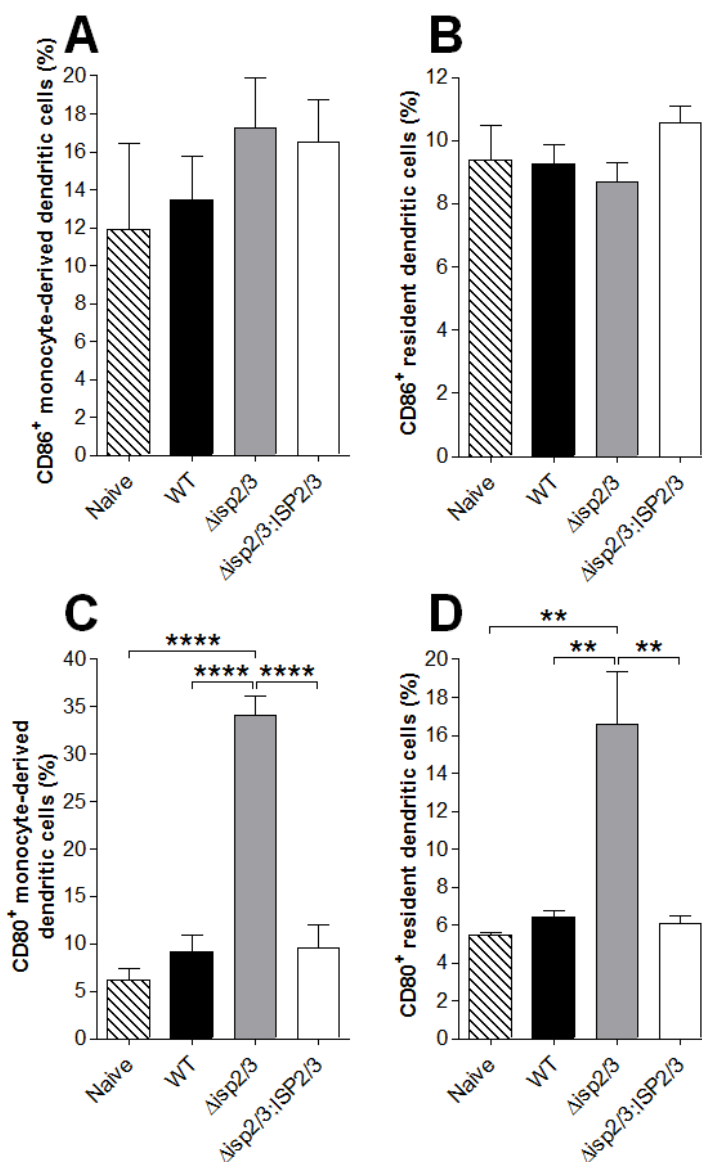


Figure 5-14 Dendritic cell co-stimulatory molecule expression at 2 wk post-infection with *L. major* WT and *ISP2* gene mutants in *Ela*^{-/-} mice. Percentage of CD86⁺ A) monocyte-derived dendritic cells and B) resident dendritic cells. Percentage of CD80⁺ C) monocyte-derived dendritic cells and D) resident dendritic cells. Asterisks indicate statistical significance between groups at $p < 0.01$ (**) and $p < 0.0001$ (****), as measured by one-way ANOVA with a Tukey post test.

5.2.4.5 Quantification of parasite loads in *Ela*^{-/-} mice

To determine whether parasite survival of *L. major* WT and the *ISP2* gene mutants was affected in the *Ela*^{-/-} mice, LDAs were performed at 5 wk post-infection. There were no significant differences in the parasite burdens in the ears or dLNs infected with *L. major* WT, Δ isp2/3, or Δ isp2/3:ISP2/3 parasites (Figure 5-15). However, parasites could only be detected in one Δ isp2/3-infected ear and two WT-infected ears, compared with Δ isp2/3:ISP2/3-infected ears, in which parasites could be detected in four out of five of the samples (Figure 5-15A).

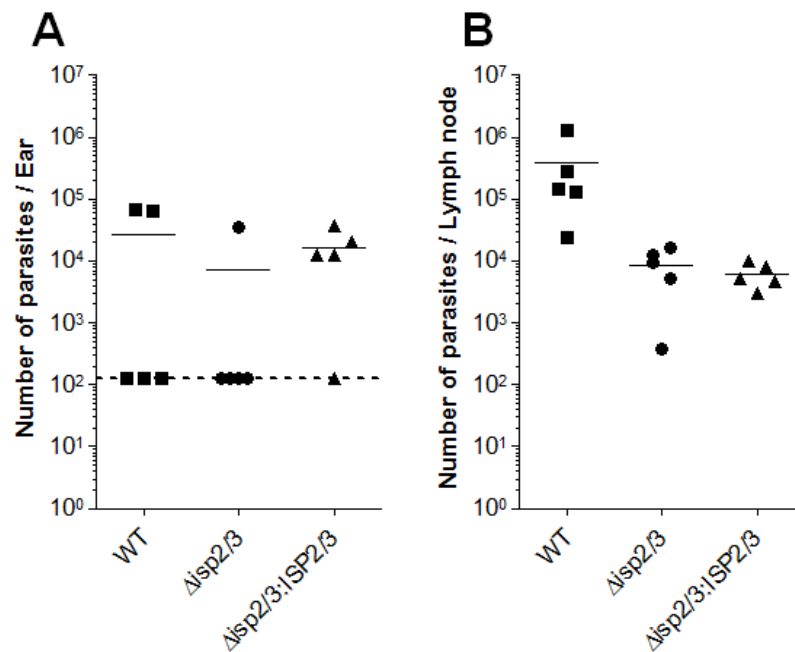


Figure 5-15 Parasite burdens at 5 wk post-infection with *L. major* WT and *ISP2* gene mutants in *Ela*^{-/-} mice. Purified metacyclic promastigotes (10^4 in 10 μ l PBS) were intradermally inoculated into the ears of *Ela*^{-/-} mice (n=5). The parasite loads in the **A**) ear and **B**) dLN at 5 wk were determined by LDA. Parasite loads from the individual samples are shown with the lines indicating the mean for the group. Dashed line indicates the lower limit of detection.

There were also no significant differences in the diameters of the dLNs, or the masses of the livers and spleens at 5 wk post-infection in *Ela*^{-/-} mice infected with *L. major* WT, Δ isp2/3, or Δ isp2/3:ISP2/3 parasites (Figure 5-16).

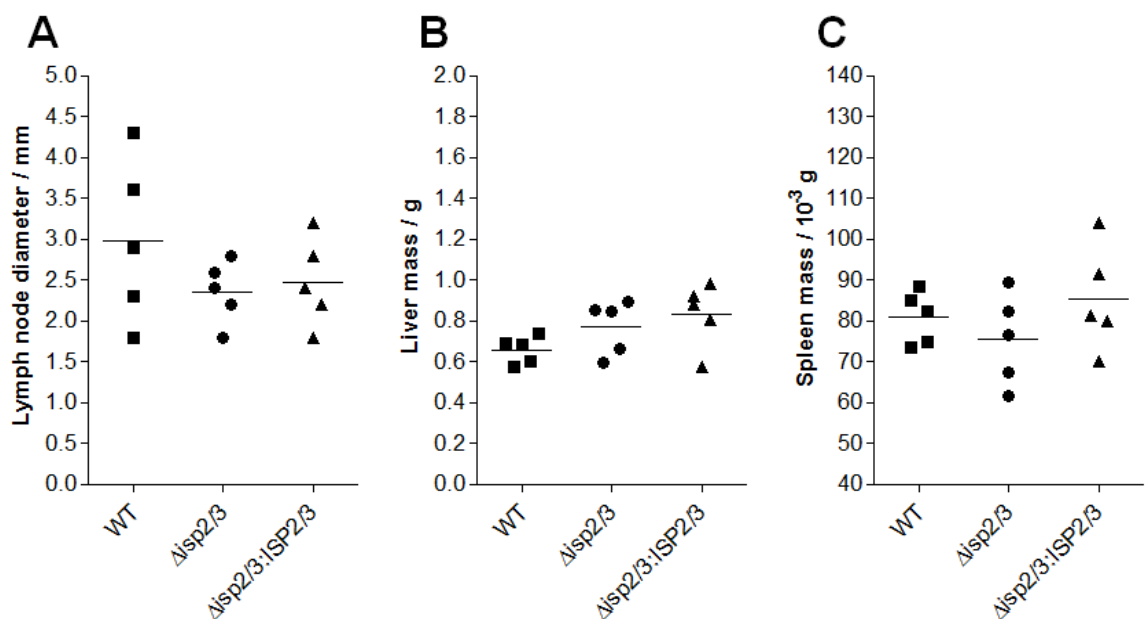


Figure 5-16 Lymph node diameters, and liver and spleen masses, at 5 wk post-infection with *L. major* WT and *ISP2* gene mutants in *Ela*^{-/-} mice. Purified metacyclic promastigotes (10^4 in 10 μ l PBS) were intradermally inoculated into the ears of *Ela*^{-/-} mice (n=5). **A**) The dLNs were removed and the diameters were measured by vernier caliper. **B**) Livers and **C**) spleens were also removed and the masses were measured.

5.3 Discussion

The results of this chapter indicate that *L. major* ISP2 may modulate host immune responses, with regards to innate immune cell infiltration and activation, during the second wave of innate cell recruitment to the site of infection which occurs around 2 wk post-infection. Ears infected with an *L. major* *ISP2/3*-deficient mutant, Δ *isp2/3*, showed an increase in inflammatory monocytes, monocyte-derived macrophages, and moDCs at 2 wk post-infection, compared with those infected with *L. major* WT parasites or an *ISP2/3* re-expressing cell line, Δ *isp2/3:ISP2/3* (Figure 5-3, G to L, and 5-6C). At 2 wk, the iNOS response, which generates NO, the toxic metabolite responsible for the majority of *Leishmania* killing *in vivo* (Stenger et al., 1994; De Trez et al., 2009), was significantly higher in Δ *isp2/3*-infected ears compared with WT- and Δ *isp2/3:ISP2/3*-infected ears (Figure 5-7B). This was due to an upregulation of iNOS expression within the inflammatory monocytes and monocyte-derived macrophages, as well as the resident macrophages and DCs (Figure 5-7, E to H). At this same time-point, the production of IFN- γ , which stimulates iNOS-generated NO production, was higher in Δ *isp2/3* infections compared with WT and Δ *isp2/3:ISP2/3* infections (Figure 5-8). The expression of DC co-stimulatory molecules, which are upregulated during the DC maturation process, was also investigated. CD80, a marker of mature DCs, was upregulated on moDCs and resident DCs in Δ *isp2/3* infections at 2 wk post-infection (Figure 5-9, E and F), which also suggests these DCs may be more posed to prime antigen-specific T cells. This could feedback to induce the iNOS response of the other innate cells present at the site of infection through the action of IFN- γ produced by Th1 cells. *In vivo* imaging also suggested that the activation of neutrophils and inflammatory monocytes from 2 wk post-infection may be higher in Δ *isp2/3* infection than WT infection, as determined by monitoring MPO-specific bioluminescence at the site of infection (Figure 5-5). The differences in the innate immune response at the site of infection in response to *L. major* WT and Δ *isp2/3* parasites suggest the effector mechanisms of the innate immune cells in the ear dermis are more primed towards the killing of *L. major* Δ *isp2/3* parasites, and the DCs more primed towards inducing an adaptive T cell response.

It was hypothesised that ISP2 would act upon the early innate immune response due to previous *in vitro* studies of the role of ISP2 in the uptake and killing of *L. major* by macrophages (Eschenlauer et al., 2009; Faria et al., 2011), and that the proposed SP targets are primarily produced by innate immune cells, including neutrophils, macrophages, and monocytes. However, there were no significant differences in the early recruitment or activation of innate cells, at time-points of less than one week, between WT and $\Delta isp2/3$ infections (Figure 5-3 and 5-5). The concentration and function of SPs in the dermis of a naive ear prior to *L. major* inoculation is unknown, in that there may be few targets for ISP2 meaning there may be little to no observed effect on immune modulation at these early time-points. The inhibitory effect of *L. major* ISP2 may only become apparent when the balance between SPs and ISP2 is affected; as may occur after the peaks of neutrophil and monocyte infiltration at 1 and 2 d post-infection respectively, and the subsequent exposure of *L. major* to the SPs, of which neutrophils and monocytes are major sources; or when the *L. major* infection becomes fully established, through intracellular replication in the host cells, leading to higher concentrations of ISP2. It could also be that ISP2 inhibits the activity of SPs from these cell types throughout infection, preventing the proteolytic modification of cytokines and chemokines, which thus affects the recruitment and activation of immune cells during the second wave of innate immune cell infiltration observed (Thalhofer et al., 2011; Ribeiro-Gomes et al., 2012).

5.3.1 Innate cell recruitment and functions during *Leishmania* infection

In this study, flow cytometry was used to assess the inflammatory response at the site of inoculation with *L. major* WT and the *ISP2* gene mutants. The cell surface markers used in this investigation were chosen to observe innate immune cell types that are important in *Leishmania* infection, as a source of SPs, have already shown to have an interaction with ISP2 *in vitro* (Faria et al., 2011), and the recruitment of which may be affected by the inhibition of SP activity (Table 5-1). The gating strategy was based on that by Ribeiro-Gomes et al. (2012), which gated resident macrophages and DCs as Ly6C⁻, and monocytes and monocyte-derived cells as Ly6C⁺, and differentiated macrophages and DC subsets by CD11c expression (Table 5-2 and Figure 5-2). Similar gating strategies with

these cell markers have been used to investigate these innate immune cell populations, although they additionally report intermediate expression of some markers, relating to cell maturation (León et al., 2007).

The ear dermis is composed of large numbers of dermal macrophages and DCs but relatively few neutrophils and inflammatory monocytes within the CD11b⁺ population (Dupasquier et al., 2004; Peters et al., 2008; Ribeiro-Gomes et al., 2012), as was shown in this study (Figure 5-3). Thalhoffer et al. (2011) investigated the inflammatory cells using the pan-leukocyte marker, CD45, over 7 d following intradermal ear inoculation of 10⁶ metacyclic *L. infantum chagasi* promastigotes into BALB/c mice. Neutrophils peaked between 6 and 24 h, whereas macrophages peaked at 3 d. Similarly, Ribeiro-Gomes et al. (2012) investigated CD11b⁺ myeloid cell populations over 14 d following intradermal ear inoculation of 2x10⁵ metacyclic *L. major* promastigotes into C57BL/6 mice. In their investigation, there was a slow increase in the total CD11b⁺ cells in ears over the first week of infection with a massive expansion over the second week. Neutrophils were detected at 1 h, peaked at 12 h, which then decreased between 1 and 4 d. In this study, a peak in the neutrophil infiltration is observed at 24 h, which then drops to levels observed in a naive ear, while resident macrophages and DCs peaked at 4 d (Figure 5-3, A to F). Sham injections without parasites only induced a neutrophil response at 1 h, likely due to the tissue damage (Ribeiro-Gomes et al., 2012); in this study the earliest time-point assessed was 1 d (Figure 5-3), at which time there were no differences in the cell populations in ears injected with PBS compared to the naive ears. At subsequent time-points, recruitment is dependent upon the infectious status of the inoculum (Peters et al., 2008). Ribeiro-Gomes et al. (2012) observed an increase in inflammatory monocytes beginning at 12 h and peaking at 24 h, with a second wave of infiltration beginning at 7 d. Whereas resident macrophages and DCs remained relatively unchanged until 7 d. The percentage of moDCs in this study represented a very small proportion of the CD11b⁺ population but expanded upon *Leishmania* infection (Figure 5-3, G and H); this level is not unusual, as moDCs are often detected in low numbers (León et al., 2007; Ribeiro-Gomes et al., 2012). These observations show that regardless of the parasite inoculation dose in the ear dermis, the sequence of innate immune cell

recruitment to *Leishmania* infection remains the same, including the timing of the peaks of infiltration for each of the innate immune cell types.

The maintenance of neutrophils at the site of infection has been shown to be affected by the delivery method; in that neutrophil recruitment at early time-points is similar whether parasites are delivered by needle inoculation or sandfly bite, however, neutrophil recruitment to sandfly bite is more prolonged (Peters et al., 2008). The initial recruitment of neutrophils appears to be independent of parasite-specific signals, as a similar response is seen in the absence of parasites (Peters et al., 2008), but the prolonged effect is likely due to the parasite-derived factors. There were no differences in the recruitment of neutrophils over the first week of infection with *L. major* WT or Δ *isp2/3* parasites suggesting that ISP2 does not have an effect on neutrophil recruitment (Figure 5-3, A and B). However, the use of flow cytometry to detect differences in the innate cell populations is subject to error due to the loss of cells during sample preparation, particularly during the ear digestion and homogenisation steps; this is especially problematic during the initial stages of infection when the total number of CD11b⁺ cells is not significantly higher than that of a naive ear (Figure 5-1). It is possible to pool biological replicates in order to retain more cells and acquire more events in flow cytometry; however, due to variations between biological samples this is not recommended, as it could skew the data making it difficult to identify differences in the innate cell populations between experimental groups. In this study, biological replicates were used for each group at each time-point, running at least one million total events per sample in order to gate cell subsets accurately, and two independent technical replicates were performed to give more confidence that any differences observed between the innate immune cell populations between the *L. major* WT and Δ *isp2/3* infections were genuine and statistically significant.

5.3.1.1 The second wave of innate cell recruitment

A second wave of innate cell infiltration has been described in the case of neutrophils, monocytes, and monocyte-derived cells at 7 d in response to *Leishmania* infection, in which their cell numbers exceed the peak numbers observed during the first wave of infiltration (Thalhofer et al., 2011; Ribeiro-Gomes et al., 2012). However, in both these reports the innate cell dynamics at

the site of infection were only investigated up to 2 wk post-infection. A second wave of neutrophil infiltration even occurs in transient neutrophil depletion suggesting that other cells at the site of infection, or the parasites themselves, induce neutrophil recruitment at this stage of infection (Thalhofer et al., 2011). A second wave of neutrophils was observed for both WT and $\Delta isp2/3$ infections, which persisted for, at least, up to 4 wk post-infection (Figure 5-3, A and B), as well as a prolonged monocyte, monocyte-derived macrophage, and moDC response during this stage of infection (Figure 5-3, G to L). The prolonged infiltration of these innate immune cells has not previously been reported for *Leishmania* infection, as investigations into the presence of innate cells at the site of inoculation typically cease at 2 wk post-infection. It is around 1 to 2 wk post-infection that the adaptive immune response is generated, after migration of APCs to the dLN to present antigen to T cells, T cell activation and clonal expansion, recruitment to the site of infection, and secretion of cytokines.

At this stage of infection, it is likely that mediators from the adaptive immune response will contribute to the neutrophil and monocyte infiltration, as at 1 wk post-infection, all the CD11b⁺ innate cell subsets investigated in this study had levels equivalent to that of a naive ear (Figure 5-3). IL-17 cytokines, such as IL-17A and IL-17F, are able to promote the recruitment of neutrophils and monocytes, mediating the persistence of an inflammatory lesion. IL-17 is released by $\gamma\delta$ T cells, CD4⁺ T cells, NK cells, as well as neutrophils. Mice deficient in IL-17 have significantly lower neutrophils in the skin compared to control mice from 4 wk post-infection with *L. major* onwards (Lopez Kostka et al., 2009). In addition, IFN- γ , secreted by Th1 cells, has been reported to promote monocyte recruitment (Gonzalez-Lombana et al., 2013). At this time-point, inflammatory cells are perhaps more apt to encounter infected cells, and they may be more “primed” for activation or exert different effects on the immune response.

There were fewer monocytes, monocyte-derived macrophages, and moDCs observed at 2 wk in WT infection than in $\Delta isp2/3$ infection (Figure 5-3, G to L); ISP2 may modulate the recruitment of these cell types to the site of inoculation, through the inhibition of SP activity. NSPs, such as NE, can proteolytically modify cytokines and chemokines to regulate immune responses (Table 5-1); in addition,

NSPs can also interact with cell receptors to modulate intracellular signalling cascades, which can affect the production and release of cytokines and chemokines from cells (Ribeiro-Gomes et al., 2007). Inhibition of NSP activity could lead to reduced parasite killing as fewer effector cells present, which means lower iNOS responses in the entire tissue, in addition, there would be fewer APCs, such as the moDCs, to prime an adaptive T cell response.

At 2 wk post-infection, there was a higher concentration of IFN- γ at the site of $\Delta isp2/3$ infection compared with that in WT and $\Delta isp2/3:ISP2/3$ infections (Figure 5-8). This could indicate that an adaptive Th1 immune response has been induced earlier in the $\Delta isp2/3$ infection than in the WT infection, meaning ISP2 could potentially delay the formation of an adaptive immune response through modulation of the innate cellular responses. The T cell response is thought to be defined during the first three days of *L. major* infection due to interaction of T cells with APCs but antigen-specific T cells are only present at the site of inoculation by 1 wk, the numbers of which peak at 3 wk post-infection (Pagán et al., 2013). The T cell response may have a feedback loop affecting the recruitment and activation of the second wave of innate cell infiltration as the presence of IFN- γ could account for the higher number of monocytes (Figure 5-3, G and H) (Gonzalez-Lombana et al., 2013), and the higher iNOS expression in the innate immune cells at the site of $\Delta isp2/3$ infection compared with those of WT and $\Delta isp2/3:ISP2/3$ infections at this time-point (Figure 5-7). A similar proposal has been suggested for *L. major* virulence factors, phosphoglycans (PGs), as *L. major* lacking PGs, *lpg2* parasites, induce higher IL-12 production from DCs and are unable to induce early IL-4 and IL-10 production from lymphocytes in BALB/c mice (Liu et al., 2009). To investigate whether the timing, magnitude, and polarisation of the T cell response is affected during infection with *L. major* WT and the *ISP2* gene mutants, it would be essential to further elucidate the cytokine microenvironment over the course of infection, in terms of IL-2, IL-12, and IFN- γ , which are indicative of a Th1 response, and IL-4 and IL-13, which are indicative of a Th2 response, as well as immuno-regulatory cytokines, IL-10 and TGF- β .

DCs are now thought to be the major cell type that harbours *Leishmania* in the dLN, and are the cell type responsible for the orchestration of an adaptive

immune response through antigen presentation and IL-12 production (von Stebut et al., 1998; Ritter et al., 2004; León et al., 2007). There were higher numbers of moDCs at the site of inoculation in *Disp2/3* infection at 2 wk compared with WT infection (Figure 5-3, K and L), with an increase in CD11b⁺ cells in the dLN at this same time-point (Figure 5-4). It would be of interest to define the innate cell subsets in the dLN over the course of infection, to determine whether there are any differences in the migration of innate immune cell types between the site of inoculation and the dLN in WT and *Disp2/3* infection.

5.3.1.2 Monocytes and monocyte-derived dendritic cells

Monocytes are recruited to the site of *L. major* infection and differentiate into moDCs, which are thought to be important in the induction of Th1 responses during *L. major* infection (León et al., 2007). Mouse CD11b⁺Ly6C^{hi}CCR2⁺ monocytes are similar to human CD14^{hi} monocytes, which constitute almost 90% of the circulating blood monocyte population and are the monocytes that are recruited to inflamed tissue (Geissmann et al., 2003). DCs are a highly heterogeneous population, defined by their specialised functions and the differential expression of specific cell surface markers, reflecting differences in their cellular origin. A DC population expressing CD11b⁺CD11c⁺Ly6C⁺MHCII⁺ and high levels of iNOS, termed inflammatory or moDCs, have been proposed to have important roles in the control of *L. major* infection, the presence of which is dependent upon a Th1 microenvironment involving IL-12 and IFN- γ (De Trez et al., 2009). These DCs have a similar phenotype to the TNF-iNOS-producing dendritic cells (Tip-DCs) reported in other models (Serbina et al., 2003), although only a small percentage are TNF-producing (De Trez et al., 2009).

Petritus et al. (2012) compared the recruitment of monocytes and moDCs to *L. major* and *L. mexicana* infections. Intradermal inoculations were performed in the ears in C57BL/6 with 10⁵ metacyclic promastigotes. Fewer monocytes were recruited, and moDCs produced less iNOS and migrated less efficiently to the dLN in *L. mexicana* infection, which was proposed to lead to insufficient priming of a Th1 response. By using a blocking antibody against the IL-10 receptor, Petritus et al. (2012) also showed an increase in monocyte and moDC recruitment to the site of *L. mexicana* infection at 2 wk post-infection. IL-10 may decrease the expression of CCL2 (MCP1), which is an important chemokine

for monocyte and DC chemotaxis, as has been reported in *T. brucei* infection (Bosschaerts et al., 2010); or the immuno-regulatory role of IL-10 may dampen Th1 responses leading to lower iNOS and IFN- γ . *L. major* also causes aggregation and activation of platelets, leading to the release of platelet-derived growth factor (PDGF), which stimulates endothelial cells, fibroblasts, and macrophages to produce CCL2 (Goncalves et al., 2011).

MoDCs are the major producers of iNOS during *L. major* infection (De Trez et al., 2009), approximately 20% of the moDCs in *L. major* infection have been shown to be iNOS⁺ at 2 wk post-infection, compared to 3% in *L. mexicana* infection (Petritus et al., 2012). In this study, up to 60% of the moDCs were iNOS⁺ in *L. major* WT, Δ *isp2/3*, and Δ *isp2/3:ISP2/3* infections (Figure 5-7I). Although there were no differences in the iNOS expression in this cell population between the infections with WT and the *ISP2* gene mutants, there were more moDCs in Δ *isp2/3* infection at 2 wk post-infection, suggesting that recruitment was affected rather than the effector mechanisms of this cell type.

MoDCs migrate to the dLN to stimulate antigen-specific Th1 responses, leading to the production of IFN- γ from Th1 cells, and are also proposed to be the major producers of IL-12 during *L. major* infection (León et al., 2007). MoDCs are detected in the dLN at 3 d after infection with *L. major*, which coincides with the expansion of the antigen-specific T cells (Pagán et al., 2013), the numbers of moDCs decrease markedly at 1 wk, then increase again at 2 wk, and continue to increase up to 4 wk post-infection (León et al., 2007). Petritus et al. (2012) investigated the migration of moDCs from the ear to the dLN at 2 wk post-infection through FITC painting of the ear; they showed a significantly higher number of moDCs in the dLNs in *L. major* infection compared with *L. mexicana* infection. MoDCs had low levels of CD86 expression in both WT and Δ *isp2/3* infection (Figure 5-9C), which has also described by León et al. (2007). During Δ *isp2/3* infection, moDCs did, however, show an upregulation in the DC co-stimulatory molecule, CD80, at 2 wk post-infection (Figure 5-9E), which suggests that these cells are more primed to induce an antigen-specific T cell response. Bosschaerts et al. (2010) have proposed that the maturation of DCs to functional Tip-DCs, expressing CD80 and CD86, in *T. brucei* infection is dependent upon IFN- γ and MyD88 signalling, which is downstream of TLR4. There was also a

corresponding increase in CD11b⁺ cells in the dLNs of $\Delta isp2/3$ -infected mice at 2 wk post-infection (Figure 5-4), although the cell subsets were not determined. *L. major*-activated DCs also induce lymph node hypertrophy to promote T cell recruitment to the dLN and enhance the protective responses (Carvalho et al., 2012), in the previous chapter the mean diameter of the dLN in $\Delta isp2/3$ infection was significantly higher than in WT and $\Delta isp2/3:ISP2/3$ infection at 5 wk (Figure 4-7A).

The presence of moDCs during *L. major* infection is further complicated by the timing of differentiation from the bone-marrow monocytes. León et al. (2007) identified two subsets in the popliteal dLNs; lymph node moDCs, which differentiated from monocytes that had migrated to the lymph node first; and dermal moDCs, which had differentiated from monocytes at the site of infection, served as hosts for *L. major*, and presented antigen to T cells to generate a Th1 response.

In vitro studies have shown that TLR activation, including TLR4, triggers the differentiation of monocytes into macrophages and DCs (Krutzik et al., 2005), which likely occurs through MyD88 signalling (De Trez et al., 2004). ISP2 has been shown to inhibit the activity of NE, preventing the activation of TLR4 signalling cascades in macrophages (Faria et al., 2011). The increase in monocyte-derived macrophages and moDCs in $\Delta isp2/3$ infection may be due to TLR4-induced differentiation of monocytes in the absence of ISP2. *L. major* ISP2 may block moDC differentiation, as it has been shown that *Salmonella typhimurium* and bacterial LPS is able to block this conversion (Rotta et al., 2003), as well as *L. amazonensis* promastigotes (Favali et al., 2007). The differentiation of monocytes into moDCs could be examined *in vitro* based on surface co-stimulatory molecule expression, such as CD40, CD80, and CD86, after co-culture with *L. major* WT and the *ISP2* gene mutants (Favali et al., 2007; Markikou-Ouni et al., 2012), in the presence or absence of TLR4 blocking antibodies.

5.3.1.3 Neutrophil-dendritic cell interactions

C57BL/6 mice depleted of neutrophils have significantly reduced *L. major* parasite loads at an intradermal site of inoculation after 1 wk post-infection

(Peters et al., 2008). The use of neutrophil-depleted mice has shown that infected DCs from these mice have higher expression levels of CD86 and CD40, and are more efficient than infected DCs from C57BL/6 mice in activating *Leishmania*-primed T cells to secrete IFN- γ (Ribeiro-Gomes et al., 2012). In addition, neutrophil-depleted mice showed a greater expansion of *Leishmania*-specific CD4⁺ T cells (Ribeiro-Gomes et al., 2012). Neutrophils are the first host cell type for *Leishmania* and are major sources of SPs. Without the neutrophil contribution of SPs at the site of infection, there may be reduced cleavage of cytokine, chemokine, and cell receptor targets, which may affect DC maturation. In this study, moDCs from Δ *isp2/3* infection showed greater expression of CD86 compared with those from WT infection.

Neutrophil granule proteins have been shown to induce monocyte recruitment and DC maturation through TLR4-dependent pathways, including human alarmins, such as β -defensins (Biragyn et al., 2002), human LL-37 and the murine homologue CRAMP (Kurosaka et al., 2005; Soehnlein et al., 2008; Chen et al., 2014), lactoferrin (de la Rosa et al., 2008), and azurocidin (Chertov et al., 1997), an inactive SP homologue, which is unable to cleave peptide bonds (Watorek, 2003). Finally, neutrophil binding to immature DCs via interactions of Mac-1 of neutrophils and DC-SIGN of DCs leads to the delivery of activation signals and antigenic molecules, causing DC maturation with increased expression of CD40, CD80, and CD86 (van Gisbergen et al., 2005). DC engulfment of apoptotic neutrophils has been shown to inhibit DC production of pro-inflammatory cytokines, expression of co-stimulatory molecules, and their ability to stimulate T cell proliferation (Sauter et al., 2000). However, the roles of neutrophil granule proteins in the pathology or protection of *Leishmania* infection have not been fully assessed.

5.3.1.4 The iNOS response

Mice deficient in iNOS have much more severe pathology during *L. major* infection, during which the lesions become necrotic (Diefenbach et al., 1998). *L. major* infection can also be reactivated in chronically infected healthy C57BL/6 mice following iNOS inhibitor treatment (Stenger et al., 1996). iNOS and the generation of NO is, therefore, essential for *Leishmania* clearance *in vivo*

(Stenger et al., 1994; Vouldoukis et al., 1995; De Trez et al., 2009; Petritus et al., 2012).

De Trez et al. (2009) performed intracellular staining for iNOS on the dLNs of C57BL/6 mice following subcutaneous footpad inoculation of 10^6 promastigotes. Their analysis showed that at the peak of iNOS expression, at 4 wk post-infection, only 0.4% of the total cells analysed were positive for iNOS; however, they did not investigate iNOS expression at the site of infection. They showed that up to 90% of iNOS-producing cells in the dLN were moDCs, whereas granulocytes represented only 10 to 15% of iNOS⁺ cells. In this study, approximately 15% of the CD11b⁺ cells at the site of *L. major* WT infection were iNOS⁺ at 2 wk (Figure 5-7B). However, during Δ *isp2/3* infection, the iNOS expression in CD11b⁺ cells was upregulated to approximately 25% due to an increase in iNOS expression in inflammatory monocytes, monocyte-derived macrophages, resident macrophages, and resident DCs (Figure 5-7, E to H). In this study, the iNOS response in the dLN was not assessed, but if the iNOS response in the dLN is lower than at site of infection, as the data from De Trez et al. (2009) would suggest, which is attributed to differences in the innate immune cell populations present (León et al., 2007), this could account for the differences in parasite burdens between the ear and the dLN in the WT and Δ *isp2/3* infections (Figure 4-7, B and C).

5.3.2 *In vivo* imaging of the innate immune responses

In vivo optical imaging reagents and substrates allow quantification of molecular and cellular responses in animal models. Luminol has previously only been used to assess the respiratory burst during *Leishmania* infections *in vitro* (al Tuwaijri et al., 1990; Vuotto et al., 2000). Luminol has since been shown to be specific for MPO activity, although the exact interaction by which bioluminescence is induced however, is still unknown (Gross et al., 2009; Tseng & Kung, 2012). Neutrophils highly express MPO, inflammatory monocytes have intermediate expression of MPO, and DCs do not express MPO (Ribeiro-Gomes et al., 2012). Circulating monocytes lose MPO activity as they infiltrate and differentiate into macrophages in tissue (Kumar et al., 2004); however, certain tissue macrophages in humans have been shown to be MPO-positive (Daugherty et al., 1994; Nagra et al., 1997). Tseng & Kung (2012) showed using purified neutrophils

and monocytes that both these cell type contribute to the MPO-specific bioluminescent signal induced by luminol. To check the MPO status of the innate immune cells analysed in this study, flow cytometry was performed with an anti-MPO antibody, which showed that all neutrophils were MPO⁺, and Ly6C^{hi} cells, which constitute monocytes, monocyte-derived macrophages, and moDCs, were approximately 48% positive for MPO staining, whereas the MPO staining in resident macrophages and DCs was negligible (Figure 5-6).

In vivo imaging of the MPO-specific bioluminescent signal during infection with *L. major* WT, $\Delta isp2/3$, or the *ISP2* overexpressing cell line, WT [pXG-*ISP2*], in C57BL/6 mice showed that ears infected with $\Delta isp2/3$ parasites appeared to have a slightly higher MPO-specific bioluminescent signal than WT-infected ears (Figure 5-5); this may have been the maximal signal, limited by the amount of luminol substrate present. It also appeared that WT-infected *Ela*^{-/-} mice had a higher MPO-specific bioluminescent signal than $\Delta isp2/3$ -infected mice (Figure 5-12, A and B), which was unexpected based on the observation in C57BL/6 mice, however, these differences were not significantly different. The signals were much more delayed in WT [pXG-*ISP2*] infection in both C57BL/6 and *Ela*^{-/-} mice, which suggests an inhibition of phagocyte recruitment or activation; it could be that the overexpression of *ISP2* enables the inhibition of other SP targets, such as CG and PR3. Flow cytometry was not performed with ears infected with WT [pXG-*ISP2*] parasites, as the episomal expression of *ISP2* was not always consistent, likely due to variation in plasmid copy number (Chakkalath et al., 2000). However, data from ears infected with $\Delta isp2/3:ISP2/3$ parasites, which slightly overexpress *ISP2* (Figure 3-1), sometimes showed a more significant decrease in innate cell recruitment than that of WT- and $\Delta isp2/3$ -infected ears (Figure 5-6, B and C).

Upon its release from neutrophils, MPO becomes inactive in the tissue microenvironment meaning that there is both enzymatically active and inactive MPO present at the site of inflammation. MPO has a direct effect on tissue damage but it is also taken up by resident macrophages expressing macrophage mannose receptors (MMRs) (Shepherd & Hoidal, 1990). MPO and MMR interaction leads to the release of ROS along with other pro-inflammatory cytokines, including TNF- α , IL-1, IL-6, IL-8, and GCSF, from macrophages (Lefkowitz et al.,

1997, 2000). As there were obvious differences in the MPO-specific bioluminescent signals from mice infected with WT [*pXG-ISP2*] parasites compared with those infected with WT and Δ *isp2/3* parasites, it would be interesting to do histological analysis over the course of these infections to determine if there are any signs of tissue damage, such as fibrinoid necrosis, particularly in the WT [*pXG-ISP2*] infection where the signal continued to increase beyond 8 wk of infection, the time at which the Δ *isp2/3* infection appeared to be resolving.

The light emitted in the luminol reaction is in the blue spectrum with a peak of 425 nm, which means it is easily scattered and absorbed by the tissues, and therefore can only be used to observe phagocyte activation at superficial surface foci, such as the mouse ear. Zhang et al. (2013) have developed a method in which the blue light emitted by luminol excites nanoparticles to emit light in the near-infrared range in a process termed chemiluminescence resonance energy transfer (CRET). Luminol-R is an administration of luminol with non-conjugated 800 nm-emitting quantum dots, improving the detectability of the luminescent signal for MPO activity in deep tissues. This could enable the detection of activated phagocyte migration from the site of infection to the dLN.

Lucigenin allows *in vivo* imaging of late phase and chronic inflammation, which detects the superoxide anion, O_2^- , dependent on generation by phagocyte NADPH oxidase activity in macrophages (Tseng & Kung, 2012). This type of *in vivo* imaging could provide additional data on the activation of, in particular, monocyte-derived macrophages during infection with *L. major* WT and the *ISP2* gene mutants, as differences were observed in the recruitment of this innate immune cell type (Figure 5-3, I and J).

Kossodo et al. (2011) have developed a near-infrared activatable fluorescence imaging agent specific to NE activity, known as Neutrophil Elastase 680 FAST, in order to detect and quantify NE activity *in vivo*. The agent is two near infrared fluorophores linked to either end of a peptide sequence, PMAVVQSVP, which is highly selective for mouse NE over mouse CG, as well as human MMP-9, and cathepsin B (Kalupov et al., 2009; Kossodo et al., 2011); although mouse PR3 also activates the imaging agent at a much lower rate (Kalupov et al., 2009). Upon peptide cleavage, the fluorophores are no longer self-quenched and

become fluorescent with a maximum emission at 690 nm. It would be interesting to use this imaging agent during infection with *L. major* WT and the *ISP2* gene mutants, as it may enable the quantification of *ISP2* inhibition *in vivo*.

5.3.3 Redundancy and synergistic effects of NSPs

Modification of chemokines by NSPs controls a temporal pattern of immune cell trafficking to the site of inflammation, which could account for the differences seen between WT and $\Delta isp2/3$ infections at the later stages in C57BL/6 mice. Neutrophil elastase-deficient mice, *Ela*^{-/-}, were used to assess the role of this host SP in the generation of immune responses to *L. major* WT and the *ISP2* gene mutants. Few studies have been conducted to investigate the roles of NSPs *in vivo*, particularly during infectious disease. However, the data for innate immune cell infiltration and DC co-stimulatory molecule expression between infection with *L. major* WT and $\Delta isp2/3$ parasites at 2 wk in *Ela*^{-/-} mice was similar to that observed in C57BL/6 mice (Figure 5-12 and 5-13).

The NSPs, NE, CG, and PR3, have a broad and overlapping range of targets (Table 5-1). The lack of difference between data from C57BL/6 and *Ela*^{-/-} mice at 2 wk post-infection could indicate potential redundancy of the NSPs, in that CG or PR3 could compensate for the loss of NE (Kessenbrock et al., 2008). NE and PR3, in particular, have similar substrate specificities. Only one time-point was investigated in the *Ela*^{-/-} mice for the innate immune cell recruitment, at the time-point which corresponded to the differences observed in C57BL/6 mice. It is possible that there may have been earlier effects that were not detected.

As shown in Table 5-1, NSPs have been shown to modify a large number of targets, and more are perhaps yet to be identified. *ISP2* may also inhibit the activity of other SP targets *in vivo*, such as CG, PR3, or the newly identified, NSP4 (Perera et al., 2012). NSP4 has been shown to have elastase activity, with 39% identity to NE and PR3. Low amounts of NSP4 have been found in the azurophilic granules of human neutrophils and, like the other NSPs, is converted to a catalytically active protease by cleavage of an N-terminal pro-dipeptide of the inactive zymogen by the lysosomal cysteine protease, dipeptidyl peptidase I (DPPI, or cathepsin C). NSP4 is also inhibited by AAT (Perera et al., 2012, 2013). NSP4 also has a homologue in mice, termed *Prss-57*. In *Prss-57*-deficient mice,

there was a marginal increase in the levels of TNF- α and CCL2 in response to LPS injection (Tang et al., 2010); however, the exact targets of NSP4 are still to be determined.

In vitro ISP2 has been shown to inhibit the activity of NE, which prevents the activation of a TLR4-NE signalling cascade in macrophages (Faria et al., 2011). It is unknown how NE activates TLR4 (Ribeiro-Gomes et al., 2007); whether NE directly engages TLR4, or cleaves another receptor which activates TLR4 signalling. TLR4 signalling cascades, however, can lead to the upregulation of cytokine and chemokine production and secretion, such as IL-8 (Ribeiro-Gomes et al., 2007; Benabid et al., 2012). NSPs may, therefore, work synergistically, for example, in the case of neutrophil recruitment, they could mediate the production and secretion of IL-8 by engaging TLRs or protease-activated receptors (PARs), or enhancing the activity of IL-8 through proteolytic modification, this would recruit more neutrophils, which are then activated to release NSPs. As neutrophils are the first cells to arrive at sites of inflammation and are a major source of NSPs, their presence at the site of inflammation could potentially influence subsequent waves of cell recruitment, and the inhibition of NSPs by ISP2 is therefore likely to have a multitude of effects *in vivo*.

Monocyte and monocyte-derived cell recruitment was higher in Δ *isp2/3* infection at 2 wk compared with WT infection. The key chemokines involved in monocyte chemotaxis to the site of infection are CCL2, CCL3, CCL5, CCL7, and CCL12 (Shi & Pamer, 2011). As yet, only CCL3 and CCL5 have been shown to be processed by NSPs (Table 5-1). Neutrophils also release CCL3 to recruit monocytes and DCs during the early stage of infection in C57BL/6 mice (Charmoy et al., 2010).

5.3.3.1 MPO and NSPs

There are contrasting views on the interaction of MPO and NSPs; the conversion of H₂O₂ to HOCl may protect NSPs from inactivation (Reeves et al., 2002), or MPO may mediate direct oxidative inactivation of NSPs (Hirche et al., 2005). HOCl does, however, inactivate AAT, the physiological inhibitor of all three NSPs. *In vivo* imaging showed that there was a slightly higher MPO-specific bioluminescent signal in the ears of Δ *isp2/3*-infected C57BL/6 mice, the presence of the MPO reaction products may, therefore, contribute the

inactivation of SP inhibitors leading to a protease-inhibitor imbalance, which augments the protective responses and the clearance of $\Delta isp2/3$ parasites.

5.3.4 Future directions

As there were differences in cellular recruitment, it would be of interest to determine if there are any specific changes in the chemokine levels during infection with *L. major* WT and the *ISP2* gene mutants. This could be achieved through tissue qPCR or luminex-based methods to determine the levels of a range of chemokines. Using both methods may also indicate differences in proteolytic modification of the chemokines. Earlier time-points could be studied; although there has been no difference in innate cell recruitment before 1 wk post-infection there may be other differences, such as the cytokine and chemokine levels, which may guide the subsequent responses. It may also be important to determine the pattern of Th1/Th2 cytokine expression during WT and $\Delta isp2/3$ infection, such as IL-2, IL-4, IL-12, and IL-13, as mentioned earlier, as the development of the Th1 response may differ between WT and $\Delta isp2/3$ infection, which could feedback to the innate cell infiltration and activation.

NSPs become enzymatically active during transport to the granules through the cleavage of an N-terminal pro-dipeptide by DPPI. In mice deficient in DPPI, NSPs have very little enzymatic activity, as well as decreased infiltration to sites of inflammation and decreased local production of cytokines (Adkison et al., 2002). Comparisons of infections with *L. major* WT and the *ISP2* gene mutants in these transgenic mice may show whether NSPs are the only targets of *ISP2* and elucidate an interaction of *ISP2* with the NSPs *in vivo*, although identification of the precise mechanism may be difficult due to the numerous targets of the NSPs. In C57BL/6 CCR2 deficient mice, in which the CCR2 receptor is not expressed on monocytes, monocytes accumulate in the bone marrow unable to respond to its chemokine partners, which include CCL2, CCL7, and CCL12, resulting in susceptibility to *L. major* infection (Sato et al., 2000; Quinones et al., 2007). In C57BL/6 mice and *Ela*^{-/-} mice, there was an increase in monocyte recruitment to $\Delta isp2/3$ infections, the use of CCR2^{-/-} mice may indicate a dependency on the chemokines mentioned, to explain the differences observed in monocyte recruitment between WT and $\Delta isp2/3$ infections.

Using fluorescently-labelled cell lines, it would be of interest to determine whether *L. major* WT and the *ISP2* gene mutants reside within the same innate immune cell types and whether there is any difference in the migration of these cell types between the site of infection and the dLN. Although macrophages are the major host cell type for *Leishmania*, neutrophils, monocytes, DCs, and fibroblasts can also harbour intracellular *Leishmania*; *L. infantum chagasi*, however, does not reside in DCs (Thalhofer et al., 2011). Parasites deficient in *ISP2/3* are internalised more efficiently by macrophages; the internalisation of Δ *isp2/3* parasites by other innate cells is currently under investigation. It could be that Δ *isp2/3* parasites are internalised more efficiently by neutrophils, which may affect the dynamics of the adaptive immune response. Thalhofer et al. (2011) showed that there were more parasite-containing cells in the dLNs of control BALB/c mice than in neutrophil-depleted mice, and that this corresponded with significantly lower numbers of leukocytes containing intracellular parasites in the skin of neutrophil-depleted mice in the first few hours of infection. It may only be possible to detect fluorescently labelled parasites inoculated at high doses, as Ribeiro-Gomes et al. (2012) recovered fewer than 10^3 red fluorescent protein (RFP)-positive cells at 1 and 4 h after intradermal inoculation of 10^5 metacyclic *L. major* promastigotes. Ribeiro-Gomes et al. (2012) did however, describe two waves of RFP⁺ recruitment at 1 d and 7 to 14 d, with monocyte-derived macrophages and moDCs harbouring RFP-expressing parasites during the second phase primarily. León et al. (2007) also reported a difference in the migration of non-infected and infected moDCs; more than 90% of the moDCs in the skin were infected, whereas less than 10% were infected in the dLN at 4 wk post-infection. This was supported by differential expression of the lymph node homing receptor CCR7 on the infected and non-infected moDCs (León et al., 2007).

5.3.5 Concluding remarks

In summary, the data reported in this chapter indicate that *L. major* *ISP2* is capable of modulating host immune responses locally *in vivo*. Flow cytometric analysis of innate immune cell infiltration at the site of intradermal *L. major* WT infection has revealed the same sequence of innate cell recruitment to the site of infection described by other groups, regardless of the initial parasite inoculation dose, showing that innate cell recruitment is highly conserved in

Leishmania infection. The use of this method has enabled the discovery of differences in the recruitment and activation of the moDCs during the second wave of innate cell infiltration to the site of infection with an *L. major* mutant deficient in *ISP2/3*, Δ *isp2/3*. Through the use of luminol, it has also been possible for the first time to image activated phagocytes in response to an infectious disease *in vivo*, taken further, it has been used to compare the phagocyte activation during infection with *L. major* WT and mutant deficient in, or overexpressing, a putative virulence factor, *ISP2*.

6 General Discussion

Leishmania are known to modulate host immune responses to facilitate their survival; however, few *Leishmania* virulence factors, which mediate these interactions, have been characterised, particularly with regards to their effect on immune responses *in vivo*. It is important to understand how parasites manipulate immune responses that facilitate parasite survival and disease initiation and persistence, and deduce which immune responses lead to pathology and protection, as this can provide insights into strategies for disease intervention.

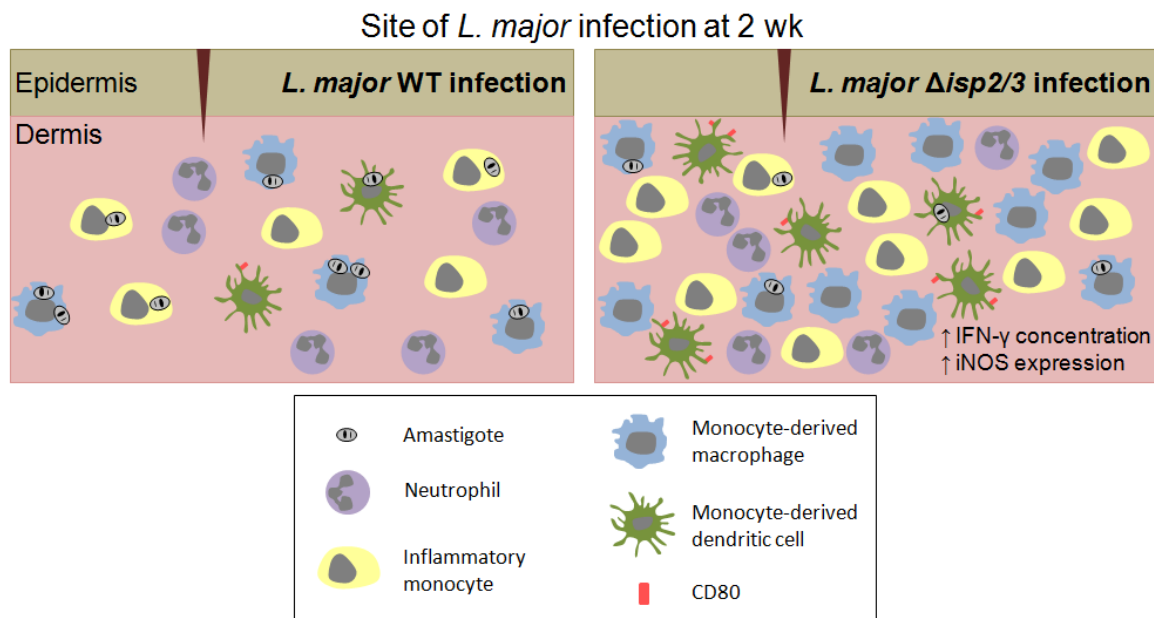
L. major has three ecotin-like peptide inhibitors of serine peptidases, which have been designated ISP1, ISP2, and ISP3 (Eschenlauer et al., 2009). *In vitro* studies have already shown that *L. major* ISP2 acts as a *Leishmania* virulence factor that inhibits the mammalian host serine peptidase, neutrophil elastase (NE) preventing the activation of a TLR4-NE signalling cascade (Faria et al., 2011). Inhibition of this signalling cascade in macrophages leads to the modulation of phagocytosis and reactive oxygen species production, which facilitates *L. major* intracellular survival (Faria et al., 2011). The potential for ISP2 to modulate host immune responses through the inhibition of host serine peptidase activity was an attractive line of investigation, as TLR4-NE signalling cascades have been shown to trigger pro-inflammatory responses in both mouse models and human cells, such as the production and release of TNF- α (Ribeiro-Gomes et al., 2007; Benabid et al., 2012), IL-6 (Benabid et al., 2012), and IL-8 (Walsh et al., 2001; Devaney et al., 2003; Benabid et al., 2012), a chemoattractant and activator of neutrophils. Hence, the presence or absence of *L. major* ISP2 could have greater effects *in vivo* on cellular recruitment and activation, and consequently on the long-term disease progression. In addition, serine peptidases of innate immune cells, which include NE, cathepsin G, and proteinase 3, are able to proteolytically modify cytokines and chemokines to regulate inflammatory responses, independent of TLR4 interaction (Pham, 2008). Therefore, the overall aim of this study was to investigate the effects of ISP2 in the wider context of the immune responses and disease progression *in vivo*. To achieve this, comparisons of the lesion development, parasite survival, and innate immune cell activation and recruitment were made between *in vivo*

infections with *L. major* WT and *ISP2* gene mutants, particularly a cell line deficient in *ISP2/3*, Δ *isp2/3* (Eschenlauer et al., 2009).

Faria et al. (2011) have previously shown reduced intracellular loads of *L. major* Δ *isp2/3* parasites in macrophages, compared with those of *L. major* WT parasites, after *in vivo* infections of less than one day. In this study, parasite burdens at the site of inoculation and in the draining lymph nodes were assessed. There were consistently lower parasite burdens of Δ *isp2/3* parasites at the site of inoculation than those of WT parasites and a cell line re-expressing *ISP2/3*, Δ *isp2/3:ISP2/3*, at later stages of *in vivo* infection, beyond 5 wk. This showed that there was not an increase in parasite loads from the early time-points studied by Faria et al. (2011), indicating that *L. major* requires *ISP2* for the initiation and persistence of disease. In addition, the parasite burdens of Δ *isp2/3:ISP2/3* parasites, which slightly overexpresses *ISP2*, were consistently higher than those of WT and Δ *isp2/3* parasites at the site of inoculation, which suggests that the levels of *ISP2* expression may affect parasite burdens. Interestingly, although parasite burdens at the site of inoculation were obviously different between the different cell lines, the parasite burdens within the draining lymph node were not significantly different, as was also observed by Faria et al. (2011) at 10 wk post-infection. Parasite burdens in the livers and spleens were also determined to discover whether *ISP2* had any effect on disease tropism; however, no parasites were detected for any of the cell lines at any of the time-points examined. It would be of interest to determine whether this is the case in the susceptible BALB/c model, which is a typical VL model for *L. donovani* and *L. infantum* infections (Nieto et al., 2011; Loría-Cervera & Andrade-Narváez, 2014). Interestingly, neutrophils from BALB/c mice release 2 to 3-fold less NE than those of C57BL/6 mice (Ribeiro-Gomes et al., 2007); the balance between NE and *ISP2* in BALB/c mice could, therefore, contribute to the greater pathology caused by *L. major* in BALB/c mice. *ISP2* has been identified in various species of *Leishmania*, including *L. mexicana*, which causes LCL and DCL, *L. braziliensis*, which causes LCL and MCL, and *L. infantum*, which causes LCL, MCL, and VL (Peacock et al., 2007). It is currently being investigated whether there is any sequence variation or any gene copy variation of the *ISP2* gene between *Leishmania* species, which could contribute to differences in gene expression and may impact upon disease tropism (Rogers et al., 2011). This may

be of particular interest in the case of PKDL, in which skin lesions are heavily parasitised (Mukhopadhyay et al., 2014), as was observed in the $\Delta isp2/3:ISP2/3$ infections.

The major findings in terms of the innate immune responses to the *L. major* WT, $\Delta isp2/3$, and $\Delta isp2/3:ISP2/3$ cell lines *in vivo* were an increase in inflammatory monocytes, monocyte-derived macrophages, and monocyte-derived DCs at the site of inoculation, coupled with an increase in iNOS expression, IFN- γ production, and DC maturation marker expression at 2 wk post-infection in the $\Delta isp2/3$ infections (Figure 6-1). Taken together, these data suggest that the immune response is more primed towards clearance of the $\Delta isp2/3$ parasites. Monocyte-derived DCs induce protective antigen-specific Th1 responses (León et al., 2007; De Trez et al., 2009; Petritus et al., 2012), which are the primary source of IFN- γ . IFN- γ stimulates the expression of iNOS in macrophages and DCs, which catalyses the production of NO, a molecule that is important for effective parasite killing (De Trez et al., 2009; Petritus et al., 2012). The modulation of these responses by ISP2 *in vivo* still requires exploration, but the increase in monocytes and monocyte-derived cells at 2 wk post-infection, in the case of $\Delta isp2/3$ infection, could be due to an increase in cytokine and chemokine production through a TLR4-NE signalling cascade. This is a line of investigation currently being pursued; preliminary results indicate that $\Delta isp2/3$ parasites induce cytokine release, including TNF- α , IL-6, CXCL1, and CXCL2 from C57BL/6 macrophages *in vitro* (Faria et al., unpublished). However, more cytokines and chemokines are to be tested, particularly chemokines that induce monocyte chemotaxis, such as CCL2, CCL3, CCL5, CCL7, and CCL12.



phosphorylation of the eukaryotic translation initiation factor eIF-2 α , but is also a translational regulator of NF- κ B, AP-1, IRF-1, STATs, ATF3 and 4, JNK, p38, and p53 (reviewed in Williams, 2001). Although the role of PKR in antiviral immunity is well characterised, the characterisation of PKR in parasitic infections is limited (Pereira et al., 2010; Ogolla et al., 2013). However, from the investigation by Faria et al. (2014), the increase in IFN- β through this signalling pathway could account for the increases in iNOS expression observed in the Δ isp2/3 infection (Diefenbach et al., 1998; Oliveira et al., 2014); therefore, it would be of interest to determine whether the levels of IFN- β also differ between WT and Δ isp2/3 infections *in vivo*.

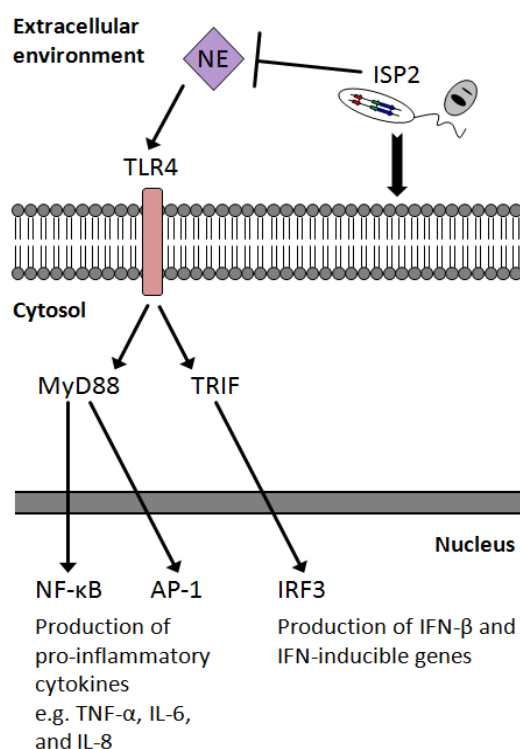


Figure 6-2 Potential effects of the prevention of TLR4 signalling cascades on immune responses *in vivo*. The *L. major* virulence factor, ISP2, has been shown to inhibit the activity of the serine peptidase neutrophil elastase (NE). This prevents the activation of a Toll-like receptor 4 (TLR4)-NE signalling cascade, which can downregulate phagocytosis and inhibit the production of reactive oxygen species (ROS) in macrophages. TLR4 signalling is commonly divided into pathways, which occur through the adaptor proteins MyD88 and TRIF. The MyD88-dependent pathway leads to activation of the transcription factors, NF- κ B and AP-1, and TRIF-dependent pathway typically leads to the activation of IRF3. NF- κ B and AP-1 activation generally leads to the production of pro-inflammatory cytokines, such as TNF- α and IL-6, whilst IRF3 leads to the production of IFN- β , which, like IFN- γ is able to stimulate the expression of inducible nitric oxide synthase (iNOS). IRF3 can induce the expression of IFN-inducible genes, such as CXCL10, which is a chemoattractant for monocytes, dendritic cells, and T cells. IRF3 has also been shown to be involved in the differentiation of monocytes into macrophages and dendritic cells, and the maturation of dendritic cells through the upregulation of CD80 and CD86 expression. There was an increase in monocyte recruitment, iNOS, and expression of the dendritic cell co-stimulatory molecule, CD80, in *L. major* Δ isp2/3 infection compared with *L. major* WT infection. These differences may be due to the inhibition of NE activity by *L. major* ISP2, which prevents the activation of the TLR4-NE signalling cascades, thus affecting the expression of cytokines, chemokines, and/or IFN-inducible genes. However, the downstream signalling cascades and effects in host cells need to be further characterised during interaction with *L. major* WT and ISP2 gene mutant parasites.

Increases in monocyte and monocyte-derived DC recruitment to the site of inoculation with $\Delta isp2/3$ parasites compared with WT parasites could lead to the other differences observed between these infections, as the monocyte-derived DCs may then prime a Th1 response causing the differences in the iNOS and IFN- γ at this time-point. It is not unusual to observe differences in innate cell recruitment occurring later in infection. Fromm et al. (2012) showed that in TNF-deficient mice, a difference in monocyte-derived DC recruitment to the draining lymph node was only observed after 2 wk post-infection, compared to the C57BL/6 mice.

ISP2 could also affect cytokine and chemokine processing through the inhibition of serine peptidase activity. This could have consequences on the recruitment of immune cells to the site of inoculation, and the differentiation, proliferation, and activation of immune cells (Wiedow & Meyer-Hoffert, 2005; Pham, 2008), which can then have consequences on the production of cytokines and chemokines, and the activation of effector mechanisms important for parasite clearance. To investigate whether there is an effect on cytokine and chemokine processing, simultaneous tissue qPCR and luminex-based methods could provide information on the cytokine/chemokine levels during infection with *L. major* WT and the *ISP2* gene mutants, and may give an indication of cytokine/chemokine processing, particularly if inactivated cytokine/chemokine proteins are efficiently degraded.

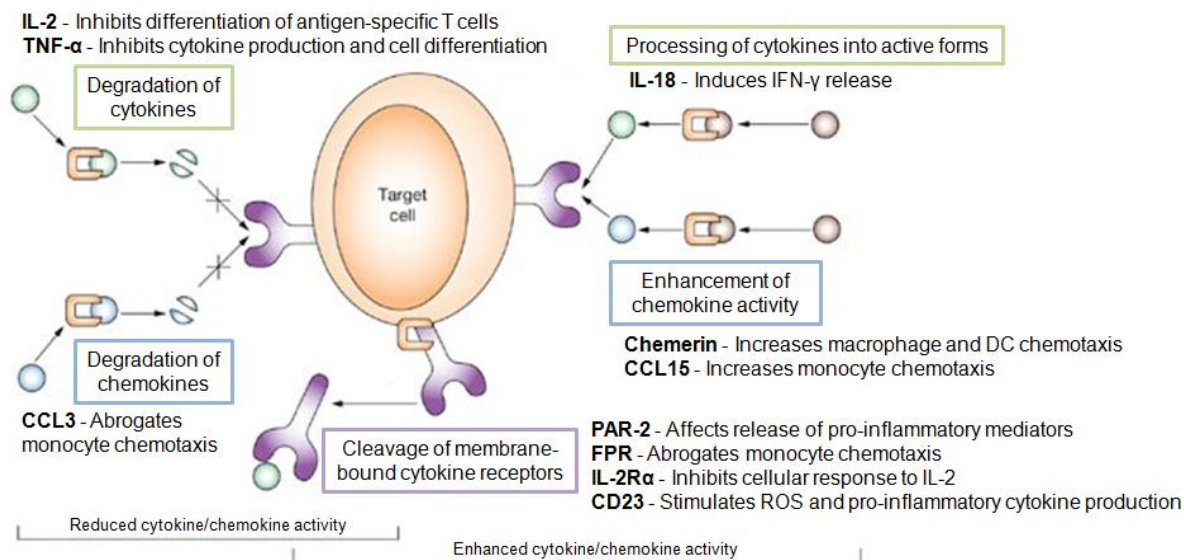


Figure 6-3 Potential effects of inhibiting serine peptidase activity by *L. major* ISP2 during *in vivo* infection. Differences were observed in the innate cell response to the site of *L. major* WT infection compared with *L. major* Δ *isp2/3* infection. ISP2 has been shown to inhibit the activity of serine peptidases of the S1A family. S1A serine peptidases, neutrophil elastase (NE), cathepsin G (CG), and proteinase 3 (PR3), play important roles in the processing of cytokines and chemokines, which can either enhance or reduce their activity. Shown above are examples of the serine peptidase targets that have already been characterised and the effect that cleavage of these targets has on the inflammatory response. *L. major* ISP2 may inhibit the activity of these serine peptidases *in vivo*, which could explain the differences observed in cellular response to the site of inoculation between *L. major* WT and Δ *isp2/3* infections. The monocyte response to *L. major* WT infection was lower than that observed in *L. major* Δ *isp2/3* infection, which may be due to ISP2 preventing the enhancement of cytokine and chemokine activity, such as chemerin and CCL15, achieved through cleavage by serine peptidase. Additionally, processing of IL-18 has been shown to induce IFN- γ release from Th1 and NK cells; there was a higher concentration of IFN- γ at the site of *L. major* Δ *isp2/3* infection compared to *L. major* WT infection. The production and processing of cytokines and chemokines needs to be further investigated during infection with *L. major* WT and the *ISP2* gene mutants to fully understand how the inhibition of serine peptidases *in vivo* may cause the differences observed in this study. Adapted from Eyles et al. (2006) with permission.

ISP2 is expressed in all *Leishmania* lifecycle stages, with particularly high levels in the infective metacyclic and amastigote stages (Eschenlauer et al., 2009). In this study all *in vivo* inoculations were performed with metacyclic promastigotes, as would be transmitted during a sandfly bite (Kimblin et al., 2008; Rogers et al., 2010). *Leishmania* metacyclic promastigotes and amastigotes interact differently with immune cells, in that amastigotes do not necessarily pass through neutrophils as observed for metacyclic promastigotes (Wenzel et al., 2012). Therefore, the interactions of *L. major* ISP2 of the metacyclic promastigotes and amastigotes will differ, as promastigotes will likely interact with serine peptidases produced by neutrophils in the first few hours before they are internalised, whereas amastigotes will interact with serine peptidases from neutrophils, monocytes, and macrophages, later in infection, when the parasites are released from cells into the extracellular environment. Hence, to determine whether there are stage-specific effects of ISP2 on the

immune responses, it could be of interest to perform infections with purified amastigotes of *L. major* WT and the *ISP2* gene mutants to observe whether recruitment of the monocytes and monocyte-derived cells is induced earlier than 2 wk post-infection. The interaction of *L. major* WT and the *ISP2* gene mutants with other innate cell types *in vitro*, neutrophils and DCs in particular, is also currently under investigation, with focus on parasite internalisation, ROS and NO production, and cytokine secretion (Faria et al., unpublished).

In this study, a low dose intradermal infection model was used to determine differences in disease progression and innate immune responses between *L. major* WT and cell lines deficient in the putative virulence factor, *ISP2*. This model proved to be sensitive enough to detect differences in parasite burdens, as assessed by limiting dilution assays, and innate immune cell populations, as assessed by flow cytometry. Luciferase-expressing cell lines also enabled an investigation into whether parasite survival was affected by the presence or absence of *ISP2* through non-invasive longitudinal *in vivo* imaging in the mouse model. In addition, bioluminescence imaging was similarly used for longitudinal *in vivo* imaging of phagocyte activation, through the detection of myeloperoxidase activity (Gross et al., 2009), in response to infection with *L. major* WT and the *ISP2* gene mutants. This is the first time that these *in vivo* imaging techniques have been used to determine the effects of putative parasite virulence factors on disease progression and phagocyte activation in real-time. *In vivo* imaging techniques are also important for the reduction of animals used in experimental procedures, as many animals are often required to perform limiting dilution assays with an appropriate number of biological replicates. In this study, these imaging experiments were performed independently, but there is potential for these techniques to be performed simultaneously, as the emission spectra are sufficiently separate, with peak emissions from the firefly luciferase and luminol reactions at 562 nm and 425 nm respectively. This is, of course, dependent upon the filters available on the *in vivo* imaging system (IVIS) used, as well as the depth of imaging required. There are other luciferase reporters with higher emission peaks available, such as red-shifted luciferase (McLatchie et al., 2013), which has a peak emission of 617 nm, as well as luminol-R, which is an administration of luminol with non-conjugated 800 nm-emitting quantum dots (Zhang et al., 2013). Dual imaging of parasite

dissemination and phagocyte activation could provide information on disease tropism through the use of different *Leishmania* species, as well as the effects of neutrophil depletion on disease pathology, which have been reported to have different effects dependent upon the *Leishmania* species, the mouse strain, and the site of infection (Lima et al., 1998; Tacchini-Cottier et al., 2000; Ribeiro-Gomes et al., 2004; McFarlane et al., 2008; Peters et al., 2008; Novais et al., 2009; Charmoy et al., 2010; Sousa et al., 2014). This technique could also be used in transgenic mice to determine the effects of certain cytokines, chemokines, and receptors on *Leishmania* infection, such as TNF- α and CCR2, which have been shown to have effects on monocyte recruitment in *Leishmania* infection (Sato et al., 2000; Quinones et al., 2007; Fromm et al., 2012).

In summary, ISP2 has been shown to be an important virulence factor in *L. major*; some of the effects of which have now been characterised *in vitro* and *in vivo*. In addition, a new infection model and imaging techniques have been proposed to enable the characterisation and comparison of *Leishmania* wild-type infections with those of cell lines deficient in, or overexpressing, putative virulence factors, for longitudinal studies of parasite survival and dissemination in concert with innate immune responses.

References

- Adkison, A.M., Raptis, S.Z., Kelley, D.G., Pham, C.T. (2002) Dipeptidyl peptidase I activates neutrophil-derived serine proteases and regulates the development of acute experimental arthritis. *J Clin Invest* 109, 363-371.
- Aga, E., Katschinski, D.M., van Zandbergen, G., Laufs, H., Hansen, B., Müller, K., Solbach, W., Laskay, T. (2002) Inhibition of the spontaneous apoptosis of neutrophil granulocytes by the intracellular parasite *Leishmania major*. *J Immunol* 169, 898-905.
- Ajdary, S., Alimohammadian, M.H., Eslami, M.B., Kemp, K., Kharazmi, A. (2000) Comparison of the immune profile of nonhealing cutaneous leishmaniasis patients with those with active lesions and those who have recovered from infection. *Infect Immun* 68, 1760-1764.
- al Tuwaijri, A.S., al Mofleh, I.A., Mahmoud, A.A. (1990) Effect of *Leishmania major* on human polymorphonuclear leucocyte function in vitro. *J Med Microbiol* 32, 189-193.
- Alexander, J. (1988) Sex differences and cross-immunity in DBA/2 mice infected with *L. mexicana* and *L. major*. *Parasitology* 96, 297-302.
- Alexander, J., Brombacher, F. (2012) T helper1/t helper2 cells and resistance/susceptibility to leishmania infection: is this paradigm still relevant? *Front Immunol* 3, 80.
- Alexander, J., Coombs, G.H., Mottram, J.C. (1998) *Leishmania mexicana* cysteine proteinase-deficient mutants have attenuated virulence for mice and potentiate a Th1 response. *J Immunol* 161, 6794-6801.
- Alvar, J., Aparicio, P., Aseffa, A., den Boer, M., Cañavate, C., Dedet, J.P., Gradoni, L., Ter Horst, R., López-Vélez, R., Moreno, J. (2008) The relationship between leishmaniasis and AIDS: the second 10 years. *Clin Microbiol Rev* 21, 334-359.
- Alvar, J., Vélez, I.D., Bern, C., Herrero, M., Desjeux, P., Cano, J., Jannin, J., den Boer, M. (2012) Leishmaniasis worldwide and global estimates of its incidence. *PLoS One* 7, e35671.
- Baldwin, T.M., Elso, C., Curtis, J., Buckingham, L., Handman, E. (2003) The site of *Leishmania major* infection determines disease severity and immune responses. *Infect Immun* 71, 6830-6834.
- Bates, P.A. (2007) Transmission of *Leishmania* metacyclic promastigotes by phlebotomine sand flies. *Int J Parasitol* 37, 1097-1106.
- Belaouaj, A., Kim, K.S., Shapiro, S.D. (2000) Degradation of outer membrane protein A in *Escherichia coli* killing by neutrophil elastase. *Science* 289, 1185-1188.
- Belaouaj, A., McCarthy, R., Baumann, M., Gao, Z., Ley, T.J., Abraham, S.N., Shapiro, S.D. (1998) Mice lacking neutrophil elastase reveal impaired host defense against gram negative bacterial sepsis. *Nat Med* 4, 615-618.
- Belkaid, Y., Kamhawi, S., Modi, G., Valenzuela, J., Noben-Trauth, N., Rowton, E., Ribeiro, J., Sacks, D.L. (1998) Development of a natural model of cutaneous leishmaniasis: powerful effects of vector saliva and saliva preexposure on the long-term outcome of *Leishmania major* infection in the mouse ear dermis. *J Exp Med* 188, 1941-1953.
- Belkaid, Y., Mendez, S., Lira, R., Kadambi, N., Milon, G., Sacks, D. (2000) A natural model of *Leishmania major* infection reveals a prolonged "silent" phase of parasite

- amplification in the skin before the onset of lesion formation and immunity. *J Immunol* 165, 969-977.
- Belkaid, Y., Piccirillo, C.A., Mendez, S., Shevach, E.M., Sacks, D.L. (2002) CD4+CD25+ regulatory T cells control Leishmania major persistence and immunity. *Nature* 420, 502-507.
- Benabid, R., Wartelle, J., Malleret, L., Guyot, N., Gangloff, S., Lebargy, F., Belaouaj, A. (2012) Neutrophil elastase modulates cytokine expression: contribution to host defense against *Pseudomonas aeruginosa*-induced pneumonia. *J Biol Chem* 287, 34883-34894.
- Bennett, C.L., Misslitz, A., Colledge, L., Aebischer, T., Blackburn, C.C. (2001) Silent infection of bone marrow-derived dendritic cells by *Leishmania mexicana* amastigotes. *Eur J Immunol* 31, 876-883.
- Benson, K.F., Li, F.Q., Person, R.E., Albani, D., Duan, Z., Wechsler, J., Meade-White, K., Williams, K., Acland, G.M., Niemeyer, G., Lothrop, C.D., Horwitz, M. (2003) Mutations associated with neutropenia in dogs and humans disrupt intracellular transport of neutrophil elastase. *Nat Genet* 35, 90-96.
- Besteiro, S., Coombs, G.H., Mottram, J.C. (2004) A potential role for ICP, a Leishmanial inhibitor of cysteine peptidases, in the interaction between host and parasite. *Mol Microbiol* 54, 1224-1236.
- Bhardwaj, S., Srivastava, N., Sudan, R., Saha, B. (2010) *Leishmania* interferes with host cell signaling to devise a survival strategy. *J Biomed Biotechnol* 2010, 109189.
- Biragyn, A., Ruffini, P.A., Leifer, C.A., Klyushnenkova, E., Shakhov, A., Chertov, O., Shirakawa, A.K., Farber, J.M., Segal, D.M., Oppenheim, J.J., Kwak, L.W. (2002) Toll-like receptor 4-dependent activation of dendritic cells by beta-defensin 2. *Science* 298, 1025-1029.
- Borovsky, D., Schlein, Y. (1987) Trypsin and chymotrypsin-like enzymes of the sandfly *Phlebotomus papatasi* infected with *Leishmania* and their possible role in vector competence. *Med Vet Entomol* 1, 235-242.
- Bosschaerts, T., Guillems, M., Stijlemans, B., Morias, Y., Engel, D., Tacke, F., Hérin, M., De Baetselier, P., Beschin, A. (2010) Tip-DC development during parasitic infection is regulated by IL-10 and requires CCL2/CCR2, IFN-gamma and MyD88 signaling. *PLoS Pathog* 6, e1001045.
- Brinkmann, V., Reichard, U., Goosmann, C., Fauler, B., Uhlemann, Y., Weiss, D.S., Weinrauch, Y., Zychlinsky, A. (2004) Neutrophil extracellular traps kill bacteria. *Science* 303, 1532-1535.
- Brittingham, A., Morrison, C.J., McMaster, W.R., McGwire, B.S., Chang, K.P., Mosser, D.M. (1995) Role of the *Leishmania* surface protease gp63 in complement fixation, cell adhesion, and resistance to complement-mediated lysis. *J Immunol* 155, 3102-3111.
- Brown, J.A., Titus, R.G., Nabavi, N., Glimcher, L.H. (1996) Blockade of CD86 ameliorates *Leishmania* major infection by down-regulating the Th2 response. *J Infect Dis* 174, 1303-1308.
- Bryson, K., Besteiro, S., McGachy, H.A., Coombs, G.H., Mottram, J.C., Alexander, J. (2009) Overexpression of the natural inhibitor of cysteine peptidases in *Leishmania mexicana* leads to reduced virulence and a Th1 response. *Infect Immun* 77, 2971-2978.

- Bunn, P.T., Stanley, A.C., de Labastida Rivera, F., Mulherin, A., Sheel, M., Alexander, C.E., Faleiro, R.J., Amante, F.H., Montes De Oca, M., Best, S.E., James, K.R., Kaye, P.M., Haque, A., Engwerda, C.R. (2014) Tissue requirements for establishing long-term CD4⁺ T cell-mediated immunity following *Leishmania donovani* infection. *J Immunol* 192, 3709-3718.
- Buxbaum, L.U., Denise, H., Coombs, G.H., Alexander, J., Mottram, J.C., Scott, P. (2003) Cysteine protease B of *Leishmania mexicana* inhibits host Th1 responses and protective immunity. *J Immunol* 171, 3711-3717.
- Cai, T.Q., Wright, S.D. (1996) Human leukocyte elastase is an endogenous ligand for the integrin CR3 (CD11b/CD18, Mac-1, alpha M beta 2) and modulates polymorphonuclear leukocyte adhesion. *J Exp Med* 184, 1213-1223.
- Cameron, P., McGachy, A., Anderson, M., Paul, A., Coombs, G.H., Mottram, J.C., Alexander, J., Plevin, R. (2004) Inhibition of lipopolysaccharide-induced macrophage IL-12 production by *Leishmania mexicana* amastigotes: the role of cysteine peptidases and the NF-kappaB signaling pathway. *J Immunol* 173, 3297-3304.
- Campbell, E.J., Owen, C.A. (2007) The sulfate groups of chondroitin sulfate- and heparan sulfate-containing proteoglycans in neutrophil plasma membranes are novel binding sites for human leukocyte elastase and cathepsin G. *J Biol Chem* 282, 14645-14654.
- Cangussú, S.D., Souza, C.C. de, Campos, C.F., Vieira, L.Q., Afonso, L.C., Arantes, R.M. (2009) Histopathology of *Leishmania major* infection: revisiting L. major histopathology in the ear dermis infection model. *Mem Inst Oswaldo Cruz* 104, 918-922.
- Carregaro, V., Costa, D.L., Brodskyn, C., Barral, A.M., Barral-Netto, M., Cunha, F.Q., Silva, J.S. (2013) Dual effect of *Lutzomyia longipalpis* saliva on *Leishmania braziliensis* infection is mediated by distinct saliva-induced cellular recruitment into BALB/c mice ear. *BMC Microbiol* 13, 102.
- Carvalho, L.P., Petritus, P.M., Trochtenberg, A.L., Zaph, C., Hill, D.A., Artis, D., Scott, P. (2012) Lymph node hypertrophy following *Leishmania major* infection is dependent on TLR9. *J Immunol* 188, 1394-1401.
- Chakkalath, H.R., Siddiqui, A.A., Shankar, A.H., Dobson, D.E., Beverley, S.M., Titus, R.G. (2000) Priming of a beta-galactosidase (beta-GAL)-specific type 1 response in BALB/c mice infected with beta-GAL-transfected *Leishmania major*. *Infect Immun* 68, 809-814.
- Charmoy, M., Brunner-Agten, S., Aebischer, D., Auderset, F., Launois, P., Milon, G., Proudfoot, A.E., Tacchini-Cottier, F. (2010) Neutrophil-derived CCL3 is essential for the rapid recruitment of dendritic cells to the site of *Leishmania major* inoculation in resistant mice. *PLoS Pathog* 6, e1000755.
- Chatelain, R., Mauze, S., Varkila, K., Coffman, R.L. (1999) *Leishmania major* infection in interleukin-4 and interferon-gamma depleted mice. *Parasite Immunol* 21, 423-431.
- Chen, K., Xiang, Y., Huang, J., Gong, W., Yoshimura, T., Jiang, Q., Tessarollo, L., Le, Y., Wang, J.M. (2014) The formylpeptide receptor 2 (Fpr2) and its endogenous ligand cathelin-related antimicrobial peptide (CRAMP) promote dendritic cell maturation. *J Biol Chem* 289, 17553-17563.
- Chertov, O., Ueda, H., Xu, L.L., Tani, K., Murphy, W.J., Wang, J.M., Howard, O.M., Sayers, T.J., Oppenheim, J.J. (1997) Identification of human neutrophil-derived cathepsin G and azurocidin/CAP37 as chemoattractants for mononuclear cells and neutrophils. *J Exp Med* 186, 739-747.

- Chhajer, R., Ali, N. (2014) Genetically modified organisms and visceral leishmaniasis. *Front Immunol* 5, 213.
- Chung, C.H., Ives, H.E., Almeda, S., Goldberg, A.L. (1983) Purification from *Escherichia coli* of a periplasmic protein that is a potent inhibitor of pancreatic proteases. *J Biol Chem* 258, 11032-11038.
- Clark, E.A., Walker, N., Ford, D.C., Cooper, I.A., Oyston, P.C., Acharya, K.R. (2011) Molecular recognition of chymotrypsin by the serine protease inhibitor ecotin from *Yersinia pestis*. *J Biol Chem* 286, 24015-24022.
- Clark, J.M., Vaughan, D.W., Aiken, B.M., Kagan, H.M. (1980) Elastase-like enzymes in human neutrophils localized by ultrastructural cytochemistry. *J Cell Biol* 84, 102-119.
- Contag, C.H., Contag, P.R., Mullins, J.I., Spilman, S.D., Stevenson, D.K., Benaron, D.A. (1995) Photonic detection of bacterial pathogens in living hosts. *Mol Microbiol* 18, 593-603.
- Cortez, M., Huynh, C., Fernandes, M.C., Kennedy, K.A., Aderem, A., Andrews, N.W. (2011) *Leishmania* promotes its own virulence by inducing expression of the host immune inhibitory ligand CD200. *Cell Host Microbe* 9, 463-471.
- Courret, N., Fréhel, C., Gouhier, N., Pouchelet, M., Prina, E., Roux, P., Antoine, J.C., (2002) Biogenesis of *Leishmania*-harbouring parasitophorous vacuoles following phagocytosis of the metacyclic promastigote or amastigote stages of the parasites. *J Cell Sci* 115, 2303-2316.
- Courret, N., Lang, T., Milon, G., Antoine, J.C. (2003) Intradermal inoculations of low doses of *Leishmania major* and *Leishmania amazonensis* metacyclic promastigotes induce different immunoparasitic processes and status of protection in BALB/c mice. *Int J Parasitol* 33, 1373-1383.
- Da Silva, R., Sacks, D.L. (1987) Metacyclogenesis is a major determinant of *Leishmania* promastigote virulence and attenuation. *Infect Immun* 55, 2802-2806.
- Daneshvar, H., Coombs, G.H., Hagan, P., Phillips, R.S. (2003) *Leishmania mexicana* and *Leishmania major*: attenuation of wild-type parasites and vaccination with the attenuated lines. *J Infect Dis* 187, 1662-1668.
- Daugherty, A., Dunn, J.L., Rateri, D.L., Heinecke, J.W. (1994) Myeloperoxidase, a catalyst for lipoprotein oxidation, is expressed in human atherosclerotic lesions. *J Clin Invest* 94, 437-444.
- de La Llave, E., Lecoeur, H., Besse, A., Milon, G., Prina, E., Lang, T. (2011) A combined luciferase imaging and reverse transcription polymerase chain reaction assay for the study of *Leishmania* amastigote burden and correlated mouse tissue transcript fluctuations. *Cell Microbiol* 13, 81-91.
- de la Rosa, G., Yang, D., Tewary, P., Varadhachary, A., Oppenheim, J.J. (2008) Lactoferrin acts as an alarmin to promote the recruitment and activation of APCs and antigen-specific immune responses. *J Immunol* 180, 6868-6876.
- De Trez, C., Brait, M., Leo, O., Aebischer, T., Torrentera, F.A., Carlier, Y., Muraille, E. (2004) Myd88-dependent in vivo maturation of splenic dendritic cells induced by *Leishmania donovani* and other *Leishmania* species. *Infect Immun* 72, 824-832.
- De Trez, C., Magez, S., Akira, S., Ryffel, B., Carlier, Y., Muraille, E. (2009) iNOS-producing inflammatory dendritic cells constitute the major infected cell type during the chronic *Leishmania major* infection phase of C57BL/6 resistant mice. *PLoS Pathog* 5, e1000494.

- Devaney, J.M., Greene, C.M., Taggart, C.C., Carroll, T.P., O'Neill, S.J., McElvaney, N.G. (2003) Neutrophil elastase up-regulates interleukin-8 via toll-like receptor 4. *FEBS Lett* 544, 129-132.
- Diefenbach, A., Schindler, H., Donhauser, N., Lorenz, E., Laskay, T., MacMicking, J., Röllinghoff, M., Gresser, I., Bogdan, C. (1998) Type 1 interferon (IFN α /beta) and type 2 nitric oxide synthase regulate the innate immune response to a protozoan parasite. *Immunity* 8, 77-87.
- Dougall, A.M., Alexander, B., Holt, D.C., Harris, T., Sultan, A.H., Bates, P.A., Rose, K., Walton, S.F. (2011) Evidence incriminating midges (Diptera: Ceratopogonidae) as potential vectors of *Leishmania* in Australia. *Int J Parasitol* 41, 571-579.
- Dupasquier, M., Stoitzner, P., van Oudenaren, A., Romani, N., Leenen, P.J. (2004) Macrophages and dendritic cells constitute a major subpopulation of cells in the mouse dermis. *J Invest Dermatol* 123, 876-879.
- Duthie, M.S., Raman, V.S., Piazza, F.M., Reed, S.G. (2012) The development and clinical evaluation of second-generation leishmaniasis vaccines. *Vaccine* 30, 134-141.
- Eggers, C.T., Murray, I.A., Delmar, V.A., Day, A.G., Craik, C.S. (2004) The periplasmic serine protease inhibitor ecotin protects bacteria against neutrophil elastase. *Biochem J* 379, 107-118.
- Ehrchen, J.M., Roebrock, K., Foell, D., Nippe, N., von Stebut, E., Weiss, J.M., Münck, N.A., Viemann, D., Varga, G., Müller-Tidow, C., Schuberth, H.J., Roth, J., Sunderkötter, C. (2010) Keratinocytes determine Th1 immunity during early experimental leishmaniasis. *PLoS Pathog* 6, e1000871.
- Eschenlauer, S.C., Faria, M.S., Morrison, L.S., Bland, N., Ribeiro-Gomes, F.L., DosReis, G. A., Coombs, G.H., Lima, A.P., Mottram, J.C. (2009) Influence of parasite encoded inhibitors of serine peptidases in early infection of macrophages with *Leishmania major*. *Cell Microbiol* 11, 106-120.
- Eyles, J.L., Roberts, A.W., Metcalf, D., Wicks, I.P. (2006) Granulocyte colony-stimulating factors and neutrophils—forgotten mediators of inflammatory disease. *Nat Clin Pract Rheumatol* 2, 500-510.
- Faria, M.S., Reis, F.C., Azevedo-Pereira, R.L., Morrison, L.S., Mottram, J.C., Lima, A.P. (2011) *Leishmania* inhibitor of serine peptidase 2 prevents TLR4 activation by neutrophil elastase promoting parasite survival in murine macrophages. *J Immunol* 186, 411-422.
- Faria, M.S., Calegari-Silva, T.C., de Carvalho Vivarini, A., Mottram, J.C., Lopes, U.G., Lima, A.P., (2014) Role of protein kinase R in the killing of *Leishmania major* by macrophages in response to neutrophil elastase and TLR4 via TNF α and IFN β . *FASEB J* 28, 3050-3063
- Favali, C., Tavares, N., Clarêncio, J., Barral, A., Barral-Netto, M., Brodskyn, C. (2007) *Leishmania amazonensis* infection impairs differentiation and function of human dendritic cells. *J Leukoc Biol* 82, 1401-1406.
- Favila, M.A., Geraci, N.S., Zeng, E., Harker, B., Condon, D., Cotton, R.N., Jayakumar, A., Tripathi, V., McDowell, M.A. (2014) Human dendritic cells exhibit a pronounced type I IFN signature following *Leishmania major* infection that is required for IL-12 induction. *J Immunol* 192, 5863-5872
- Franco, L.H., Beverley, S.M., Zamboni, D.S. (2012) Innate immune activation and subversion of Mammalian functions by leishmania lipophosphoglycan. *J Parasitol Res* 2012, 165126.

- Fromm, P.D., Kling, J., Mack, M., Sedgwick, J.D., Körner, H. (2012) Loss of TNF signaling facilitates the development of a novel Ly-6Clow macrophage population permissive for Leishmania major infection. *J Immunol* 188, 6258-6266.
- Gabriel, C., McMaster, W.R., Girard, D., Descoteaux, A. (2010) Leishmania donovani promastigotes evade the antimicrobial activity of neutrophil extracellular traps. *J Immunol* 185, 4319-4327.
- García, M.A., Gil, J., Ventoso, I., Guerra, S., Domingo, E., Rivas, C., Esteban, M. (2006) Impact of protein kinase PKR in cell biology: from antiviral to antiproliferative action. *Microbiol Mol Biol Rev* 70, 1032-1060.
- Geissmann, F., Jung, S., Littman, D.R. (2003) Blood monocytes consist of two principal subsets with distinct migratory properties. *Immunity* 19, 71-82.
- Giannini, M.S. (1974) Effects of promastigote growth phase, frequency of subculture, and host age on promastigote-initiated infections with Leishmania donovani in the golden hamster. *J Protozool* 21, 521-527.
- Giraud, E., Lecoeur, H., Rouault, E., Goyard, S., Milon, G., Lang, T. (2014) A combined luciferase-expressing Leishmania imaging/RT-qPCR assay provides new insights into the sequential bilateral processes deployed in the ear pinna of C57BL/6 mice. *Parasitol Int* 63, 245-253
- Gollob, J.A., Kawasaki, H., Ritz, J. (1997) Interferon-gamma and interleukin-4 regulate T cell interleukin-12 responsiveness through the differential modulation of high-affinity interleukin-12 receptor expression. *Eur J Immunol* 27, 647-652
- Gomes, R., Teixeira, C., Teixeira, M.J., Oliveira, F., Menezes, M.J., Silva, C., de Oliveira, C.I., Miranda, J.C., Elnaiem, D.E., Kamhawi, S., Valenzuela, J.G., Brodskyn, C.I. (2008) Immunity to a salivary protein of a sand fly vector protects against the fatal outcome of visceral leishmaniasis in a hamster model. *Proc Natl Acad Sci USA* 105, 7845-7850.
- Goncalves, R., Zhang, X., Cohen, H., Debrabant, A., Mosser, D.M. (2011) Platelet activation attracts a subpopulation of effector monocytes to sites of Leishmania major infection. *J Exp Med* 208, 1253-1265.
- Gonzalez-Lombana, C., Gimblet, C., Bacellar, O., Oliveira, W.W., Passos, S., Carvalho, L.P., Goldschmidt, M., Carvalho, E.M., Scott, P. (2013) IL-17 mediates immunopathology in the absence of IL-10 following Leishmania major infection. *PLoS Pathog* 9, e1003243.
- Gossage, S.M., Rogers, M.E., Bates, P.A. (2003) Two separate growth phases during the development of Leishmania in sand flies: implications for understanding the life cycle. *Int. J Parasitol* 33, 1027-1034.
- Gross, S., Gammon, S.T., Moss, B.L., Rauch, D., Harding, J., Heinecke, J.W., Ratner, L., Piwnica-Worms, D. (2009) Bioluminescence imaging of myeloperoxidase activity in vivo. *Nat Med* 15, 455-461.
- Guimarães-Costa, A.B., DeSouza-Vieira, T.S., Paletta-Silva, R., Freitas-Mesquita, A.L., Meyer-Fernandes, J.R., Saraiva, E.M. (2014) 3'-nucleotidase/nuclease activity allows Leishmania parasites to escape killing by neutrophil extracellular traps. *Infect Immun* 82, 1732-1740.
- Guimarães-Costa, A.B., Nascimento, M.T., Froment, G.S., Soares, R.P., Morgado, F.N., Conceição-Silva, F., Saraiva, E.M. (2009) Leishmania amazonensis promastigotes induce and are killed by neutrophil extracellular traps. *Proc Natl Acad Sci USA* 106, 6748-6753.

- Güler, M.L., Gorham, J.D., Hsieh, C.S., Mackey, A.J., Steen, R.G., Dietrich, W.F., Murphy, K.M. (1996) Genetic susceptibility to Leishmania: IL-12 responsiveness in Th1 cell development. *Science* 271, 984-987.
- Hart, D.T., Vickerman, K., Coombs, G.H. (1981) A quick, simple method for purifying *Leishmania mexicana* amastigotes in large numbers. *Parasitology* 82, 345-355.
- Hassani, K., Antoniak, E., Jardim, A., Olivier, M. (2011) Temperature-induced protein secretion by *Leishmania mexicana* modulates macrophage signalling and function. *PLoS One* 6, e18724.
- Heinzel, F.P., Schoenhaut, D.S., Rerko, R.M., Rosser, L.E., Gately, M.K. (1993) Recombinant interleukin 12 cures mice infected with *Leishmania major*. *J Exp Med* 177, 1505-1509.
- Heinzel, F.P., Rerko, R.M., Ahmed, F., Pearlman, E. (1995) Endogenous IL-12 is required for control of Th2 cytokine responses capable of exacerbating leishmaniasis in normally resistant mice. *J Immunol* 155, 730-739.
- Hirche, T.O., Gaut, J.P., Heinecke, J.W., Belaaouaj, A. (2005) Myeloperoxidase plays critical roles in killing *Klebsiella pneumoniae* and inactivating neutrophil elastase: effects on host defense. *J Immunol* 174, 1557-1565.
- Hsu, A.C., Scott, P. (2007) *Leishmania mexicana* infection induces impaired lymph node expansion and Th1 cell differentiation despite normal T cell proliferation. *J Immunol* 179, 8200-8207.
- Huntington, J.A. (2011) Serpin structure, function and dysfunction. *J Thromb Haemost* 9 Suppl 1, 26-34.
- Hurdal, R., Brombacher, F. (2014) The role of IL-4 and IL-13 in cutaneous leishmaniasis. *Immunol Lett* 161, 179-183
- Ireland, P.M., Marshall, L., Norville, I., Sarkar-Tyson, M. (2014) The serine protease inhibitor Ecotin is required for full virulence of *Burkholderia pseudomallei*. *Microb Pathog* 67-68, 55-58.
- Ivens, A.C., Peacock, C.S., Worthey, E.A., Murphy, L., Aggarwal, G., Berriman, M., Sisk, E., Rajandream, M.-A., Adlem, E., Aert, R., Anupama, A., Apostolou, Z., Attipoe, P., Bason, N., Bauser, C., Beck, A., Beverley, S.M., Bianchetti, G., Borzym, K., Bothe, G., Bruschi, C. V, Collins, M., Cadag, E., Ciarloni, L., Clayton, C., Coulson, R.M., Cronin, A., Cruz, A.K., Davies, R.M., De Gaudenzi, J., Dobson, D.E., Duesterhoeft, A., Fazelina, G., Fosker, N., Frasch, A.C., Fraser, A., Fuchs, M., Gabel, C., Goble, A., Goffeau, A., Harris, D., Hertz-Fowler, C., Hilbert, H., Horn, D., Huang, Y., Klages, S., Knights, A., Kube, M., Larke, N., Litvin, L., Lord, A., Louie, T., Marra, M., Masuy, D., Matthews, K., Michaeli, S., Mottram, J.C., Müller-Auer, S., Munden, H., Nelson, S., Norbertczak, H., Oliver, K., O'neil, S., Pentony, M., Pohl, T.M., Price, C., Purnelle, B., Quail, M.A., Rabbinowitsch, E., Reinhardt, R., Rieger, M., Rinta, J., Robben, J., Robertson, L., Ruiz, J.C., Rutter, S., Saunders, D., Schäfer, M., Schein, J., Schwartz, D.C., Seeger, K., Seyler, A., Sharp, S., Shin, H., Sivam, D., Squares, R., Squares, S., Tosato, V., Vogt, C., Volckaert, G., Wambutt, R., Warren, T., Wedler, H., Woodward, J., Zhou, S., Zimmermann, W., Smith, D.F., Blackwell, J.M., Stuart, K.D., Barrell, B., Myler, P.J. (2005) The genome of the kinetoplastid parasite, *Leishmania major*. *Science* 309, 436-442.
- Jacobs, T., Andrä, J., Gaworski, I., Graefe, S., Mellenthin, K., Krömer, M., Halter, R., Borlak, J., Clos, J. (2005) Complement C3 is required for the progression of cutaneous lesions and neutrophil attraction in *Leishmania major* infection. *Med Microbiol Immunol* 194, 143-149.

- Kalupov, T., Brillard-Bourdet, M., Dadé, S., Serrano, H., Wartelle, J., Guyot, N., Juliano, L., Moreau, T., Belaouaj, A., Gauthier, F. (2009) Structural characterization of mouse neutrophil serine proteases and identification of their substrate specificities: relevance to mouse models of human inflammatory diseases. *J Biol Chem* 284, 34084-34091.
- Kamhawi, S. (2006) Phlebotomine sand flies and Leishmania parasites: friends or foes? *Trends Parasitol* 22, 439-445.
- Kamhawi, S., Belkaid, Y., Modi, G., Rowton, E., Sacks, D. (2000) Protection against cutaneous leishmaniasis resulting from bites of uninfected sand flies. *Science* 290, 1351-1354.
- Kargi, H.A., Campbell, E.J., Kuhn, C. (1990) Elastase and cathepsin G of human monocytes: heterogeneity and subcellular localization to peroxidase-positive granules. *J Histochem Cytochem* 38, 1179-1186.
- Kautz-Neu, K., Noordegraaf, M., Dinges, S., Bennett, C.L., John, D., Clausen, B.E., von Stebut, E. (2011) Langerhans cells are negative regulators of the anti-Leishmania response. *J Exp Med* 208, 885-891.
- Kébaïer, C., Louzir, H., Chenik, M., Ben Salah, A., Dellagi, K. (2001) Heterogeneity of wild Leishmania major isolates in experimental murine pathogenicity and specific immune response. *Infect Immun* 69, 4906-4915.
- Kessenbrock, K., Fröhlich, L., Sixt, M., Lämmermann, T., Pfister, H., Bateman, A., Belaouaj, A., Ring, J., Ollert, M., Fässler, R., Jenne, D.E. (2008) Proteinase 3 and neutrophil elastase enhance inflammation in mice by inactivating antiinflammatory progranulin. *J Clin Invest* 118, 2438-2447.
- Killick-Kendrick, R., Molyneux, D.H., Ashford, R.W. (1974) Leishmania in phlebotomid sandflies. I. Modifications of the flagellum associated with attachment to the mid-gut and oesophageal valve of the sandfly. *Proc R Soc Lond B Biol Sci* 187, 409-419.
- Kimblin, N., Peters, N., Debrabant, A., Secundino, N., Egen, J., Lawyer, P., Fay, M.P., Kamhawi, S., Sacks, D. (2008) Quantification of the infectious dose of Leishmania major transmitted to the skin by single sand flies. *Proc Natl Acad Sci USA* 105, 10125-10130.
- Kolaczowska, E., Kubes, P. (2013) Neutrophil recruitment and function in health and inflammation. *Nat Rev Immunol* 13, 159-175.
- Korkmaz, B., Horwitz, M.S., Jenne, D.E., Gauthier, F. (2010) Neutrophil elastase, proteinase 3, and cathepsin G as therapeutic targets in human diseases. *Pharmacol Rev* 62, 726-759.
- Körner, U., Fuss, V., Steigerwald, J., Moll, H. (2006) Biogenesis of Leishmania major-harboring vacuoles in murine dendritic cells. *Infect Immun* 74, 1305-1312.
- Kossodo, S., Zhang, J., Groves, K., Cuneo, G.J., Handy, E., Morin, J., Delaney, J., Yared, W., Rajopadhye, M., Peterson, J.D. (2011) Noninvasive in vivo quantification of neutrophil elastase activity in acute experimental mouse lung injury. *Int J Mol Imaging* 2011, 581406.
- Krutzik, S.R., Tan, B., Li, H., Ochoa, M.T., Liu, P.T., Sharfstein, S.E., Graeber, T.G., Sieling, P.A., Liu, Y.J., Rea, T.H., Bloom, B.R., Modlin, R.L. (2005) TLR activation triggers the rapid differentiation of monocytes into macrophages and dendritic cells. *Nat Med* 11, 653-660.

- Kuchroo, V.K., Das, M.P., Brown, J.A., Ranger, A.M., Zamvil, S.S., Sobel, R.A., Weiner, H.L., Nabavi, N., Glimcher, L.H. (1995) B7-1 and B7-2 costimulatory molecules activate differentially the Th1/Th2 developmental pathways: application to autoimmune disease therapy. *Cell* 80, 707-718.
- Kumar, A.P., Piedrafita, F.J., Reynolds, W.F. (2004) Peroxisome proliferator-activated receptor gamma ligands regulate myeloperoxidase expression in macrophages by an estrogen-dependent mechanism involving the -463GA promoter polymorphism. *J Biol Chem* 279, 8300-8315.
- Kumar, R., Engwerda, C. (2014) Vaccines to prevent leishmaniasis. *Clin Transl Immunol* 3, e13.
- Kurosaka, K., Chen, Q., Yarovinsky, F., Oppenheim, J.J., Yang, D. (2005) Mouse cathelin-related antimicrobial peptide chemoattracts leukocytes using formyl peptide receptor-like 1/mouse formyl peptide receptor-like 2 as the receptor and acts as an immune adjuvant. *J Immunol* 174, 6257-6265.
- Lainson, R., Ward, R.D., Shaw, J.J. (1977) Leishmania in phlebotomid sandflies: VI. Importance of hindgut development in distinguishing between parasites of the *Leishmania mexicana* and *L. braziliensis* complexes. *Proc R Soc Lond B Biol Sci* 199, 309-320.
- Lang, T., Goyard, S., Lebastard, M., Milon, G. (2005) Bioluminescent *Leishmania* expressing luciferase for rapid and high throughput screening of drugs acting on amastigote-harboring macrophages and for quantitative real-time monitoring of parasitism features in living mice. *Cell Microbiol* 7, 383-392.
- Larson, R.S., Springer, T.A. (1990) Structure and function of leukocyte integrins. *Immunol Rev* 114, 181-217.
- Laufs, H., Müller, K., Fleischer, J., Reiling, N., Jahnke, N., Jensenius, J.C., Solbach, W., Laskay, T. (2002) Intracellular survival of *Leishmania major* in neutrophil granulocytes after uptake in the absence of heat-labile serum factors. *Infect Immun* 70, 826-835.
- Lazarski, C.A., Ford, J., Katzman, S.D., Rosenberg, A.F., Fowell, D.J. (2013) IL-4 attenuates Th1-associated chemokine expression and Th1 trafficking to inflamed tissues and limits pathogen clearance. *PLoS One* 8, e71949.
- Lefkowitz, D.L., Lincoln, J.A., Lefkowitz, S.S., Bollen, A., Moguilevsky, N. (1997) Enhancement of macrophage-mediated bactericidal activity by macrophage-mannose receptor-ligand interaction. *Immunol Cell Biol* 75, 136-141.
- Lefkowitz, D.L., Roberts, E., Grattendick, K., Schwab, C., Stuart, R., Lincoln, J., Allen, R.C., Moguilevsky, N., Bollen, A., Lefkowitz, S.S. (2000) The endothelium and cytokine secretion: the role of peroxidases as immunoregulators. *Cell Immunol* 202, 23-30.
- Leifso, K., Cohen-Freue, G., Dogra, N., Murray, A., McMaster, W.R. (2007) Genomic and proteomic expression analysis of *Leishmania* promastigote and amastigote life stages: the *Leishmania* genome is constitutively expressed. *Mol Biochem Parasitol* 152, 35-46.
- León, B., López-Bravo, M., Ardavín, C. (2007) Monocyte-derived dendritic cells formed at the infection site control the induction of protective T helper 1 responses against *Leishmania*. *Immunity* 26, 519-531.

- Lima, G.M., Vallochi, A.L., Silva, U.R., Bevilacqua, E.M., Kiffer, M.M., Abrahamsohn, I.A. (1998) The role of polymorphonuclear leukocytes in the resistance to cutaneous leishmaniasis. *Immunol Lett* 64, 145-151.
- Lipoldová, M., Demant, P. (2006) Genetic susceptibility to infectious disease: lessons from mouse models of leishmaniasis. *Nat Rev Genet* 7, 294-305.
- Lira, R., Doherty, M., Modi, G., Sacks, D. (2000) Evolution of lesion formation, parasitic load, immune response, and reservoir potential in C57BL/6 mice following high- and low-dose challenge with *Leishmania major*. *Infect Immun* 68, 5176-5182.
- Liu, D., Kebaier, C., Pakpour, N., Capul, A.A., Beverley, S.M., Scott, P., Uzonna, J.E. (2009) *Leishmania major* phosphoglycans influence the host early immune response by modulating dendritic cell functions. *Infect Immun* 77, 3272-3283.
- Locksley, R.M., Heinzel, F.P., Holaday, B.J., Mutha, S.S., Reiner, S.L., Sadick, M.D. (1991) Induction of Th1 and Th2 CD4+ subsets during murine *Leishmania major* infection. *Res Immunol* 142, 28-32.
- Lodes, M.J., Merlin, G., DeVos, T., Ghosh, A., Madhubala, R., Myler, P.J., Stuart, K. (1995) Increased expression of LD1 genes transcribed by RNA polymerase I in *Leishmania donovani* as a result of duplication into the rRNA gene locus. *Mol Cell Biol* 15, 6845-6853.
- Lopez Kostka, S., Dinges, S., Griewank, K., Iwakura, Y., Udey, M.C., von Stebut, E. (2009) IL-17 promotes progression of cutaneous leishmaniasis in susceptible mice. *J Immunol* 182, 3039-3046.
- Loría-Cervera, E.N., Andrade-Narváez, F.J. (2014) Animal models for the study of leishmaniasis immunology. *Rev Inst Med Trop Sao Paulo* 56, 1-11.
- Louzir, H., Melby, P.C., Ben Salah, A., Marrakchi, H., Aoun, K., Ben Ismail, R., Dellagi, K. (1998) Immunologic determinants of disease evolution in localized cutaneous leishmaniasis due to *Leishmania major*. *J Infect Dis* 177, 1687-1695.
- MacIvor, D.M., Shapiro, S.D., Pham, C.T., Belaaouaj, A., Abraham, S.N., Ley, T.J. (1999) Normal neutrophil function in cathepsin G-deficient mice. *Blood* 94, 4282-4293.
- Markikou-Ouni, W., Ben Achour-Chenik, Y., Meddeb-Garnaoui, A. (2012) Effects of *Leishmania major* clones showing different levels of virulence on infectivity, differentiation and maturation of human dendritic cells. *Clin Exp Immunol* 169, 273-280.
- Maurer, M., Lopez Kostka, S., Siebenhaar, F., Moelle, K., Metz, M., Knop, J., von Stebut, E. (2006) Skin mast cells control T cell-dependent host defense in *Leishmania major* infections. *FASEB J* 20, 2460-2467.
- McDowell, M.A., Marovich, M., Lira, R., Braun, M., Sacks, D. (2002) *Leishmania* priming of human dendritic cells for CD40 ligand-induced interleukin-12p70 secretion is strain and species dependent. *Infect Immun* 70, 3994-4001.
- McFarlane, E., Perez, C., Charmoy, M., Allenbach, C., Carter, K.C., Alexander, J., Tacchini-Cottier, F. (2008) Neutrophils contribute to development of a protective immune response during onset of infection with *Leishmania donovani*. *Infect Immun* 76, 532-541.
- McLatchie, A.P., Burrell-Saward, H., Myburgh, E., Lewis, M.D., Ward, T.H., Mottram, J.C., Croft, S.L., Kelly, J.M., Taylor, M.C. (2013) Highly sensitive in vivo imaging of *Trypanosoma brucei* expressing "red-shifted" luciferase. *PLoS Negl Trop Dis* 7, e2571.

- Metzler, K.D., Fuchs, T. a, Nauseef, W.M., Reumaux, D., Roesler, J., Schulze, I., Wahn, V., Papayannopoulos, V., Zychlinsky, A. (2011) Myeloperoxidase is required for neutrophil extracellular trap formation: implications for innate immunity. *Blood* 117, 953-959.
- Michel, G., Ferrua, B., Lang, T., Maddugoda, M.P., Munro, P., Pomares, C., Lemichez, E., Marty, P. (2011) Luciferase-expressing *Leishmania infantum* allows the monitoring of amastigote population size, in vivo, ex vivo and in vitro. *PLoS Negl Trop Dis* 5, e1323.
- Miralles, G.D., Stoeckle, M.Y., McDermott, D.F., Finkelman, F.D., Murray, H.W. (1994) Th1 and Th2 cell-associated cytokines in experimental visceral leishmaniasis. *Infect Immun* 62, 1058-1063.
- Misslitz, A., Mottram, J.C., Overath, P., Aebischer, T. (2000) Targeted integration into a rRNA locus results in uniform and high level expression of transgenes in *Leishmania* amastigotes. *Mol Biochem Parasitol* 107, 251-261.
- Misslitz, A.C., Bonhagen, K., Harbecke, D., Lippuner, C., Kamradt, T., Aebischer, T. (2004) Two waves of antigen-containing dendritic cells in vivo in experimental *Leishmania major* infection. *Eur J Immunol* 34, 715-725.
- Mollinedo, F., Janssen, H., de la Iglesia-Vicente, J., Villa-Pulgarin, J.A., Calafat, J. (2010) Selective fusion of azurophilic granules with *Leishmania*-containing phagosomes in human neutrophils. *J Biol Chem* 285, 34528-34536.
- Moradin, N., Descoteaux, A. (2012) *Leishmania* promastigotes: building a safe niche within macrophages. *Front Cell Infect Microbiol* 2, 121.
- Morris, R.V., Shoemaker, C.B., David, J.R., Lanzaro, G.C., Titus, R.G. (2001) Sandfly maxadilan exacerbates infection with *Leishmania major* and vaccinating against it protects against *L. major* infection. *J Immunol* 167, 5226-5230.
- Morrison, L.S., Goundry, A., Faria, M.S., Tetley, L., Eschenlauer, S.C., Westrop, G.D., Dostalova, A., Volf, P., Coombs, G.H., Lima, A.P., Mottram, J.C. (2012) Ecotin-like serine peptidase inhibitor ISP1 of *Leishmania major* plays a role in flagellar pocket dynamics and promastigote differentiation. *Cell Microbiol* 14, 1271-1286
- Moser, M (2001) Regulation of Th1/Th2 development by antigen-presenting cells in vivo. *Immunobiology* 204, 551-557.
- Mottram, J.C., Souza, A.E., Hutchison, J.E., Carter, R., Frame, M.J., Coombs, G.H. (1996) Evidence from disruption of the *lmcpb* gene array of *Leishmania mexicana* that cysteine proteinases are virulence factors. *Proc Natl Acad Sci USA* 93, 6008-6013.
- Mottram, J.C., Coombs, G.H., Alexander, J. (2004) Cysteine peptidases as virulence factors of *Leishmania*. *Curr Opin Microbiol* 7, 375-381.
- Mukbel, R.M., Patten, C., Gibson, K., Ghosh, M., Petersen, C., Jones, D.E. (2007) Macrophage killing of *Leishmania amazonensis* amastigotes requires both nitric oxide and superoxide. *Am J Trop Med Hyg* 76, 669-675.
- Mukhopadhyay, D., Dalton, J.E., Kaye, P.M., Chatterjee, M. (2014) Post kala-azar dermal leishmaniasis: an unresolved mystery. *Trends Parasitol* 30, 65-74.
- Müller, K., van Zandbergen, G., Hansen, B., Laufs, H., Jahnke, N., Solbach, W., Laskay, T. (2001) Chemokines, natural killer cells and granulocytes in the early course of *Leishmania major* infection in mice. *Med Microbiol Immunol* 190, 73-76.

- Munday, J.C., McLuskey, K., Brown, E., Coombs, G.H., Mottram, J.C. (2011) Oligopeptidase B deficient mutants of *Leishmania major*. *Mol Biochem Parasitol* 175, 49-57.
- Muraille, E., Gounon, P., Cazareth, J., Hoebeke, J., Lippuner, C., Davalos-Misslitz, A., Aebischer, T., Muller, S., Glaichenhaus, N., Mougneau, E. (2010) Direct visualization of peptide/MHC complexes at the surface and in the intracellular compartments of cells infected in vivo by *Leishmania major*. *PLoS Pathog* 6, e1001154.
- Murray, H.W., Nathan, C.F. (1999) Macrophage microbicidal mechanisms in vivo: reactive nitrogen versus oxygen intermediates in the killing of intracellular visceral *Leishmania donovani*. *J Exp Med* 189, 741-746.
- Musa, A., Khalil, E., Hailu, A., Olobo, J., Balasegaram, M., Omollo, R., Edwards, T., Rashid, J., Mbui, J., Musa, B., Abuzaid, A.A., Ahmed, O., Fadlalla, A., El-Hassan, A., Mueller, M., Mucee, G., Njoroge, S., Manduku, V., Mutuma, G., Apadet, L., Lodenyo, H., Mutea, D., Kirigi, G., Yifru, S., Mengistu, G., Hurissa, Z., Hailu, W., Weldegebreal, T., Tafes, H., Mekonnen, Y., Makonnen, E., Ndegwa, S., Sagaki, P., Kimutai, R., Kesusu, J., Owiti, R., Ellis, S., Wasunna, M. (2012) Sodium stibogluconate (SSG) & paromomycin combination compared to SSG for visceral leishmaniasis in East Africa: a randomised controlled trial. *PLoS Negl Trop Dis* 6, e1674.
- Myburgh, E., Coles, J.A., Ritchie, R., Kennedy, P.G., McLatchie, A.P., Rodgers, J., Taylor, M.C., Barrett, M.P., Brewer, J.M., Mottram, J.C. (2013) In vivo imaging of trypanosome-brain interactions and development of a rapid screening test for drugs against CNS stage trypanosomiasis. *PLoS Negl Trop Dis* 7, e2384.
- Nagra, R.M., Becher, B., Tourtellotte, W.W., Antel, J.P., Gold, D., Paladino, T., Smith, R.A., Nelson, J.R., Reynolds, W.F. (1997) Immunohistochemical and genetic evidence of myeloperoxidase involvement in multiple sclerosis. *J. Neuroimmunol* 78, 97-107.
- Ndjamen, B., Kang, B.H., Hatsuzawa, K., Kima, P.E. (2010) *Leishmania* parasitophorous vacuoles interact continuously with the host cell's endoplasmic reticulum; parasitophorous vacuoles are hybrid compartments. *Cell Microbiol* 12, 1480-1494.
- Ng, L.G., Hsu, A., Mandell, M. A., Roediger, B., Hoeller, C., Mrass, P., Iparraguirre, A., Cavanagh, L.L., Triccas, J. A, Beverley, S.M., Scott, P., Weninger, W. (2008) Migratory dermal dendritic cells act as rapid sensors of protozoan parasites. *PLoS Pathog.* 4, e1000222.
- Nieto, A., Domínguez-Bernal, G., Orden, J.A., De La Fuente, R., Madrid-Elena, N., Carrión, J. (2011) Mechanisms of resistance and susceptibility to experimental visceral leishmaniasis: BALB/c mouse versus Syrian hamster model. *Vet Res* 42, 39.
- Noben-Trauth, N., Lira, R., Nagase, H., Paul, W.E., Sacks, D.L. (2003) The relative contribution of IL-4 receptor signaling and IL-10 to susceptibility to *Leishmania major*. *J Immunol* 170, 5152-5158.
- Novais, F.O., Santiago, R.C., Báfica, A., Khouri, R., Afonso, L., Borges, V.M., Brodskyn, C., Barral-Netto, M., Barral, A., de Oliveira, C.I. (2009) Neutrophils and macrophages cooperate in host resistance against *Leishmania braziliensis* infection. *J Immunol* 183, 8088-8098.
- Novais, F.O., Carvalho, L.P., Graff, J.W., Beiting, D.P., Ruthel, G., Roos, D.S., Betts, M.R., Goldschmidt, M.H., Wilson, M.E., de Oliveira, C.I., Scott, P. (2013) Cytotoxic T cells mediate pathology and metastasis in cutaneous leishmaniasis. *PLoS Pathog.* 9, e1003504.

- O'Shea, J.J., Paul, W.E. (2010) Mechanisms underlying lineage commitment and plasticity of helper CD4+ T cells. *Science* 327, 1098-1102.
- Ogolla, P.S., Portillo, J.A., White, C.L., Patel, K., Lamb, B., Sen, G.C., Subauste, C.S. (2013) The protein kinase double-stranded RNA-dependent (PKR) enhances protection against disease cause by a non-viral pathogen. *PLoS Pathog* 9, e1003557.
- Oliveira, F., Lawyer, P.G., Kamhawi, S., Valenzuela, J.G. (2008) Immunity to distinct sand fly salivary proteins primes the anti-Leishmania immune response towards protection or exacerbation of disease. *PLoS Negl Trop Dis* 2, e226.
- Oliveira, L.S., de Queiroz, N.M., Veloso, L.V., Moreira, T.G., Oliveira, F.S., Carneiro, M.B., Faria, A.M., Vieira, L.Q., Oliveira, S.C., Horta, M.F. (2014) A defective TLR4 signaling for IFN- β expression is responsible for the innately lower ability of BALB/c macrophages to produce NO in response to LPS as compared to C57BL/6. *PLoS One* 9, e98913.
- Opperdoes, F.R., Michels, P.A. (2007) Horizontal gene transfer in trypanosomatids. *Trends Parasitol* 23, 470-476.
- Pagán, A.J., Peters, N.C., Debrabant, A., Ribeiro-Gomes, F., Pepper, M., Karp, C.L., Jenkins, M.K., Sacks, D.L. (2013) Tracking antigen-specific CD4+ T cells throughout the course of chronic Leishmania major infection in resistant mice. *Eur J Immunol* 43, 427-438.
- Papayannopoulos, V., Metzler, K.D., Hakkim, A., Zychlinsky, A. (2010) Neutrophil elastase and myeloperoxidase regulate the formation of neutrophil extracellular traps. *J Cell Biol* 191, 677-691.
- Park, A.Y., Hondowicz, B.D., Scott, P. (2000) IL-12 is required to maintain a Th1 response during Leishmania major infection. *J Immunol* 165, 896-902.
- Peacock, C.S., Seeger, K., Harris, D., Murphy, L., Ruiz, J.C., Quail, M.A., Peters, N., Adlem, E., Tivey, A., Aslett, M., Kerhornou, A., Ivens, A., Fraser, A., Rajandream, M.-A., Carver, T., Norbertczak, H., Chillingworth, T., Hance, Z., Jagels, K., Moule, S., Ormond, D., Rutter, S., Squares, R., Whitehead, S., Rabinowitsch, E., Arrowsmith, C., White, B., Thurston, S., Bringaud, F., Baldauf, S.L., Faulconbridge, A., Jeffares, D., Depledge, D.P., Oyola, S.O., Hilley, J.D., Brito, L.O., Tosi, L.R.O., Barrell, B., Cruz, A.K., Mottram, J.C., Smith, D.F., Berriman, M. (2007) Comparative genomic analysis of three Leishmania species that cause diverse human disease. *Nat Genet* 39, 839-847.
- Pereira, R.M., Teixeira, K.L., Barreto-de-Souza, V., Calegari-Silva, T.C., De-Melo, L.D., Soares, D.C., Bou-Habib, D.C., Silva, A.M., Saraiva, E.M., Lopes, U.G. (2010) Novel role for the double-stranded RNA-activated protein kinase PKR: modulation of macrophage infection by the protozoan parasite Leishmania. *FASEB J* 24, 617-626.
- Perera, N.C., Schilling, O., Kittel, H., Back, W., Kremmer, E., Jenne, D.E. (2012) NSP4, an elastase-related protease in human neutrophils with arginine specificity. *Proc Natl Acad Sci USA* 109, 6229-6234.
- Perera, N.C., Wiesmüller, K.H., Larsen, M.T., Schacher, B., Eickholz, P., Borregaard, N., Jenne, D.E. (2013) NSP4 is stored in azurophil granules and released by activated neutrophils as active endoprotease with restricted specificity. *J Immunol* 191, 2700-2707.
- Peters, N.C., Egen, J.G., Secundino, N., Debrabant, A., Kimblin, N., Kamhawi, S., Lawyer, P., Fay, M.P., Germain, R.N., Sacks, D. (2008) In vivo imaging reveals an essential role for neutrophils in leishmaniasis transmitted by sand flies. *Science* 321, 970-974.

- Petritus, P.M., Manzoni-de-Almeida, D., Gimblet, C., Gonzalez Lombana, C., Scott, P. (2012) *Leishmania mexicana* induces limited recruitment and activation of monocytes and monocyte-derived dendritic cells early during infection. *PLoS Negl Trop Dis* 6, e1858.
- Peysseelon, F., Launay, G., Lisacek, F., Duclos, B., Ricard-Blum, S. (2013) Comparative analysis of *Leishmania* exoproteomes: implication for host-pathogen interactions. *Biochim Biophys Acta* 1834, 2653-2662.
- Pham, C.T. (2006) Neutrophil serine proteases: specific regulators of inflammation. *Nat Rev Immunol* 6, 541-550.
- Pham, C.T. (2008) Neutrophil serine proteases fine-tune the inflammatory response. *Int J Biochem Cell Biol* 40, 1317-1333.
- Piedrafita, D., Proudfoot, L., Nikolaev, A.V., Xu, D., Sands, W., Feng, G.J., Thomas, E., Brewer, J., Ferguson, M.A., Alexander, J., Liew, F.Y. (1999) Regulation of macrophage IL-12 synthesis by *Leishmania* phosphoglycans. *Eur J Immunol* 29, 235-244.
- Pimenta, P.F., Saraiva, E.M., Rowton, E., Modi, G.B., Garraway, L.A., Beverley, S.M., Turco, S.J., Sacks, D.L. (1994) Evidence that the vectorial competence of phlebotomine sand flies for different species of *Leishmania* is controlled by structural polymorphisms in the surface lipophosphoglycan. *Proc Natl Acad Sci USA* 91, 9155-9159.
- Pimenta, P.F., Modi, G.B., Pereira, S.T., Shahabuddin, M., Sacks, D.L. (1997) A novel role for the peritrophic matrix in protecting *Leishmania* from the hydrolytic activities of the sand fly midgut. *Parasitology* 115, 359-369.
- Pollock, K.G., McNeil, K.S., Mottram, J.C., Lyons, R.E., Brewer, J.M., Scott, P., Coombs, G.H., Alexander, J. (2003) The *Leishmania mexicana* cysteine protease, CPB2.8, induces potent Th2 responses. *J Immunol* 170, 1746-1753.
- Quinones, M.P., Estrada, C.A., Jimenez, F., Martinez, H., Willmon, O., Kuziel, W.A., Ahuja, S.K., Ahuja, S.S. (2007) CCL2-independent role of CCR2 in immune responses against *Leishmania major*. *Parasite Immunol.* 29, 211-217.
- Rakotomanga, M., Blanc, S., Gaudin, K., Chaminade, P., Loiseau, P.M. (2007) Miltefosine affects lipid metabolism in *Leishmania donovani* promastigotes. *Antimicrob Agents Chemother* 51, 1425-1430.
- Ramalho-Ortigão, J.M., Kamhawi, S., Rowton, E.D., Ribeiro, J.M.C., Valenzuela, J.G. (2003) Cloning and characterization of trypsin- and chymotrypsin-like proteases from the midgut of the sand fly vector *Phlebotomus papatasi*. *Insect Biochem Mol Biol* 33, 163-171.
- Reeves, E.P., Lu, H., Jacobs, H.L., Messina, C.G., Bolsover, S., Gabella, G., Potma, E.O., Warley, A., Roes, J., Segal, A.W. (2002) Killing activity of neutrophils is mediated through activation of proteases by K⁺ flux. *Nature* 416, 291-297.
- Reimão, J.Q., Trinconi, C.T., Yokoyama-Yasunaka, J.K., Miguel, D.C., Kalil, S.P., Uliana, S.R. (2013) Parasite burden in *Leishmania (Leishmania) amazonensis*-infected mice: validation of luciferase as a quantitative tool. *J Microbiol Methods* 93, 95-101.
- Ribeiro-Gomes, F.L., Otero, A.C., Gomes, N.A., Moniz-De-Souza, M.C., Cysne-Finkelstein, L., Arnholdt, A.C., Calich, V.L., Coutinho, S.G., Lopes, M.F., DosReis, G.A. (2004) Macrophage interactions with neutrophils regulate *Leishmania major* infection. *J Immunol* 172, 4454-62.

- Ribeiro-Gomes, F.L., Moniz-de-Souza, M.C., Alexandre-Moreira, M.S., Dias, W.B., Lopes, M.F., Nunes, M.P., Lungarella, G., DosReis, G.A. (2007) Neutrophils activate macrophages for intracellular killing of *Leishmania major* through recruitment of TLR4 by neutrophil elastase. *J Immunol* 179, 3988-3994.
- Ribeiro-Gomes, F.L., Peters, N.C., Debrabant, A., Sacks, D.L. (2012) Efficient capture of infected neutrophils by dendritic cells in the skin inhibits the early anti-leishmania response. *PLoS Pathog* 8, e1002536.
- Ribeiro-Gomes, F.L., Roma, E.H., Carneiro, M.B., Doria, N.A., Sacks, D.L., Peters, N.C. (2014) Site dependent recruitment of inflammatory cells determines the effective dose of *Leishmania major*. *Infect Immun* 82,2713-2727
- Ritter, U., Meissner, A., Scheidig, C., Körner, H., (2004) CD8 alpha- and Langerin-negative dendritic cells, but not Langerhans cells, act as principal antigen-presenting cells in leishmaniasis. *Eur J Immunol* 34, 1542-1550.
- Ritter, U., Frischknecht, F., van Zandbergen, G. (2009) Are neutrophils important host cells for *Leishmania* parasites? *Trends Parasitol* 25, 505-510.
- Rittig, M.G., Bogdan, C. (2000) *Leishmania*-host-cell interaction: complexities and alternative views. *Parasitol Today* 16, 292-297.
- Rogers, K.A., Titus, R.G. (2003) Immunomodulatory effects of Maxadilan and *Phlebotomus papatasi* sand fly salivary gland lysates on human primary in vitro immune responses. *Parasite Immunol* 25, 127-134.
- Rogers, M.B., Hilley, J.D., Dickens, N.J., Wilkes, J., Bates, P.A., Depledge, D.P., Harris, D., Her, Y., Herzyk, P., Imamura, H., Otto, T.D., Sanders, M., Seeger, K., Dujardin, J.C., Berriman, M., Smith, D.F., Hertz-Fowler, C., Mottram, J.C. (2011) Chromosome and gene copy number variation allow major structural change between species and strains of *Leishmania*. *Genome Res* 21, 2129-2142.
- Rogers, M.E., Chance, M.L., Bates, P.A. (2002) The role of promastigote secretory gel in the origin and transmission of the infective stage of *Leishmania mexicana* by the sandfly *Lutzomyia longipalpis*. *Parasitology* 124, 495-507.
- Rogers, M.E., Ilg, T., Nikolaev, A.V, Ferguson, M.A., Bates, P.A. (2004) Transmission of cutaneous leishmaniasis by sand flies is enhanced by regurgitation of fPPG. *Nature* 430, 463-467.
- Rogers, M.E., Bates, P.A. (2007) *Leishmania* manipulation of sand fly feeding behavior results in enhanced transmission. *PLoS Pathog.* 3, e91.
- Rogers, M.E., Hajmová, M., Joshi, M.B., Sadlova, J., Dwyer, D.M., Volf, P., Bates, P.A. (2008) *Leishmania* chitinase facilitates colonization of sand fly vectors and enhances transmission to mice. *Cell Microbiol* 10, 1363-72.
- Rogers, M.E., Corware, K., Müller, I., Bates, P.A. (2010) *Leishmania infantum* proteophosphoglycans regurgitated by the bite of its natural sand fly vector, *Lutzomyia longipalpis*, promote parasite establishment in mouse skin and skin-distant tissues. *Microbes Infect* 12, 875-879.
- Romão, P.R., Da Costa Santiago, H., Ramos, C.D., De Oliveira, C.F., Monteiro, M.C., De Queiroz Cunha, F., Vieira, L.Q. (2009) Mast cell degranulation contributes to susceptibility to *Leishmania major*. *Parasite Immunol.* 31, 140-146.
- Ronet, C., Voigt, H., Himmelrich, H., Doucey, M.A., Hauyon-La Torre, Y., Revaz-Breton, M., Tacchini-Cottier, F., Bron, C., Louis, J., Launois, P. (2008) *Leishmania major*-

- specific B cells are necessary for Th2 cell development and susceptibility to L. major LV39 in BALB/c mice. *J Immunol* 180, 4825-4835.
- Rotta, G., Edwards, E.W., Sangaletti, S., Bennett, C., Ronzoni, S., Colombo, M.P., Steinman, R.M., Randolph, G.J., Rescigno, M. (2003) Lipopolysaccharide or whole bacteria block the conversion of inflammatory monocytes into dendritic cells in vivo. *J Exp Med* 198, 1253-1263.
- Roy, G., Dumas, C., Sereno, D., Wu, Y., Singh, A.K., Tremblay, M.J., Ouellette, M., Olivier, M., Papadopoulou, B. (2000) Episomal and stable expression of the luciferase reporter gene for quantifying Leishmania spp. infections in macrophages and in animal models. *Mol Biochem Parasitol* 110, 195-206.
- Sacks, D.L., Hieny, S., Sher, A. (1985) Identification of cell surface carbohydrate and antigenic changes between noninfective and infective developmental stages of Leishmania major promastigotes. *J Immunol* 135, 564-569.
- Saha, A.K., Mukherjee, T., Bhaduri, A. (1986) Mechanism of action of amphotericin B on Leishmania donovani promastigotes. *Mol Biochem Parasitol* 19, 195-200.
- Sanderson, S.J., Westrop, G.D., Scharfstein, J., Mottram, J.C., Coombs, G.H. (2003) Functional conservation of a natural cysteine peptidase inhibitor in protozoan and bacterial pathogens. *FEBS Lett* 542, 12-16.
- Sato, N., Ahuja, S.K., Quinones, M., KostECKI, V., Reddick, R.L., Melby, P.C., Kuziel, W.A., Ahuja, S.S. (2000) CC chemokine receptor (CCR)2 is required for langerhans cell migration and localization of T helper cell type 1 (Th1)-inducing dendritic cells. Absence of CCR2 shifts the Leishmania major-resistant phenotype to a susceptible state dominated by Th2 cytokines, B cell outgrowth, and sustained neutrophilic inflammation. *J Exp Med* 192, 205-218.
- Sauter, B., Albert, M.L., Francisco, L., Larsson, M., Somersan, S., Bhardwaj, N. (2000) Consequences of cell death: exposure to necrotic tumor cells, but not primary tissue cells or apoptotic cells, induces the maturation of immunostimulatory dendritic cells. *J Exp Med* 191, 423-434.
- Schuster, S., Hartley, M.A., Tacchini-Cottier, F., Ronet, C. (2014) A scoring method to standardize lesion monitoring following intra-dermal infection of Leishmania parasites in the murine ear. *Front Cell Infect Microbiol.* 4, 67.
- Seblova, V., Sadlova, J., Carpenter, S., Volf, P. (2012) Development of Leishmania parasites in Culicoides nubeculosus (Diptera: Ceratopogonidae) and implications for screening vector competence. *J Med Entomol* 49, 967-970.
- Serbina, N.V, Salazar-Mather, T.P., Biron, C.A., Kuziel, W.A., Pamer, E.G. (2003) TNF/iNOS-producing dendritic cells mediate innate immune defense against bacterial infection. *Immunity* 19, 59-70.
- Shepherd, V.L., Hoidal, J.R. (1990) Clearance of neutrophil-derived myeloperoxidase by the macrophage mannose receptor. *Am J Respir Cell Mol Biol* 2, 335-340.
- Shi, C., Pamer, E.G. (2011) Monocyte recruitment during infection and inflammation. *Nat Rev Immunol* 11, 762-774.
- Shio, M.T., Hassani, K., Isnard, A., Ralph, B., Contreras, I., Gomez, M.A., Abu-Dayyeh, I., Olivier, M. (2012) Host cell signalling and leishmania mechanisms of evasion. *J Trop Med* 2012, 819512.

- Silverman, J.M., Chan, S.K., Robinson, D.P., Dwyer, D.M., Nandan, D., Foster, L.J., Reiner, N.E. (2008) Proteomic analysis of the secretome of *Leishmania donovani*. *Genome Biol* 9, R35.
- Silverman, J.M., Clos, J., De'Oliveira, C.C., Shirvani, O., Fang, Y., Wang, C., Foster, L.J., Reiner, N.E. (2010a) An exosome-based secretion pathway is responsible for protein export from *Leishmania* and communication with macrophages. *J Cell Sci* 123, 842-852.
- Silverman, J.M., Clos, J., Horakova, E., Wang, A.Y., Wiesgigl, M., Kelly, I., Lynn, M.A., McMaster, W.R., Foster, L.J., Levings, M.K., Reiner, N.E. (2010b) *Leishmania* exosomes modulate innate and adaptive immune responses through effects on monocytes and dendritic cells. *J Immunol* 185, 5011-5022.
- Singh, O.P., Sundar, S. (2014) Immunotherapy and targeted therapies in treatment of visceral leishmaniasis: current status and future prospects. *Front Immunol* 26: 296
- Snider, H., Lezama-Davila, C., Alexander, J., Satoskar, A.R., 2009. Sex hormones and modulation of immunity against leishmaniasis. *Neuroimmunomodulation* 16, 106-113.
- Soehnlein, O., Zernecke, A., Eriksson, E.E., Rothfuchs, A.G., Pham, C.T., Herwald, H., Bidzhekov, K., Rottenberg, M.E., Weber, C., Lindbom, L., (2008) Neutrophil secretion products pave the way for inflammatory monocytes. *Blood* 112, 1461-1471.
- Sousa, L.M., Carneiro, M.B., Resende, M.E., Martins, L.S., Dos Santos, L.M., Vaz, L.G., Mello, P.S., Mosser, D.M., Oliveira, M.A., Vieira, L.Q. (2014) Neutrophils have a protective role during early stages of *Leishmania amazonensis* infection in BALB/c mice. *Parasite Immunol* 36, 13-31.
- Späth, G.F., Epstein, L., Leader, B., Singer, S.M., Avila, H.A., Turco, S.J., Beverley, S.M. (2000) Lipophosphoglycan is a virulence factor distinct from related glycoconjugates in the protozoan parasite *Leishmania major*. *Proc Natl Acad Sci USA* 97, 9258-9263.
- Späth, G.F., Garraway, L.A., Turco, S.J., Beverley, S.M. (2003) The role(s) of lipophosphoglycan (LPG) in the establishment of *Leishmania major* infections in mammalian hosts. *Proc Natl Acad Sci USA* 100, 9536-9541.
- Stenger, S., Thüning, H., Rölinghoff, M., Bogdan, C. (1994) Tissue expression of inducible nitric oxide synthase is closely associated with resistance to *Leishmania major*. *J Exp Med* 180, 783-793.
- Stenger, S., Donhauser, N., Thüning, H., Rölinghoff, M., Bogdan, C. (1996) Reactivation of latent leishmaniasis by inhibition of inducible nitric oxide synthase. *J Exp Med* 183, 1501-1514.
- Stierhof, Y.D., Bates, P.A., Jacobson, R.L., Rogers, M.E., Schlein, Y., Handman, E., Ilg, T. (1999) Filamentous proteophosphoglycan secreted by *Leishmania* promastigotes forms gel-like three-dimensional networks that obstruct the digestive tract of infected sandfly vectors. *Eur J Cell Biol* 78, 675-689.
- Sundar, S., Chakravarty, J., Agarwal, D., Rai, M., Murray, H.W. (2010) Single-dose liposomal amphotericin B for visceral leishmaniasis in India. *N Engl J Med* 362, 504-512.
- Sundar, S., Sinha, P.K., Rai, M., Verma, D.K., Nawin, K., Alam, S., Chakravarty, J., Vaillant, M., Verma, N., Pandey, K., Kumari, P., Lal, C.S., Arora, R., Sharma, B., Ellis, S., Strub-Wourgaft, N., Balasegaram, M., Olliaro, P., Das, P., Modabber, F. (2011) Comparison of short-course multidrug treatment with standard therapy for

- visceral leishmaniasis in India: an open-label, non-inferiority, randomised controlled trial. *Lancet* 377, 477-486.
- Tacchini-Cottier, F., Zweifel, C., Belkaid, Y., Mukankundiye, C., Vasei, M., Launois, P., Milon, G., Louis, J.A. (2000) An immunomodulatory function for neutrophils during the induction of a CD4⁺ Th2 response in BALB/c mice infected with *Leishmania major*. *J Immunol* 165, 2628-2636.
- Talmi-Frank, D., Jaffe, C.L., Nasereddin, A., Baneth, G. (2012) *Leishmania tropica* experimental infection in the rat using luciferase-transfected parasites. *Vet Parasitol* 187, 57-62.
- Tang, T., Li, L., Tang, J., Li, Y., Lin, W.Y., Martin, F., Grant, D., Solloway, M., Parker, L., Ye, W., Forrest, W., Ghilardi, N., Oravec, T., Platt, K.A., Rice, D.S., Hansen, G.M., Abuin, A., Eberhart, D.E., Godowski, P., Holt, K.H., Peterson, A., Zambrowicz, B.P., de Sauvage, F.J. (2010) A mouse knockout library for secreted and transmembrane proteins. *Nat Biotechnol* 28, 749-755.
- Tay, S.P., Cheong, S.K., Hamidah, N.H., Ainoon, O. (1998) Flow cytometric analysis of intracellular myeloperoxidase distinguishes lymphocytes, monocytes and granulocytes. *Malays J Pathol* 20, 91-94.
- Teixeira, C., Gomes, R., Oliveira, F., Meneses, C., Gilmore, D.C., Elnaïem, D.E., Valenzuela, J.G., Kamhawi, S. (2014) Characterization of the early inflammatory infiltrate at the feeding site of infected sand flies in mice protected from vector-transmitted *Leishmania major* by exposure to uninfected bites. *PLoS Negl Trop Dis* 8, e2781.
- Telleria, E.L., de Araújo, A.P., Secundino, N.F., D'Avila-Levy, C.M., Traub-Csekö, Y.M. (2010) Trypsin-like serine proteases in *Lutzomyia longipalpis*--expression, activity and possible modulation by *Leishmania infantum* chagasi. *PLoS One* 5, e10697.
- Thalhofer, C.J., Graff, J.W., Love-Homan, L., Hickerson, S.M., Craft, N., Beverley, S.M., Wilson, M.E. (2010) In vivo imaging of transgenic *Leishmania* parasites in a live host. *J Vis Exp* 27, 1980.
- Thalhofer, C.J., Chen, Y., Sudan, B., Love-Homan, L., Wilson, M.E. (2011) Leukocytes infiltrate the skin and draining lymph nodes in response to the protozoan *Leishmania infantum* chagasi. *Infect Immun* 79, 108-117.
- Titus, R.G., Marchand, M., Boon, T., Louis, J.A. (1985) A limiting dilution assay for quantifying *Leishmania major* in tissues of infected mice. *Parasite Immunol* 7, 545-555.
- Titus, R.G., Ribeiro, J.M. (1988) Salivary gland lysates from the sand fly *Lutzomyia longipalpis* enhance *Leishmania* infectivity. *Science* 239, 1306-1308.
- Tkalcevic, J., Novelli, M., Phylactides, M., Iredale, J.P., Segal, A.W., Roes, J. (2000) Impaired immunity and enhanced resistance to endotoxin in the absence of neutrophil elastase and cathepsin G. *Immunity* 12, 201-210.
- Tseng, J.C., Kung, A.L. (2012) In vivo imaging of inflammatory phagocytes. *Chem Biol* 19, 1199-1209.
- Ulrichs, P., Tavernier, J. (2008) MAPPIT analysis of early Toll-like receptor signalling events. *Immunol Lett* 116, 141-148.
- van Gisbergen, K.P., Sanchez-Hernandez, M., Geijtenbeek, T.B., van Kooyk, Y. (2005) Neutrophils mediate immune modulation of dendritic cells through glycosylation-dependent interactions between Mac-1 and DC-SIGN. *J Exp Med* 201, 1281-1292.

- van Zandbergen, G., Hermann, N., Laufs, H., Solbach, W., Laskay, T. (2002) Leishmania promastigotes release a granulocyte chemotactic factor and induce interleukin-8 release but inhibit gamma interferon-inducible protein 10 production by neutrophil granulocytes. *Infect Immun* 70, 4177-4184.
- van Zandbergen, G., Klinger, M., Mueller, A., Dannenberg, S., Gebert, A., Solbach, W., Laskay, T. (2004) Cutting edge: neutrophil granulocyte serves as a vector for Leishmania entry into macrophages. *J Immunol* 173, 6521-6525.
- Villaseñor-Cardoso, M.I., Salaiza, N., Delgado, J., Gutiérrez-Kobeh, L., Pérez-Torres, A., Becker, I. (2008) Mast cells are activated by Leishmania mexicana LPG and regulate the disease outcome depending on the genetic background of the host. *Parasite Immunol* 30, 425-434.
- von Stebut, E., Belkaid, Y., Jakob, T., Sacks, D.L., Udey, M.C. (1998) Uptake of Leishmania major amastigotes results in activation and interleukin 12 release from murine skin-derived dendritic cells: implications for the initiation of anti-Leishmania immunity. *J Exp Med* 188, 1547-1552.
- Vouldoukis, I., Riveros-Moreno, V., Dugas, B., Ouaz, F., Bécherel, P., Debré, P., Moncada, S., Mossalayi, M.D. (1995) The killing of Leishmania major by human macrophages is mediated by nitric oxide induced after ligation of the Fc epsilon RII/CD23 surface antigen. *Proc Natl Acad Sci USA* 92, 7804-7808.
- Vuotto, M.L., De Luna, R., Ielpo, M.T., De Sole, P., Moscatiello, V., Simeone, I., Gradoni, L., Mancino, D. (2000) Chemiluminescence activity in whole blood phagocytes of dogs naturally infected with Leishmania infantum. *Luminescence* 15, 251-255.
- Wakid, M.H., Bates, P.A. (2004) Flagellar attachment of Leishmania promastigotes to plastic film in vitro. *Exp Parasitol* 106, 173-178.
- Walsh, D.E., Greene, C.M., Carroll, T.P., Taggart, C.C., Gallagher, P.M., O'Neill, S.J., McElvaney, N.G. (2001) Interleukin-8 up-regulation by neutrophil elastase is mediated by MyD88/IRAK/TRAF-6 in human bronchial epithelium. *J Biol Chem* 276, 35494-35499.
- Walters, L.L., Chaplin, G.L., Modi, G.B., Tesh, R.B. (1989) Ultrastructural biology of Leishmania (Viannia) panamensis (=Leishmania braziliensis panamensis) in Lutzomyia gomezi (Diptera: Psychodidae): a natural host-parasite association. *Am J Trop Med. Hyg* 40, 19-39.
- Warburg, A., Schlein, Y. (1986) The effect of post-bloodmeal nutrition of Phlebotomus papatasi on the transmission of Leishmania major. *Am J Trop Med Hyg* 35, 926-930.
- Watorek, W. (2003) Azurocidin -- inactive serine proteinase homolog acting as a multifunctional inflammatory mediator. *Acta Biochim Pol* 50, 743-752.
- Wege, A.K., Florian, C., Ernst, W., Zimara, N., Schleicher, U., Hanses, F., Schmid, M., Ritter, U. (2012) Leishmania major infection in humanized mice induces systemic infection and provokes a nonprotective human immune response. *PLoS Negl Trop Dis* 6, e1741.
- Wenzel, U.A., Bank, E., Florian, C., Förster, S., Zimara, N., Steinacker, J., Klinger, M., Reiling, N., Ritter, U., van Zandbergen, G. (2012) Leishmania major parasite stage-dependent host cell invasion and immune evasion. *FASEB J* 26, 29-39.
- Wiedow, O., Meyer-Hoffert, U. (2005) Neutrophil serine proteases: potential key regulators of cell signalling during inflammation. *J Intern Med* 257, 319-328.

- Williams, B.R. (2001) Signal integration via PKR. *Sci. STKE* 2001, re2.
- Xu, X., Oliveira, F., Chang, B.W., Collin, N., Gomes, R., Teixeira, C., Reynoso, D., My Pham, V., Elnaiem, D.E., Kamhawi, S., Ribeiro, J.M., Valenzuela, J.G., Andersen, J.F. (2011) Structure and function of a “yellow” protein from saliva of the sand fly *Lutzomyia longipalpis* that confers protective immunity against *Leishmania major* infection. *J Biol Chem* 286, 32383-32393.
- Yang, S.Q., Wang, C.I., Gillmor, S.A., Fletterick, R.J., Craik, C.S. (1998) Ecotin: a serine protease inhibitor with two distinct and interacting binding sites. *J Mol Biol* 279, 945-57.
- Young, R.E., Thompson, R.D., Larbi, K.Y., La, M., Roberts, C.E., Shapiro, S.D., Perretti, M., Nourshargh, S. (2004) Neutrophil elastase (NE)-deficient mice demonstrate a nonredundant role for NE in neutrophil migration, generation of proinflammatory mediators, and phagocytosis in response to zymosan particles in vivo. *J Immunol* 172, 4493-4502.
- Zhang, N., Francis, K.P., Prakash, A., Ansaldi, D. (2013) Enhanced detection of myeloperoxidase activity in deep tissues through luminescent excitation of near-infrared nanoparticles. *Nat Med* 19, 500-505.
- Zheng, Y., Manzotti, C.N., Liu, M., Burke, F., Mead, K.I., Sansom, D.M. (2004) CD86 and CD80 differentially modulate the suppressive function of human regulatory T cells. *J Immunol* 172, 2778-2784